UNIVERSITÀ DEGLI STUDI DI TRIESTE

XXVIII Ciclo
Scuola di Dottorato in Scienze e Tecnologie Chimiche e Farmaceutiche

Innovative phase I clinical trials based on patient genotype monitoring

Settore scientifico-disciplinare: ING-IND/24

Ph.D. STUDENT
Bianca Posocco

Ph.D. PROGRAM COORDINATOR
Prof. Mauro Stener

THESIS SUPERVISORS
Prof. Mario Grassi

Giuseppe Toffoli, M.D.

CO-SUPERVISOR
Elena Marangon, Ph.D.

ACADEMIC YEAR 2014 / 2015

Questo lavoro di tesi è stato svolto presso la Scuola di Dottorato in Scienze e Tecnologie Chimiche e Farmaceutiche dell'Università degli Studi di Trieste, diretta dal Prof. Mauro Stener in collaborazione con la Struttura Operativa Complessa di Farmacologia Sperimentale e Clinica del Centro di Riferimento Oncologico di Aviano (Istituto di ricerca e cura a carattere scientifico), diretta dal Dott. Giuseppe Toffoli.

Contents

List of abbreviations

For pharmacokinetic parameters see **Table 1**

6α-OH-PTX: 6α-hydroxy paclitaxel

ABCB1: ATP Binding Cassette gene

ANC: absolute neutrophil count

BSA: body surface area

CPT-11: irinotecan

CT: computed-tomography

CYP: cytochrome P450

DLT: dose-limiting toxicity

ECOG: Eastern Cooperative Oncology Group

EGFR: epidermal growth factor receptor

ESI: electrospray Ionization

FOLFIRI: irinotecan in combination with 5-fluorouracil/leucovorin

IS: internal standard

LC-MS/MS: liquid chromatography tandem mass spectrometry

LLE: liquid-liquid extraction

LLOQ: lower limit of quantification

LOD: limit of detection

mCRC: metastatic colorectal cancer

MRM: multiple reaction monitoring

MTD: maximum tolerated dose

OS: overall survival

PD: pharmacodynamics

PFS: progression-free survival

PGx: pharmacogenetics

PK: pharmacokinetics

PP: protein precipitation

PS: performance status

PTX: paclitaxel

QC: quality control

SNP: single-nucleotide polymorphism

SPE: Solid phase extraction

SRM: selective reaction monitoring

TDM: therapeutic drug monitoring

UGT1A1: UDP glucuronosyltransferase A1

ULOQ: upper limit of quantification

VEGF: vascular endothelial growth factor

ABSTRACT

BACKGROUND

Most of the chemotherapeutic agents are characterized by a low therapeutic index and significant variability in therapeutic and toxic effects. Thus, despite the increasing amount of knowledge produced in the last years on the molecular bases of anticancer therapy, a large part of the anticancer treatments still result to be ineffective. For this reason, many efforts have been made to optimize the dosage and the administration of antiblastic drugs in order to obtain a maximal anti-tumour effect with acceptable levels of toxicity. This has led to the *personalized therapy* concept, which aims at tailoring the medical treatment to the individual characteristics and needs of the single patient.

In particular, important advances in the pharmacogenetics (PGx) field deserve the inclusion of patient genetic profiling in the optimization of antineoplastic chemotherapy and in clinical drug development. In this context, our group has developed new strategies for phase I studies driven by patient's genetic makeup, that is *genotype-guided phase I clinical trials*. This approach aimed at redefining the dose of cytotoxic drugs, already used in clinical setting, taking into account the pharmacogenetic determinants associated to tumour response and toxicities.

The phase I studies here proposed are related to: (1) irinotecan (CPT-11) administered in combination with 5-fluorouracil/leucovorin (FOLFIRI) and bevacizumab in metastatic colorectal cancer (mCRC) patients; (2) CPT-11 administered in FOLFIRI regimen and cetuximab as first-line therapy in mCRC patients; (3) weekly paclitaxel (PTX) in ovarian cancer patients.

These clinical studies were also supported by the analysis of the drugs pharmacokinetics (PK). In addition, in this thesis a different strategy to personalize the treatment has been explored for a tyrosine kinase inhibitor, sunitinib. Since no PGx biomarkers are known up–to-date for dosage optimization of this drug, a therapeutic drug monitoring approach should be consider in order to maintain the plasma drug concentration within the therapeutic window.

AIMS

The primary aim of these clinical studies was to redefine the maximum tolerated dose (MTD) and the dose limiting toxicity (DLT) of CPT-11, administered in FOLFIRI regimen plus bevacizumab or cetuximab, and of weekly PTX according to *UGT1A1*28* and *ABCB1-2677G>T/A* patient's genotype, respectively. Additional aims were to evaluate the correlation between the PK of CPT-11 and PTX and patients' different genotypes, as well as the effect of the PK on toxicity and response rate. In the case of CPT-11, the possible effect of bevacizumab and cetuximab on the drug PK has also been investigated. In order to obtain these data, an important part of this PhD project has been employed for the development and validation of LC-MS/MS methods for the quantification of these drugs and their metabolites in human plasma.

Regarding sunitinib, the project aimed to develop and validate an analytical method, suitable for the clinical practice, for the quantification of sunitinib and its main metabolite, N-desethyl sunitinib.

METHODS

Phase I trials (1) and (2): eligible patients were stratified in two groups, based on the *UGT1A1 *1/*1* or **1/*28* genotype. For ethical reasons, high risk toxicity patients (**28/*28*) were excluded. CPT-11 was administered as a 2-h continuous i.v. infusion once every 2 weeks over 28-day cycles. The starting dose was fixed at 260 mg/m^2, and the following dose at 310 and 370 mg/m^2. The study has been designed to evaluate the PK of CPT-11 and its main metabolites in absence and presence of bevacizumab/cetuximab during the first chemotherapy cycle, in order to define the potential effect of the biological agents.

Phase I trial (3): eligible patients were stratified in two groups based on the *ABCB1-2677G>T/A* polymorphism: group 1 (*ABCB1-2677GG* genotype) and group 2 (*ABCB1-2677GT; GA, AA, TT, AT* genotypes). PTX was administered as 1-h i.v. infusion every week over 28-day cycles. The starting dose was 80 mg/m^2 and was escalated by steps of 10 mg/m^2. The pharmacokinetic profile of the drug was evaluated twice during the first chemotherapy cycle, during the first and the fourth administration, in order to investigate the phenomenon of metabolic autoinduction of this taxane, which has been reported.

The "3+3" dose escalation method has been applied in all these phase I studies. The MTD was defined as the dose at which <4/10 patients had a DLT (grade 3-4 non hematologic or grade 4 hematologic toxicity during the first one or 2 cycles of therapy in study (1)-(2) and (3), respectively).

Bioanalytical methods: the LC-MS/MS methods have been developed using a HPLC system consisted of a SIL-20AC XR auto-sampler and LC-20AD UFLC XR pumps coupled with an API 4000 triple quadrupole mass spectrometer AB SCIEX. To quantify the chromatographic peaks, data were processed with Analyst 1.5.2 software package (AB SCIEX). Pharmacokinetic parameters were calculated using the non-compartmental model with Phoenix® WinNonlin™ 6.4, Pharsight, Certara Company.

RESULTS

Development and validation of bioanalytical methods: Two LC-MS/MS methods have been developed for the quantification of: 1) CPT-11 and its main metabolites, SN-38, SN-38G, and APC; 2) PTX and its 6α-hydroxy metabolite (6α-OH-PTX). Moreover, beyond the phase I projects, a third method has been developed for the quantification of sunitinib and its active metabolite, N-desethyl sunitinib. These methods require a small plasma volume and a simple and fast protein precipitation as sample proccessing. The concentration ranges, defined for all the analytes, generously covered the clinical expected drug quantities, and resulted appropriate both for pharmacokinetic studies and for dose escalation trials (high doses). They have also been fully validated according to FDA-EMA guidelines on bioanalytical method validation. In fact, the recovery, linearity, intra- and inter-day precision and accuracy, reproducibility, limit of detection and quantification, selectivity, matrix effect, and stability have been successfully assessed. Noteworthy, the method for the quantification of sunitinib, molecule that undergoes Z-E isomerization, does not require the light protection during the sample handling, thus resulting more suitable for the clinical laboratory routine.

Phase I study (1): 48 patients were enrolled (47 were evaluable for DLTs: 24 **1/*1* patients and 23 **1/*28* patients). For **1/*1* patients, 2 DLTs were observed among 10 patients at 310 mg/m^2, while 370 mg/m^2 was not tolerated (2 DLTs in 4 patients). For **1/*28* patients, 2 DLTs were observed among 10 patients at 260 mg/m^2, while 310 mg/m^2 was not tolerated (4 DLTs in 10 patients). Therefore, the MTD resulted 260

mg/m^2 in the **1/*28* cohort and 310 mg/m^2 in the **1/*1* cohort. No significant differences in the pharmacokinetic parameters of CPT-11 and its main metabolites have been observed among the two genotype groups. Moreover, changes in the AUCs of CPT-11 and SN-38 associated with bevacizumab treatment were marginal.

Phase I study (2): at the moment, 2 patients were enrolled in this study. The PK of these patients was followed, as per protocol, during the days 1-3 and the days 15-17 of the first chemotherapy cycle.

Phase I study (3): until now, 37 patients were enrolled (35 patients were evaluable: 10 in the group 1 and 25 in the group 2). For group 2 no DLTs were observed among 10 patients at 120 mg/m^2, while 130 mg/m^2 was not tolerated (2 DLTs in 3 patients). Hence, the MTD resulted 120 mg/m^2 for this group. For group 1, 1 DLT was observed among the first 3 patients at 110 mg/m^2, thus the cohort needs to be enlarged up to 6 patients before to proceed with the dose escalation. Preliminary analyses have showed no significant difference in the pharmacokinetic parameters of both PTX and 6α-OH-PTX among the two genotype groups. Moreover, on the basis of the results related to the comparison between the I and the IV administration it is possible to exclude the PTX metabolism autoinduction. Furthermore, a switching from linear to non-linear PK has been observed when doses higher than 110 mg/m^2 were administered.

CONCLUSIONS

Our genotype-guided phase I studies have demonstrated that doses of both CPT-11 and PTX higher than the standard level (180 and 80 mg/m^2, respectively) can be safely administered. In particular, different MTDs have been assessed according to the patient's genotype, thus demonstrating the effective role of genetic stratification to deliver safe doses of anticancer drugs to patients. Moreover, the different LC-MS/MS methods, developed and validated according to FDA-EMA guidelines, have been successfully applied to plasma samples collected from the patients enrolled in our phase I studies and pharmacokinetic data have been obtained to more deeply investigate the PK/PD relationship.

1 INTRODUCTION

1.1 Chemotherapy: from cytotoxic agents to targeted therapies

The use of chemotherapy to treat cancer began at the start of the 20th century. The term "chemotherapy" was coined by the famous German chemist Paul Ehrlich, in the early 1900s, and was defined as the use of chemicals to treat diseases (DeVita and Chu, 2008). Nitrogen mustards were the first anticancer agents to be used clinically. The effects of an accidental spill of sulphur mustards on troops from a bombed ship in Bari Harbour, Italy, during the World War II led to the observation that both bone marrow and lymph nodes were markedly depleted in those men exposed to the mustard gas (DeVita and Chu, 2008) (Thurston, 2006). In 1942, Alfred Gilman and Louis Goodman began clinical studies of intravenous nitrogen mustards in patients with lymphoma, launching the modern era of cancer chemotherapy (Gilman and Philips, 1946).

Since then, important improvements have been made in the development of new anticancer drugs. Advances in understanding the molecular basis of malignant transformation have led to dramatic changes in the strategy for the discovery of anticancer drugs. In prior years, most of the anticancer agents were synthetic chemicals and natural products, and their mechanism of action was based on the interaction with DNA or its precursor, inhibiting the synthesis of new genetic material and causing broad-based damage to DNA in both malignant and normal cells.

More recently, the expanding knowledge of the molecular changes underlying cancer has led to the development of new anticancer agents for targeted therapy (Sawyers, 2004). The term "targeted therapy" refers to a new generation of anticancer drugs designed to interfere with a specific molecular target (typically a protein) that is believed to have a critical role in tumour growth or progression (e.g. growth factor receptors, intracellular signalling pathways, tumour vascularity). This approach contrasts with the conventional, more empirical approach used to develop cytotoxic chemotherapeutics — the mainstay of cancer drug development in past decades.

1.1.1 Cytotoxic agents

The cytotoxic compounds actually used in chemotherapy are different in structure and mechanism of action. They include: 1) alkylating agents and platinum coordination complexes, 2) antimetabolite analogs of folic acid, pyrimidine, and purine, and 3) natural products (Brunton et al., 2011) (Nussbaumer et al., 2011).

1) *Alkylating agents*. At present, six major types of alkylating agents are used: nitrogen mustards, ethyleneimines, alkyl sulfonates, nitrosoureas, the triazenes, and DNA-methylating drugs, including procarbazine, temozolomide, and dacarbazine. These agents have in common the property of forming highly reactive carbonium ion intermediates, which covalently link to sites of high electron density, such as phosphates, amines, sulfhydryl, and hydroxyl groups. Their chemotherapeutic and cytotoxic effects are directly related to the alkylation of reactive amines, oxygens, or phosphates on DNA, which leads to the creation of DNA strand breaks by repair enzymes, and an apoptotic response. In addition, because of similarities in their mechanisms of action and resistance, platinum complexes are listed in this category. They do not form carbonium ion intermediates like other alkylating agents or formally alkylate DNA but instead covalently bind to nucleophilic sites on it and share many pharmacological attributes with alkylators.
2) *Antimetabolites.* This class of drugs occupies a special place in the history of cancer treatment since they produced the first striking, although temporary, remission in leukaemia (Farber and Diamond, 1948) and the first cure of the choriocarcinoma (Berlin et al., 1963). The mechanism of action is based on the interaction with essential biosynthesis pathways. These drugs are structural analogues of pyrimidine or purine and, therefore, they are incorporated into cell components to disrupt the synthesis of nucleic acids. 5-fluorouracil and mercaptopurine are typical pyrimidine and purine analogues, respectively. Other antimetabolites, such as methotrexate, interfere with essential enzymatic processes of metabolism.
3) *Natural products*. Many anticancer drugs are either natural compounds or have been developed from naturally occurring parent compounds. Among them, several compounds act as antitubulin agents, interfering with microtubule dynamics (i.e.

spindle formation or disassembly), blocking division of the nucleus and thus leading to cell death. The main members of this family include taxanes and vinca alkaloids. A new class of agents, the epothilones, resembles the taxanes in their action but has limited cross-resistance with taxanes. Natural products as anticancer drugs include also topoisomerase inhibitors (e.g. irinotecan and etoposide), which inhibit the responsible enzyme for the cleavage, annealing, and topological state of DNA. Moreover, the family includes intercalating agents that act by binding between base pairs, such as anthracyclines (e.g., doxorubicin, epirubicin), mitoxantrone and actinomycin-D. Lastly, DNA-cleaving agents, such as bleomycin, are included, and they interact with DNA and cause strand scission at the binding site.

An understanding of the life cycle of tumours is essential for the rational use of antineoplastic agents. Since many cytotoxic agents act by damaging DNA, their toxicity is greatest during the S, or DNA synthetic, phase of the cell cycle. Others block the formation of a functional mitotic spindle in the M phase. Therefore, these agents are most effective on cells entering mitosis, the most vulnerable phase of the cell cycle. Accordingly, human malignant neoplasms most susceptible to chemotherapy are those having a high percentage of proliferating cells (e.g. leukaemias and lymphomas). Likewise, normal tissues that proliferate rapidly (bone marrow, hair follicles, and intestinal epithelium) are thus highly vulnerable to damage from cytotoxic drugs (Brunton et al., 2011). For this reason, unpleasant side effects such as bone marrow suppression, gastrointestinal tract lesions, alopecia, nausea, as well as the rapid development of clinical resistance represent the main disadvantages of many cytotoxic agents (Thurston, 2006) (Brunton et al., 2011).

Moreover, in some cases, cytotoxicity may also depend on the presence, in the pharmaceutical preparations, of organic solvents/detergents necessary to improve the poor solubility in water of many of these cytotoxic agents. Thus, the toxicity can be decreased significantly combining the cytotoxic compounds with a variety of drug carrier vehicles, which alter also the drug pharmacokinetics (PK) (Figure 1).

Recent advances in drug delivery include the use of biocompatible polymers with functional monomers attached in such a way as to permit linkage of drug molecules to the polymer (Posocco et al., 2015). A drug-polymer conjugate can be designed to be a stable, long-circulating prodrug by varying the molecular weight of the polymer and the

cleavable linkage between the drug and the polymer. The linkage is designed to keep the drug inactive until it is released from the backbone polymer by a disease- specific trigger, typically pH condition or enzyme activity in the targeted tissue that delivers the active drug at or near the site of pathology. Thus, an increasing interest in the development of targeted drug delivery systems has been showed, giving rise to new intriguing scenarios in chemotherapy.

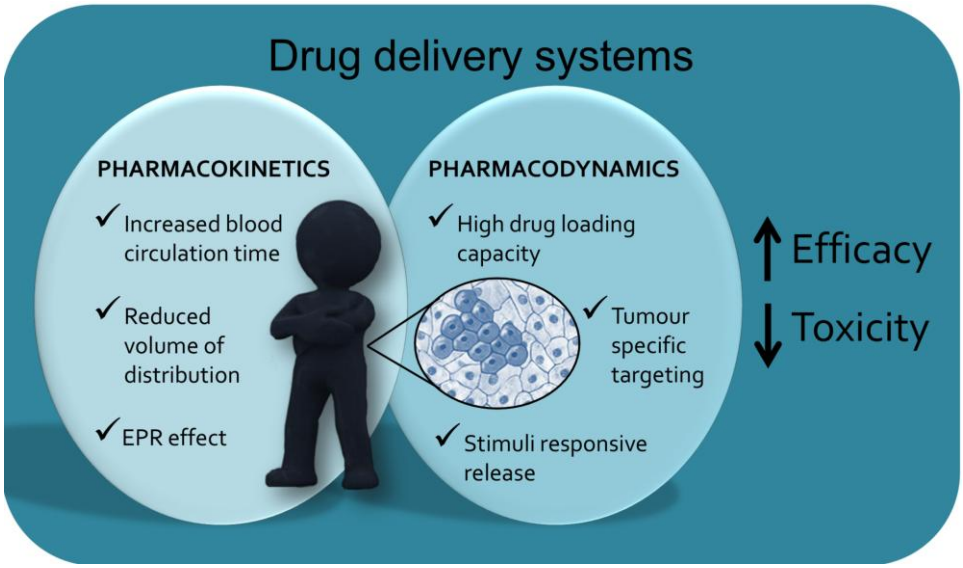

Figure 1 Schematic representation of the main benefits derived from the use of drug delivery systems. EPR effect: Enhanced Permeability and Retention Effect. Adapted from (Posocco et al., 2015)

1.1.2 Targeted therapies

The targeted therapies include two main classes of drugs with very different pharmacological properties: monoclonal antibodies that attack cell surface receptors and antigens, and synthetic small molecules that enter cells and inhibit multiple enzymatic sites. It is convenient to distinguish the different drugs belonging to the targeted therapies on the basis of their specific target: 1) protein tyrosine kinase inhibitors, 2) epidermal growth factor receptor (EGFR) inhibitors, 3) inhibitors of angiogenesis (Brunton et al., 2011) (Sawyers, 2004).

1) *Protein tyrosine kinase inhibitors*. Protein kinases are critical components of signal transduction pathways that regulate cell growth and adaption to the extracellular environment. These signalling pathways influence gene transcription and/or DNA synthesis, as well as cytoplasmic events. Growth factors and other ligands bind to

and activate the receptor tyrosine kinases under physiological conditions. In a growing number of human malignancies, mutations that constitutively activate protein tyrosine kinases are implicated in malignant transformation; thus, protein tyrosine kinases are targets for cancer therapy. For instance, imatinib targets the BCR-ABL tyrosine kinase, which underlies chronic myelogenous leukemia (CML). A single molecular event, in this case the 9:22 translocation, leads to expression of the Abelson proto-oncogene kinase *ABL* fused to *BCR* (breakpoint cluster region), yielding a constitutively activated protein kinase. Imatinib binds to a segment of the kinase domain that fixes the enzyme in a closed or non-functional state, in which the protein is unable to bind its substrate/phosphate donor, ATP (Weisberg et al., 2005). As a result, these cells stop growing, and even die by apoptosis (Goldman and Melo, 2003). Other protein tyrosine kinase inhibitors are dasatinib and nilotinib.

2) *Epidermal growth factor receptor inhibitors.* The EGFR belongs to the ErbB family of transmembrane receptor tyrosine kinases. EGFR, also known as ErbB1 or HER1, is essential for the growth and differentiation of epithelial cells. Ligand binding to the extracellular domain of EGFR family members causes receptor dimerization and stimulates the protein tyrosine kinase activity of the intracellular domain, resulting in autophosphorylation of several Tyr residues in the C-terminal domain. Recognition of the phosphotyrosines by other proteins initiates protein-protein interactions that result in stimulation of a variety of signalling pathways that regulate cell proliferation, metabolism, and survival (Schlessinger, 2000). Drugs targeting EGFR pathway have become important agents in the therapy of solid tumours and can be divided in two main classes: the EGFR tyrosine kinase inhibitors, such erlotinib and gefitinib, which bind to the kinase domain and block the enzymatic function of EGFR, and the monoclonal antibodies. Cetuximab and panitumumab, belonging to this latter class, bind specifically the extracellular domain of EGFR. They inhibit EGFR-dependent signalling through the inhibition of ligand-dependent activation and receptor dimerization, the downregulation of EGFR expression, and the induction of antibody-dependent cell mediated cytotoxicity (Ciardiello and Tortora, 2008).
3) *Inhibitors of angiogenesis*. Angiogenesis is the formation of new capillaries from pre-existing vessels and circulating endothelial precursors. It is a tightly controlled

dynamic process that can occur physiologically in those tissues that undergo active remodelling in response to stress and hypoxia (El-Kenawi and El-Remessy, 2013). However, it can be aberrantly activated during many pathological conditions such as cancer. In fact, tumour cells secrete angiogenic factors that induce the formation of new blood vessels that guarantee the flow of nutrients to the tumour cells. An additional benefit of anti-angiogenic agents derived from the observation that leaky capillaries within tumours have increased permeability and cause an enhancement in tumour interstitial pressure. This increased pressure inhibits blood flow, decreases oxygenation, and prevents drug delivery within the tumour (Jain, 2009). Antibodies directed at the primary angiogenic factor, vascular endothelial growth factor (VEGF), "normalize" interstitial pressure and improve blood flow, thus enhancing the ability of chemotherapeutic agents to reach the tumour. An example of antibody targeting VEGF is bevacizumab, which was the first FDA-approved molecule that specifically targeted angiogenesis. Moreover, three small molecules (pazopanib, sorafenib, and sunitinib), which inhibit the kinase function of VEGF-2, have been approved for clinical use.

Although molecularly targeted drugs have had outstanding successes in selected type of cancer, traditional cytotoxics are not likely to be replaced by these new therapies in the near future. Rather, targeted drugs and cytotoxics will continue to be used in combination (Brunton et al., 2011) (Nussbaumer et al., 2011). Moreover, cytotoxic agents are also used as a support to either surgery or radiotherapy (Brunton et al., 2011).

In the present thesis, about all the different chemotherapy treatments reported above has been taken in consideration: from a single cytotoxic agent-based therapy related to paclitaxel (PTX) in ovarian cancer patients to two combination therapies of irinotecan (CPT-11) with 5-fluorouracil/leucovorin in association with targeted agents (bevacizumab and cetuximab) in metastatic colorectal cancer (mCRC) patients. Finally, also a tyrosine kinase inhibitor (sunitinib)-based therapy for metastatic renal-cell cancer patients has been considered.

1.2 Determining the optimal dose: phase I study and pharmacokinetics

The theoretical aim of an anticancer therapy is to treat the patient with the highest possible dose in order to achieve the maximum possible effect on tumour cells. Nevertheless, many of anticancer treatments, be they cytotoxic chemotherapy drugs, biologic agents, or radiation, are associated with acute toxicities that can affect a wide range of organ systems and are frequently life threatening (Shanholtz, 2001). Therefore, the challenge has been and still remains to find a balance between efficacy and toxicity. This requires the definition of dose-limiting toxicity (DLT) and the so-called maximum tolerated dose (MTD). The main principle is indeed that the observed dose-limiting toxicities define the maximal tolerable dose (Mathijssen et al., 2014). Thus, this recommendation was determined according to safety aspects and the assumption that toxicity is a surrogate of activity: the highest safe dose is assumed to be the one most likely to be efficacious (Eisenhauer et al., 2000). As a consequence, the therapeutic window of cytotoxic agents is commonly narrow (Figure 2), meaning that relatively small changes in drug concentration may lead to a lower drug activity or extreme toxicities.

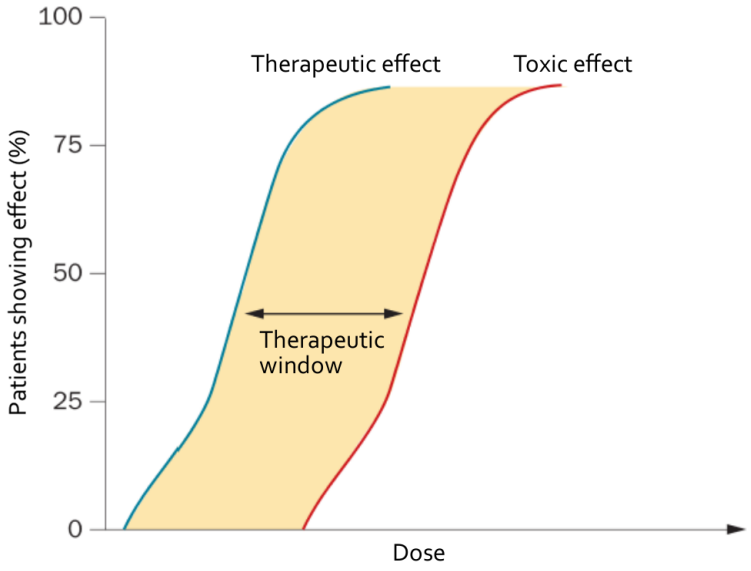

Figure 2 Schematic representation of the therapeutic window. Below a certain threshold- concentration the drug is inactive, while above a certain concentration side effects appear.

1.2.1 Development of anticancer drugs: clinical phase I-II-III-IV

The conventional approach for the identification of the optimal dose is based on identifying the MTD in phase I trials and incorporating it within subsequent trials. In Figure 3 the different phases involved in the translation of new cancer therapies from bench to bedside are represented.

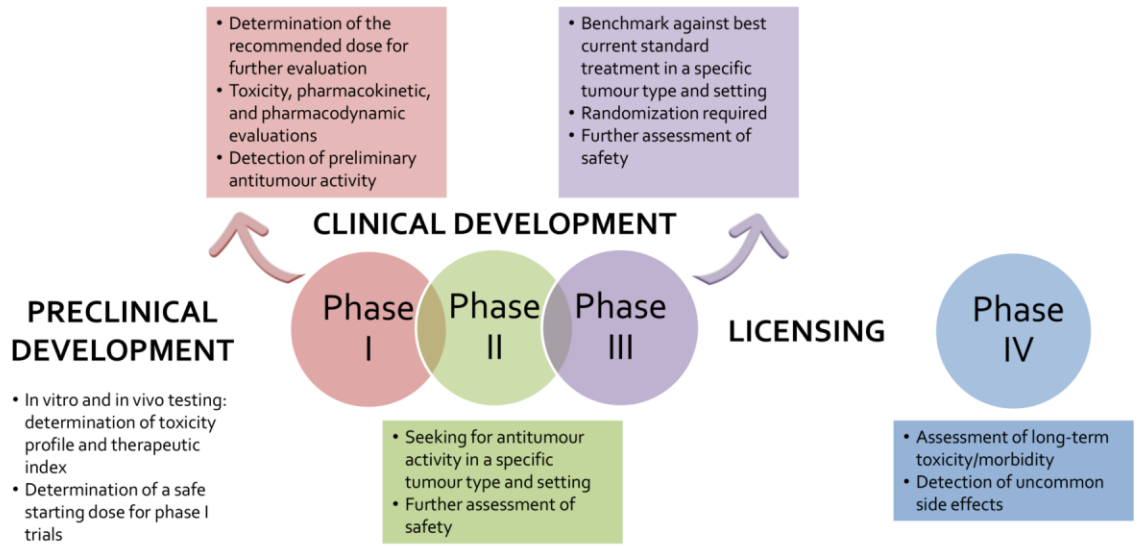

Figure 3 Main steps of anticancer-drug development.

They are designed to answer a specific research question (Arrondeau et al., 2010):

- *Phase I*: a new drug or drug combination is tested in a small group of patients for the first time to evaluate its safety, determine a safe dosage range, and identify side effects. The phase I for anticancer drug/therapy development differs from non-oncology phase I in that it is usually performed in patients with a terminal diagnosis, who typically have exhausted standard treatment options, rather than in healthy volunteers (Miller and Joffe, 2008) (Ivy et al., 2010). This choice has a dual purpose: to prevent healthy volunteers from being exposed to very toxic drugs and to give to some patients suffering from cancer the possibility to benefit from the investigational drug. The primary goal of phase I cancer trials is to collect data on toxicity, pharmacologic and pharmacodynamic properties of a specific drug or therapy regimen, allowing determination of the recommended phase II dose. Moreover, pharmacokinetic analyses are performed to determine the relationship of increasing dose to drug absorption, distribution, and

metabolism. In addition, drug interactions are also investigated in combination regimen phase I trials.

- *Phase II*: they are screening studies aiming to identify signals of anti-tumour activity in a homogenous population of patients with a particular tumour type (Dhani et al., 2009). The gold standard for evaluation of any new cancer therapy is the improvement in overall survival (OS), that is the length of time from either the date of diagnosis or the start of treatment for the disease that patients diagnosed with the disease are still alive (www.cacer.gov). However, OS has limited utility in phase II trials due to the limited length of observation and the confounding effects of subsequent therapies and, thus, other endpoints such as progression-free survival (PFS- the length of time during and after the treatment of the disease that a patient lives with the disease but it does not get worse (www.cacer.gov)) and biomarkers may be preferable (Dhani et al., 2009) (Seymour et al., 2010).
- *Phase III*: this kind of trial is a critical step before licensing and it consists of the evaluation of the new treatment efficacy against the best current standard therapy. In order to conduct a scientifically valid comparison between the two treatment cohorts, the groups need to be alike as much as possible, with the only exception being the specific treatments under investigation (Thall, 2008). Phase III trials can be classified by their goals. On the one side, difference (superiority) trials, the most frequent studies, aim to determine if sufficient evidence exists that one treatment arm is different from another. On the other side, equivalence trials aim to determine whether two treatment arms are equivalent (or nearly so). Equivalence trials are performed to demonstrate that a less expensive or less toxic new treatment provides similar clinical benefit to the standard therapy.
- *Phase IV*: after licensing, phase IV post-marketing trials may be undertaken to explore the long-term safety/morbidity of the treatment. However, these phase IV trials are infrequently done (Arrondeau et al., 2010).

More in details regarding the phase I trials, objects of this thesis, the guiding principle for dose escalation in these studies is to avoid unnecessary exposure of patients to very low doses of an agent while preserving safety and maintaining rapid accrual. Phase I

clinical studies are conducted by selecting a safe starting dose deduced from animal toxicology testing (i.e. one tenth of the lethal dose in mouse (Eisenhauer et al., 2000)). In a stepwise manner the dose is subsequently increased in defined cohorts of patients until DLT is reached in a given number of patients. Dose escalation methods are divided in two main categories: the rule-based designs, which include the traditional "3+3" design; and the model-based designs (Le Tourneau et al., 2009).

The former design proceeds with cohorts of three patients; the first cohort is treated at a starting dose that is considered to be safe based on extrapolation from animal toxicological data, and the subsequent cohorts are treated at increasing dose levels that have been fixed in advance (Figure 4).

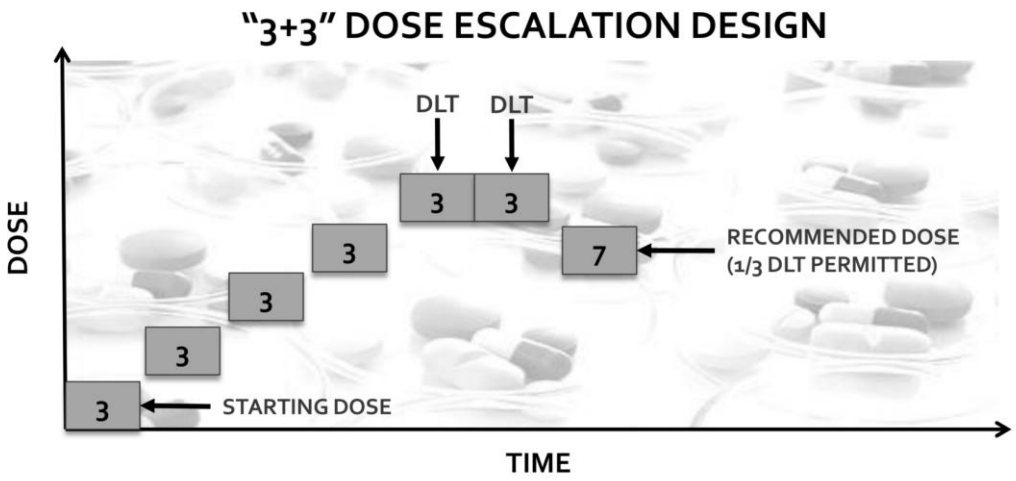

Figure 4 Schematic description of the 3+3 cohort expansion design.

Historically, dose escalation has followed a modified Fibonacci sequence in which the dose increments become smaller as the dose increases (e.g. the dose first increases by 100% of the preceding dose, and thereafter by 67%, 50%, 40%, and 30% – 35% of the preceding doses). In most of the cases, the pre-specified dose levels do not fit the exact Fibonacci sequence (Le Tourneau et al., 2009). If none of the three patients in a cohort experienced a dose-limiting toxicity, another three patients will be treated at the next higher dose level. Otherwise, if one of the first three patients experienced a dose-limiting toxicity, three more patients will be treated at the same dose level. The dose escalation continues until at least two patients among a cohort of three to six patients experience dose-limiting toxicities (i.e. ≥ 33% of patients with a DLT at that dose level). The MTD recommended for phase II studies is conventionally defined as the dose level

immediately below the one at which ≥33% of patients have experienced DLT. Therefore at the MTD, ≤1/3 out of at least 10 patients experienced DLT.

Despite the traditional "3+3" design is safe and easy to implement, it presents a limitation due to the fact that the early dose levels involve treating patients at very low doses which are almost certainly biologically inactive, while few patients actually receive doses at or near the recommended phase II dose (Arrondeau et al., 2010). An alternative rule-based strategy, known as the accelerated titration design attempts to minimize this problem. In this case, a single patient is treated per cohort, with the dose doubling between each cohort in the absence of any grade 2 toxicities. As soon as a grade 2 toxicity occurs, dose escalation is switched to the slower and more traditional "3+3" design. In some of these designs, intrapatient dose escalation is also allowed (Arrondeau et al., 2010).

The second dose escalation method for phase I clinical trials, the model-based design mentioned above, is based on the use of statistical models that actively seek a dose level that produces a prespecified probability of DLTs by using toxicity data from all enrolled patients and compute a more precise dose – toxicity curve. It also attempts to reduce the number of patients treated at very low doses (Le Tourneau et al., 2009). However, the use of this design is challenging, as it needs biostatistical expertise and available software on site to perform model fitting in real time, as well as expedited collection of data from each cohort of patients to fit the model (Arrondeau et al., 2010). For these reasons, the traditional "3+3" design remains the prevailing method for conducting phase I cancer clinical trials (Arrondeau et al., 2010) (Le Tourneau et al., 2009). Hence, the phase I trials objects of this PhD project have been designed adopting this traditional dose-escalation model.

According to the Italian legislation (DPR n°439/2001,art.3), it is necessary to design a Phase I study with:

- New pharmaceutical products never tested in human subjects;
- Pharmaceutical products resulted from a new association of already registered agents;
- Pharmaceutical products already registered in other countries but declared new by the Italian Ministry of Health;

- Pharmaceutical agents already registered but for which new pharmaceutical forms, excipients, recommendations, dosages, administration routes are proposed.

The last category identifies the so-called *phase Ib* studies, specifically object of this thesis.

1.2.2 Pharmacokinetic principles

As reported in the previous section, the determination of the pharmacokinetic properties of the study drug represents an important aim of phase I clinical trials.

PK describes the temporal patterns of response to drug administration following acute or chronic dosing. In order to understand and control the therapeutic action of drugs in the human body, it is necessary to know how much drug will reach the site(s) of drug action and when this will occur. In fact, understanding and employing pharmacokinetic principles can increase the probability of therapeutic success and reduce the occurrence of adverse drug effects in the body (Brunton et al., 2011). Pharmacokinetic studies are essential to determine how the body handles drug, that is, how drug is absorbed, distributed, metabolized and eliminated (Figure 5).

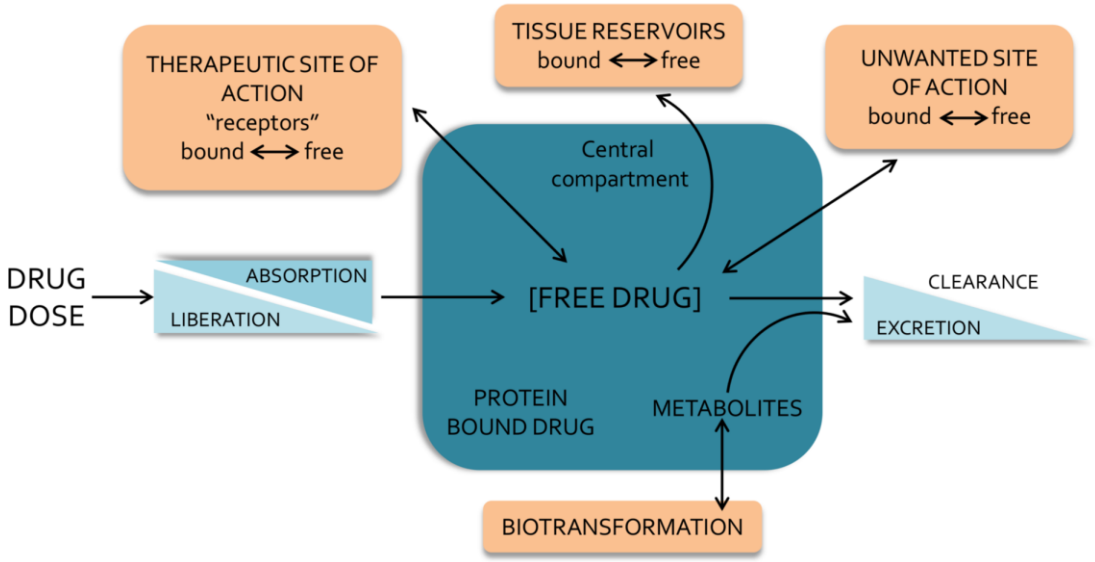

Figure 5 The interrelationship of the absorption, distribution, binding, metabolism, and excretion of a drug and its concentration at its sites of action (possible distribution and binding of metabolites in relation to their potential actions at receptors are not depicted).

All these processes, collectively called ADME, are influenced by patient's characteristics (i.e. genetics, body size, age, and co-morbidity) and by dosage, drug formulation, route of administration and by the possible co-administration of other drugs.

Bioavailability is a term used to indicate the fractional extent to which a dose of drug reaches its site of action or a biological fluid from which the drug has access to its site of action. By definition, when a drug is administered intravenously, its bioavailability is 100% and, on the contrary, when a drug is administered via other routes, its bioavailability decreases because of several losses during the absorption phase. For example, a drug given orally must be absorbed first from the gastrointestinal tract, but net absorption may be limited by the characteristics of the dosage form, the drug's physicochemical properties, the intestinal metabolism, and the transporter export back into the intestinal lumen.

Following absorption or systemic administration into the bloodstream, a drug distributes into interstitial and intracellular fluids. This process reflects a number of physiological factors and the particular physicochemical properties of the individual drug. Drug circulating in the bloodstream is responsible of pharmacological activity and several processes regulate its level: 1) the organs uptake; 2) the drug binding with plasma proteins (albumin is a major carrier for acidic drugs; α1-acid glycoprotein binds basic drugs. The binding is usually reversible), red cells or platelets; 3) the permeability of tissue membranes, and 4) the drug metabolism and elimination.

Drugs are eliminated from the body either unchanged by the process of excretion or converted to metabolites. In fact, drug elimination occurs by two processes, excretion and metabolism; excretion is the irreversible loss of chemically unchanged drug in urine and in faeces (renal excretion of unchanged drug is a major route of elimination for 25–30% of drugs), while metabolism is the conversion of one chemical species to another. Excretory organs, the lung excluded, eliminate polar compounds more efficiently than substances with high lipid solubility. Lipid-soluble drugs thus are not readily eliminated until they are metabolized to more polar compounds. Drug metabolism is obtained by two types of enzymatic reactions: phase I (biotransformation) characterized by reactions of oxidation, hydroxylation, reduction and hydrolysis and phase II (conjugation) characterized by reactions of addition of a new functional group such as glucuronide, sulphate, methyl and acetyl groups, glutathione and amino acids.

Although drug metabolism is the physiological way of detoxification, some metabolites can retain (or increase) the pharmacological activity. Understanding drug metabolism has spawned the new disciplinary focus of pharmacogenetics, which offers the promise that understanding the expression and activities of specific metabolizing enzyme isoforms in a given individual will permit the clinician to tailor treatments, particularly in chemotherapy (Dawood and Leyland-Jones, 2009), to maximize therapeutic outcomes and minimize risks of toxicity or drug-drug interactions. Anyway, this aspect will discussed more in details in the following chapter.

The most important parameters governing drug disposition are reported in Table 1.

Table 1 Main pharmacokinetic parameters and their clinical significance.

Parameter	Name	Significance	Key features
C_{max}	Maximum plasma concentration	The highest drug concentration observed in plasma following administration	C_{max} and T_{max} are correlated and both depend on how quickly the drug enters into and is eliminated from the body
T_{max}	Time until C_{max} is reached	The time at which the highest drug concentration occurs	
AUC	Area under the concentration-time curve	The measure of the total systemic exposure to the drug	It represents the amount of unchanged drug that has reached the general circulation and it is useful to define the bioavailability of a drug
V_d	Volume of distribution	The apparent volume into which the drug is dissolved	It depends on binding to plasma proteins and tissues and it is useful to correlate the drug concentration in plasma with its amount in the body
$t_{1/2}$	Half-life in the terminal phase	The time taken for the plasma concentration to fall by one half once distribution equilibrium has been achieved	It is independent of the amount of drug in the body and it is useful for the determination of the frequency of drug administration
Cl	Clearance	The rate of drug elimination by all routes normalized to the concentration of the drug	It is the sum of all organs clearance, especially hepatic and renal clearance

1.2.2.1 Mass spectrometry for pharmacokinetic analysis

Measuring drug plasma concentration in samples collected at specific time points, it is possible to obtain the plasma concentration-time profile and the shape and the mathematical elaboration of this profile provide the main pharmacokinetic parameters reported in the previous Table 1.

In order to obtain the plasma concentration-time profile, the method and the analytical technique used are fundamental. A higher method sensitivity correlates with a the better description of the drug kinetics, in terms of a much longer monitoring of drug concentration, which also means a better measurement of the area under the concentration-time curve (AUC) and a description of the half-life in the terminal phase ($t_{1/2}$). In the last 35 years, there have been significant improvements in analytical technologies applied in cancer pharmacology to measure drug concentration and to study drug metabolism. At the beginning, the concentration data from plasma or other biological matrix were usually obtained by LC-UV/VIS methods. The next step was to prefer, when possible, the use of a fluorescence detector (FLD), but the real change in bio-analysis began with the development of bench-top mass spectrometry instruments, combined with liquid chromatography (LC-MS). Within a few years, LC-MS has become the method of choice for quantitative drug analysis to support PK and drug metabolism studies (Hopfgartner and Bourgogne, 2003) (Crotti et al., 2015). Coupling the mass spectrometer with LC provided significant improvements in assay sensitivity, specificity and capability to analyze samples with very different concentration ranges. The increase in sensitivity and specificity caused three important effects:

- the possibility to detect drugs and metabolites at very low concentration;
- the possibility to use very small amount of sample (that is particularly important in preclinical studies conducted in small animals or in paediatric studies);
- a selective analytes detection in presence of complex matrices such as tissues or whole blood.

Mass spectrometry owes its success to its performances in drug quantitative (PK) and qualitative (metabolites identification) analysis. Accurate and sensible quantitation is obtained by operating in tandem mass (MS/MS) mode (Saint-Marcoux et al., 2007). MS/MS is necessary because of possible interfering compounds present in the biological

sample exhibiting the same integer mass, while the fragmentation pattern is compound specific. Tandem mass experiments, performed by means of triple quadrupole instrumentation, are obtained through collision-induced dissociation (CID). Detection is based on selective reaction monitoring (SRM), also called multiple reaction monitoring (MRM), based on monitoring of fragmentation reaction(s) from the analyte molecular ion to analyte specific fragment ion(s) (de Hoffmann, 1996). The combination of parent mass and its fragment ions is used to monitor selectively the compound that has to be quantified.

Despite the need for chromatographic separation is often low with MRM detection mode thanks to its specificity, co-eluting matrix components may cause problems in the ionization process by so called matrix effects. Moreover, other factors such as the drug-proteins binding ant the analyte instability during the untreated sample storage could affect the quantitative drug analysis. Sample preparation is one of the most time-consuming steps in the bioanalysis aiming to isolate, clean-up and pre-concentrate analytes of interest from biological matrices (Nováková, 2013). Sample preparation procedures mainly employed in PK studies are schematized in Figure 6.

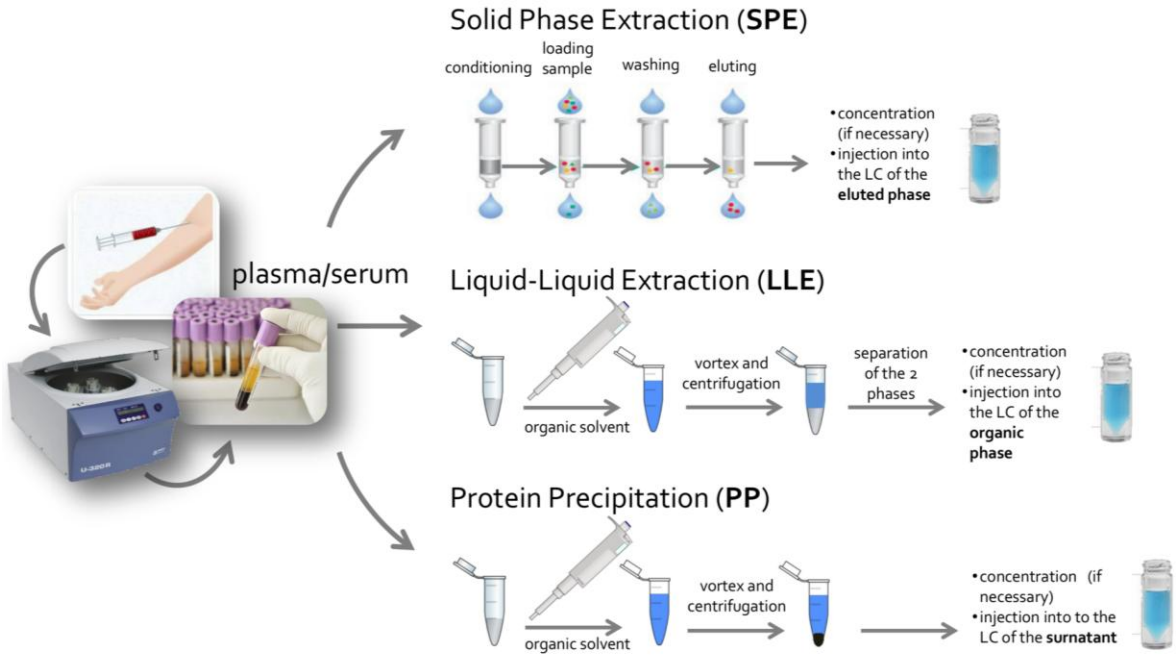

Figure 6 Schematic representation of the conventional sample preparation techniques used in pharmacokinetic analysis.

Solid phase extraction (SPE), liquid-liquid extraction (LLE) and protein precipitation (PP) are considered the conventional sample preparation techniques still highly employed in contrast to modern approaches such as on-line techniques or microextractions (Nováková, 2013). Basically, LLE and SPE provide selective analytes recovery (depending on the solvent and/or stationary phase choice) and result in cleaner extracts with respect to PP. SPE has advantages in terms of less sample amount required, a minor solvent consumption, and the possibility to be used in on-line systems.

In LC-MS analysis the analytes are introduced into the ion source of mass spectrometer after their separation in a LC column. There are different types of MS ion sources, but the most commonly employed in pharmacokinetic studies is Electrospray Ionization (ESI), an atmospheric pressure ionization. ESI is a soft ionization technique - as very little internal energy is retained by the analyte after ionization - and does not cause decomposition of labile compounds. It is characterized by an efficient ion production, mainly by protonation or cationization reactions, and it can operate in either positive or negative ion mode. In a typical ESI source, schematized in Figure 7, the solution is injected in a stainless steel capillary.

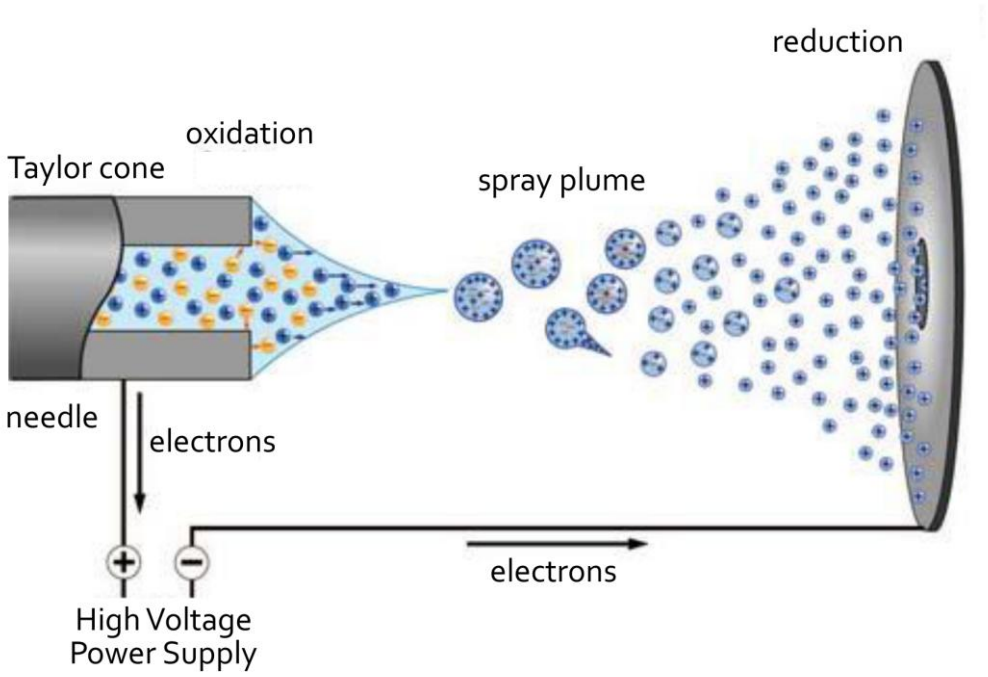

Figure 7 Ions formation in positive electrospray ionization. Under these conditions the capillary is placed at a positive voltage, while the counter electrode is placed to a negative voltage. Adapted from (Crotti et al., 2011).

Between this capillary and their counter electrode, a voltage in the order of 3-5 kV is applied. Under these conditions, the formation of a solution cone just outside the capillary occurs. The cone formation is due to the presence of charged species inside the solution, which experiment the electrostatic field existing between the capillary and the counter electrode (Taylor, 1964). After the cone production, the droplets formation from the cone apex is observed, charged droplets further migrate through the atmosphere to the counter electrode (Taylor, 1964). Droplets formation is strongly influenced by solvent chemical-physical characteristics, ionic analytes concentration, inorganic salts concentration, and the applied voltage. The so generated charged droplets, decrease their radius after solvent evaporation still conserving their total charge amount. The energy required for the solvent evaporation is due to the environment thermal energy, further enhanced through by the use of a heated capillary or by collisions with heated gas flow. As the droplet radius decrease, the surface charge density increases; when the radius reaches the Rayleigh stability limit, the electrostatic repulsion equals the surface tension. For lower radii, the charged droplets are unstable and decompose through a process defined "Columbic Fission" (Rayleigh, 1882). This produces smaller droplets that ultimately liberate unsolvated charged analyte molecules. Alternatively, the "ion evaporation" mechanism has been proposed, based on the direct emission of ions from the charged droplets occurring when the surface charge density shows a large increase. Far to be fully understood, the mechanism(s) of gas phase ions production from the small/highly charged droplets has been investigated by several authors, as discussed in some recent reviews (Crotti et al., 2011) (Kebarle and Verkerk, 2009). Typically, in ESI the production of smaller droplets is enhanced by lower mobile phase flow rate and by the use of volatile mobile phases; the pH and volatility of the LC eluent has a very high role in ionization efficiency and thus detection sensitivity.

Another, commonly used, ionization type is atmospheric pressure chemical ionization (APCI), which is based on the interaction of solution vapours with a corona discharge, leading to gas phase ionization reactions. APCI has been used typically for less polar (neutral) analyte compounds, such as steroid-like compounds.

Physicochemical properties (i.e. hydrophilicity and ionization behaviour) of the analyte have a major role in affecting the method performance in both chromatographic separation step and mass spectrometric detection. The detection response of

compounds varies due to the ionization efficacy and co-presence of interfering molecules, thus quantitative analysis by LC-MS should require that pure standards are available for each analyte. The use of isotope labelled compounds as internal standards is recommend to reduce those problems caused by matrix effects.

1.2.2.2 Validation of a bioanalytical method

Selective, sensitive, and validated analytical methods for the quantitative evaluation of drugs and their metabolites are critical for the successful conduction of nonclinical and clinical pharmacology studies. Indeed, the quantitative measurements of drugs, metabolites, and biomarkers provide essential information in the assessment of safety and efficacy of drugs. Moreover, drug or biomarker concentrations frequently serve as the primary or secondary endpoints of many clinical studies in drug development. Consequently, the reliability or quality of that data underpins the study outcome (Booth et al., 2015; FDA, 2013a). For this reason, validating bioanalytical methods includes performing all of the procedures that demonstrate that a particular method used for quantitative measurement of analytes in a given biological matrix (e.g. blood, plasma, serum, or urine) is reliable and reproducible for the intended use (FDA, 2013a).

The measurements should be based on established principles and scientists should utilize a common, vetted paradigm of practices, independent of the analytical platform to demonstrate that the assays provide reliable data. The necessity to establish the main guiding principles for the validation of an analytical method and to disseminate them to the pharmaceutical community was received, in 1990, by the first American Association of Pharmaceutical Scientist (AAPS)/ FDA Bioanalytical Workshop (Shah et al., 1991). Scientists in the bioanalytical field worked with the regulatory community to establish a common language and expectations in generating pharmacokinetic data for drugs and metabolites. These validation principles were introduced into regulations by Health Canada in 1992 (Canadian Minister of Health, 1991) and then by the FDA which published the first edition of its Guidance on Bioanalytical Method Validation in 2001 (FDA, 2001).

This guidance explains the course of action for the validation of analytical procedures such as gas chromatography; high-pressure liquid chromatography; GC-MS; LC-MS; ligand binding assays, immunological assays and microbiological procedures. In doing

so, the specific features of these methods in the quantitative determination of drugs and metabolites in biological matrices are taken into account. Validation involves documenting, through the use of specific laboratory investigations, that the performance characteristics of the method are suitable and reliable for the intended analytical applications. The acceptability of analytical data corresponds directly to the criteria used to validate the method. Fundamental parameters for this validation include the following: accuracy, precision, selectivity, sensitivity, reproducibility, stability. The FDA guidance described in detail all these parameters and the correct way to validate them.

Since the publishing of this guidance in 2001, the dialogue has broadened significantly through scientific conferences not only within the USA, but globally. In 2011 the Guidance on Bioanalytical Method Validation was introduced in EU (EMA, 2011). Successively, in September 2013 the FDA released a draft revision of the Guidance for Industry Bioanalytical Method Validation that included a number of changes to the expectations for bioanalysis (FDA, 2013a).

In particular, taking into account the AAPS/FDA Workshop on Incurred Sample Reanalysis (Fast et al., 2009), this revised version has introduced an additional measure of assay reproducibility: the Incurred Sample Reanalysis (ISR). This analysis is now well established as an important element of bioanalysis and it is intended to verify the reliability of the reported subject sample analyte concentrations. ISR is conducted by repeating the analysis of a subset of subjects' samples from a given study in a separate run to critically support the performance of assays.

Accordingly to what reported above, the development and validation processes of the LC-MS/MS methods, represent an essential task of the PhD project herein reported in order to correctly define the drug PK as a support to the phase I studies conducted by our group.

1.3 New challenge in cancer chemotherapy: the personalization of the therapy

Personalized medicine represents one of the most important challenges in cancer therapy. The increasing amount of knowledge produced in the last years on the molecular bases of anticancer therapy has led to the development of new therapeutic targeted molecules and to a better understanding of the molecular bases of chemotherapy with traditional drugs. Nevertheless, cancer still remains an enormous global health burden (the second most common cause of death in the US, exceeded only by heart disease, accounting for nearly 1 of every 4 deaths). Today, cancer accounts for about 1 in every 7 deaths worldwide – more than HIV/AIDS, tuberculosis, and malaria combined. In 2016 about 1685210 new cancer cases are expected to be diagnosed in US and about 595690 Americans are expected to die of cancer (Cancer Facts and Figures, 2016). More than 60% of cancer deaths occurs in low- and middle-income countries, many of which lack the medical resources and health systems to support the disease burden (Cancer Facts and Figures, 2016). Anyway, a large part of patient's treatment results to be ineffective: it is estimated that in only 25% of patients a response is achieved (Spear et al., 2001) (FDA, 2013b). This represents a big issue not only in oncology, but also in medicine in general: everyday millions of people take drugs that will not help them, as depicted in the Figure 8.

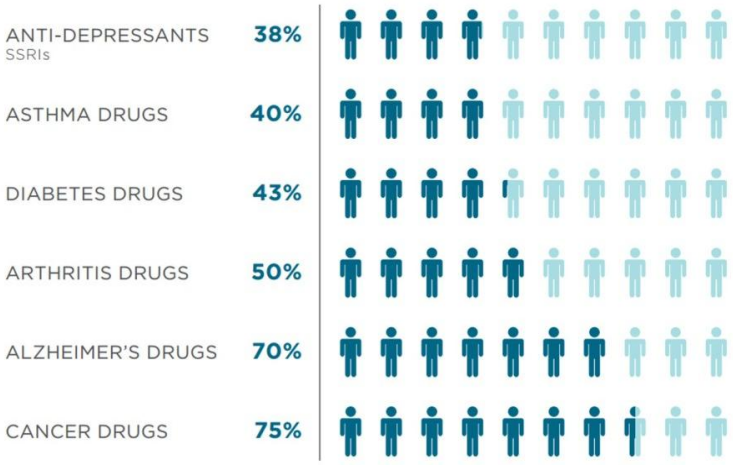

Figure 8 Imprecision medicine: average percentage of the patient population for which a particular drug in a class is ineffective (Spear et al., 2001).

Certainly, this problem becomes particularly serious considering drugs characterized by both severe side effects and a low therapeutic index such as those administered in cancer patients.

1.3.1 Current practice for individualize anticancer drug dose: the Body Surface Area

In the early days of cancer chemotherapy, cytotoxic drug doses were either fixed at the level defined by the phase I studies or recalculated on the basis of the body weight (BW) (Pinkel, 1998). Successively, the huge variability in cancer patients' outcomes in terms of both toxicity and efficacy along with the narrow therapeutic index characterising anticancer drugs has led clinicians to propose a new strategy for a corrected chemotherapy dosing.

In 1883, it was discovered that small animals utilise relatively more oxygen and produce relatively more heat than larger animals. These findings could be explained because smaller animals have relatively larger surface areas per unit mass, when compared with larger animals. These observations were confirmed and applied to humans, giving rise to the practice of expressing human basal metabolism in terms of body surface area (BSA) rather than BW (Pinkel, 1958).

Initially, BSA was recommended in dosage calculations for intravenous fluids, electrolytes, drugs and blood replacement needs in children, as it gave better outcomes than dosing based on BW or age. Then, prompted by publications by Pinkel (Pinkel, 1958) and Freireich et al. (Freireich et al., 1966), recommending the use of BSA to extrapolate chemotherapy doses from animals to human phase I studies and for the dosing of patients, many paediatricians started using BSA for anti-cancer drug dosing, and they were followed by medical oncologists (Pinkel, 1998). In fact, correlations between blood volume and BSA were observed, and in the 1940s-1950s relationships were found between BSA and the total amount of circulating plasma proteins. The relationship between BSA and renal function was also considered, as the total number of glomeruli and kidney weight were found to be proportional to BSA for various mammals, and the ratio of kidney weight to BSA were similar for rat, dog, and man. The Addis urea excretion rate (used as a measure of renal function) was in turn proportional

to kidney weight, and consequently it was considered that there was a relationship between renal function and BSA (Pinkel, 1958).

Body surface area is a measurement that is extremely difficult to reproduce. Several different formulae for predicting surface area from measurements of height and weight have been derived. In 1916, Du Bois and Du Bois examined nine individuals of varying age, shape, and size and measured their BSA directly using moulds. From these measurements, they derived a formula to estimate BSA using height and weight alone (DuBois and DuBois, 1916):

$$BSA\ (m^2) = 0.007184 * (\text{height (cm)}^{0.725} * \text{weight (kg)}^{0.425})$$

Although the Du Bois formula was determined on only nine individuals and certain assumptions were made in developing the formula (e.g. Du Bois and Du Bois only measured one leg and one arm, assuming the body to be symmetrical (Jones et al., 1985)), it has prevailed from other proposed formula and it is the most popular one for BSA calculation in current use. Anyway, many limitations have been pointed out in the use of BSA dose individualization. Except for the inherent inaccuracies in methods for BSA calculation (Du Bois and Du Bois estimated the maximal error as ±5% (DuBois and DuBois, 1916)), there is a substantial risk of arithmetical errors. In fact, mistakes in the use of dosage equations have been found to account for more than 15% of medication prescribing errors (Lesar, 1998). On the one side, the patient's BSA calculation is dependent on the accuracy of weight and height measurements. For many cancer patients, body size will probably vary during the course of the disease, due to conditions such as cachexia and anorexia. Despite this, BSA is not always re-calculated between treatment cycles, although there are recommendations that BSA should be re-calculated when BW has changed by more than 5-10%. On the other side, in clinical practice, the calculated cytotoxic drug doses are also frequently manipulated by rounding to the nearest convenient dose (Kaestner and Sewell, 2007). Furthermore, given the complexity of drug clearance, drug-related toxicity and anti-tumour activity, it is unlikely that only one factor such as BSA can be used to adjust the dosage. Moreover, once a specific dose is determined for a specific patients' population, this does not necessary mean that this dose will be the best dose for each individual patient even if calculated in respect of BSA.

Another important point to highlight regarding the anticancer dosage is that toxicity is commonly regarded as the most important effect to control, partly because it is easier to measure, but the risk of under-dosing and reduced efficacy must also be considered. In clinical practice it is more common to reduce doses, increase dose intervals, or skip courses in response to adverse effects than to increase the dose intensity in cases where treatment is well tolerated and there is no significant toxicity. This approach may reduce the severity of toxic effects, but it could also result in a suboptimal therapeutic effect (Kaestner and Sewell, 2007). For all these reasons, in order to overcome the BSA approach and to optimize the dose, the recent progresses in the cancer field introduced the concept of *personalized therapy* with the aim of tailoring medical treatment to the individual characteristics and needs of the single patient.

1.3.2 Beyond the BSA-based dose: the genomic era

Many parameters are responsible for the different responses observed in patients with the same diagnosis and treated with the same drugs, such as age, gender, comorbidities, dietary factors, lifestyle, and molecular background (Figure 9).

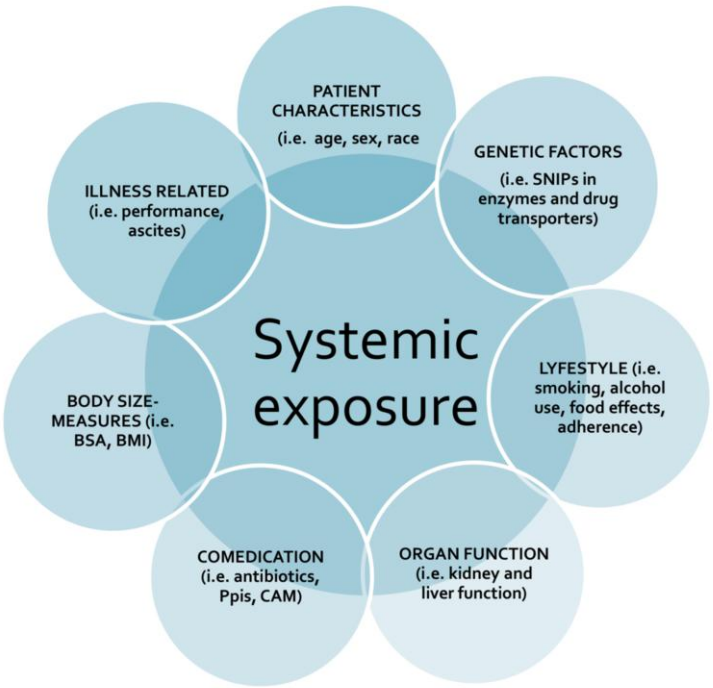

Figure 9 Schematic summary of the main factors that can influence the systemic exposure to a drug. BMI: body-mass index; CAM: complementary and alternative medicine; PPI: proton-pump inhibitor; SNPs: single-nucleotide polymorphisms. Adapted from (Mathijssen et al., 2014).

The resulting marked interpatient variability caused by all these factors is not considered by the current used BSA-dosing approach that results insufficient for adequately dosing cytotoxic drugs (Mathijssen et al., 2014).

This has led clinicians and researchers to change the way to conceive patients, highlighting the uniqueness of each clinical case, and paved the way to the so called era of *personalized (or precision) medicine*. The goal of personalized medicine is to streamline clinical decision-making by distinguishing in advance those patients most likely to benefit from a given treatment from those who will suffer side effects and incur costs without gaining benefit.

As reported by FDA (FDA, 2013b), many definitions of personalized therapy have been proposed and coined. In particular, we can mention these ones:

- "*The use of new methods of molecular analysis to better manage a patient's disease or predisposition to disease*" (Personalized Medicine Coalition)
- "*Providing the right treatment to the right patient, at the right dose at the right time*" (European Union)
- "*The tailoring of medical treatment to the individual characteristics of each patient*" (President's Council of Advisors on Science and Technology)
- "*Health care that is informed by each person's unique clinical, genetic, and environmental information*" (American Medical Association)
- "*A form of medicine that uses information about a person's genes, proteins, and environment to prevent, diagnose, and treat disease*" (National Cancer Institute, NIH)

From these definitions it is clear that heavy importance is given to the individual peculiarity in terms of clinical-, genetic-, and environmental information, factors that can impact disease prevention, diagnosis and treatment.

The concept of personalized medicine dates back many hundreds of years, but only now the possibility to sequence the entire genome and the enormous evolution in computational biology and other medical areas, have created the possibility for scientists to transform the personalized medicine from an idea to a practice. Indeed, personalized oncology is actually mainly based on the effect of genetic (germline and

somatic) differences among individuals on the response of cancer patients to chemotherapy.

These genetic variations led to the definition of biomarkers, generally described as "any substance, structure, or process that can be measured in the body or its products and influence or predict the incidence of outcome or disease" (Strimbu and Tavel, 2010). To date, the labelling (drug labelling is intended to provide a summary of the essential scientific information needed for the safe and effective use of the drug) of more than 100 approved drugs contains information on genomic biomarkers (including gene variants, functional deficiencies, expression changes, chromosomal abnormalities, and others) (www.fda.gov). Some, but not all, of the labelling include specific actions to be taken based on genetic information. Moreover, among the new drugs approved by the FDA since 2011, approximately one-third included in the submission some types of genetic or other biomarker data to characterize efficacy, safety, or PK. Data from the last few years indicate that more and more drugs are being designed for small populations, a trend that is consistent with the increasing use of stratification in drug development (FDA, 2013b).

On the one side, genomic and proteomic technologies have made possible to subclassify different kinds of solid tumours according to differences in gene sequence and/or expression patterns, thus leading to the development of new personalized drugs (Figure 10).

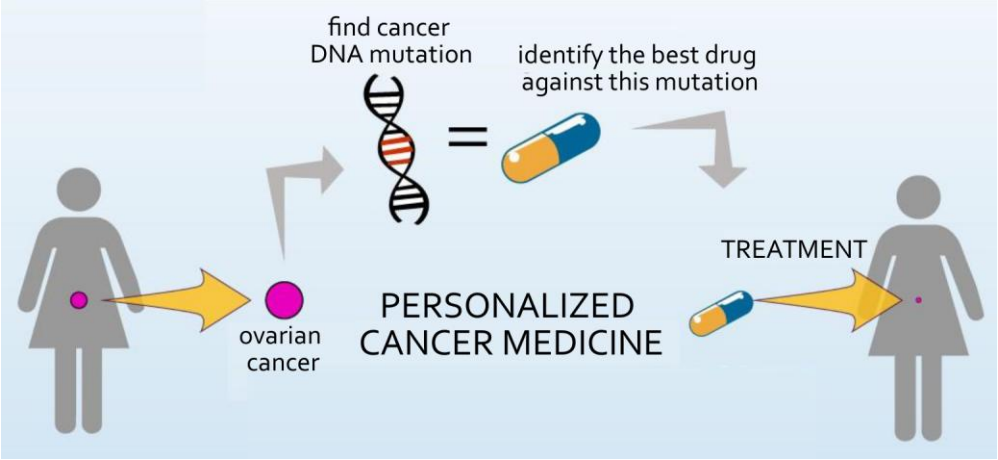

Figure 10 Using the genetic changes in a patient's tumour to determine their treatment is known as personalized medicine (www.cancer.gov).

For instance, the development of imatinib against chronic myelocytic leukemia (CML) is the greatest success in the personalized cancer field so far (Gravitz, 2014). In CML, a single molecular event, the 9:22 translocation, leads to expression of the Abelson proto-oncogene kinase ABL fused to BCR (breakpoint cluster region), yielding a constitutively activated protein kinase, BCR-ABL, and then the malignant phenotype. Imatinib attacks the unique and specific protein obtained with the BCR-ABL translocation, inducing clinical and molecular remissions in >90% of CML patients in the chronic phase of disease (Gharwan and Groninger, 2015).

On the other side, genetic information can be used to explain interindividual differences in drug ADME (PK) and physiological drug response (pharmacodynamics-PD), identifying responders and non-responders to a drug, and predicting its efficacy and/or toxicity (FDA, 2013b) (Figure 11). This research field, called pharmacogenetics (PGx), arises from the convergence of advances in pharmacology (the science of drugs) and genetics (the study of genes and their functions).

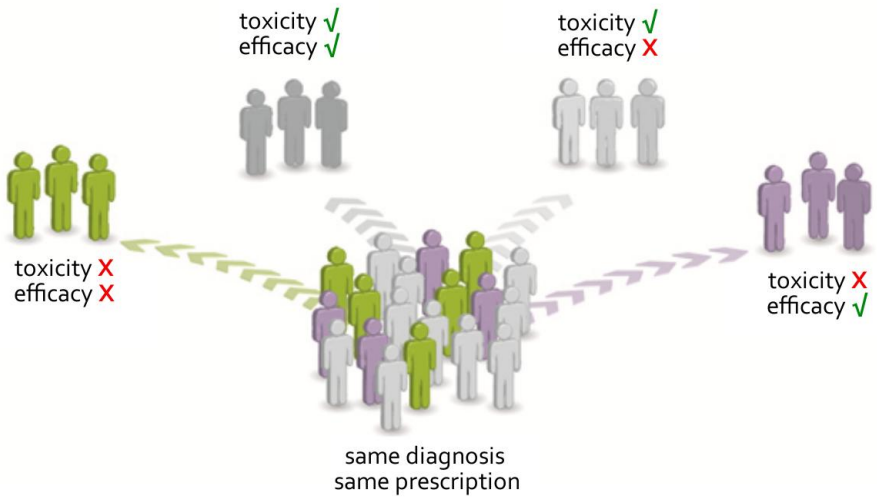

Figure 11 Genetic information can be used to explain interindividual differences in drug PK and physiological drug response, identifying responders and non-responders to a drug, and predicting its efficacy and/or toxicity.

Despite the extraordinary advances that have been made till now, we have a long way to go in understanding why different individuals respond differently to treatments. The issue is of such importance that in January 2015, the American President Barack Obama launched a national Precision Medicine Initiative, founding it with 215 million dollars,

aiming at promoting the introduction of personalized medicine concepts into the clinical practice, with a special focus on oncology and genetics (Schork, 2015).

1.3.3 Personalized chemotherapy: pharmacogenetics and phase I clinical trials

PGx, the study of those DNA and RNA mutations related to drug response, is one of the most exciting areas of personalized medicine today. As reported above, patients typically have variability in response to many drugs that are currently available. PGx tries to understand how genetic mutations affect the body's response to medications, in order to predict who will benefit from a medication, who will not respond at all, and who will experience adverse effects (FDA, 2013b).

Physiological variations within the human genome have a frequency of about 1 every 500±1000 bases. These cause the interindividual variability that is observed also in drug response and are the object of PGx. Although there are a huge number of different types of polymorphic markers, over the last years, the scientific community has focused on single-nucleotide polymorphisms (SNPs), and on the potentiality they offer in determining the individual drug response profile. Conventionally, a SNP is defined as a nucleotide variation having an allele frequency greater than 1%, whereas, when the frequency is lower, the genetic variation is indicated as mutation or as rare variant (Chakravarti, 2001).

On the one hand, predictive PGx biomarkers are usually SNPs located in genes that are direct targets of drugs, such as molecules involved in DNA repair or in drug metabolism, and are specifically associated with the response to a therapy, that can be defined as the probability to have a response or as the risk to develop toxicities. Prognostic PGx biomarkers, on the other hand, predict the natural course of a specific disease and patients' outcome (Sawyers, 2008). Examples of prognostic oncology markers are SNPs located in proteins involved in tumour cell proliferation, dedifferentiation, angiogenesis, invasion or metastasis.

As discussed in the previous section, using SNPs as predictive and prognostic biomarkers, it may possible to tailor drug prescription and dosage, moving from "one

dose fits all" model to the introduction of the "personalized medicine" model (Figure 12) (Duffy et al., 2011) (Patel, 2014) (Shankaran et al., 2008).

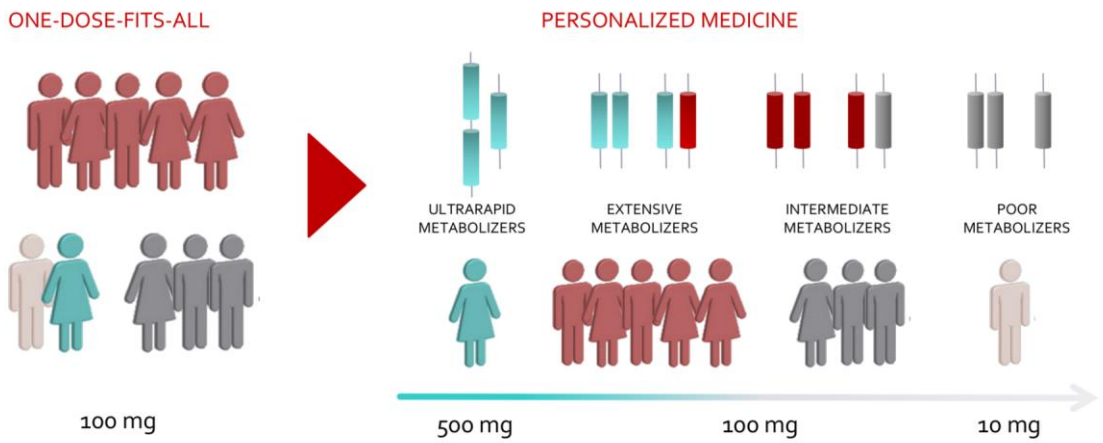

Figure 12 Representation of the "one-dose-fits-all" approach versus personalized medicine. The left panel shows a situation in which everyone gets the same dose of a drug. The right panel shows a personalized medicine approach in which the drug dose is selected on the basis of specific characteristics of the patients (FDA, 2013b).

Furthermore, the introduction of predictive and prognostic biomarkers in the clinical practice enables to enhance patients' quality of life and to decrease overall health care costs (Huang and Ratain, 2009).

PGx allows, on the basis of genotype analysis, the "stratification" of patients with a particular disease into subgroups as who respond more frequently to a particular drug or, alternatively, who are at decreased risk of side effects in response to a certain treatment (Patel, 2014).

This possibility could be used as a new strategy for phase I clinical trials, in order to select a study population in which the assessment of a drug dose is more efficient, in term of both efficacy and toxicity, than it would be in an unselected population (Carden et al., 2010) (Hollingsworth and Biankin, 2015). In fact, the feasibility of incorporating genotype into early phase clinical trials could really improve the optimization of the MTD, thereby enhancing clinical efficacy. Moreover, selecting patients by genetic biomarkers is becoming a common practice to reduce the size of trials and achieve end points faster and at a lower cost (Innocenti et al., 2014) (FDA, 2013b).

In fact, many drugs under development never reach the stage of being submitted to FDA (Food and Drug Administration) in an application requesting approval for

marketing. High attrition rates indeed stem largely from failure of drugs to meet expected efficacy levels, to demonstrate improved outcomes over a comparator drug, or to demonstrate sufficient safety to justify their use (FDA, 2013b). This problem is particularly huge for the newer molecular-targeted treatments. Although it has been suggested that targeted agents might have more successful development rates than conventional cytotoxic chemotherapies, attrition rates are still unacceptably high (Walker and Newell, 2009). Only 1 in 20 cancer drugs entering clinical trials gains regulatory approval: of the agents tested at each stage, 70% fail at Phase II, 59% fail at Phase III and 30% fail at the registration stage (Carden et al., 2010). The major causes for failure are inadequate therapeutic activity (30%) and toxicity (30%) (Kola and Landis, 2004). Moreover, the cost of developing an anticancer drug are typically US$ 700–1700 million, amount that are strongly influenced by the high rate of failure of evaluated agents and the length of time the process typically takes (eight to ten years from discovery to registration) (DiMasi and Grabowski, 2007).

In this context of an inefficient drug development process, there is a clear scientific, ethical and financial imperative to improve phase I trial design.

For instance, it has been recently proposed to design phase I and phase II studies to redefine the dose or the treatment modalities with conventional cytotoxic drugs taking into account the newer pharmacogenetic knowledge: the so called *genotype-guided phase Ib clinical trials* (Toffoli et al., 2010) (Marcuello et al., 2011) (Innocenti et al., 2014) (Lu et al., 2015). These genotype-based phase I studies, indeed, require the patients stratification on the basis of patient's genetic profile in order to find the MTD accordingly. Thus, these studies are intended to produce not one optimal dose for the unselected population, but different dose levels for different patient's genetic profiles, as required by the personalized approach (Figure 12).

The genotype-guided phase I trials are not widespread. At the best of our knowledge, only four published papers report this kind of approach, and all aimed at redefining the optimal dose of CPT-11 according to *UGT1A1* genotype (more details about it will be provided in following sections) (Toffoli et al., 2010) (Marcuello et al., 2011) (Innocenti et al., 2014) (Lu et al., 2015). The fundamental principle in order to design a phase I trial genotype-guided is indeed a strong pharmacogenetic rationale. Surely, one barrier to genotype-guided phase I studies implementation is the lack of freely available, peer-

reviewed, updatable, and detailed information about PGx biomarkers to be introduced in drug guidelines. Moreover, despite traditional chemotherapeutic agents still represent the core of cancer treatment, most of them have an "off-patent" status and pharmaceutical companies generally do not perform further profit research on these drugs.

For all these reasons, our group has developed, starting from a strong PGx background, several genotype-guided phase I clinical trials of traditional, off-patent, and extensively used against several solid tumours, cytotoxic drugs: PTX and CPT-11.

In order to obtain additional information about the drug's PK and its relationship with PD, particularly with toxicities, two LC-MS/MS methods have been developed and validated, according to FDA and EMA guidelines, for the drug quantification in human plasma samples.

1.3.3.1 Genotype-guided phase I study of irinotecan administered in combination with 5-fluorouracil/leucovorin (FOLFIRI) and bevacizumab in advanced colorectal cancer patients

The genotype-guided approach was applied to a phase I study, developed in our group, related to the administration of CPT-11 in combination with 5-fluorouracil/leucovorin (FOLFIRI) and bevacizumab in mCRC patients.

CRC is the third leading cause of cancer death in both men and women and the second leading cause of cancer death when men and women are combined. An estimated 49190 deaths from this malignancy are expected to occur in 2016. The 5- and 10-year relative survival rates for CRC are 65% and 58%, respectively. Although 5-year survival for localized disease is 90%, only 39% of patients are diagnosed at this stage, in part due to the underuse of screening (Cancer Facts and Figures, 2016).

5- FU and folinate calcium (leucovorin (LV)) have been the standard therapy against CRC until chemotherapy has improved with the introduction of several new cytotoxic and biologic agents in the therapeutic armamentarium. These agents include CPT-11 and newer monoclonal antibodies (e.g. bevacizumab and cetuximab) (Hegde et al., 2008).

Randomized trials have shown improvements in clinical efficacy as related to overall response rates (ORR), time to tumour progression (TTP), and median OS when CPT-11

has been added to either infusional (FOLFIRI) (Douillard et al., 2000) or bolus (IFL) (Saltz et al., 2001) of 5-FU and LV in the initial treatment of patients with mCRC. These two studies demonstrated, in terms of overall response and survival, the superiority of CPT-11 in combination with 5-FU/LV compared to 5-FU/LV or CPT-11 alone.

In 2007 FDA approved the bevacizumab (Avastin®) in combination with fluoropyrimidine-based chemotherapy for first-line treatment of patients with mCRC (Krämer and Lipp, 2007). Bevacizumab is a recombinant humanized monoclonal antibody that binds and neutralizes effects induced by human vascular endothelial growth factor (VEGF) (Presta et al., 1997) in cell proliferation and new blood vessel formation (angiogenesis process). The addition of bevacizumab (5 mg/kg every 2 weeks) as an intravenous infusion in combination with CPT-11 5-fluorouracil and leucovorin (FOLFIRI) has been found to increase the response rates from 34.8% to 44.8% and extend median OS from 15.6 months to 20.3 months. Moreover, this treatment prolonged the duration of response from a median of 6.2 months to 10.6 months as compared to FOLFIRI alone (Hurwitz et al., 2004). Although the improvements offered by the introduction of bevacizumab, a great inter-patient variability in both response and toxicity associated to CPT-11 treatment still remain the major concern.

In this context, our group has developed a phase I clinical study of CPT-11, in FOLFIRI regimen in combination with bevacizumab, guided by the advanced CRC patient's genotype. The principal aim of this study was indeed to apply the personalization approach to the clinical practice, addressing the role of PGx on the MTD of CPT-11, in combination therapy. Hence, this section will present the main aspects characterizing the pharmacology of CPT-11 and the rationale underlying our phase I study.

Irinotecan

CPT-11 is a camptothecin analogue. Camptothecins are potent, cytotoxic antineoplastic agents that target the nuclear enzyme topoisomerase I (TOP1). Camptothecin (CPT), the lead compound of this class, was first isolated from the bark of the Chinese tree, *Camptotheca acuminata* (Wall et al., 1966). Several aspects make the camptothecins pharmacologically unique. Indeed, TOP1 is their only target, as it has been shown using yeast cells, which become totally resistant to CPT when the TOP1 gene is removed

(Wall and Wani, 1995). Moreover, all camptothecins have a fused five-ring backbone that includes a labile lactone ring (at physiological pH): the hydroxyl group and S-conformation of the chiral centre in the lactone ring are required for biological activity (Brunton et al., 2011). The camptothecins bind to and stabilize the normally transient DNA-TOP1 cleavable complex, leading to the accumulation of single-stranded breaks in DNA. The collision of a DNA replication fork with this cleaved strand of DNA causes an irreversible double-strand DNA break, ultimately leading to cell death (Tsao et al., 1993). Since the cytotoxic activity of camptothecins depends on cellular cycle and is more pronounced during S phase, a sufficient exposure of tumour cells to drug concentrations above a minimum threshold is necessary for the implementation of the cytotoxic activity of these agents (Brunton et al., 2011) (Lorusso et al., 2010).

Camptothecin carboxylate was tested clinically in the mid-1970s and showed anticancer activity, but was discontinued because of its severe and unpredictable toxicity, principally myelosuppression and haemorrhagic cystitis (Muggia et al., 1972) (Moertel et al., 1972) (Schaeppi et al., 1974). After the discovery that TOP1 was the cellular target of this drug, more soluble and less toxic analogs of CPT, topotecan and CPT-11, were successfully developed. CPT-11 received accelerated approval by FDA in 1996 and the full approval in 1998 (www.accessdata.fda.gov) for the treatment of CRC. Nowadays it is one of the most active drugs in the first- and second-line treatment of this malignancy (Conti et al., 1996) (Saltz et al., 2001).

CPT-11 differs from topotecan in that it is a prodrug. In fact, it is activated by the enzyme carboxylesterase to 7-ethyl-10-hydroxycamptothecin (SN-38), that, compared with the parent drug, is 100- to 1000-times more cytotoxic (Newton et al., 2012) (Figure 13).

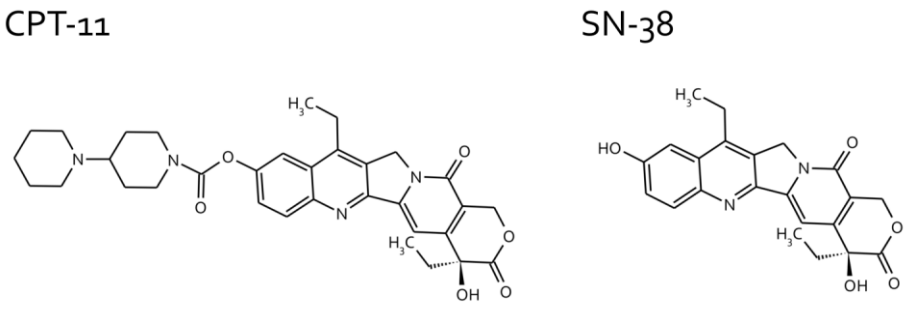

Figure 13 Chemical structures of the prodrug CPT-11 and its active metabolite SN-38.

Approved single-agent dosage schedules of CPT-11 in the U.S. include 125 mg/m^2 as a 90-min infusion administered weekly (on days 1, 8, 15, and 22) for 4 out of 6 weeks, and 350 mg/m^2 given every 3 weeks. In patients with advanced CRC, CPT-11 is used as first-line therapy in combination with fluoropyrimidines or as a single agent or in combination with cetuximab following failure of a 5-FU/oxaliplatin regimen (Brunton et al., 2011). The DLT with all dosing schedules is delayed diarrhoea, with or without neutropenia (Brunton et al., 2011). In the initial studies, indeed, up to 35% of patients experienced severe diarrhoea. The second most common CPT-11-associated toxicity is myelosuppression. Severe neutropenia occurs in 14-47% of the patients treated with the every-3-weeks schedule and is less frequently encountered among patients treated with the weekly schedule. Febrile neutropenia is observed in 3% of patients and may be fatal, particularly when associated with concomitant diarrhoea.

Irinotecan pharmacokinetics

Despite CPT-11 is present as two forms (lactone and carboxylate), monitoring of total (lactone and carboxylate forms) CPT-11, as well as total SN-38, has essentially the same clinical significance as the monitoring of lactone forms of the two agents, because the PK of total CPT-11 and total SN-38 are significantly correlated with those of lactone CPT-11 and lactone SN-38, respectively (www.accessdata.fda.gov). Most of the initial studies have been performed with the drug administered as a short i.v. infusion (0.5–1.5 h). After such administration, peak plasma concentrations were reached at the end of the infusion, with a rapid decrease thereafter as a result of multiple distribution and elimination pathways (Sparreboom et al., 1998) (Rivory et al., 1994) (Chabot et al., 1995) (Rivory et al., 1997). A rebound peak in the concentration-curve has been noticed in some studies (Abigerges et al., 1995) (Catimel et al., 1995) (Gupta et al., 1997) (Rivory et al., 1997) and it was initially ascribed to enterohepatic recirculation. More recently, it has been suggested that this phenomenon is related to substantial uptake of CPT-11 lactone by erythrocytes and its subsequent release, followed by accumulation of the carboxylate form in the plasma compartment (Loos et al., 1999). The peak concentration of CPT-11 appears to be dose-proportional in a large dose range (100–750 mg/m^2), although substantial interpatient variability has been noted (Canal et al., 1996) (Abigerges et al., 1995) (Rowinsky et al., 1994) (Catimel et al., 1995) (Rothenberg et al.,

1996). This variability seemed to increase at later time points (Mick et al., 1996). CPT-11 AUC also increases in a dose-dependent way at doses ranging from 33 to 180 mg/m^2 (Rothenberg et al., 1993) (Catimel et al., 1995) (Rothenberg et al., 1996) , indicating linear PK. CPT-11 and SN-38 have differential binding affinity for several plasma proteins: from 30% to 68% of CPT-11 is bound to plasma protein (predominantly albumin) while SN-38 is highly bound (approximately 95% bound) (Combes et al., 2000). The volume of distribution of CPT-11 is large, suggesting extensive tissue distribution, and remained unchanged with an increase in dose (Slatter et al., 2000) (Abigerges et al., 1995) (Rothenberg et al., 1993) (Gupta et al., 1997). Similarly, the total plasma clearance of CPT-11 was found to be dose-independent, with a value of 13.5 ± 3.5 L/h/m^2 (Chabot et al., 1995). The clearance is unaltered during repeated cycles, despite a mean interpatient variability of ~30% and an intra-patient variability of ~13.5% (Canal et al., 1996) (Chabot et al., 1995).

Irinotecan metabolism

As mentioned above, CPT-11 acts as a soluble prodrug of the biologically active form SN-38, generated in vivo from the parent drug through the cleavage of the ester-bond at C10 by liver carboxylesterase (Mathijssen et al., 2001). SN-38 AUC of is only 4% of the CPT-11 AUC, suggesting that only a relatively small fraction of the dose is ultimately converted to the active form of the drug ((www.accessdata.fda.gov). Moreover, SN-38 concentrations have been shown to increase with the CPT-11 dose over the dose range studied (100–750 mg/m^2) (Chabot et al., 1995).

After formation, SN-38 is further metabolized in human liver by conjugation with glucuronic acid to form the inactive SN-38 glucuronide (SN-38G) through an enzymatic reaction mediated by the UDP-glucuronosyl transferase 1A1 isoform (UGT1A1). Mostly, the plasma concentrations of SN-38G are related to SN-38 plasma concentrations, with peak values at ~1.2 h after the end of infusion (Gupta et al., 1997) (Kehrer et al., 2000).

Simultaneously, CPT-11 undergoes an oxidative degradation mediated by CYP3A4 to form the inactive 7-ethyl-10-(4-N-[5-aminopentanoic-acid]- 1-piperidino)-carbonyl-oxycamptothecin (APC) and 7-ethyl- 10-(4-amino-1-piperidino) carbonyloxy-camptothecine (NPC) metabolites. APC is the major metabolite detectable in plasma and it is formed by a CYP3A-mediated oxidation of the distal piperidine group at C10 of

CPT-11. NPC is also formed through this pathway, by cleavage of the distal piperidino group of CPT-11 (Lokiec et al., 1996) (Haaz et al., 1998) (Santos et al., 2000) (Figure 14). APC peaks at ~2 h after the end of infusion, and AUC values increase linearly with increasing CPT-11 dose, despite important interpatient variation (Rivory et al., 1997).
Biliary excretion appears to be the primary elimination route of the oxidation compounds (APC and NPC), the parent drug, and the SN-38 metabolite (Mathijssen et al., 2001).

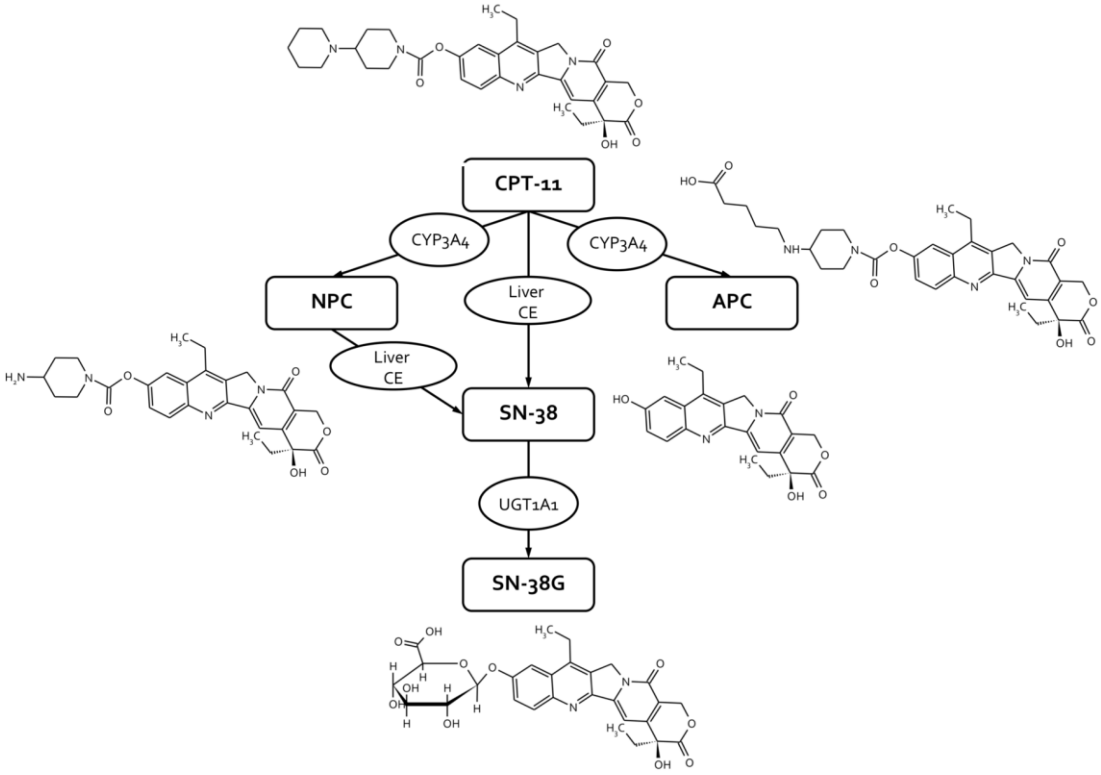

Figure 14 Metabolic pathways of CPT-11 showing carboxylesterase (CE)-mediated formation of the active metabolite SN-38 and its subsequent conversion to SN-38G by UGT1A1. CPT-11 can also undergo CYP3A4-mediated oxidative metabolism to form APC and NPC, of which the latter can be hydrolyzed by CE to release SN-38.

Rationale of the phase I study

Despite the improvements offered by the introduction of bevacizumab, a great inter-patient variability in both response and toxicity associated to CPT-11 treatment still remain the major concern. This could be related to differential plasma levels of the active metabolite SN-38 (Mathijssen et al., 2001) among patients. Several factors can affect SN-38 plasma levels, such as the activation of CPT-11 to SN-38 by

carboxylesterase enzymes or glucuronidation of SN-38 to the inactive SN-38G by UGT1A1.

In particular, the PGx research mainly focused on the UGT1A family, responsible for conjugation of the active SN-38 to inactive SN-38G. Among the most studied SNPs within these genes, *UGT1A1*28* (rs81753479) SNP is surely one of the most well-known. The *UGT1A1*28* allele is characterized by seven thymine-adenine (TA) repeats within the promoter region, as opposed to six that characterizes the wild-type allele (*UGT1A1*1*). These extra repeats impair proper gene transcription, resulting in decreased gene expression by approximately 70% (Tukey et al., 2002) (Bosma et al., 1995). This SNP is thought to be associated with a reduced glucuronidation of SN-38 compared with wild-type genotype, leading to variability in PK of SN38 (Ando et al., 2002) (Innocenti et al., 2004) (Iyer et al., 2002). Moreover, patients homozygous or heterozygous for the *UGT1A1*28* commonly develop dose limiting severe neutropenia and late diarrhoea and the current US package insert includes homozygosity of *UGT1A1*28* as a risk factor for severe neutropenia (www.fda.gov). Recently, a French joint working group comprising the National Pharmacogenetics Network (RNPGx) and the Group of Clinical Onco-pharmacology (GPCO-Unicancer) have published an itemized guideline for the use of *UGT1A1*28* genotype when prescribing CPT-11 (Etienne-Grimaldi et al., 2015) (Figure 15).

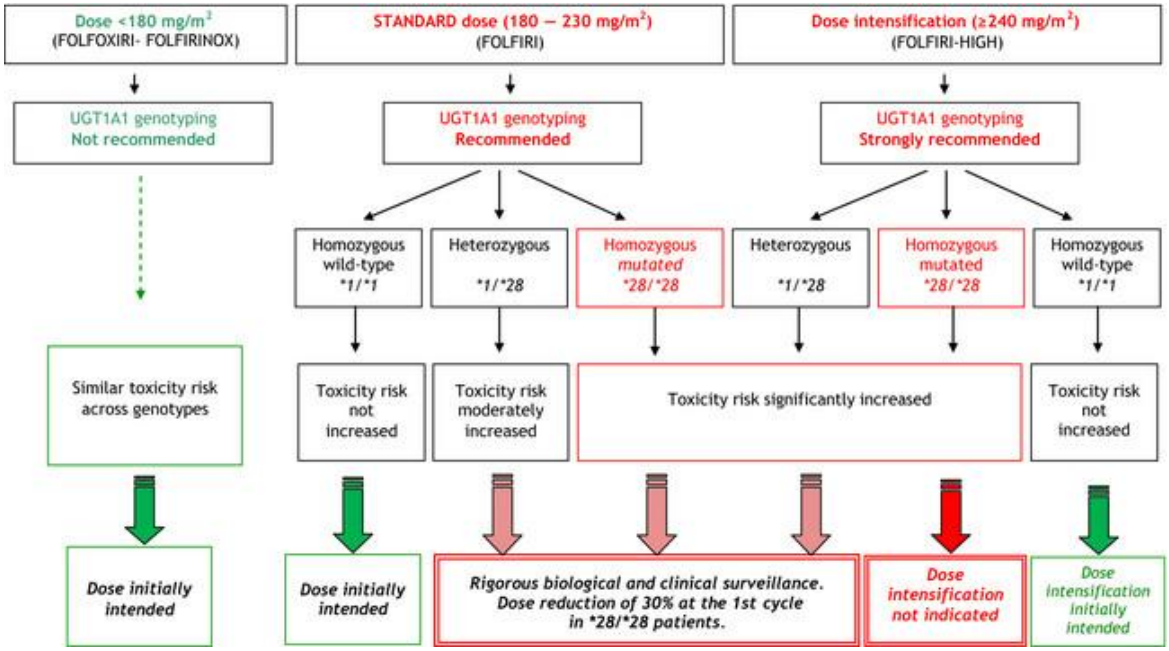

Figure 15 Scheme of the guidelines for the use of UGT1A1*28 genotype when prescribing CPT-11.

Thus, on the background of the CPT-11 PGx dosing guidelines described above, this drug is a perfect candidate for genotype-driven phase Ib studies.

Previously, our group performed a dose-finding study in mCRC patients treated with FOLFIRI regimen and with the *UGT1A1*1/*1* and *UGT1A1*1/*28* genotypes. By dose escalating CPT-11 only in patients without the high-risk *UGT1A1*28*/*28 genotype (10% on average in patients of European descent), they demonstrated that the recommended dose of 180 mg/m^2 for CPT-11 in FOLFIRI is considerably lower than the dose that can be tolerated by the non–*UGT1A1*28*/*28 patients. Specifically, patients with *UGT1A1**1/*1 genotype can safely be treated with dose of 370 mg/m^2, while the MTD for *UGT1A1**1/*28 was assessed at 310 mg/m^2 (Toffoli et al., 2010).

In early registration studies, where FOLFIRI was given with bevacizumab, the CPT-11 plasma concentrations were found similar to those observed in patients receiving FOLFIRI alone. However the concentrations of the active metabolite SN38 were 33% higher in patients receiving FOLFIRI plus bevacizumab as compared with FOLFIRI alone that can in part explain the higher incidence of NCI-CTC Grade 3-4 diarrhoea and neutropenia observed in the group of patients receiving FOLFIRI plus bevacizumab (McCormack and Keam, 2008) (Avastin® product information). This observation imposes caution to CPT-11 dose increment when administrated in combination with bevacizumab.

In this contest, our group proposed a phase I study to assess the recommended dose of CPT-11 according to *UGT1A1* genotype for FOLFIRI plus bevacizumab regimen in patients with mCRC with the intent of increasing the overall efficiency of the treatment.

1.3.3.2 Genotype-guided phase I study of irinotecan administered in combination with 5-fluorouracil/leucovorin (FOLFIRI) and cetuximab as first-line therapy in metastatic colorectal cancer patients

This genotype-guided phase I study was designed on the basis of the initial results obtained from the previous trial (Section 1.3.3.1). In fact, in a preliminary analysis of 22 patients, bevacizumab decreased the AUC of SN-38 ($p = 0.026$ by Wilcoxon matched pairs signed rank test), suggesting a role of this monoclonal antibody in the PK of CPT-11 (Manish, 2014). Hence, a following phase I study of CPT-11 administered in FOLFIRI regimen in combination with cetuximab was designed and approved, in order 1) to

define the CPT-11 MTD in this combination therapy according to *UGT1A1*28* genotype, and 2) to investigate the potential effect of this targeted agent on CPT-11 PK.

At present, cetuximab combined with FOLFIRI represents one of the most active therapeutic options for mCRC patients with EGFR+/K-RAS wild-type tumours. This is based on the results of a phase III trial (CRYSTAL trial), conducted as first-line treatment for mCRC, comparing cetuximab plus FOLFIRI with FOLFIRI alone, showed improved progression-free survival, and, in patients with K-RAS wild-type tumours, a particularly significant increase in response rates (59.3%) and metastasis resection rates (7.0% vs 3.7%) (Van Cutsem et al., 2009).

The role of K-RAS mutational status in predicting tumour responsiveness to cetuximab has been previously shown in studies aimed to compare the administration of cetuximab alone or in combination with CPT-11 to patients with mCRC that had progressed after previous treatment (Lièvre et al., 2008) (De Roock et al., 2008) (Karapetis et al., 2008). Thus, as data from multiple clinical trials of cetuximab in mCRC have demonstrated that patients whose tumours contain activating mutations in the *K-RAS* gene do not derive clinical benefit from antibody therapy, and have significantly shortened survival compared to patients whose tumour expresses wild-type *K-RAS* (Amado et al., 2008) (Lièvre et al., 2008), cetuximab use is limited to EGFR-positive *K-RAS* wild-type tumours.

The effect of cetuximab on the PK of high-dose of CPT-11 is also not known, although the non-overlapping pharmacology of both drugs is not suggestive of clinically-relevant drug-drug interactions at the level of drug disposition. Hence, we proposed to study the safety and PK of genotype-driven higher doses of CPT-11 in mCRC patients treated with FOLFIRI plus cetuximab.

Thus, this second study, as the previous reported, will define the recommended dose of CPT-11 according to *UGT1A1* genotype for FOLFIRI plus cetuximab regimen in patients with mCRC. The definition of MTD of CPT-11 (FOLFIRI) associated to cetuximab is essential to define the optimal CPT-11 dose for phase II-III studies in which CPT-11 dosage will be based on *UGT1A1* genotype.

1.3.3.3 Genotype-guided phase I study for weekly paclitaxel in ovarian cancer patients

The American Cancer Society estimates about 22280 new diagnoses of ovarian cancer and 14240 deaths for this cancer in the United States for 2016. Ovarian cancer ranks fifth in cancer deaths among women, accounting for more deaths than any other cancer of the female reproductive system.

Despite the fact that this cancer is highly treatable when caught early and confined to the ovary, less than one-fifth of cases are diagnosed while still in this early stage (American Cancer Society. Ovarian Cancer Detailed Guide). As a result, the 5- and 10-year relative survival rates for ovarian cancer patients are 46% and 35%, respectively. However, survival varies substantially by age; women younger than 65 are twice as likely to survive 5 years as women 65 and older (58% versus 28%). Overall, only 15% of cases are diagnosed at a local stage, for which 5-year survival is 92% (Cancer Facts and Figures, 2016).

To date, intensive surgical staging and cytoreduction, followed by first-line chemotherapy with the carboplatin-PTX regimen, are considered the gold standard for the management of this disease.

The weekly administration of PTX, the treatment applied in our phase I study, has been investigated as treatment of platinum resistant ovarian cancer by several groups, with reports suggesting that approximately 10-20% of patients will achieve an objective response to the regimen (Fennelly et al., 1997) (Markman et al., 2002) (Kita et al., 2004). The results of a phase I study conducted by Takano et al., in 2002 (Takano et al., 2002) showed that weekly PTX has a different toxicity profile than higher-dosed schedules with less neutropenia, alopecia and neurotoxicity.

In this context, our group has developed a third phase I clinical study of weekly PTX based on the ovarian cancer patient's genetic profile. The genotype-guided phase I study design and aim are the same reported for the previously described trial. Hence, this section will present the main aspects characterizing the pharmacology of PTX and the rationale underlying our phase I study.

Paclitaxel

PTX is a natural product isolated in 1971 from the bark of the Pacific Yew (*Taxus brevifolia*) (Wani et al., 1971). It belongs to taxanes, a very important class of anticancer agents available for clinical use since 1990s. It is approved for the treatment of several solid tumours, including ovarian (du Bois et al., 2003) (Parmar et al., 2003), breast (Sparano et al., 2008) (Sledge et al., 2003), non-small cell lung cancer (NSCLC) (Belani et al., 2005), and AIDS-related Kaposi Sarcoma (KS). It is administered in monotherapy or in association with other antineoplastic agents in several therapeutic schemes.

PTX is a microtubule-interfering agent. Microtubules are part of cytoskeleton -within the cell's cytoplasm - and are involved in numerous cellular functions, including the maintenance of cell shape, intracellular transport, secretion and neurotransmission. Microtubules are made up of polymers of tubulin, which, in their turn, are made up of a heterodimer consisting of α- and β-tubulin subunits. Microtubules are highly dynamic and unstable structures that are constantly incorporating free dimers and releasing dimers into the soluble tubulin pool (Figure 16).

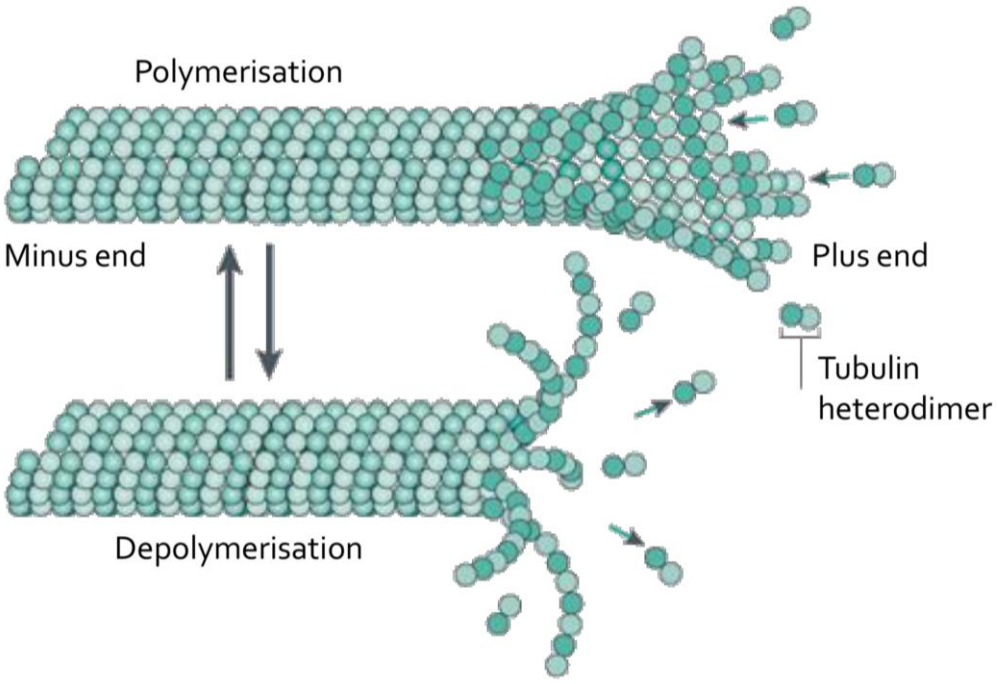

Figure 16 Microtubules dynamic instability (polymerization and depolymerization Interconversion). They are dynamic polymers that are assembled from tubulin heterodimers, which are organized such that the microtubules have an intrinsic polarity. Although microtubules exhibit dynamic instability at both ends of the microtubule, the plus ends are more dynamic than the minus ends. Adapted from (Walczak et al., 2010).

PTX binds to the β-tubulin subunit of the tubulin heterodimer, accelerate the polymerization of tubulin and stabilize the resultant microtubules inhibiting their depolymerization. This inhibition results in the arrest of the cell division cycle which triggers the cell signalling cascade, leading to apoptosis of cancer cells (Schiff and Horwitz, 1980) (Schiff and Horwitz, 1981).

PTX is insoluble in aqueous solution and it is therefore formulated in 50% ethanol and 50% cremophor-EL (a polyoxyethylated castor oil derivative that forms micelle) to improve its solubility (Gelderblom et al., 2001). This vehicle is responsible for increasing the risk of neuropathy and hypersensitive reactions in neoplastic patients (ten Tije et al., 2003). PTX is a substrate of P-glycoprotein (P-gp). Being P-gp expressed in the luminal side of plasma membrane of gut epithelial cells (Cordon-Cardo et al., 1990) (Thiebaut et al., 1987), the absorption in the gut of PTX is prevented (Helgason et al., 2006), explaining its low bioavailability (5-8%) and the necessity to administer it only intravenously. It is administered as a 3-h i.v. infusion of 135-175 mg/m^2 every 3 weeks or as a weekly 1-h i.v. infusion of 80-100 mg/m^2. The most concerning side effects of PTX are neutropenia and neuropathy. Many patients experience myalgias for several days. Mucositis is prominent in 72- or 96-h i.v. infusions and in weekly schedule. Hypersensitivity reactions occurred in patients receiving PTX infusions of 1 to 6 hours but have largely been averted by premedication (Brunton et al., 2011)

Paclitaxel pharmacokinetics

A substantial number of clinical pharmacokinetic studies with PTX have been performed and have shown a nonlinear pharmacokinetic behaviour. The elimination of PTX has been described by a three-phase elimination curve and by a non linear profile, particularly with shorter infusions (Huizing et al., 1997). Moreover, a disproportional increase in C_{max} and AUC at the increasing of the dose suggests the saturation of both elimination and distribution processes (where the saturable distribution has been described as saturable transport (Sonnichsen et al., 1994) or saturable binding (Karlsson et al., 1999)) at higher concentrations of PTX (Henningsson et al., 2001) (Mross et al., 2000) (Gianni et al., 1995). Several studies with PTX given as a 6-h i.v. infusion documented nonlinear PK with doses higher than 250 mg/m^2 (Brown et al., 1991) (Wiernik et al., 1987) (Grem et al., 1987), while others reported that a lower dose of 135

mg/m^2 is the critical threshold for non-linear kinetics (Ohtsu et al., 1995) (Panday et al., 1998). Similar findings were noted with 3-h i.v. infusion schedules in patients who received doses of 135 and 175 mg/m^2, (Gianni et al., 1995) (Ohtsu et al., 1995) (Ye et al., 2000).

Cremophor-EL has been proposed to augmented the nonlinear pharmacokinetic behaviour of PTX in plasma by trapping the drug in micelles (because the highly hydrophobic PTX favours partitioning in cremophor-EL micelles) and thereby making it less available for distribution to tissues, metabolism, and biliary excretion (Sparreboom et al., 1996) (Van Tellingen et al., 1999) (van Zuylen et al., 2001). It has been reported indeed that the volume of distribution for cremophor-EL is small (ten Tije et al., 2003), thereby indicating that its distribution is more or less limited to plasma. Additionally cremophor-EL itself shows nonlinear kinetics. Although in minor extent, other mechanisms by which cremophor-EL affects PTX PK are hemodynamic changes (Bowers et al., 1991) and alteration in P-gp function (Schuurhuis et al., 1990). In the blood stream, the protein binding is 95-98 % (Longnecker et al., 1987) (Wiernik et al., 1987). PTX binds α1-glycoprotein-acid and, in minor extent, albumin and lipoproteins (Kumar et al., 1993). Supporting extensive drug binding *in vivo*, total volumes of distribution have been reported as significantly variable, dependent from the dose/schedule and larger than that of total body water, ranging from 50 L/m^2 to over 650 L/m^2 (Brown et al., 1991) (Tamura et al., 1994) (Wiernik et al., 1987). In addition, PTX shows high distribution in specific tissue of organs as kidney, lung, spleen, and in third space fluids, including ascitic and pleural fluid (Wiernik et al., 1987), while it does not penetrate in tumour sanctuary tissues, including testicles and brain, and it is not present in cerebral spinal fluid (Glantz et al., 1995) (Lesser et al., 1995). PTX clearance is nonlinear and decreases with increasing dose or dose rate. It disappears from plasma with a half-life of 10-14 hours and a clearance ranging from 15 to 18 L/hr/m^2 (Brunton et al., 2011). The major route of elimination is biliary excretion (Monsarrat et al., 1993) (Walle et al., 1995), while renal excretion and other extrahepatic excretion mechanisms account for less than 10% of elimination (Longnecker et al., 1987) (Wiernik et al., 1987). The best model to predict the relationship between PTX plasma concentration and effects is the *threshold model*, in which the length of time that PTX concentration exceeds a threshold concentration is predictive of toxicity. In fact, it has been reported a

higher incidence of neutropenia and neuropathy in relation to how long the PTX plasma concentration exceeds 0.05 µmol/L (Gianni et al., 1995), 0.1 µmol/L (Huizing et al., 1993), or 0.197 µmol/L (Henningsson et al., 2001). In a subsequent study, the estimated threshold concentration of 0.05 µmol/L was found correlated with the development of peripheral neuropathy (Mielke et al., 2005b). Moreover, patients with progressive disease showed significantly lower times of PTX concentrations above 0.05 µmol/L (Mielke et al., 2005a). Finally, an exposure-response relation was found in chemotherapy-naive patients with advanced NSCLC receiving PTX and carboplatin, whereas PTX concentrations above 0.1 µmol/L for >15 hours were related to improve OS (Huizing et al., 1997).

Paclitaxel metabolism

The major human metabolite identified is 6α-hydroxypaclitaxel (6α-OH-PTX) and corresponds to a stereospecific hydroxylation at the 6-position on the taxane ring as determined by nuclear magnetic resonance (Harris et al., 1994). Moreover, multiple hydroxylated products were found in plasma, such as 3′-p-hydroxypaclitaxel, corresponding to an hydroxylation at the para-position on the phenyl ring at the C3'-position of the C13 side chain, and 6α,3′-p-dihydroxypaclitaxel (Figure 17) (Cresteil et al., 1994) (Monsarrat et al., 1997).

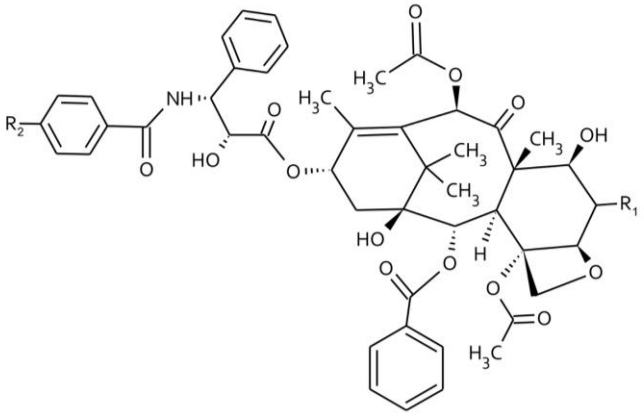

Compound	R_1	R_2
paclitaxel	H	H
6α-hydroxypaclitaxel	OH	H
3′-p-hydroxypaclitaxel	H	OH
6α,3′-p-dihydroxypaclitaxel	OH	OH

Figure 17 PTX and its main metabolites chemical structures.

Rahman et al. and more recently Henningsson et al. showed the role of cytochrome P450 2C8 (CYP2C8) in metabolism of PTX to 6α-OH-PTX (Henningsson, 2005) (Rahman et al., 1994). Cresteil et al. also showed that cytochrome P450 3A4 (CYP3A4) was responsible for the metabolism of PTX to 3'-p-hydroxypaclitaxel (Cresteil et al., 1994). 6α-OH-PTX is approximately 30 times less cytotoxic than PTX when tested against ovarian and CRC cell lines and, thus, the formation of 6α-OH-PTX is likely an important detoxification pathway (Harris et al., 1994).

Moreover, Kang et al. demonstrated that PTX cytotoxicity in HL60 and K562 human leukaemia cells had been increased in the presence of noncytotoxic concentrations of 6α-OH-PTX (Kang et al., 2001). Activity of 3'-p-hydroxypaclitaxel was, in contrast, reduced but not absent in ovarian cancer cell lines. All the three metabolites cited before retained bone marrow toxicity when tested on human bone marrow cells (Sparreboom et al., 1995).

Rationale of the phase I study

Understanding the mechanism underneath the interindividual differences observed in the PTX PK and the related pharmacodynamic profile (toxicity and tumour response), could make treatment individualization feasible.

As reported above, the systemic elimination of PTX involves CYP3A4 (that converts PTX to 3'-p-hydroxypaclitaxel) and CYP2C8 (that converts PTX to 6α-OH-PTX). Genes encoding these well-known metabolizing enzymes have been investigated in a large number of studies. The genetic variants *CYP2C8*3* (Gréen et al., 2009) (Bosó et al., 2014) (Hertz et al., 2012) (Leskelä et al., 2011) for PTX have shown predictive potential for haematological toxicity and neurotoxicity, although these positive associations could not be confirmed by other groups, as recently revised by Frederiks et al. (Frederiks et al., 2015).

CYP3A4 expression is known to be regulated by the pregnane/steroid X receptor (PXR), coded by the *NR1I2* gene. PXR is a well established regulator of many other genes including *CYP3A5*, *CYP2C8* and *ABCB1*. Polymorphisms in the *NR1I2* gene have been reported to modulate *CYP3A4* expression (He et al., 2006), although their clinical effect remains to be elucidated. A novel genetic polymorphism in *CYP3A4*, *CYP3A4*22*, has

been identified as possible risk factor for neurotoxicity in patients receiving a PTX-containing regimen (de Graan et al., 2013).

PTX is a substrate of P-gp; a reduced P-gp mediated transport from blood to intestine indeed would increase systemic drug exposure, affecting PTX PK. Thus, cancer cells with an ineffective P-gp efflux should be more sensitive to the drug. P-gp is encoded by the ATP Binding Cassette gene (*ABCB1*).

Among at least 50 common SNPs described in *ABCB1* gene in Caucasians, *2677G>T/A* (responsible for the substitution from alanine to serine or threonine) and *3435C>T* (responsible for the wobble effect on the glutamic acid) SNPs have been shown to correlate with the P-gp expression and phenotype. In particular, the *2677G>T/A* allele has demonstrated to impact PTX PK and PD in ovarian cancer patients (Hamidovic et al., 2010). Johnatty et al. (Johnatty et al., 2008) found a significant association between *ABCB1-2677G>T/A* and progression free survival in 309 patients from the Australian Ovarian Cancer Study treated with PTX/carboplatin. The SCOTROC1 trial failed to confirm this evidence in the entire group of 914 ovarian cancer patients treated with taxanes (Marsh et al., 2007), but in a selected subset of patients with optimal debulking, the significant association with progression free survival, was confirmed (Johnatty et al., 2008). An association of the SNP with higher risk of severe haematological and non-haematological toxicity was demonstrated in 118 ovarian cancer patients of Asian ethnicity treated with PTX and carboplatin (Kim et al., 2009).

The mechanism underneath the association of *ABCB1-2677G>T/A* with toxicity and efficacy seems related to an effect on the PK: the presence of the *2677T/A* genotype affects PTX clearance, that resulted lowered in patients carrying the variant allele (Green, 2008) (Wong et al., 2005). Moreover, a pilot study on 20 carboplatin/PTX treated ovarian cancer patients conducted by our group confirmed a lowered PTX clearance for patients carrying the variant *2677T/A* allele (unpublished data).

Based on this background, our group designed a genotype-guided phase I clinical trial of weekly PTX in order to define the MTD and DLTs according to the *ABCB1-2677G>T/A* SNP in epithelial ovarian cancer patients.

1.3.4 Personalized chemotherapy: therapeutic drug monitoring

Therapeutic drug monitoring (TDM), introduced in the clinical care from the early 1960s, involves the measurement and interpretation of drug concentrations in biological fluids in order to individualize the drug dosages or schedules thus maximizing the therapeutic outcomes and/or minimizing toxicities (Alnaim, 2007).

In theory, a drug should fulfil several criteria in order to apply the TDM approach (Sanavio and Krol, 2015):

- presence of considerable inter- or intra-individual variability in PK;
- existence of a defined and ascertainable relationship between concentration and pharmacological effects;
- narrow therapeutic window;
- absence of a simple accessible parameter to evaluate clinical efficacy;
- availability of a defined and accurate method for drug quantification in biological fluids.

TDM is broadly applied to drugs from different therapeutic classes, such as cardiovascular agents, antiepileptics, antibiotics, respiratory smooth muscle relaxants, anti-inflammatory agents, immunosuppressants, and antidepressants (Bardin et al., 2014). Anticancer drugs also fit many of the criteria commonly defined as prerequisites for utilizing TDM approaches. Firstly, the extent of inter-individual pharmacokinetic variability exhibited is large in the majority of cases, with coefficients of clearance variation of more than 50%. Variability in PK leads also to plasma concentration fluctuation that may vary over 10-fold range when fixed doses of chemotherapeutic agents are administered (Bardin et al., 2014). Secondly, relationships have been described between drug plasma concentrations and PD end-points such as percentage decrease in neutrophil counts between pretreatment and nadir values (Paci et al., 2014). Moreover, TDM in cancer chemotherapy has additional advantages like enhancement of compliance, dose adjustment in patients with hepatic and renal dysfunction, and detection of drug interactions (Reynolds and Aronson, 1993). Furthermore, adjusting the drug dose on the basis of its plasma concentration potentially allow to take in

consideration simultaneously all the individual factors that affect the systemic exposure (Figure 9) in order to minimize the pharmacokinetic variability among patients.

Despite the potential benefits deriving from the application of TDM in cancer chemotherapy, the clinical value of TDM for antineoplastic agents still remains restricted by several factors (Alnaim, 2007). First of all, there is naturally a long lag time between the measurement of drug in plasma and evaluation of the definitive pharmacodynamic effect, which is, usually, cure. If improvement in cure rate is used as the outcome variable, this usually requires at least 5 years of follow-up to dependably evaluate the outcome. Consequently, studies require more time and more complex process than that of studies for drugs with quicker effects, such as antibiotics.

Furthermore, the identification of the concentration–effect relationships results complicated since antineoplastic agents are almost always given in combination (Chatelut et al., 2000), condition that renders very difficult to accurately define the PK of each individual agent. In addition, combination therapy also complicates the PK of drug toxicity.

Another limitation in implementing TDM in clinical practice is due to the heterogeneous feature of cancer, with inherent characteristics that affect the concentration–effect relationship for antineoplastic agents. They display heterogeneity in blood supply and cellular characteristics, leading to different levels of sensitivity and resistance to antineoplastic agents (Pignon et al., 1994).

Lastly, sensitive, precise and reproducible assays available for the clinical use are required in order to implement TDM use in daily practice. Equally, the implementation of the analytical assays for a rapid and sensitive quantification of drugs in human plasma could enhance the effort in order to better and more extensively define the concentration–effect relationship with antineoplastic agents.

1.3.4.1 Therapeutic drug monitoring: the case of sunitinib

Despite targeted therapies are now revolutionizing cancer treatment by transforming some previously deadly malignancies into chronically manageable conditions, poor tolerability and therapeutic failure are not uncommon, and relapse is a nearly inevitable consequence of treatment interruption (Widmer et al., 2014). In addition, oral administration of these drugs is, on the one side, associated with a better quality of life

but, on the other side, also generates a complex step in the PK of these drugs. Thus, standard dosage regimens rarely result in comparable circulating concentrations of the active drug in all patients, possibly favouring the selection of resistant cellular clones (in case of sub-therapeutic drug exposure) or the development of undesirable toxicity (in case of overexposure) (Gao et al., 2012).

Moreover, retrospective studies have shown that targeted drug exposure, reflected in the AUC, correlates with treatment response (efficacy/toxicity) in various cancers (Widmer et al., 2014).

Surely, these characteristics render the targeted therapies suitable for TDM. In particular, this section will take in consideration the case of sunitinib.

Sunitinib

Sunitinib (SUTENT) is an oral multi-targeted tyrosine kinase inhibitor. It competitively inhibits the binding of ATP to the tyrosine kinase domain on the VEGF receptor-2, which mediates the majority of the downstream effects of VEGF-A, including vascular permeability, endothelial cell proliferation, invasion, migration, and survival (Dvorak, 2002). This inhibitor is a low molecular-weight, ATP-mimetic agent that binds to the ATP-binding catalytic site of the tyrosine kinase domain of VEGFR, resulting in a blockade of intracellular signalling. It has both direct antiproliferative effects and antiangiogenic properties. Sunitinib also inhibits other protein tyrosine kinases (FLT3, PDGFR-α, PDGFR-β, RET, CSF-1R, and c-KIT) at concentrations of 5-100 nM (Fabian et al., 2005). It has activity in metastatic renal-cell cancer (mRCC), producing a higher response rate (31%) and a longer progression-free survival than any other approved anti-angiogenic drug (Motzer et al., 2007). Sunitinib is also approved for treatment of gastrointestinal stromal tumour (GIST) that has developed resistance to imatinib as a consequence of c-KIT mutations (Heinrich et al., 2008). Sunitinib is administered orally in doses of 50 mg once a day. The typical cycle of sunitinib is 4 weeks on treatment followed by 2 weeks off treatment. The dosage and schedule of sunitinib can be increased or decreased according to toxicity (hypertension, fatigue). Dosages <25 mg/day typically are ineffective (Brunton et al., 2011).

Sunitinib is primarily metabolized by CYP3A4 to an equipotent N-desethyl metabolite (N-desethyl sunitinib) (Sakamoto, 2004) (Figure 18).

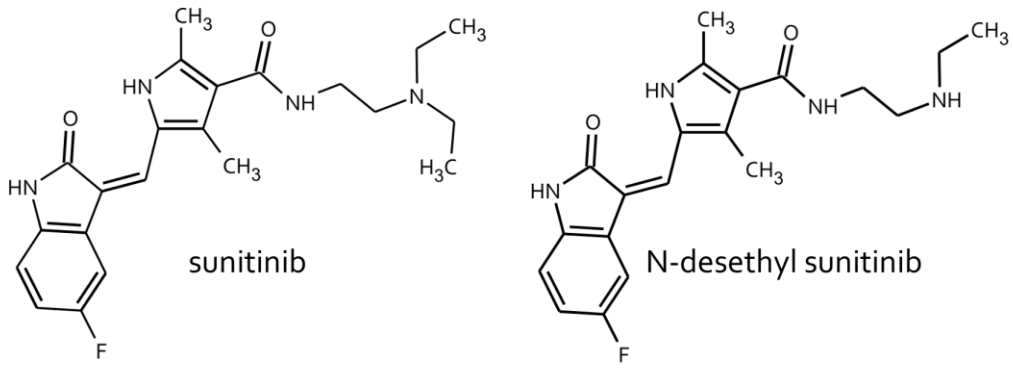

Figure 18 Chemical structures of sunitinib and its metabolite, N-desethyl sunitinib.

Protein binding of sunitinib and N-desethyl sunitinib is 95% and 90%, respectively. AUC and C_{max} are increasing proportionally with increasing dose within a range of 25–100 mg and are not affected by food. Maximum plasma concentrations of sunitinib are reached between 6 and 12 h and the terminal half-lives of sunitinib and N-desethyl sunitinib are 40–60 h and 80–110 h, respectively (Le Tourneau et al., 2007) (Goodman et al., 2007) (Mendel et al., 2003).

Recent studies suggested sunitinib as a candidate for a TDM program. In fact, increased exposure to sunitinib in patients with advanced solid tumours is associated with improved clinical outcomes (longer time to tumour progression, longer overall survival, a higher probability of a response and greater tumour-size decreases), as well as some increased risks of adverse effects (incidence of fatigue, increase of diastolic blood pressure, decrease of absolute neutrophil count) (Houk et al., 2009). Additionally, a recent retrospective analysis of 521 patients with mRCC has shown that plasma concentration might be better correlated to PFS than to the administered dose of drug (Khosravan, 2012). Thus, based on preclinical data (Houk et al., 2010) and on a phase I study (Faivre, 2006), a target plasma concentration of sunitinib and active metabolite in the range of 50–100 ng/mL has been suggested.

The analytical issue

Despite this information, in order to introduce the TDM of sunitinib in the clinical practice it is necessary also to have a rapid, specific, sensitive and reproducible analitycal method. One of the most challenging peculiarities of sunitinib for the setup of an analytical method is represented by its isomerization in presence of light. In fact,

sunitinib and N-desethyl sunitinib are 5-fluoro-2-oxindoles attached to a dimethyl pyrrole carboxamide by an exocyclic double bond prone to showing light-induced Z/E-isomerism (Figure 19).

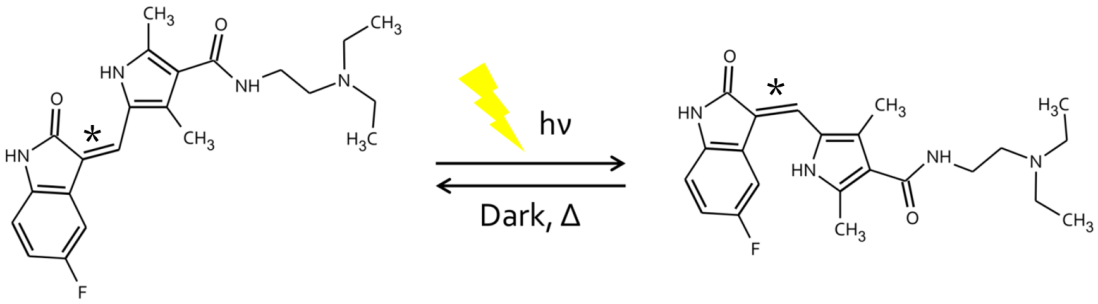

Figure 19 Z/E-isomerism of sunitinib. The symbol * indicates the double bond that undergoes isomerization.

Similar photo induced isomerism of molecules with double bonds has been reported in literature and have shown to result in the formation of the less stable isomer (Whitesides et al., 1969) (Zhang et al., 2001). In this case, the predominance of Z-isomer results from an intramolecular hydrogen bond between the C-2 carbonyl oxygen atom of the indolin-2-one ring and the proton of the pyrrole NH-group (Rodamer et al., 2011). The group of Sistla studied the isomerization of a precursor of sunitinib, semaxanib, and, in order to determine the reversion kinetics, they exposed an analytical solution of this drug to light for 23 hours to attain equilibrium between the two Z and E isomers. This solution was then protected from light at different temperatures to study the E- to Z-isomer conversion. The E-isomer was observed to revert to the Z-isomer following storage in the dark with an increase in the reconversion rate at higher temperatures. This observation indicates that the reversion of E- to Z- isomer is a thermal reversion (Sistla and Shenoy, 2005). Their infusate studies indicated also that <2% E-isomer will be dosed to patients and would likely convert to the Z-isomer, following administration. This report implies no limitations towards ensuring pharmaceutical product quality. Anyway, special attention must be paid to both isomers during any patient's plasma analysis steps, from the collection to the samples treatment and analysis.

In this context, a LC-MS/MS method has been developed, particularly taking into account the isomerisation issue, and validated in order to set up a simple, rapid and sensitive analytical assay for the application of TDM in the sunitinib-based therapy.

2 AIMS

The great inter-patient variability in the PK and PD of the anticancer drugs and their low therapeutic index dramatically complicate the dosing of these drugs, leading to a significant variability in both therapeutic and toxic effects. Moreover, the traditional method based on the measurement of the BSA does not account for the complex processes of anticancer drug metabolism and elimination and, over the years, the need for a new dosing approach has become increasingly evident.

The recent progresses in the research field against cancer introduced the concept of personalized therapy with the aim of tailoring medical treatment to the individual characteristics and needs of the single patient. In particular, the giant steps made in the PGx field paved the way for a tailoring therapy leading to personalize the anticancer drugs dose on the basis of the patient genotype. However, for drugs such as targeted anti-cancer agents, which are only recently introduced in the clinical practice, no PGx biomarkers are known up-to-date for dosage optimization. Thus, in these cases there is the necessity to apply other methods to personalize the therapy, such as the TDM.

On the one hand, the object of this PhD project has been the redefinition of the MTD of two conventional and widely used anticancer drugs, CPT-11 and PTX, on the basis of patient's genotype, in order to move from "one dose fits all" model to the "personalized medicine" approach. For this reason, innovative *genotype-guided phase I clinical studies* have been designed using PGx biomarkers for patients stratification.

On the other hand, additional purpose of this thesis has been the development of different LC-MS/MS methods for the quantification of both the two cytotoxic drugs cited before and sunitinib, one of the most important targeted anti-cancer agent. These methods were developed to quantify these drugs, along with their main metabolites, in human plasma samples in order to obtain the pharmacokinetic data related to the phase I studies for CPT-11 and PTX, and TDM for sunitinib. These methods have also been validated according to FDA-EMA guidelines, in order to assess the robustness of the methods and the reliability of the obtained data.

The specific aims of each clinical study are reported below:

Genotype-guided phase I study of irinotecan administered in combination with 5-fluorouracil/leucovorin (FOLFIRI) and bevacizumab in advanced colorectal cancer patients

The primary aim of this study was:

- to define the MTD and the DLTs of CPT-11 administered in the FOLFIRI regimen plus bevacizumab in mCRC patients according to *UGT1A1*28* genotype.

The secondary purposes of this trial were:

- to develop and validate a LC-MS/MS method for the quantification of CPT-11 and its main metabolites (SN-38, SN-38G, and APC) in human plasma samples;
- to evaluate the variability of CPT-11 PK in patients with **1/*1* and **1/*28* genotype and the effect of the PK on toxicity and response rate;
- to evaluate a possible effect of bevacizumab on CPT-11 PK.

Genotype-guided phase I study of irinotecan administered in combination with 5-fluorouracil/leucovorin (FOLFIRI) and cetuximab as first-line therapy in metastatic colorectal cancer patients

This second phase I study shares the same aims of the previous one, since it has been designed on the basis of the preliminary results obtained:

- to define the MTD and the DLTs of CPT-11, administered in the FOLFIRI regimen plus cetuximab in mCRC patients treated as first-line chemotherapy according to *UGT1A1*28* genotype;
- to evaluate the variability of CPT-11 PK in patients with **1/*1* and **1/*28* genotype and the effect of the PK on toxicity and response rate;
- to evaluate a possible effect of cetuximab on the CPT-11 PK.

Genotype-guided phase I study for weekly paclitaxel in ovarian cancer patients

The primary aim of this study was:

- to define the MTD and the DLTs of weekly PTX according to the *ABCB1-2677G>T/A* polymorphism in epithelial ovarian cancer patients;

Secondary aims of the study were:

- to develop and validate a LC-MS/MS method for the quantification of PTX and its main metabolite, 6α-OH-PTX, in human plasma samples;

- to evaluate the PK of PTX and its 6α-hydroxylated metabolite in human plasma and the correlation of PTX PK with the *ABCB1-2677G>T/A* different genotypes;
- to define the effect of PTX PK on toxicity and response rate.

3 MATERIALS AND METHODS

3.1 Phase I clinical trials

3.1.1 Genotype-guided phase I study of irinotecan administered in combination with 5-fluorouracil/leucovorin (FOLFIRI) and bevacizumab in advanced colorectal cancer patients

The protocol of this trial (EudraCT n. 2009-012227-28) has been revised and approved by the CRO ethical committee, the AIFA (Agenzia Italiana del Farmaco) and the ISS (Istituto Superiore di Sanità). It has been conducted in collaboration with University of Chicago Medical Center (IL, U.S.A) and San Filippo Neri Hospital of Rome (Italy) and the protocol was approved by the ethical committee of each participating site. All patients signed a written informed consent before entering the study. The main characteristics of this study are briefly described above.

3.1.1.1 Patients characteristics

The eligibility criteria for this study are:

- ✓ histologically or cytologically confirmed diagnosis of mCRC;
- ✓ no prior chemotherapy for metastatic disease;
- ✓ age ≥18 or ≤75 years;
- ✓ Eastern Cooperative Oncology Group (ECOG) performance status (PS) of 0 or 1;
- ✓ life expectancy > 3 months;
- ✓ measurable or evaluable disease (defined as > 1 cm on spiral computed tomography scan);
- ✓ adequate organ function, including bone marrow (absolute neutrophil count (ANC) ≥1500/μL, haemoglobin ≥9g/dL, platelets ≥100000/μL); hepatic (total bilirubin <1.6 mg/dL, international normalized ratio or ≤2x for Gilbert's Syndrome, aspartate aminotransferase/alanine aminotransferase <2.5 x upper limit of normal for patients without liver metastases, <5 x upper limit of normal for patients with liver metastases); and kidneys (serum creatinine ≤1.5 x upper limit of normal) function;

- ✓ patients who are eligible to be registered in the study, based upon the above criteria, will be genotyped for *UGT1A1*28* polymorphism and stratified into two groups based on the presence of **1/*1* or **1/*28* genotype. Patients with both variant alleles **28/*28* will be excluded;
- ✓ for patients valuable for response (secondary end point), at least one measurable cancer lesion as defined by RECIST, i.e. lesions that can be accurately measured in at least one dimension with the longest diameter ≥20 mm using conventional techniques or ≥10 mm using spiral computerized tomography scan;
- ✓ signed informed consent and local ethical committee approval are requested.

The exclusion criteria are:

- ✓ prior CPT-11 and bevacizumab treatment;
- ✓ chronic enteric diseases (Crohn disease, ulcerous colitis);
- ✓ unresolved diarrhea and bowel obstruction;
- ✓ documented cerebral metastasis;
- ✓ serious active infectious disease;
- ✓ serious functional alteration of visceral and metabolic disease;
- ✓ pregnancy status;
- ✓ radiotherapy or major surgery within 4 weeks;
- ✓ all patients in fertile age must have been under contraceptive treatment;
- ✓ presence of previous or concomitant neoplasm with exclusion of *in situ* cervical cancer;
- ✓ patients who could not attend periodic clinical check-ups.

3.1.1.2 Drug administration, dose escalation and DLT/MTD definitions

Patients have been treated with the FOLFIRI regimen plus bevacizumab, where CPT-11 has been administered at doses higher than the standard dose in patients with the *UGT1A1 *1/*1* and **1/*28* genotypes. The initial dose of CPT-11 for the two groups of patients (the *UGT1A1 *1/*1* and **1/*28*) was 260 mg/m^2 administered as a 120 min intravenous infusion every 2 weeks (base on the previous phase I (Toffoli et al., 2010)). As per protocol, the CPT-11 dosage could be increased to 310, 370, and 420 mg/m^2, and further CPT-11 doses would be increased of 14%; 5-FU was administered as 400 mg/m^2 bolus right after the end of the CPT-11 infusion, followed by 2400 mg/m^2 over a 46 h

continuous infusion plus leucovorin 200 mg/m^2 every two weeks. Bevacizumab was administered at a dose of 5 mg/kg by 90 min IV on day 3 and 15 during the first 28 day-cycle of treatment. No dose modification has been performed for 5-FU, LV and bevacizumab. Before starting CPT-11, patients have been pre-treated with atropine 0.5 mg, dexamethasone 8 mg, granisetron 3 mg or ondansetron 8 mg. Diarrhoea has been treated promptly with loperamide 4 mg at the onset, and then with 2 mg every 2 h, until the patient would be diarrhoea-free for at least 12 h. Growth factors (i.e., G-CSF) have been allowed only in patients who had grade 3-4 neutropenia at previous cycles. DLT was defined as haematological grade 4 toxicity or non haematological grade 3-4 toxicity recorded at cycle 1 that developed or persisted despite supportive measures (i.e. anti-diarrhoeas or anti-emetics). Toxicity was classified and graded according to the U.S. NCI's Common Terminology Criteria for Adverse Events (version 3.0). Under a "3+3" design, three patients have been enrolled at any dose level, they have been treated with CPT-11 at 260 mg/m^2 and if DLT was observed in <1/3 of them, dose level would be escalated and 3 patients would be treated at the next dose level (310 mg/m^2). If DLT was observed in 1/3 of the patients, 3 additional patients were enrolled at the same dose level and the escalation to the next dose level (310 mg/m^2) continued if DLT occurred in ≤1/6 of the 6 patients treated at 260 mg/m^2. If DLT was observed in ≥1/3 or >1/6 patients treated at any given dose level, the dose escalation was stopped, and 10 patients total were then enrolled at one dose level below to assess the safety and the inter-patient pharmacokinetic variability. If DLT was observed in <1/3 of patients enrolled at this dose level experience DLT, this dose level was declared as the MTD. The MTD recommended for phase II studies has been defined as the dose level immediately below that at which ≥1/3 of patients out of three patients or ≥1/6 out of six patients experienced DLT. Therefore at the MTD, ≤1/3 out of at least 10 patients experienced DLT. No intra-patient dose escalation was allowed.

3.1.1.3 Efficacy and toxicity assessment

Blood counts were measured at baseline, weekly during cycle 1, and within 48 hours before each administration during following cycles. Clinical evaluation, haematological, hepatic and renal function tests were performed at baseline and within 48 hours before each CPT-11 administration, during which patients were questioned about nausea and

vomiting, mucositis, diarrhoea, malaise, and appetite. Computed-tomography (CT) scans of measurable lesions were assessed at baseline and repeated every two cycles, with a minimum of one on-treatment CT required to be evaluable for efficacy (unless there was clinical disease progression). Objective tumour response, limited to those patients with measurable disease at enrolment, was assessed according to RECIST (version 1.0) (Therasse et al., 2000). The response criteria were:

- *Complete response* (CR): Disappearance of all target lesions;
- *Partial response* (PR): At least a 30% decrease in the sum of the longest diameter (LD) of target lesions, taking as reference the baseline sum LD;
- *Progressive disease* (PD): At least a 20% increase in the sum of the LD of target lesions, taking as reference the smallest sum LD recorded since the treatment started or the appearance of one or more new lesions;
- *Stable disease* (SD): Neither sufficient shrinkage to qualify for PR nor sufficient increase to qualify for PD, taking as reference the smallest sum LD since the treatment started.

PFS was measured from the time of drug administration to the occurrence of progressive disease or death, whichever came first.

Patients could continue receiving the same dose of CPT-11 in absence of major toxicity according to the following criteria: before re-treatment, full recovery from any non haematological toxicity, an ANC ≥1500/μL and platelet count ≥100000/mm^3, were required. Chemotherapy was discontinued on evidence of disease progression, or the appearance of new lesions on serial magnetic resonance or CT scans. Patients experiencing a major toxicity during the first or successive cycles of therapy were allowed to receive additional treatment with a 25% reduction in the CPT-11 dose. The cumulative haematological and non haematological toxicity as well as the number of dose reductions and a delay in starting the next cycle of treatment have been used as secondary indicators to differentiate the two genotype cohorts of patients.

3.1.1.4 Pharmacokinetic study

To improve current knowledge about the potential PK and PD interaction between bevacizumab and CPT-11, the pharmacokinetic profile of CPT-11 has been evaluated in absence and presence of bevacizumab in the same patient. In fact, in all patients

enrolled in the study and at each dose level the pharmacokinetic profile of CPT-11 alone has been evaluated at the first chemotherapy treatment during which bevacizumab was administered on day 3 (46h from the end of CPT-11 administration). Instead, CPT-11 PK in combination with bevacizumab was performed at day 1 of the second treatment where a second dose of bevacizumab was administered concomitantly to CPT-11.

Thus, serial blood samples were collected into heparinised tubes before drug administration, and at 1.0, 2.0, 2.25, 2.50, 3.0, 4.0, 6.0, 8.0, 10.0, 14.0, 26.0, 50.0 h following the start of the CPT-11 infusion (Figure 20).

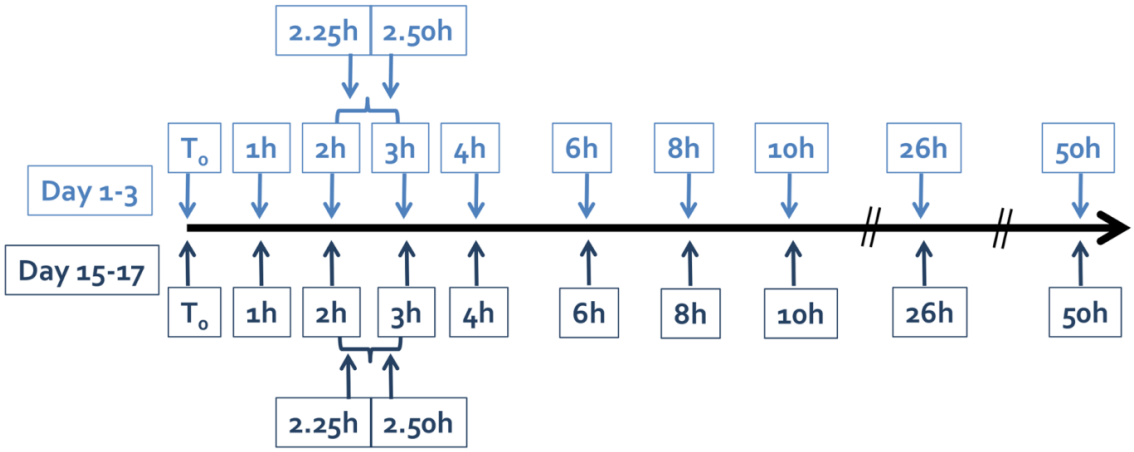

Figure 20 Schematic representation of the sampling times scheduled for the pharmacokinetic study during the first (day 1-3) and second administration (day 15-17) of the first chemotherapy cycle.

Plasma was obtained immediately by centrifugation of the blood samples at 3,000 g for 15 min at 4°C, and stored at -80°C.

The quantification of CPT-11 and its main metabolites, SN-38, SN-38G, and APC, in patients' plasma sample has been performed with the validated LC-MS/MS method specifically developed for this study (Marangon et al., 2015).

Non-compartmental analysis was used to generate the PK data, as described in more details in Section 3.4. Moreover, the extent of glucuronidation of SN38 to SN38G in plasma was defined as the ratio of SN38G AUC_{last}/SN38 AUC_{last} (glucuronidation ratio - GR).

3.1.2 Genotype-guided phase I study of irinotecan administered in combination with 5-fluorouracil/leucovorin (FOLFIRI) and cetuximab as first-line therapy in metastatic colorectal cancer patients

This phase I clinical trial has been conducted in collaboration with University of Chicago Medical Center (IL, U.S.A).The protocol of this trial (EudraCT n.2013-005618-37) has been revised and approved by the ethical committee of each participating site, the AIFA (Agenzia Italiana del Farmaco) and the ISS (Istituto Superiore di Sanità). All patients signed a written informed consent before entering the study. The main characteristics of this study are briefly described above.

3.1.2.1 Patients characteristics

The eligibility criteria for this study are:

- ✓ histologically or cytologically confirmed diagnosis of mCRC expressing EGFR;
- ✓ *RAS* wild-type status;
- ✓ no prior chemotherapy for metastatic disease;
- ✓ age ≥18;
- ✓ ECOG PS of 0 or 1;
- ✓ life expectancy > 3 months;
- ✓ measurable or evaluable disease (defined as > 1 cm on spiral computed tomography scan);
- ✓ adequate organ function, including bone marrow ANC ≥1500/μL, haemoglobin ≥9g/dL, platelets ≥100000/μL); hepatic (total bilirubin <1.6 mg/dL, international normalized ratio or ≤2x for Gilbert's Syndrome, aspartate aminotransferase/alanine aminotransferase <2.5 x upper limit of normal for patients without liver metastases, <5 x upper limit of normal for patients with liver metastases); and kidneys (serum creatinine ≤1.5 x upper limit of normal) function;
- ✓ patients who are eligible to be registered in the study, based upon the above criteria, will be genotyped for *UGT1A1*28* polymorphism and stratified into two

groups based on the presence of **1/*1* or **1/*28* genotype. Patients with both variant alleles **28/*28* will be excluded;

- ✓ for patients valuable for response (secondary end point), at least one measurable cancer lesion as defined by RECIST, i.e. lesions that can be accurately measured in at least one dimension with the longest diameter ≥20 mm using conventional techniques or ≥10 mm using spiral computerized tomography scan;
- ✓ signed informed consent and local ethical committee approval are requested.

The exclusion criteria are:

- ✓ cardiac pathology (cardiac decompensation, infarction during the period of 6 months preceding the study, atrioventricular block, serious arrhythmia);
- ✓ patients with specific contraindications for the use of EGFR inhibitors (pulmonary fibrosis, interstitial pneumonia history);
- ✓ unresolved diarrhoea and bowel obstruction;
- ✓ haemorrhagic syndrome;
- ✓ documented cerebral metastasis;
- ✓ serious active infectious disease;
- ✓ serious functional alteration of visceral and metabolic disease;
- ✓ pregnancy status;
- ✓ radiotherapy or major surgery within 4 weeks;
- ✓ all patients in fertile age must have been under contraceptive treatment;
- ✓ presence of previous or concomitant neoplasm with exclusion of *in situ* cervical cancer;
- ✓ non collaborative and/or unreliable patients;
- ✓ patients with a chronic toxicity ≥grade 2;
- ✓ refusal of informed consent;
- ✓ patients who could not attend periodic clinical check-ups.

3.1.2.2 Drug administration, dose escalation and DLT/MTD definitions

Patients are treated with FOLFIRI regimen plus cetuximab, where CPT-11 is administered at doses higher than the standard dose in patients with *UGT1A1 *1/*1* and **1/*28* genotypes. The starting dose of CPT-11 for the two groups of patients (*UGT1A1 *1/*1* and **1/*28* group) is 260 mg/m^2 administered as a 120 min intravenous infusion

every 2 weeks. The CPT-11 dosage will be increased to 310, 370, and 420 mg/m^2, and further CPT-11 doses will be increased of 14%; 5-FU is administered as 400 mg/m^2 bolus right after the end of the CPT-11 infusion, followed by 2400 mg/m^2 over a 46-h continuous infusion plus LV 200 mg/m^2 every two weeks. Cetuximab is administered as an intravenous infusion at a dose of 500 mg/m^2 with prophylactic intravenous steroids and anti-histaminic agents. Cetuximab is administered every 2 weeks. No dose modification will be performed for 5-FU, LV and cetuximab. One cycle is 28 days (two CPT-11 administrations). Before starting CPT-11, patients are pre-treated with atropine 0.5 mg, dexamethasone 8 mg, granisetron 3 mg or ondansetron 8 mg. Diarrhoea will be promptly treated with loperamide 4 mg at the onset, and then with 2 mg every 2 h, until the patient will be diarrhoea-free for at least a minimum of 12 h. Growth factors (i.e., G-CSF) is allowed only in patients who will have grade ≥ 3 neutropenia at previous cycles.

The dosage of CPT-11 is escalated applying a "3 + 3" cohort expansion design to reach the MTD. There will be two genotype cohorts of patients: one for each genotype (*UGT1A1 *1/*1* and **1/*28* groups), and the escalation study will proceed accordingly. Three patients will be enrolled and treated with CPT-11 at the starting dose (260 mg/m^2). If DLT is observed in <1/3 of them, the dose level will be escalated and three patients more will be treated at the next dose level (310 mg/m^2). If DLT is observed in 1/3 of the patients, 3 additional patients will be enrolled at the same dose level. The escalation to the next dose level will continue if DLT occurs in ≤1/6 of the 6 patients treated at the first dose level (260 mg/m^2). If DLT is observed in >1/3 or >1/6 of the patients treated at any given dose level, the dose escalation will be stopped, and 10 patients in total will then be enrolled at one dose level lower to assess the safety and the inter-patient pharmacokinetic variability.

The MTD recommended for phase II studies will be defined as the dose level immediately below the one at which ≥1/3 of patients out of three patients or ≥1/6 out of six patients experienced DLT. Therefore at the MTD, ≤1/3 out of at least 10 patients experienced DLT. No intra-patient dose escalation is allowed.

DLT is defined as haematological grade 4 toxicity or non-haematological grade 3-4 toxicity and developed or persisted despite supportive measures (i.e. anti-diarrhoeas or anti-emetics). DLT will be evaluated during the first cycle of chemotherapy (2

administrations). Toxicity is classified and graded according to the United States NCI's common toxicity criteria (version 4.03).

The cumulative haematological and non haematological toxicities as well as the number of dose reductions and a delay in starting the next cycle of treatment will be used as secondary indicators to differentiate the two genotype cohorts of patients.

3.1.2.3 Efficacy and toxicity assessment

See section 3.1.1.3.

3.1.2.4 Pharmacokinetic study

To improve the current knowledge about the potential pharmacokinetic and pharmacodynamic interactions between cetuximab and CPT-11, this open label drug-drug interaction study evaluates the pharmacokinetic profile of CPT-11 in absence and presence of cetuximab in the same patient within the first chemotherapy cycle.

In all patients enrolled in the study and at each dose level, the pharmacokinetic profile of CPT-11 alone will be evaluated at the first chemotherapy treatment (on days 1-3) during which cetuximab will be administered on day 3 (48 h from the end of CPT-11 administration). Instead, the PK of CPT-11 in combination with cetuximab will be performed on days 15-17 of the second treatment of the first cycle of therapy where a second dose of cetuximab will be administered concomitantly to CPT-11.

Thus, serial blood samples are collected into tubes containing K-EDTA (4.9 mL). The sampling times is: before drug administration and at 1.0, 2.0, 2.25, 2.50, 3.0, 4.0, 6.0, 8.0, 10.0, 26.0 and 50.0 h following the start of the CPT-11 infusion during both the treatments of the first cycle of therapy, as schematized in Figure 21. Plasma is obtained immediately by centrifugation of blood samples (3000 g for 10 min at 4°C), then split into 2 aliquots and stored at -80°C in 2 different freezers.

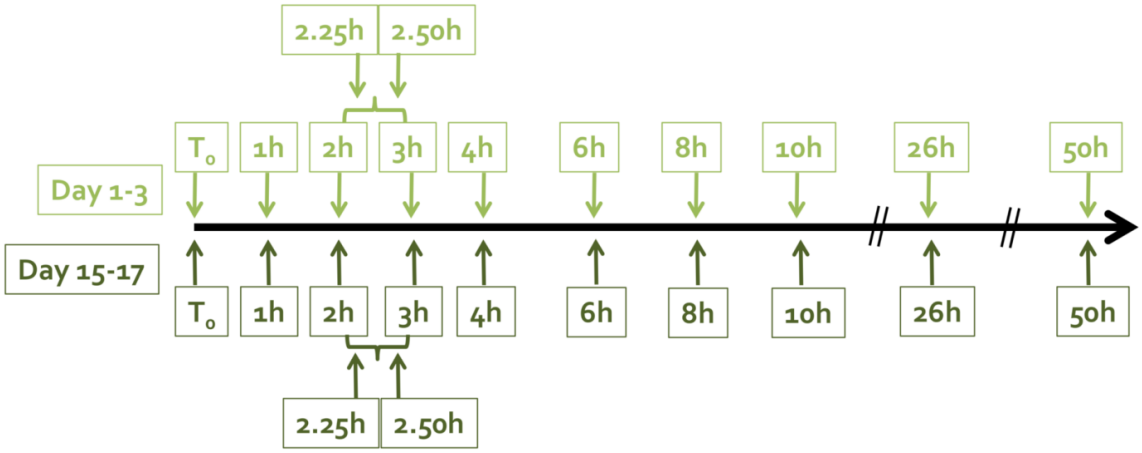

Figure 21 Schematic representation of the sampling times scheduled for the pharmacokinetic study during the first (day 1-3) and second administration (day 15-17) of the first chemotherapy cycle.

The quantification of CPT-11 and its main metabolites in patients' plasma sample has been performed with the validated LC-MS/MS method specifically developed for the previous phase I study and already published (Marangon et al., 2015).

3.1.3 Genotype-guided phase I study for weekly paclitaxel in ovarian cancer patients

The protocol of this trial (EudraCT n. 2010-021619-18) has been revised and approved by the CRO ethical committee, the AIFA (Agenzia Italiana del Farmaco) and the ISS (Istituto Superiore di Sanità). All patients signed a written informed consent before entering the study. The main characteristics of this study are briefly described above.

3.1.3.1 Patients characteristics

The eligibility criteria for this study are:

- ✓ histologically confirmed diagnosis of relapsed epithelial ovarian cancer;
- ✓ indication for chemotherapy treatment;
- ✓ age ≥18 years and ≤75 years (for patients ≥70 years a multidisciplinary geriatric evaluation will be performed);
- ✓ ECOG PS ≤ 2;
- ✓ life expectancy >3 months;
- ✓ pretreatment with adequate dose of platinum based regimens;

- ✓ measurable disease according to GCIG guidelines (RECIST and/or CA-125 criteria);
- ✓ patients enrolled in the study according to the previous eligibility criteria will be genotyped for the *ABCB1-2677G>T/A* polymorphism and stratified in two groups based on the presence of at least one *ABCB1-2677T/A* variant allele (i.e. group 1: *ABCB1-2677GG* genotype; group 2: *ABCB1-2677GT; GA, AA, TT, AT* genotypes).

The exclusion criteria are:

- ✓ cardiac pathology (cardiac decompensation, infarction during the period of 6 months preceding the study, atrioventricular block, serious arrhythmia);
- ✓ ANC <1,500/μL, platelets <100,000/μL;
- ✓ alterations of renal function (serum creatinine ≥1.25 fold the normal limit);
- ✓ alterations of hepatic function (GOT or GPT ≥1.25 fold the normal limit unless clearly due to hepatic metastasis);
- ✓ hemorrhagic syndrome;
- ✓ chronic neuropathy grade ≥2;
- ✓ non collaborative and/or unreliable patients;
- ✓ patients' impossibility of coming to CRO;
- ✓ patients previously treated with >3 therapy lines for the metastatic disease;
- ✓ patients with a chronic toxicity grade ≥2;
- ✓ refusal of informed consent.

3.1.3.2 Drug administration, dose escalation and DLT/MTD definitions

Patients have been treated with weekly PTX starting from an 80 mg/m^2 dose for both groups: the high risk of toxicity (group 2, *ABCB1-2677GT, GA, AA, TT, AT* genotypes) and the low (group 1, *ABCB1*-2677GG genotype). Dose escalation steps have been of 10 mg/m^2 for dose level. PTX was administered as 60 minutes intravenous infusion every week following anti-hypersensitivity premedication with corticosteroid and anti H1–H2 histamine receptor.

DLT was defined as haematological toxicity grade 4 or non-haematological toxicity grade ≥ 3. DLTs have been evaluated during the first two cycles of chemotherapy (8 weekly administrations). Additionally, it has been considered DLT if the recovery from any non haematological toxicity, of ANC to ≥1500/μl and platelet count to

≥100000/mm^3 has taken longer than 14 days. Toxicity has been classified and graded according to the United States NCI's common toxicity criteria (version 3).

Three patients has been treated with PTX at the starting dose and if DLT was observed in <1/3 of them, dose level would be escalated and other 3 patients would be treated at the next dose level. If DLT was observed in 1/3 of the patients, 3 additional patients would be enrolled at the same dose level. The escalation to the next dose level would continue if DLT occurred in ≤1/6 of the 6 patients treated at the first dose level. If DLT was observed in >1/3 or >1/6 of the patients treated at any given dose level, the dose escalation would be stopped, and a total of 10 would then be enrolled at one dose level lower to assess the safety and the inter-patient pharmacokinetic variability. The MTD recommended for phase II studies would be defined as the dose level immediately below the one at which ≥1/3 of patients out of three or ≥1/6 out of six have experienced DLT. Therefore at the MTD, ≤1/3 out of at least 10 patients experienced DLT. No intra-patient dose escalation is allowed.

The cumulative haematological and non haematological toxicities, as well as the number of dose reductions and a delay in starting the next cycle of treatment, has been used as secondary indicators to differentiate the two genotype cohorts of patients.

3.1.3.3 Efficacy and toxicity assessment

Blood counts were measured at baseline, weekly during cycle 1, and within 48 hours before each administration during following cycles. Clinical evaluation, haematological, hepatic and renal function tests were performed at baseline and within 48 hours before each PTX administration, during which patients were questioned about nausea and vomiting, mucositis, diarrhoea, malaise, and appetite. CT scans of measurable lesions were assessed at baseline and repeated every two cycles, with a minimum of one on-treatment CT required to be evaluable for efficacy (unless there was clinical disease progression). Objective tumour response, was assessed according to RECIST (version 1.0) (Therasse et al., 2000) and/or CA-125 criteria (according to Gynecological Cancer Intergroup -GCIG guidelines). PFS was measured from the time of drug administration to the occurrence of progressive disease or death, whichever came first.

Patients could continue receiving the same dose of PTX in absence of major toxicity according to the following criteria: before re-treatment, full recovery from any non

haematological toxicity, an ANC ≥1500/μl and platelet count ≥100000/mm^3, were required. Chemotherapy was discontinued on evidence of disease progression, or the appearance of new lesions on serial magnetic resonance or CT scans.

Patients experiencing a major toxicity during the first or successive cycles of therapy were allowed to receive additional treatment with a 25% reduction in the dose of PTX. The cumulative haematological and non haematological toxicity as well as the number of dose reductions and a delay in starting the next cycle of treatment will be used as secondary indicators to differentiate the two genotype cohorts of patients.

3.1.3.4 Pharmacokinetics study

A pharmacokinetic study has been performed to clarify relationship between *ABCB1-2677G>T/A* polymorphism and PTX Cl or AUC. In all patients enrolled in the study, the PTX pharmacokinetic profile has been evaluated twice during the first chemotherapy cycle: on the first PTX administration and on the fourth one, because of the metabolic autoinduction effect of this taxane. In fact, it seems that frequent dosing of PTX (i.e. a more constant drug exposure) can induce the metabolism and elimination of the drug (Gustafson et al., 2005). According with this aim, even the PK of 6α-OH-PTX will be determined.

Thus, serial blood samples will be collected into tubes containing K_2EDTA. For what concerns the first PTX administration, pharmacokinetic sampling will be done before drug infusion, at 59 minutes since its start (just before the end of the infusion, to precisely define the Cmax), and at 15 and 30 minutes and 1, 3, 7, 24 and 48 hours after the end of the infusion. On the fourth drug administration, the sampling will be done before drug infusion, at 59 minutes and at 30 minutes, 1, 4, 10-12, 24 and 48 hours after the end of the infusion (Figure 22). Plasma will be obtained immediately by centrifugation of blood samples and stored at -80°C.

The plasma concentration of PTX and its 6α-hydroxymetabolite has been determined using a new LC-MS/MS method that has been specifically developed and validated.

To determine the pharmacokinetic parameters, a non-compartmental analysis has been applied (see Section 3.4).

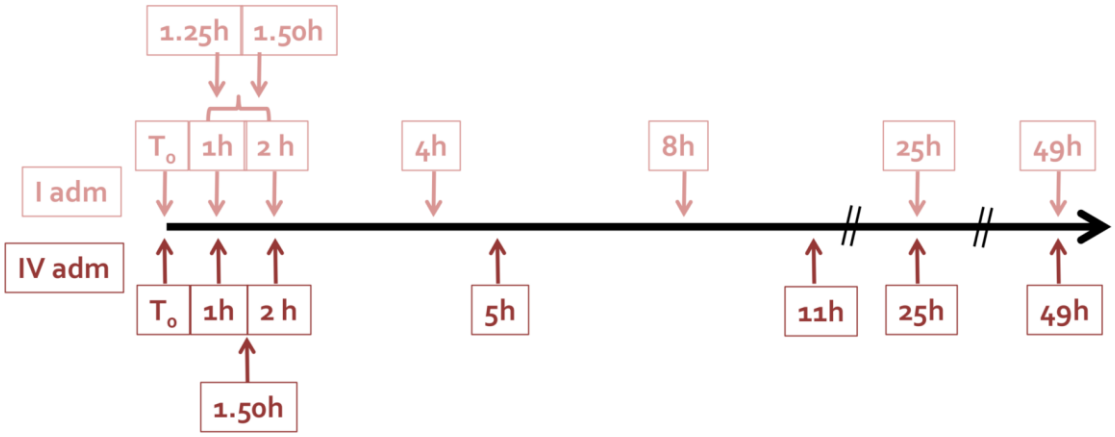

Figure 22 Schematic representation of the sampling times scheduled for the pharmacokinetic study during the first and fourth administration (adm) of the first chemotherapy cycle.

3.2 LC-MS/MS methods: development

The LC-MS/MS methods have been developed using a HPLC system consisted of a SIL-20AC XR auto-sampler and LC-20AD UFLC XR pumps (Shimadzu, Tokyo, Japan) coupled with an API 4000 triple quadrupole mass spectrometer AB SCIEX (Massachusetts, USA). To quantify the chromatographic peaks, data were processed with Analyst 1.5.2 (quantification with MultiQuant 2.1) software package (AB SCIEX).

3.2.1 High-performance liquid chromatography–tandem mass spectrometry method for the simultaneous determination of irinotecan and its main metabolites in human plasma

3.2.1.1 Standards and chemicals

Analytical reference standards of CPT-11 (7-ethyl-10-[4-(1-piperidino)-1-piperidino]-carbonyloxycamptothecin, batch 059K1163, purity ≥97%), SN-38 (7-ethyl-10-hydroxycamptothecin, batch 088K1267, purity ≥98%) and CPT ((S)-(+)-Camptothecin, batch SLBB9623V, purity ≥90%), used as Internal Standard (IS), were purchased from Sigma-Aldrich Co. (Milan, Italy). APC (7-ethyl-10-[4-N-(5-aminopentanoic acid)-1-piperidino]-carbonyloxycamptothecin, batch 5-PSB-149-1, purity ≥98%) was purchased from Toronto Research Chemicals, Inc. (North York, Ontario, Canada) and SN-38G (7-ethyl-10-[3,4,5-trihydroxy-pyran-2-carboxylic acid]-camptothecin, batch MS0366) was kindly provided by Yakult Honsha Co., Ltd (Tokyo, Japan).

Dimethyl sulfoxide (DMSO, batch 037K07663) and LC-MS grade acetonitrile were purchased from Sigma-Aldrich Co. LC-MS grade methanol and acetic acid were supplied by Carlo Erba (Milan, Italy) and Baker (JT Baker, Deventer, NL) respectively. Filtered, deionized water was obtained from a Milli-Q Plus system (Millipore, Billerica, MA, USA).

Control human plasma/K_2EDTA, used to prepare daily standard calibration curves and quality control (QC) samples was provided by the transfusion unit of the National Cancer Institute (Aviano, Italy) from healthy volunteers.

3.2.1.2 Standards and quality control solutions

For CPT-11, APC, SN-38 and SN-38G two stock solutions (for standards and QCs) for each compound were prepared in DMSO at a concentration of 5000.0 µg/mL for CPT-11, 1000.0 µg/mL for APC and 100.0 µg/mL for SN-38 and SN-38G. The stock solution for the IS was prepared at 5 µg/mL in methanol. These solutions were stored at -80°C. A series of working solutions (F to A) to prepare the plasma standard points of the calibration curve and the plasma QC samples (L, M and H) were obtained by mixing and diluting the stock solutions with methanol in order to obtain the final concentrations reported in Table 2. Aliquots of these solutions were kept in polypropylene tubes at -80°C. The IS working solution was prepared at 0.5 µg/mL by diluting the stock solution with methanol.

Table 2 Standard and quality control working solutions.

Standards	Concentrations (µg/mL)								
	F	E	D	C	B	A	QCL	QCM	QCH
CPT11	0.20	2.00	20.00	100.00	160.00	200.00	0.50	120.00	180.00
APC	0.02	0.20	2.00	20.00	50.00	100.00	0.04	40.00	80.00
SN38	0.02	0.10	0.50	2.00	5.00	10.00	0.04	3.00	8.00
SN38G	0.02	0.10	0.50	2.00	5.00	10.00	0.04	3.00	8.00

3.2.1.3 Preparation of standards and quality control samples

A six-point plasma calibration curve was prepared freshly every day during the validation study. Each calibration sample was prepared by adding 5 µL of the respective standard solution from F to A (ULOQ) to 95 µL of pooled blank human plasma to obtain the final concentrations reported in Table 3.

Table 3 Final concentrations of calibration curve and QC samples.

Standards	Concentrations (ng/mL)								
	F	E	D	C	B	A	QCL	QCM	QCH
CPT11	10.00	100.00	1000.00	5000.00	8000.00	10000.00	25.00	6000.00	9000.00
APC	1.00	10.00	100.00	1000.00	2500.00	5000.00	2.00	2000.00	4000.00
SN38	1.00	5.00	25.00	100.00	250.00	500.00	2.00	150.00	400.00
SN38G	1.00	5.00	25.00	100.00	250.00	500.00	2.00	150.00	400.00

Each calibration curve included a blank sample (plasma processed without IS) and a zero blank sample (plasma processed with the IS). Three QC samples were used for each concentration level. To prepare QC samples, 5.7 mL aliquots of control human plasma were mixed with 300 µL of each working QC solutions (L, M and H) obtaining the QC plasma concentration reported in Table 3. Several 100 µL-aliquots of the three QCs were stored at −80°C to check the analytes stabilities and as controls for future assays. The calibration curve samples and QCs were processed as described below.

3.2.1.4 Processing samples

After have thawed plasma samples in an ice bath, they were vortexed for 10 s and centrifuged at 3000 g for 10 min at nominally 4°C. Then 100 µL of the actual sample, standard or QC sample were transferred to a 1.5 mL Eppendorf polypropylene tube, and 5 µL of the IS working solution (0.5 µg/mL) were added and the mixture was vortexed. After that, 300 µL of 0.1% CH_3COOH/CH_3OH were added. Each tube was thoroughly vortexed for 10 s and centrifuged at 16000 g for 10 min at nominally 4°C. Then 150 µL of the obtained supernatant were transferred to an autosampler glass vial. Different amounts (3–5 µL), inversely related to the concentrations, were injected into the HPLC system to minimize the carry-over effect. Moreover, after the injection of the ULOQ, three samples of mobile phase and one blank sample were injected to demonstrate the absence of carry-over effect. This procedure guaranteed that no peak higher than 10% of LLOQ was detected. For the same reason, patients' samples were analyzed on the basis of expected concentrations (lowest to highest), and three samples of mobile phase were injected between successive test samples.

3.2.1.5 Chromatographic conditions

Samples were separated on a Gemini C18 chromatographic column (3 µM 110A, 100 x 2.0 mm) coupled with a Security Guard Cartridge (Gemini-NX C18 4.0 x 2.0 mm), both provided by Phenomenex (Torrance, CA, USA) and thermostatically controlled at 25°C. The mobile phases (MP) used for chromatographic separation were 0.1% CH_3COOH/bidistilled water (MP A) and 0.1% CH_3COOH/acetonitrile (MP B). The HPLC system was set up with a flow rate of 0.3 mL/min and the following linear gradient: *step 1*: the initial condition of 95% MP A held for 1 min; *step 2*: from 95% MP A to 30% over

5.5 min; *step 3*: constant for 1.5 min; *step 4*: from 30% MP A to 10% over 0.5 min; *step 5*: kept constant for 1.5 min; *step 6*: from 10% MP A to the initial condition over 1 min and reconditioning for 7 min. The total run time was 18 min.

3.2.1.6 Mass spectrometry

Standard solutions prepared in 0.1% CH_3COOH acetonitrile/water 1:1 (50 ng/mL) of CPT-11, SN-38, SN-38G, APC and IS were infused at a flow rate of 10 µL/min in order to optimize all the MS parameters. Positive ion mode was used to obtain the mass spectra (MS_1) and the product ion spectra (MS_2). The instrument was equipped with a Turbo IonSpray source operated at 650°C and with ion spray voltage of 5500 V. The biological samples were analyzed with ESI, using zero air as nebulizer gas (30 psi) and as heater gas (65 psi). Nitrogen was employed as curtain gas (20 psi) and as collision gas at medium intensity (CAD). After fragmentation, the characteristic product ions of the five compounds were monitored in the third quadrupole at *m/z* 124.2, *m/z* 167.2 and *m/z* 195.2 for CPT-11, at *m/z* 349.3, *m/z* 249.1 and *m/z* 293.2 for SN-38, at *m/z* 393.2, *m/z* 349.2 and *m/z* 249.2 for SN-38G, at *m/z* 393.3, *m/z* 227.1 and *m/z* 349.2 for APC and at *m/z* 305.1, *m/z* 248.9 and *m/z* 220.1 for IS. Quantification was done in SRM mode using the following transitions: *m/z* 587.4 > 124.2 for CPT-11, *m/z* 393.3 > 349.3 for SN-38, *m/z* 569.3 > 393.2 for SN-38G, *m/z* 619.2 > 393.3 for APC and *m/z* 349.2 > 305.1 for the IS (CPT).

3.2.2 High-performance liquid chromatography–tandem mass spectrometry method for the simultaneous determination of paclitaxel and its main metabolite 6α-hydroxy-paclitaxel in human plasma

3.2.2.1 Standards and chemicals

Analytical reference standards of PTX (2α,4α,5β,7β,10β,13α-4,10-Bis(acetyloxy)-13-{[(2R,3S)-3-(benzoylamino)-2-hydroxy-3-phenylpropanoyl]oxy}-1,7-dihydroxy-9-oxo-5,20-epoxytax-11-en-2-yl benzoate, batch 061M1664V, purity ≥97%), and docetaxel (DTX) (1,7β,10β-trihydroxy-9-oxo-5β,20-epoxytax-11-ene-2α,4,13α-triyl 4-acetate 2-

benzoate 13-{(2R,3S)-3-[(tert-butoxycarbonyl)amino]-2-hydroxy-3-phenylpropanoate}, batch 1425738V, purity ≥97%), used as Internal Standard (IS), were purchased from Sigma-Aldrich Co. (Milan, Italy). 6α-OH-PTX (batch 1JAB113-2, purity ≥98%) was purchased from Toronto Research Chemicals, Inc. (North York, Ontario, Canada). LC-MS grade acetonitrile, methanol and formic acid were purchased from Sigma-Aldrich Co. Filtered, deionized water was obtained from a Milli-Q Plus system (Millipore, Billerica, MA, USA). Control human plasma/K_2EDTA, used to prepare daily standard calibration curves and QC samples was provided by the transfusion unit of the National Cancer Institute (Aviano, Italy) from healthy volunteers.

3.2.2.2 Standards and quality control solutions

For PTX and 6α-OH-PTX two stock solutions (for standards and QCs) for each compound were prepared in methanol at a concentration of 2000.0 µg/mL for PTX and 100.0 µg/mL for 6α-OH-PTX. The stock solution for the IS was prepared at 100 µg/mL in methanol. These solutions were stored at -80°C. A series of working solutions (G to A) to prepare the plasma standard points of the calibration curve and the plasma QC samples (L, M and H) were obtained by mixing and diluting the stock solutions with methanol in order to obtain the final concentrations: 0.02, 0.20, 1.00, 5.00, 20.00, 100.00, 200.00 (G to A) and 0.06, 12.50, 150.00 (QCL, M, H) µg/mL for PTX, and 0.02, 0.10, 0.50, 1.00, 2.00, 10.00, 20.00 (from G to A) and 0.06, 1.50, 15.00 (QCL, M, H) µg/mL for 6α-OH-PTX. Aliquots of these solutions were kept in polypropylene tubes at -80°C. The IS working solution was prepared at 4 µg/mL by diluting the stock solution with methanol.

3.2.2.3 Preparation of standards and quality control samples

A seven-point plasma calibration curve was prepared freshly every day during the validation study. Each calibration sample was prepared by adding 5 µL of the respective standard solution from G to A (ULOQ) to 95 µL of pooled blank human plasma to obtain the final concentrations: 1.00, 10.00, 50.00, 250.00, 1000.00, 5000.00, 10000.00 (G to A) and 3.00, 625.00, 7500.00 (QCL, M, H) ng/mL for PTX, and 1.00, 5.00, 25.00, 50.00, 100.00, 500.00, 1000.00 (G to A) and 3.00, 75.00, 750.00 (QCL, M, H) ng/mL for 6α-OH-PTX. Each calibration curve included a blank sample (plasma processed without IS) and

a zero blank sample (plasma processed with the IS). Three QC samples were used for each concentration level. To prepare QC samples, 5.7 mL aliquots of control human plasma were mixed with 300 µL of each working QC solutions (L, M and H), obtaining the QC plasma concentration reported above. Several 100 µL-aliquots of the three QCs were stored at –80°C to check the analytes stabilities and as controls for future assays. The calibration curve samples and QCs were processed as described below.

3.2.2.4 Processing samples

After have thawed plasma samples at room temperature, they were vortexed for 10 s and centrifuged at 3000 g for 10 min at nominally 4°C. Then 100 µL of the actual sample, standard or QC sample were transferred to a 1.5 mL Eppendorf polypropylene tube, and 5 µL of the IS working solution (4 µg/mL) were added and the mixture was vortexed. After that, 400 µL of 0.1% HCOOH/CH_3OH were added. Each tube was thoroughly vortexed for 10 s and centrifuged at 16000 g for 15 min at nominally 4°C. Then 150 µL of the obtained supernatant were transferred to an autosampler glass vial. Different amounts (3–5 µL), inversely related to the concentrations, were injected into the HPLC system to minimize the carry-over effect. Moreover, after the injection of the ULOQ, three samples of mobile phase and one blank sample were injected to demonstrate the absence of carry-over effect. This procedure guaranteed that no peak higher than 10% of LLOQ was detected. For the same reason, patients' samples were analyzed on the basis of expected concentrations (lowest to highest), and three samples of mobile phase were injected between successive test samples.

3.2.2.5 Chromatographic conditions

Samples were separated on a SunFireTM C18 chromatographic column (3.5 µM, 92 Å, 2,1 x 150 mm) coupled with a Security Guard Cartridge (SunFireTM C18 2.1 x 10 mm), both provided by Waters (Milford, MA, USA) and thermostatically controlled at 30°C. The mobile phases (MP) used for chromatographic separation were 0.1% HCOOH/bidistilled water (MP A) and 0.1% HCOOH/acetonitrile (MP B). The HPLC system was set up with a flow rate of 0.2 mL/min and the following linear gradient: *step 1*: from the initial condition of 60% MP A to 0% over 12 min; *step 2*: kept constant for 2

min; *step 3*: from 0% MP A to the initial condition over 1 min; *step 4*: reconditioning for 6 min. The total run time was 21 min.

3.2.2.6 Mass spectrometry

Standard solutions prepared in 0.1% HCOOH acetonitrile/water 1:1 (50 ng/mL) of PTX, 6α-OH-PTX and IS were infused at a flow rate of 10 µL/min in order to optimize all the MS parameters. Positive ion mode was used to obtain the mass spectra (MS_1) and the product ion spectra (MS_2). The instrument was equipped with a Turbo IonSpray source operated at 250°C and with ion spray voltage of 5500 V. The biological samples were analyzed with ESI, using zero air as nebulizer gas (50 psi) and as heater gas (50 psi). Nitrogen was employed as curtain gas (20 psi) and as collision gas at medium intensity (CAD). After fragmentation, the characteristic product ions of the two analytes were monitored in the third quadrupole at *m/z* 569.3, *m/z* 286.3 and *m/z* 105.1 for PTX, at *m/z* 286.3, *m/z* 105.1 and *m/z* 525.3 for 6α-OH-PTX, and at *m/z* 226.3 and *m/z* 527.3 for IS. Quantification was done in SRM mode using the following transitions: *m/z* 854.5 > 569.3 for PTX, *m/z* 870.5 > 286.3 for 6α-OH-PTX, and *m/z* 808.5 > 226.3 for the IS (DTX).

3.2.3 High-performance liquid chromatography–tandem mass spectrometry method for the simultaneous determination of sunitinib and its main metabolite N-desethyl sunitinib in human plasma

3.2.3.1 Standards and chemicals

Analytical reference standard of sunitinib (N-(2-diethylaminoethyl)-5-[(Z)-(5-fluoro-2-oxo-1H-indol-3-ylidene)methyl]-2,4-dimethyl-1H-pyrrole-3-carboxamide) was purchased from Sigma-Aldrich Co. (Milan, Italy) while N-desethyl sunitinib (N-[2-(Ethylamino)ethyl]-5-[(Z)-(5-fluoro-1,2-dihydro-2-oxo-3H-indol-3-ylidene)methyl]-2,4-dimethyl-1H-pyrrole-3-carboxamide) and the deuterated internal standard sunitinib D10 were purchased from Toronto Research Chemicals, Inc. (North York, Ontario, Canada). LC-MS grade methanol and formic acid were supplied by Sigma-Aldrich Co. (Milan, Italy) and Baker (JT Baker, Deventer, NL), respectively. Filtered, deionized water

was obtained from a Milli-Q Plus system (Millipore, Billerica, MA, USA). The transfusion unit of the National Cancer Institute (Aviano, Italy) provided control human plasma/K_2EDTA, used to prepare daily standard calibration curves and QC samples from healthy volunteers.

3.2.3.2 Standards and quality control solutions

Two different stock solutions (for standards and QCs) of each compound (sunitinib, N-desethyl and IS) were prepared in dimethyl sulfoxide (DMSO) at a concentration of 1.00 mg/mL. Dilution in acetonitrile from the solutions of sunitinib and N-desethyl sunitinib (for standards and QC) were prepared at concentration of 100 µg/mL, 10 µg/mL and 1 µg/mL. A series of working solutions (G to A) to prepare the plasma standard points of the calibration curve and the plasma QC samples (L, M and H) were obtained by mixing and diluting the stock in order to obtain the final concentrations: 0.002, 0.010, 0.050, 0.200, 1.000, 5.000, and 10.000 (G to A) and 0.005, 0.500, and 8.000 (L, M and H) µg/mL for sunitinib and 0.002, 0.010, 0.050, 0.200, 1.000, 2.000, and 5.000 (G to A) and 0.005, 0.500, and 4.000 (L, M and H) µg/mL for N-desethyl sunitinib. The IS working solution was prepared at 0.1 µg/mL by diluting the stock solution with acetonitrile. All the solutions were kept in polypropylene tubes and stored at -80°C.

3.2.3.3 Preparation of standards and quality control samples

A seven-point plasma calibration curve was prepared freshly every day during the validation study. Each calibration sample was prepared by adding 1.5 µL of the respective standard solution from G to A (ULOQ) to 28.5 µL of pooled blank human plasma to obtain the following final concentrations: 0.1, 0.5, 2.5, 10.0, 50.0, 250.0, and 500.0 ng/mL for sunitinib and 0.1, 0.5, 2.5, 10.0, 50.0, 100.0 and 250.0 ng/mL for N-desethyl sunitinib. Each calibration curve included a blank sample and a zero blank sample (plasma processed with the IS). At least three concentrations of QC need to be prepared: one within three times the LLOQ (low QC), one in the midrange (middle QC), and one approaching the high end (high QC) of the range of the expected study concentrations. To prepare QC samples, 1.14 mL aliquots of control human plasma were mixed with 60 µL of each working QC solutions (L, M and H) obtaining the following QC plasma concentration: 0.25, 25.00, and 400.00 ng/mL for sunitinib and

0.25, 25.00, and 200.00 ng/mL for N-desethyl sunitinib. Several 30 µL-aliquots of the three QCs were stored at –80°C to check the analytes stabilities and as controls for future assays.

3.2.3.4 Processing samples

After have thawed plasma samples, they were vortexed for 10 s and centrifuged at 3000 g for 10 min. Then, 30 µL of the actual sample, standard or QC sample were transferred to a 1.5 mL Eppendorf polypropylene tube, and 1.5 µL of the IS working solution (0.1 µg/mL) were added and the mixture was vortexed. Sample treatment was based on a simple protein precipitation, made adding 150 µL of CH_3OH to the mixture. Each tube was thoroughly vortexed for 10 s and centrifuged at 13000 g for 10 min. Then 100 µL of the obtained supernatant were transferred to an autosampler glass vial pending analysis. Since all the sample handling steps described above occur without any light-protection, an additional step has been introduced in order to revert the isomerisation and thus to obtain only the active Z-isomer to be measured. For this reason, the samples were heated at 90°C for 5 min in a thermostatic bath and, then, transferred into the autosampler. This last step is the only one in the entire processing procedure that needs to be done in the dark (Figure 23).

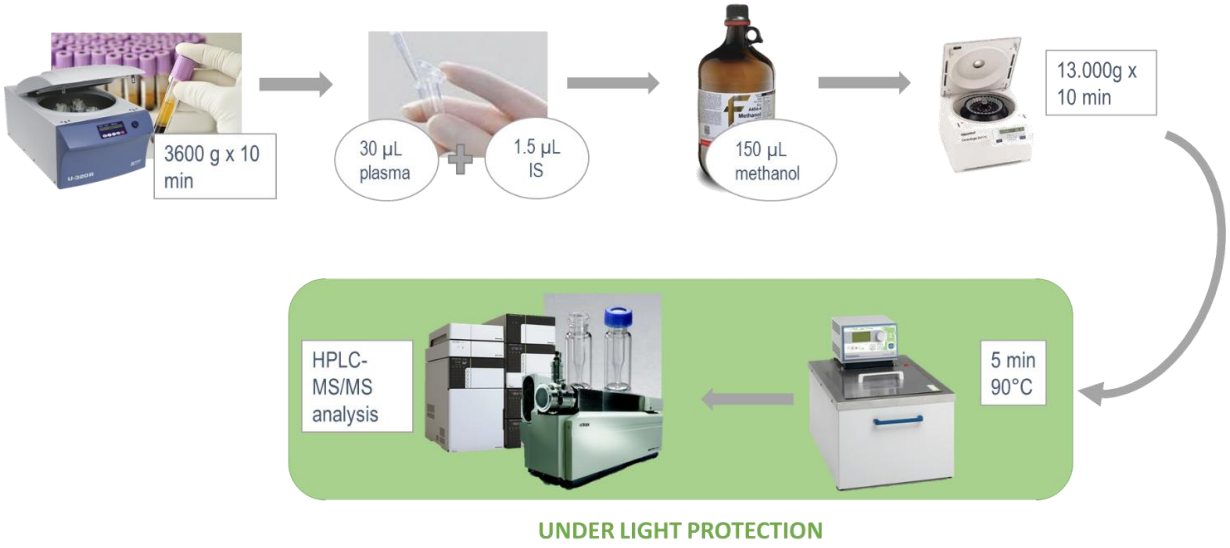

Figure 23 Schematic representation of the processing sample procedure.

Different amounts (2–5 µL), inversely related to the concentrations, were injected into the HPLC system to minimize the carry-over effect. Moreover, after the injection of the

ULOQ, three samples of mobile phase and one blank sample were injected to demonstrate the absence of carry-over effect. This procedure guaranteed that no peak higher than 10% of LLOQ was detected.

3.2.3.5 Chromatographic conditions

Samples were separated on a Synergy Fusion RP C18, 4 µM, 80 Å, 2 x 50 mm (pre-column: Gemini-NX C18 4.0 x 2.0 mm) and thermostatically controlled at 50°C. The mobile phases were 0.1% HCOOH/bidistilled water (MP A) and 0.1% HCOOH/acetonitrile (MP B). The HPLC system was set up with a flow rate of 0.3 mL/min and the following linear gradient: *step 1:* the initial condition of 90% MP A held for 0.5 min; *step 2*: from 90% MP A to 30% over 1 min; *step 3:* constant for 1.2 min; *step 4*: from 30% MP A to 60% over 0.3 min; *step 5*: from 60% MP A to the initial condition over 0.5 min and reconditioning for 4 min. The total run time was 7.5 min.

3.2.3.6 Mass spectrometry

Standard solutions prepared in 0.1% CH_3COOH acetonitrile/ water 1:1 (50 ng/mL) of sunitinib, N-desethyl sunitinib, and IS were infused at a flow rate of 10 µL/min in order to optimize all the MS parameters. Positive ion mode was used to obtain the mass spectra (MS_1) and the product ion spectra (MS_2). The instrument was equipped with a Turbo Ion Spray source operated at 625°C and with ion spray voltage of 5000 V. The biological samples were analyzed with ESI, using zero air as nebulizer gas (30 psi) and as heater gas (70 psi). Nitrogen was employed as curtain gas (20 psi) and as collision gas at medium intensity (CAD). After fragmentation, the characteristic product ions of the compounds were monitored in the third quadrupole at *m/z* 326.2, *m/z* 283.2 and *m/z* 238.2 for each analyte. Quantification was done in SRM mode using the following transitions: *m/z* 399.2 > 326.2 for sunitinib, *m/z* 371.2 > 283.2 for N-desethyl sunitinib, and *m/z* 409.2 > 328.2 for IS.

3.3 LC-MS/MS methods: validation study

All the three methods above described have been validated in accordance with the EMA and the FDA guidance on bio-analytical method validation (EMA, 2011) (FDA, 2013) (FDA, 2001). In particular, the validation study was conducted by examining the following parameters: recovery, linearity, intra- and inter-day precision and accuracy, reproducibility, limit of detection (LOD), LLOQ, selectivity, matrix effect, and stability.

3.3.1 Recovery

The percentage extraction recovery was determined for each analyte at three plasma concentrations (QCL, QCM and QCH) prepared in quintuplicate. The peak areas of each analyte extracted from plasma QC samples were compared to those from external standards prepared in methanol.

The recovery of IS was evaluated in the same way at the specific plasma concentration chosen for each method. Recovery of the analyte and the IS need not to be 100%, but it is important that the extent of recovery is consistent, precise and reproducible.

3.3.2 Linearity

The linearity of calibration curves was validated on five different working days. For each standard point, the ratio of the HPLC–MS/MS peak area for each analyte to the IS was calculated and plotted against the nominal concentration of each analyte in the sample. A weighted quadratic regression function ($1/x^2$) was applied to generate calibration curves.

The linearity of the standard curves was checked by regression analysis and the goodness of the regression by calculating the Pearson's determination coefficient R^2 and by comparison of the true and back-calculated concentrations of the calibration standards.

The accuracy of back-calculated values of an individual point had to be within 85–115% of the theoretical concentration (80–120% at the LLOQ), and a minimum of five standards had to meet these criteria, including the LLOQ and highest calibrator, ULOQ.

3.3.3 Intra-day and inter-day precision and accuracy and reproducibility

The precision of an analytical method describes the closeness of individual measures of an analyte when the procedure is applied repeatedly to multiple aliquots of a single homogeneous volume of biological matrix. The accuracy of an analytical method describes the closeness of mean test results obtained by the method to the actual value (concentration) of the analyte. This parameter was determined by expressing the mean calculated QC concentration as percentage of the nominal concentration.

Precision and accuracy were evaluated on five different days by measuring the analytes in three replicates at the three QC levels. To analyze the QC samples, different standard calibration curves were plotted and processed on each of the five days of the validation study. The precision of the method at each concentration was reported as the coefficient of variation (CV%), expressing the standard deviation as a percentage of the mean calculated concentration. The accuracy was determined by expressing the mean calculated concentration as a percentage of the nominal concentration. In each run, the measured concentration for at least six out of nine QC samples had to be within 15% of the nominal value. Only one QC sample could be excluded at each concentration level. As indicated in the FDA Draft Guidance for Industry on Bioanalytical Method Validation -September 2013-(Biopharmaceutics, Revision 1) (FDA, 2013), a revised version of the guidance published in May 2001 (FDA, 2001) taking into account the AAPS/FDA Workshop on Incurred Sample Reanalysis (Fast et al., 2009), evaluation of bioanalytical methods by re-analysis of incurred samples should be performed and can be considered as an additional measure of assay reproducibility. Incurred Sample Reanalysis (ISR) is a necessary component of bioanalytical method validation and is intended to verify the reliability of the reported subject sample analyte concentrations. ISR is conducted by repeating the analysis, with the same bioanalytical method procedures, of a subset of subject samples from a given study in separate runs on different days to critically support the precision and accuracy measurements established with spiked QCs. Therefore, the accuracy of the present method was assessed by re-analyzing the incurred plasma samples of one patient from the pharmacokinetic study in a further analytical session. The selection of samples for reanalysis was done guaranteeing adequate coverage of the pharmacokinetic profile in its entirety including a sample

around the maximum concentration (C_{max}) and in the elimination phase. The analyses can be considered equivalent if two-thirds (67%) of the percentage difference [(repeat-original)*100/mean] of the results is within 20%.

3.3.4 Limit of detection, limit of quantification, and selectivity

The LOD is the concentration at which the signal-to-noise ratio (S/N) is at least 3. The LLOQ of the bioanalytical method is the concentration of the lowest standard. The analyte response at the LLOQ should be at least 5 times the response compared to blank response. The LLOQ of the present method was assessed by adding F working solution to six samples of blank human plasma. Selectivity was proved using six independent sources of blank human plasma, which were individually analyzed and evaluated for interference: a single 95 µL-aliquot from each of the six matrices was spiked with the analytes at the LLOQ. Both LLOQ and selectivity had to have acceptable accuracy (≤20%) and precision (between 80% and 120%).

3.3.5 Matrix effect

Matrix effects arise due to effects of endogenous components of the plasma matrix on the ionization of the analytes of interest and IS. In the ESI source a process of charging and desolvation transforms the analytes in the liquid phase into gas ions that are introduced in MS analyzer. It seems clear that the coeluting compounds interfering with either the desolvation or the charging step alter the ionization of the analyte (González et al., 2014). Although they are generally the principal cause, not only endogenous components in the biological matrix (e.g. salts, amines, triglycerides) cause matrix effect, also some exogenous compounds (plasticizers from sample containers or anticoagulants in case of plasma) are susceptible to alter the ionization process (Mei et al., 2003). Furthermore, other substances can be present in the mobile phase and can alter the signal of the analyte by causing ion suppression or enhancement. Nevertheless this is not considered a matrix effect source since it is not sample specific (González et al., 2014).

Current FDA requirements underline the importance to assess this phenomenon in mass spectrometry, because it may compromise the precision, the accuracy, the sensitivity and the selectivity of the developed method and, consequently, the

reliability of analytical data produced. The same definition reported in the FDA guidance for matrix effect is given by EMA in the *Guideline on bioanalytical method validation* of 2011 (EMA, 2011). Both guides agree that the variability in the matrix effect, which would cause lack of reproducibility in the method, should be studied using six lots of blank matrix from individual donors. Indeed, a quantitative evaluation of matrix effect should be achieved by comparing the response of the analyte in solvent to the response obtained by spiking the analyte into six extracted independent sources of black human plasma. The matrix effect is calculated as the ratio of the peak area in the presence of matrix to the peak area in absence of matrix at the three different QC concentrations (L, M and H) of each analyte. The CV should be within 15%.

In addition, a common method to evaluate qualitatively the matrix effect is the post-column infusion, described by Bonfiglio and colleagues (Bonfiglio et al., 1999), which permits to identify the chromatographic region where the matrix effect manifests itself (González et al., 2014). A constant concentration of the analyte is introduced in the ion source of the mass spectrometer by using an infusion pump connected with a zero-dead-volume "T" junction after the HPLC column, while a blank extracted sample is injected onto the chromatographic system. The signal of the infused drug, followed in a SRM scan mode, is steady, unless endogenous components eluting from the column cause a reduction or a gain of the response. To assure the reliability of the results, it is important that these ion suppression or enhancement effects do not happen near the analyte retention time. To perform the post-column infusion experiments standard solutions, prepared in 0.1% CH_3COOH acetonitrile/water 1:1 (50 ng/mL) for each analyte and IS, were infused by a syringe pump.

3.3.6 Stability

Studying the stability of the analyte in stock solutions and matrix is vital to ensure the reliability of the results provided by the analytical method. These include assesses that cover all the situations that can be encountered during the whole analytical procedure such as freeze-thaw stability, short and long term stability, stock stability and post preparative stability.

Plasma stability each analyte was assessed by analyzing QC samples for each standard at the three different concentrations (L, M and H) during sample storage and handling.

Bench-top stability was determined after 2- or 4 h at room temperature (or in ice bath in the case of the CPT-11 method) and the stability of the processed samples in the autosampler was determined repeatedly analyzing the processed QC samples 24, 48 and 96 h after the first injection. To check freeze/thaw stability, a freshly prepared aliquot of each QC sample concentration was processed and analyzed, and then again after one and two freeze/thaw cycles. Long-term stability was assessed in plasma and in working solutions stored at approximately −80°C. Each analyte was considered stable at each concentration when the differences between the freshly prepared samples and the stability of testing samples did not deviate more than 15% from the nominal concentrations.

3.4 Calculation of the pharmacokinetic parameters

Pharmacokinetic parameters were calculated with Phoenix® WinNonlin™ 6.4, Pharsight, Certara Company (Princeton, New Jersey, USA). Data were fitted using the non-compartmental model (Urso et al., 2002) (Gabrielsson and Weiner, 2012).

A linear-log trapezoidal numerical integration method was used to calculate the area under the drugs and their main metabolites plasma concentration-time curve ($AUC_{0\text{-}last}$) from time 0 to the last sampling time:

(1) $$AUC_0^{t_{last}} = \sum_{i=1}^{n} \frac{C_i + C_{i+1}}{2} \cdot \Delta t$$

The closer time points are, the closer the trapezoids reflect the actual shape of the concentration-time curve. For this reason is very important to have tight samples time points especially near the C_{max}.

The extrapolation of the AUC from the last measurable concentration to infinity ($AUC_{0\text{-}\infty}$) was computed assuming that the wash-out in the terminal phase follows a monoexponential profile. Despite often in PK the drug profile is not monoexponential, it has been observed that the log-concentrations of many drugs in plasma and tissues decay linearly in the terminal phase.

A monoexponential function can be written as:

(2) $$C(t) = C_0 \cdot e^{-\lambda t}$$

Where C(t) is the drug concentration at time t and C_0 and λ (the elimination constant rate) are the parameters to be estimated. Ideally, to obtain a reliable estimate of the terminal slope, 3–4 half-lives would need to have elapsed. However, sometimes this is not possible and in this case it is allowed to consider 3–4 observations for the terminal slope to consider the estimation accurate. For this reason, the points used in the estimation should always be declared when the estimate of the terminal half-life is presented.

Integrating the equation (2) between 0 and infinity, we get:

(3) $$AUC_{t_{last}}^{\infty} = \int_{t_{last}}^{\infty} C_{last} \cdot e^{-\lambda_z (t - t_{last})} dt = \frac{C_{last}}{\lambda_z}$$

Starting from the monoexponential function (2) and taking into account that at $t_{1/2}$ the drug plasma concentration helves its value respect to the C_0, the following equation is obtained for the elimination half-life:

(4) $$t_{1/2} = \frac{ln2}{\lambda_z}$$

The most useful parameter for the evaluation of an elimination mechanism is the Cl that, in the non-compartmental analysis, represents the sum of all organs clearance, especially hepatic and renal clearance, the two major organs of elimination. Clearance can be defined as the drug amount eliminated per unit of time, which is the rate of excretion (X_e), over drug concentration in plasma:

(5) $$Cl = \frac{dX_e}{dt} \cdot \frac{1}{C(t)}$$

Integrating the equation (5) between 0 and infinity it is possible to obtain:

(6) $$Cl = \frac{D}{AUC_0^{\infty}}$$

Where D is the total amount of drug that enters into the systemic circulation that is, after an intravenous administration, the dose.

The V_d is the apparent volume into which the total amount of drug needs to be dissolved to maintain the same concentration as the plasma. This parameter it is useful to correlate the drug in the body to the measured concentration in the plasma, in fact V_d can be defined as:

(7) $$V_d = \frac{D}{C_0}$$

Using monoexponential function to redefine C_0 (2) and making the integration between 0 and infinity of the equation obtained, it is possible to express the V_d on the basis of the dose (D), $AUC_{0-\infty}$ and λ_z:

(8) $$V_d = \frac{D}{AUC_0^{\infty}} \cdot \frac{1}{\lambda_z}$$

3.5 Statistics

Differences in the pharmacokinetic parameters of the drugs and their metabolites between the different administrations (day1-3 vs day15-17 in the case of CPT-11, and I vs IV administration in case of PTX) were tested by the non-parametric Wilcoxon signed rank matched pairs test.

The correlation between CPT-11/PTX dose and pharmacokinetic parameters was tested by Spearman's rank correlation test.

The effects of drugs doses and patient's genotype on PFS were estimated using the Kaplan-Meier estimator, and differences were tested using the log-rank test. ORRs (complete + partial response) between groups were compared using Fisher's exact test for count data. For all comparisons, a two-sided p value <0.05 was considered significant, not adjusted for multiple comparisons due to the exploratory nature of the analyses.

4 RESULTS

4.1 LC-MS/MS methods: development and validation

4.1.1 High-performance liquid chromatography–tandem mass spectrometry method for the simultaneous determination of irinotecan and its main metabolites in human plasma

4.1.1.1 HPLC-MS/MS

To optimize the mass spectrometer conditions, an infusion of each standard solution at 50 ng/mL in mobile phases (50:50) was used. The source and compound dependent parameters so optimized are reported in Table 4, together with the ion transitions of each analyte used for the mass spectrometer method.

Table 4 Source- and compound-dependent parameters and ion transitions of each analyte and IS used for the mass spectrometer method. The dwell time of each transition was set up at 50 msec. DP: declustering potential; EP: entrance potential; CE: collision energy; CXP: collision cell exit potential.

Precursor Ion				**Daughter Ion**		
Analyte	**Q1 (amu)**	**DP (volts)**	**EP (volts)**	**Q3 (amu)**	**CE (volts)**	**CXP (volts)**
CPT-11	587.4	125	11	**124.2**	51	6
				167.2	58	10
				195.2	44	13
SN-38	393.3	103	13	**349.3**	35	8
				249.1	68	15
				293.2	47	13
SN-38G	569.3	113	11	**393.2**	40	8
				349.2	60	7
				249.2	104	16
APC	619.2	115	12	**393.3**	45	9
				227.1	36	14
				349.2	62	7
CPT (IS)	349.2	75	10	**305.1**	33	15
				248.9	43	16
				220.1	48	13

The fragmentation patterns are represented in Figure 24. For each compound, the daughter ion with the highest signal was used as quantifier, as follows: 587.4 >124.2 for

CPT-11, 393.3>349.3 for SN-38, 569.3>393.2 for SN-38G, 619.2>393.3 for APC and 349.2>305.1 for IS, all expressed in *m/z*.

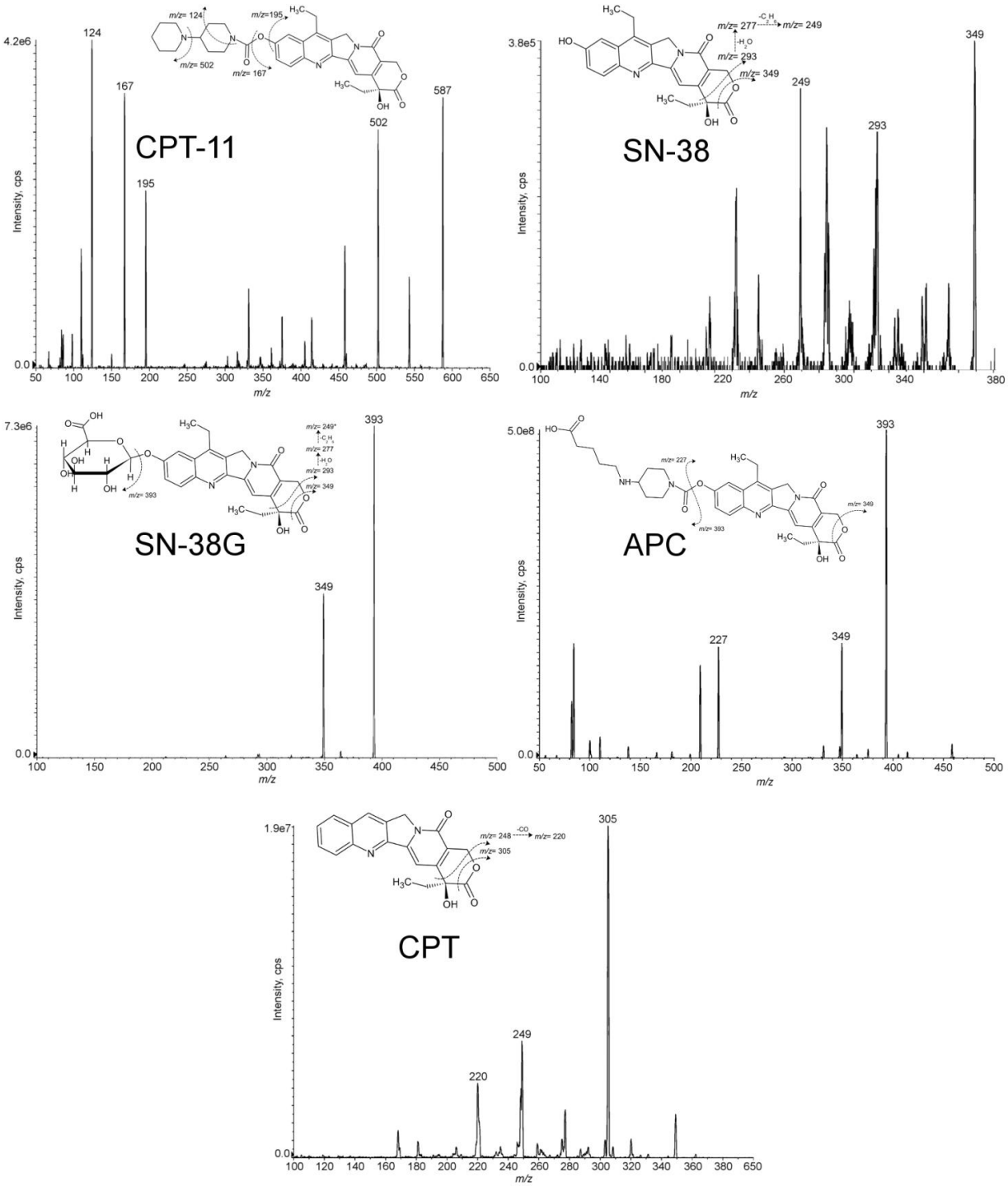

Figure 24 MS/MS mass spectra of CPT-11, SN-38, SN-38G and APC with chemical structures and identification of the main fragment ions. The fragment ion at *248 *m/z* of SN-38G is not shown in the MS/MS mass spectrum because it requires, for its formation, a higher collision energy than the other fragments.

Figure 25 presents typical SRM chromatograms, using the quantifier transitions noted above.

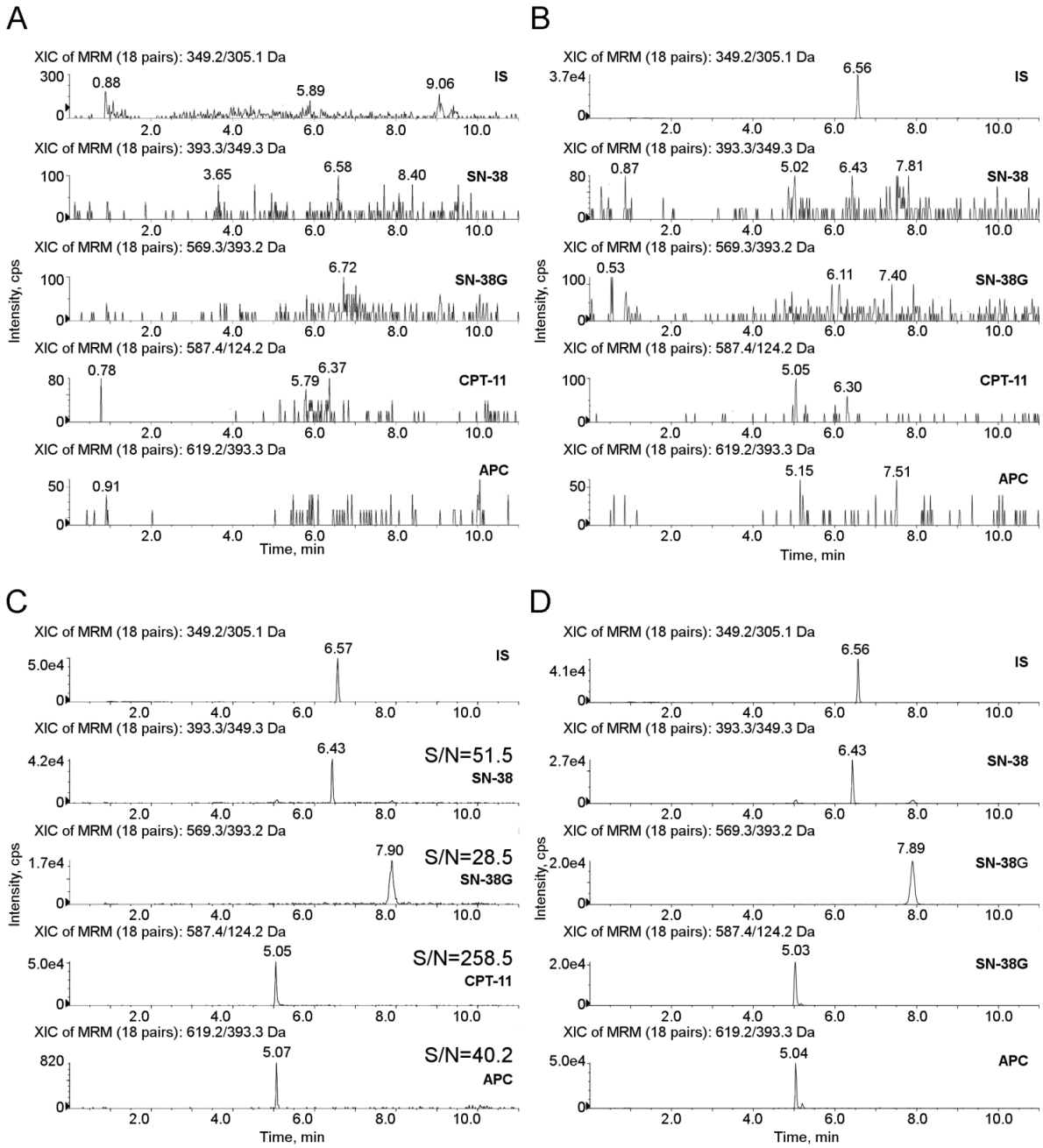

Figure 25 Representative SRM chromatograms. **Panel A**: SRM chromatograms of a human blank plasma sample; **Panel B**: SRM chromatograms of a human blank plasma sample with IS added; **Panel C**: S/N of SN-38, SN-38G, CPT-11 and APC at the LLOQ (10 ng/mL for CPT-11 and 1 ng/mL for SN-38, SN-38G and APC); **Panel D**: SRM chromatograms of an extracted plasma sample of a treated patient showing IS, SN-38, SN-38G, CPT-11 and APC.

Panel A shows an extracted blank plasma sample; Panel B displays an extracted blank plasma sample with IS added; Panel C shows an extracted plasma sample at the LLOQ with IS added and Panel D displays an extracted plasma sample of a patient, drawn 26 h after the drug dose of 310 mg/m^2. The peaks correspond to a concentration of 80.27, 7.42, 16.57 and 12.91 ng/mL of CPT-11, SN-38, SN-38G, APC, respectively. The elution of the analytes was rapid and selective with adequate separation of all the peaks within 9 min: CPT-11, SN-38, SN-38G, APC and IS were eluted at approximately 5.05, 6.43, 7.9, 5.07 and 6.57 min, respectively. No interfering peaks were observed at these retention times, and the peaks were completely resolved from plasma matrix, with a good shape. The specificity of the method was confirmed by analyzing six independent sources of blank human plasma.

4.1.1.2 Validation of the method

Recovery. The extraction method is based on simple deproteinization with three volumes of 0.1% CH_3COOH/CH_3OH relative to plasma sample (Table 5).

Table 5 Recovery of the analytes and the IS from human plasma.

Analyte	Nominal concentration (ng/mL)	Recovery (%) ± SD	CV %
CPT-11	25.00	66.4 ± 5.7	8.6
	6000.00	68.3 ± 1.6	2.3
	9000.00	68.8 ± 1.6	2.3
SN-38	2.00	77.2 ± 7.3	9.4
	150.00	83.8 ± 2.8	3.4
	400.00	84.1 ± 1.0	1.2
SN-38G	2.00	58.6 ± 7.1	12.1
	150.00	54.8 ± 2.6	4.8
	400.00	56.4 ± 0.8	1.4
APC	2.00	44.0 ± 4.7	10.6
	2000.00	47.6 ± 2.3	4.7
	4000.00	49.1 ± 0.9	1.9
CPT (IS)	25.00	30.6 ± 2.1	6.9

The recovery, evaluated in five replicates at three QC concentrations, was in the range 66.4-68.8% (CV ≤8.6%) for CPT-11, 77.2-84.1% (CV ≤9.4%) for SN-38, 54.8-58.6% (CV ≤12.1%) for SN-38G and within 44.0-49.1% (CV ≤10.6%) for APC. The recovery of IS was 30.6% (CV 6.9%).

Calibration Curves. Table 6 reports the results for the calibration curves of CPT-11 and its main metabolites freshly prepared every day during the validation study, and the accuracy and precision for each standard (Figure 26).

Table 6 Linearity, accuracy and precision data for calibration curves of CPT-11 and its main metabolites.

Analyte	Nominal conc. (ng/mL)	Mean ± SD	Precision %	Accuracy %
CPT-11	10.00	9.88 ± 0.03	0.3	98.8
	100.00	111.90 ± 3.18	2.8	111.9
	1000.00	1070.91 ± 61.18	5.7	107.1
	5000.00	4671.81 ± 114.51	2.5	93.4
	8000.00	7568.46 ± 500.11	6.6	94.6
	10000.00	9420.12 ± 513.90	5.5	94.2
SN-38	1.00	1.00 ± 0.01	1.0	99.8
	5.00	5.01 ± 0.29	5.9	100.2
	25.00	25.70 ± 0.86	3.4	102.8
	100.00	99.35 ± 5.09	5.1	99.4
	250.00	251.99 ± 10.01	4.0	100.8
	500.00	484.99 ± 31.86	6.6	97.0
SN-38G	1.00	1.00 ± 0.01	1.5	100.1
	5.00	4.98 ± 0.38	7.7	99.6
	25.00	24.67 ± 0.86	3.5	98.7
	100.00	101.40 ± 3.48	3.4	101.4
	250.00	253.43 ± 14.12	5.6	101.4
	500.00	494.14 ± 34.95	7.1	98.8
APC	1.00	1.00 ± 0.01	0.7	99.7
	10.00	10.38 ± 0.68	6.5	103.8
	100.00	105.44 ± 5.01	4.8	105.4
	1000.00	943.42 ± 39.02	4.1	94.3
	2500.00	2469.92 ± 207.95	8.4	98.8
	5000.00	4935.06 ± 264.42	5.4	98.7

The calibration curves prepared on five different days showed good linearity and acceptable results of the back-calculated concentrations over the validated range of

10.00-10000.00 ng/mL for CPT-11, of 1.00-500.00 ng/mL for SN-38 and SN-38G and of 1.00-5000.00 ng/mL for APC. Pearson's coefficient of determination R^2 was ≥0.9962 for each run, the mean accuracy was always close to 100% (range 93.4-111.9% for CPT-11, 97.0-102.8% for SN-38, 98.7-101.4% for SN-38G and 94.3-105.4% for APC) and the precision, expressed as CV%, ranged from 0.3% for the lowest calibrator (10.00 ng/mL) to 6.6% for CPT-11, from 1.0 to 6.6% for SN-38, from 1.5 to 7.7% for SN-38G and from 0.7 to 8.4% for APC. In order to quantify patients' samples, a calibration curve was freshly prepared every analysis run and the samples' concentrations were back-calculated from the calibration curve.

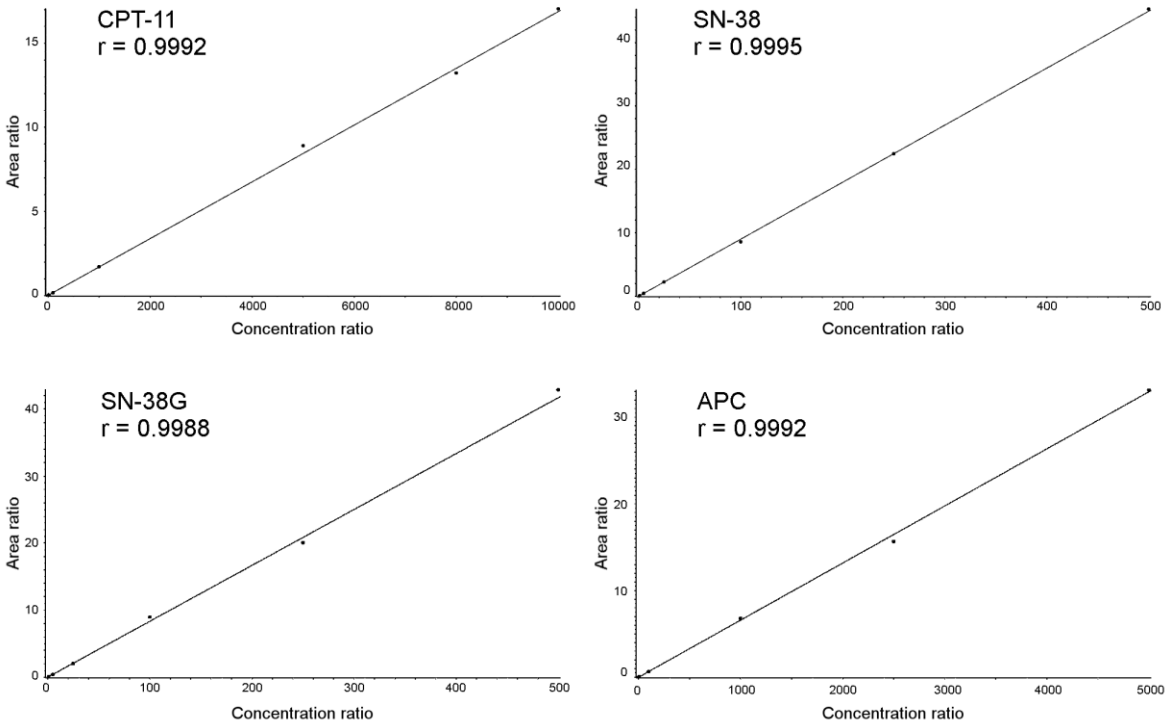

Figure 26 Calibration curve of CPT-11 and its main metabolites SN-38, SN-38G and APC in human plasma.

***Intra-day and inter-day Precision and Accuracy and Reproducibility*.** The precision and accuracy of the method were evaluated by analysing three replicates of QC samples (QCL, QCM and QCH) within a single-run analysis for intra-day assessment and over five consecutive runs for inter-day assessment. The accuracy and precision (CV%) obtained are shown in Table 7. The method was very precise, with intra- and inter-day CV ≤8.9% and ≤8.7% for CPT-11, ≤11.6% and ≤9.9% for SN-38, ≤9.0% for SN-38G and ≤10.7% and ≤12.2% for APC.

Table 7 Intra and inter-day precision and accuracy of the method for the analysis of CPT-11 and its main metabolites in human plasma samples.

	Analyte	Nominal conc. (ng/mL)	Mean ± SD	Precision %	Accuracy %
Intra-day (N=5)	CPT-11	25.00	25.42 ± 2.26	8.9	101.7
		6000.00	6379.41 ± 520.23	8.2	106.3
		9000.00	9090.55 ± 369.12	4.1	101.0
	SN-38	2.00	2.17 ± 0.14	6.5	108.7
		150.00	163.43 ± 18.97	11.6	109.0
		400.00	384.85 ± 14.03	3.6	96.2
	SN-38G	2.00	1.85 ± 0.17	9.0	92.3
		150.00	169.52 ± 3.73	2.2	113.0
		400.00	405.40 ± 15.15	3.7	101.3
	APC	2.00	2.10 ± 0.22	10.7	105.2
		2000.00	1788.03 ± 83.27	4.7	89.4
		4000.00	4242.35 ± 170.47	4.0	106.1
Inter-day (N=14)	CPT-11	25.00	24.77 ± 2.16	8.7	99.1
		6000.00	5986.95 ± 483.98	8.1	99.8
		9000.00	8667.00 ± 580.72	6.7	96.3
	SN-38	2.00	2.02 ± 0.20	9.9	101.2
		150.00	158.78 ± 13.97	8.8	105.9
		400.00	387.53 ± 21.46	5.5	96.9
	SN-38G	2.00	1.98 ± 0.18	9.0	98.9
		150.00	153.45 ± 11.89	7.8	102.3
		400.00	393.07 ± 20.94	5.3	98.3
	APC	2.00	2.06 ± 0.25	12.2	103.2
		2000.00	1881.31 ± 158.89	8.4	94.1
		4000.00	3984.00 ± 346.26	8.7	99.6

Moreover, the method showed intra- and inter-day accuracy within the range 101.0-106.3% and 96.3-99.8% for CPT-11, 96.2-109.0% and 96.9-105.9% for SN-38, 92.3-113.0% and 98.3-102.3% for SN-38G and 89.4-106.1% and 94.1-103.2% for APC. The good reproducibility and accuracy of the method were further demonstrated by re-

analysis of incurred plasma samples of one patient treated at the dose of 260 mg/m^2 (Figure 27).

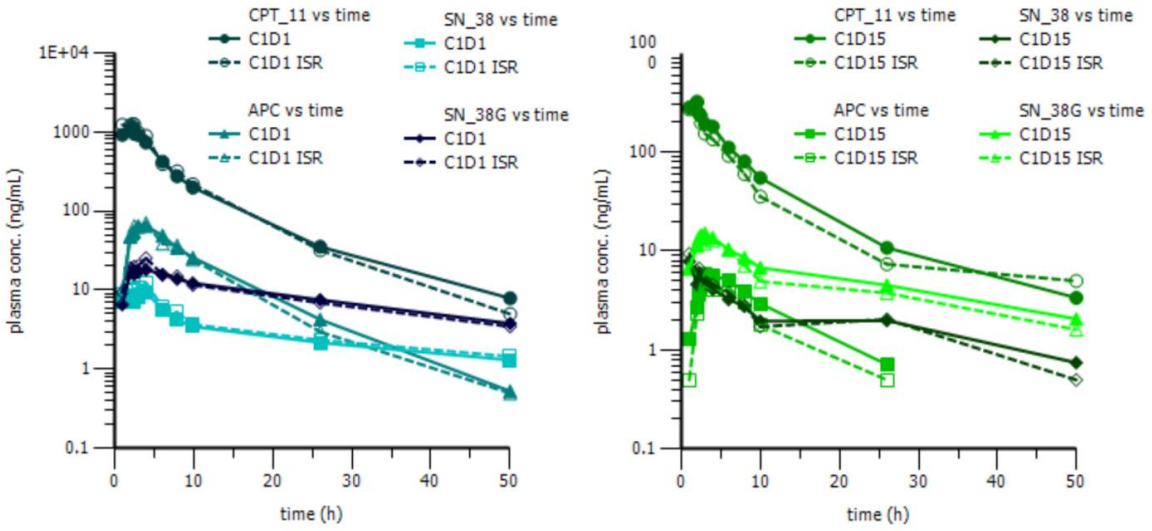

Figure 27 Re-analysis of incurred plasma samples of one patient treated at the dose of 260 mg/m^2 during the first (C1D1, on the left) and the second (C1D15, on the right) of the first chemotherapy cycle.

The concentrations of CPT-11 and its main metabolites determined on the two analytical runs were very similar in all samples, being the percentage difference of the results within 20% for more than 71% of the total amount of samples re-analyzed. This range encompasses the accepted variability of the analytical method; hence, the two measurements can be considered equivalent.

Limit of Detection, Limit of Quantification, Selectivity and Matrix Effect. The LOD was defined as the concentration at which the S/N was at least 3. The LOD was 58 pg/mL for SN-38, 105 pg/mL for SN-38G, 116 pg/mL for CPT-11 and 75 pg/mL for APC. As shown in Panel C of Figure 25, with the high S/N obtained (S/N range: 28.5-258.5), it would have been possible to fix a lower LLOQ for each analyte. However, the LLOQ values were chosen on the basis of the concentration range expected in plasma samples of patients enrolled in the phase I study. Therefore, the LLOQ was fixed at 1 ng/mL for SN-38, SN-38G and APC and at 10 ng/mL for CPT-11 and was validated through analysis of six replicates. The accuracy and precision at the LLOQ were determined by analyzing six replicates of the sample at the LLOQ concentration. The accuracy and CV% were,

respectively, 91.0% and 4.9% for CPT-11, 111.4% and 5.2% for SN-38, 94.2% and 7.9% for SN-38G and 98.3% and 11.2% for APC. The method was not affected by endogenous components in the matrix or other components in the sample; on spiking six different sources of human plasma with CPT-11 and its main metabolites at a concentration corresponding to the LLOQ the precision was 4.9, 5.2, 7.9 and 11.2% for CPT-11, SN-38, SN-38G and APC, respectively and the accuracy was 91.0, 111.4, 94.2 and 98.3%, respectively. There were no significant variations (<15%) in the peak area of each analyte in the six lots of matrix, therefore it was possible to exclude the presence of any matrix effect of ion suppression or enhancement. The absence of the matrix effects has been determined also by the post column infusion test and by comparing the peak area of the analyte extracted from plasma QC samples with the peak area of the extracted matrix prepared in five replicates and added with the same amount of the analyte (data not shown).

Stability. CPT-11 and its main metabolites resulted stable for 2 h in ice bath and for 96 h in the autosampler at 4°C after extraction (Table 8).

CPT-11 and its main metabolites were stable in human plasma over two freeze/thaw cycles: precision as CV% and accuracy for freeze/thaw samples were ≤5.3% and within 86.7-97.6% for CPT-11, ≤6.5% and within 101.3-105.4% for SN-38, ≤3.2% and within 88.1-90.7% for SN-38G and ≤11.0% and within 94.6-95.3% for APC (Table 9).

After 4 months of storage in human plasma, at approximately -80°C, precision (CV%) and accuracy obtained were ≤9.9% and within 94.4-102.2% for CPT-11, ≤8.3% and within 93.5-103.6% for SN-38, ≤8.6% and within 85.2-92.0% for SN-38G and ≤8.3% and within 92.5-104.5% for APC (Table 9).

The standard working solutions of CPT-11, SN-38, SN-38G and APC used for calibration curve and QC samples, prepared in methanol and stored at –80°C, were stable after 9 months: CV% and accuracy were ≤5.9% and within 107.1-108.9% for CPT-11, ≤4.4% and within 100.3-104.9% for SN-38, ≤6.5% and within 99.0-109.1% for SN-38G and ≤14.4% and within 97.1-111.3% for APC (Table 10).

Table 8 Short term stability of CPT-11 and its main metabolites in human plasma samples.

Analytes	Nominal conc. (ng/mL)	T = 2 h			T = 96 h in autosampler (4°C)		
		Mean ± SD	Prec %	Acc %	Mean ± SD	Prec %	Acc %
CPT-11	25.00	23.93 ± 2.83	11.8	95.7	22.71 ± 0.80	3.5	90.8
	6000.00	5983.16 ± 268.62	4.5	99.7	5443.19 ± 270.24	5.0	90.7
	9000.00	8645.98 ± 303.46	3.5	96.1	8337.48 ± 963.60	11.6	92.6
SN38	2.00	1.96 ± 0.02	1.2	98.1	1.89 ± 0.25	13.4	94.6
	150.00	154.21 ± 2.16	1.4	102.8	136.06 ± 7.51	5.5	90.7
	400.00	402.43 ± 17.77	4.4	100.6	360.09 ± 26.21	7.3	90.0
SN-38 G	2.00	1.90 ± 0.02	1.1	95.2	1.80 ± 0.11	6.1	90.2
	150.00	147.04 ± 2.68	1.8	98.0	127.55 ± 0.84	0.7	85.0
	400.00	379.76 ± 24.29	6.4	94.9	360.82 ± 34.01	9.4	90.2
APC	2.00	2.08 ± 0.19	8.9	103.9	1.84 ± 0.12	6.8	91.9
	2000.00	1864.57 ± 86.08	4.6	93.2	1715.93 ± 13.10	0.8	85.8
	4000.00	3955.31 ± 235.24	5.9	98.9	3716.48 ± 424.53	11.4	92.9

Table 9 Stability of CPT-11 and its metabolites after 2 freeze-thaw cycles and after 4 months at -80°C.

Analytes	Nominal conc. (ng/mL)	After 2 freeze-thaw cycles			Stored at -20°C over 4 months		
		Mean ± SD	Prec %	Acc %	Mean ± SD	Prec %	Acc %
CPT-11	25.00	21.67 ± 0.12	0.6	86.7	25.55 ± 2.53	9.9	102.2
	6000.00	5853.32 ± 237.66	4.1	97.6	5941.81 ± 322.04	5.4	99.0
	9000.00	8381.75 ± 445.81	5.3	93.1	8496.65 ± 605.20	7.1	94.4
SN38	2.00	2.11 ± 0.06	2.8	105.4	2.07 ± 0.17	8.3	103.6
	150.00	151.97 ± 9.86	6.5	101.3	154.76 ± 3.98	2.6	103.2
	400.00	412.38 ± 16.19	3.9	103.1	374.05 ± 30.58	8.2	93.5
SN-38 G	2.00	1.81 ± 0.05	2.8	90.5	1.84 ± 0.16	8.6	92.0
	150.00	136.10 ± 3.72	2.7	90.7	130.48 ± 2.60	2.0	87.0
	400.00	352.52 ± 11.30	3.2	88.1	340.69 ± 0.28	0.1	85.2
APC	2.00	1.91 ± 0.21	11.0	95.3	2.09 ± 0.17	8.3	104.5
	2000.00	1891.29 ± 160.58	8.5	94.6	1870.85 ± 136.92	7.3	93.5
	4000.00	3791.48 ± 280.50	7.4	94.8	3699.92 ± 254.86	6.9	92.5

Table 10 Stability of the working solutions of CPT-11 and its main metabolites stored at -80°C over 9 months.

Analytes	Nominal conc. (ng/mL)	Stored at -80°C over 9 months		
		Mean ± SD	Prec. %	Acc. %
CPT-11	25.00	26.78 ± 1.08	4.0	107.1
	6000.00	6533.20 ± 388.29	5.9	108.9
	9000.00	9798.46 ± 396.30	4.0	108.9
SN38	2.00	2.01 ± 0.06	2.8	100.3
	150.00	154.57 ± 6.09	3.9	103.0
	400.00	419.47 ± 18.31	4.4	104.9
SN-38 G	2.00	1.98 ± 0.05	2.5	99.0
	150.00	149.18 ± 9.72	6.5	99.5
	400.00	436.51 ± 21.69	5.0	109.1
APC	2.00	1.94 ± 0.28	14.4	97.1
	2000.00	2058.05 ± 74.43	3.6	102.9
	4000.00	4451.13 ± 107.37	2.4	111.3

4.1.2 High-performance liquid chromatography–tandem mass spectrometry method for the simultaneous determination of paclitaxel and its main metabolite 6α-hydroxy-paclitaxel in human plasma

4.1.2.1 HPLC-MS/MS

An infusion of each standard solution at 50 ng/mL in mobile phases (50:50) was used to optimize the mass spectrometer parameters, reported in the following table (Table 11).

Table 11 Source- and compound-dependent parameters and ion transitions of each analyte and IS used for the mass spectrometer method The dwell time of each transition was set up at 50 msec. DP: declustering potential; EP: entrance potential; CE: collision energy; CXP: collision cell exit potential.

Precursor Ion				**Daughter ion**		
Analyte	**Q1 (amu)**	**DP (volts)**	**EP (volts)**	**Q3 (amu)**	**CE (volts)**	**CXP (volts)**
PTX	854.5	63	9	**569.3**	15	18
				286.3	23	7
				105.1	95	19
6α-OH-PTX	870.5	63	8	**286.3**	23	7
				105.1	94	18
				525.3	22	16
DTX	808.5	50	7	**226.3**	23	22
				527.3	14	16

The fragmentation patterns are represented in Figure 28. For each compound, the daughter ion with the highest signal was used as quantifier, as follows: 854.5 >569.3 for PTX, 870.5>286.3 for 6α-OH-PTX, and 808.5>226.3 for IS, all expressed in *m/z*. Figure 29 presents typical SRM chromatograms, using the quantifier transitions noted above. Panel A shows an extracted blank plasma sample; Panel B displays an extracted blank plasma sample with IS added; Panel C shows an extracted plasma sample at the LLOQ with IS added and Panel D displays an extracted plasma sample of a patient, drawn at the end of the 1-h intravenous infusion of 80 mg/m^2 of PTX. The peaks correspond to a concentration of 1997.39 and 93.67 ng/mL of PTX and 6α-OH-PTX, respectively. The

elution of the analytes was rapid and selective with adequate separation of all the peaks within 10 min: PTX, 6α-OH-PTX and IS were eluted at approximately 8.40, 7.15 and 8.04 min, respectively. No interfering peaks were observed at these retention times, and the peaks were completely resolved from plasma matrix, with a good shape. The specificity of the method was confirmed by analyzing six independent sources of blank human plasma.

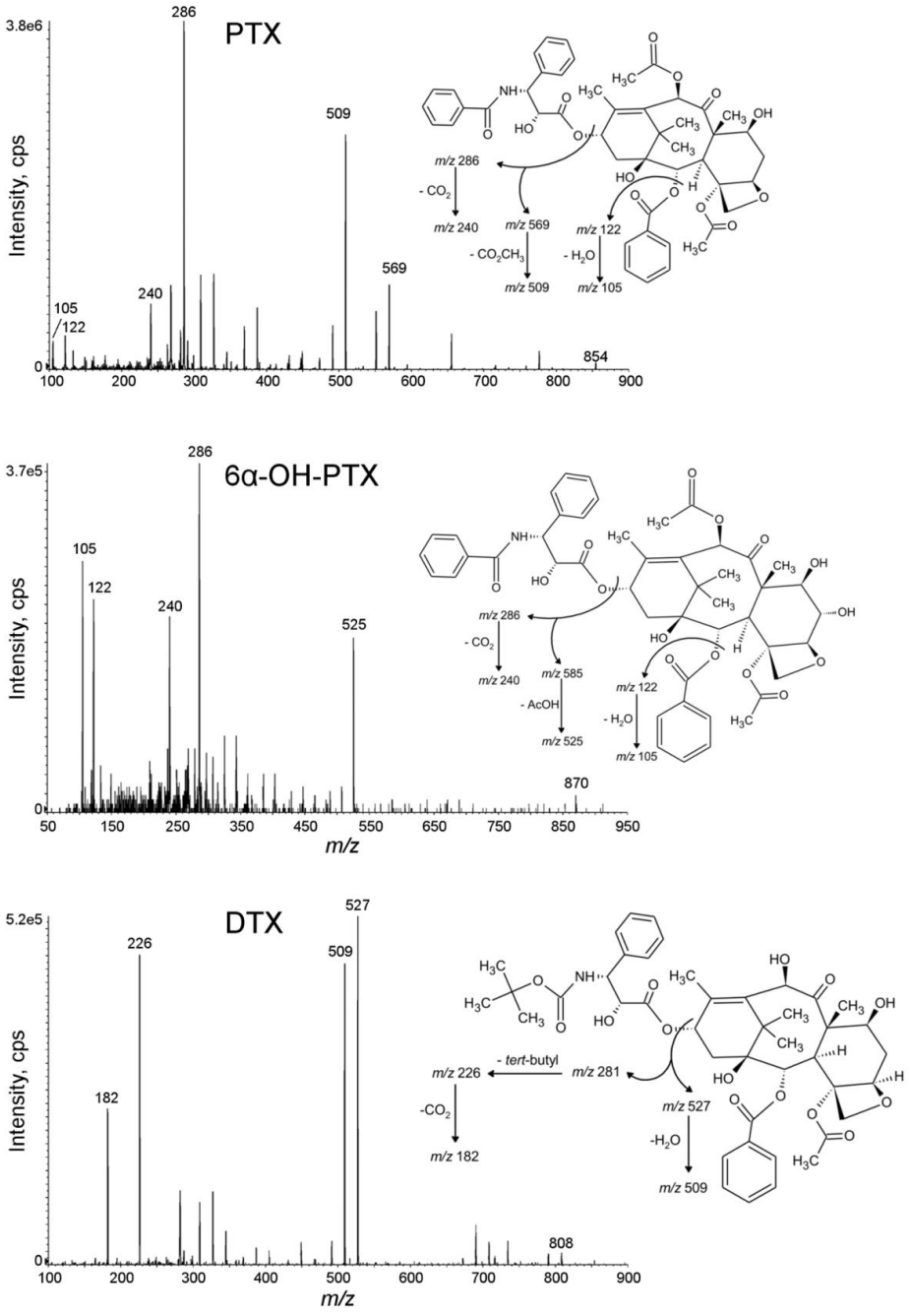

Figure 28 MS/MS mass spectra of PTX and 6α-OH-PTX with chemical structures and identification of the main fragment ions.

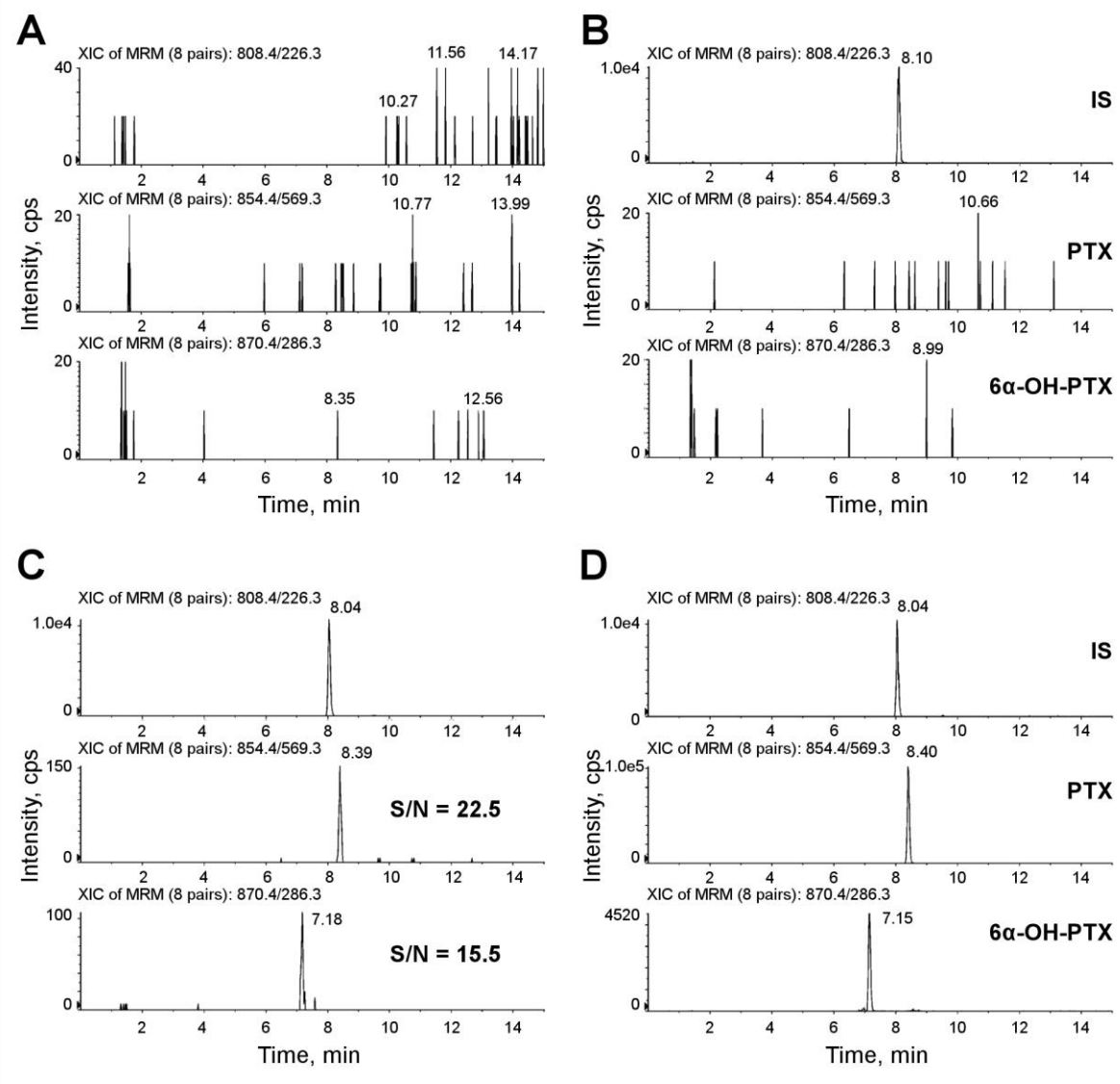

Figure 29 Representative SRM chromatograms. **Panel A**: SRM chromatograms of a human blank plasma sample; **Panel B**: SRM chromatograms of a human blank plasma sample with IS added; **Panel C**: S/N of PTX and 6α-OH-PTX at the LLOQ (1 ng/mL for both analytes); Panel D: SRM chromatograms of an extracted plasma sample of a treated patient showing IS, PTX and 6α-OH-PTX.

4.1.2.2 Validation of the method

Recovery. The extraction method is based on simple deproteinization with four volumes of 0.1%HCOOH/CH_3OH relative to plasma sample. The recovery, evaluated in five replicates at three QC concentrations, was in the range 92.4-95.7% (CV ≤6.9%) for PTX and 93.4-97.7% (CV ≤5.5%) for 6α-OH-PTX, as shown in Table 12. The recovery of IS was 101.2% (CV 4.4%).

Table 12 Recovery of the analytes and the IS from human plasma.

Analyte	Nominal concentration (ng/mL)	Recovery (%) ± SD	CV %
PTX	3	95.7 ± 6.4	6.6
	625	92.4 ± 6.4	6.9
	7500	93.8 ± 1.3	1.4
6α-OH-PTX	3	94.2 ± 1.9	2.0
	75	97.7 ± 5.4	5.5
	750	93.4 ± 2.6	2.8
DTX (IS)	200	101.2 ± 4.5	4.4

Calibration Curves. Table 13 reports the results for the calibration curves of PTX and its main metabolite 6α-OH-PTX freshly prepared every day during the validation study, and the accuracy and precision for each standard.

Table 13 Linearity, accuracy and precision data for calibration curves of PTX and its metabolite 6α-OH-PTX.

Analytes	Nominal conc. (ng/mL)	Mean ± SD	Precision %	Accuracy %
PTX	1	0.99 ± 0.01	0.6	99.4
	10	10.59 ± 0.68	6.4	105.9
	50	50.91 ± 1.74	3.4	101.8
	250	269.00 ± 9.05	3.4	107.6
	1000	1020.79 ± 52.28	5.1	102.1
	5000	4488.84 ± 161.87	3.6	89.8
	10000	9292.7 ± 736.14	7.9	92.9
6α-OH-PTX	1	1.01 ± 0.01	0.8	100.8
	5	4.82 ± 0.27	5.7	96.5
	25	21.74 ± 0.48	2.2	87.0
	50	53.40 ± 3.63	6.8	106.8
	100	102.43 ± 4.12	4.0	102.4
	500	512.77 ± 17.90	3.5	102.6
	1000	1011.36 ± 71.36	7.1	101.1

The calibration curves (Figure 30) prepared on five different days showed good linearity and acceptable results of the back-calculated concentrations over the validated range of 1.00-10000.00 ng/mL for PTX and of 1.00-1000.00 ng/mL for 6α-OH-PTX. Pearson's coefficient of determination R^2 was ≥0.9948 for each run, the mean accuracy was always close to 100% (range 89.8-107.6% for PTX and 87.01-106.8% for 6α-OH-PTX) and the precision, expressed as CV%, ranged from 0.6% for the lowest calibrator (1.00 ng/mL) to 7.9% for PTX and from 0.8 to 7.1% for 6α-OH-PTX. In order to quantify patients' samples, a calibration curve was freshly prepared every analysis run and the samples' concentrations were back-calculated from the calibration curve.

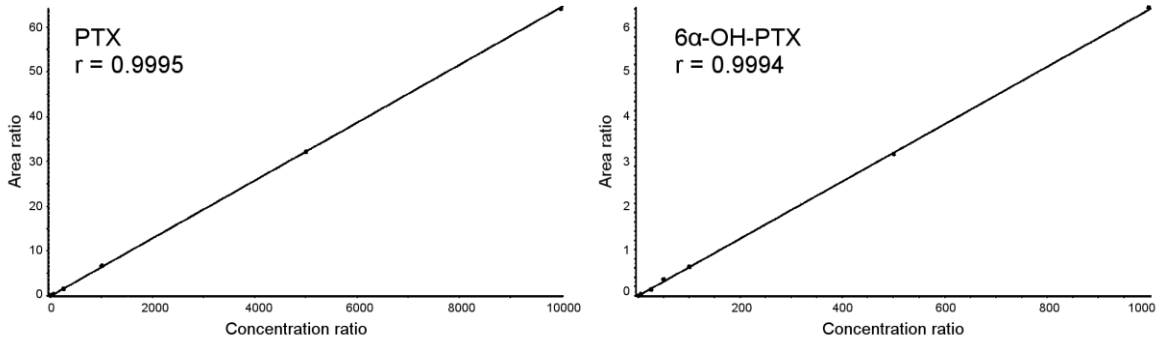

Figure 30 Calibration curve of PTX and its main metabolite 6α-OH-PTX in human plasma.

Intra-day and inter-day Precision and Accuracy and Reproducibility. The precision and accuracy of the method were evaluated by analysing three replicates of QC samples (QCL, QCM and QCH) within a single-run analysis for intra-day assessment and over five consecutive runs for inter-day assessment. The accuracy and precision (CV%) obtained are shown in Table 14. The method was very precise, with intra- and inter-day CV ≤9.2% and ≤7.0% for PTX and ≤7.9% and ≤9.9% for 6α-OH-PTX. Moreover, the method showed intra- and inter-day accuracy within the range 91.1-98.4% and 94.0-104.8% for PTX and 92.8-103.3% and 99.5-104.0% for 6α-OH-PTX. The good reproducibility and accuracy of the method were further demonstrated by re-analysis of incurred plasma samples of one patient treated at the dose of 100 mg/m^2. The concentrations of PTX and its main metabolite determined on the two analytical runs were very similar in all samples, being the percentage difference of the results within 20% for more than 94.1 and 91.7% of the total amount of samples re-analyzed for PTX

and 6α-OH-PTX, respectively. This range encompasses the accepted variability of the analytical method; hence, the two measurements can be considered equivalent.

Table 14 Intra and inter-day precision and accuracy of the method for the analysis of PTX and its metabolite 6α-OH-PTX in human plasma samples.

	Analytes	Nominal concentration (ng/mL)	Mean ± SD	Precision %	Accuracy %
Intra-day (N=5)	PTX	3	3.18 ± 0.29	9.2	94.4
		625	685.97 ± 40.72	5.9	91.1
		7500	7619.62 ± 370.09	4.9	98.4
	6α-OH-PTX	3	2.91 ± 0.23	7.9	103.3
		75	80.85 ± 4.24	5.2	92.8
		750	808.02 ± 50.47	6.2	92.8
Inter-day (N=15)	PTX	3	3.14 ± 0.19	5.9	104.8
		625	644.20 ± 45.22	7.0	103.1
		7500	7047.92 ± 477.06	6.8	94.0
	6α-OH-PTX	3	2.99 ± 0.29	9.9	99.5
		75	77.99 ± 5.73	7.3	104.0
		750	766.42 ± 58.58	7.6	102.2

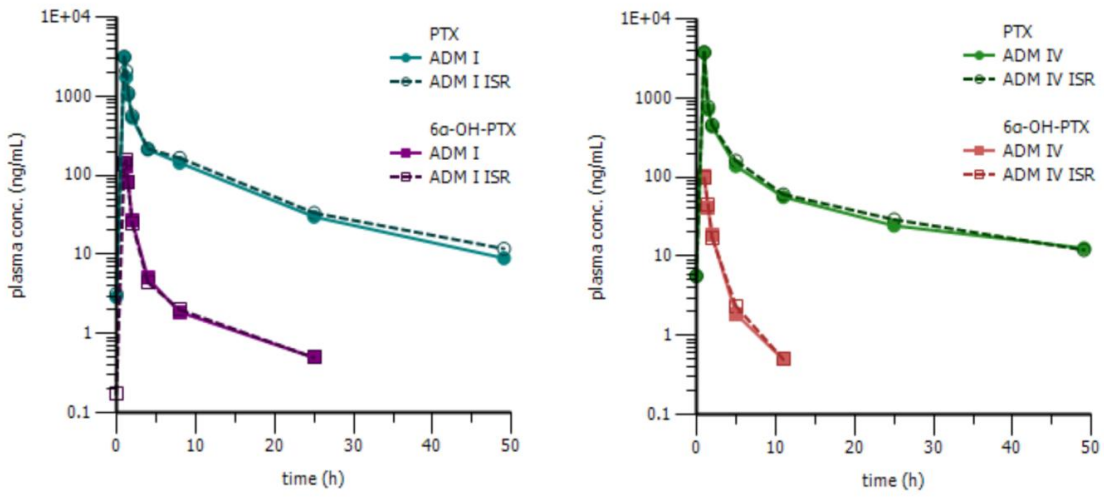

Figure 31 Re-analysis of incurred plasma samples of one patient treated at the dose of 100 mg/m^2 during the first (I ADM, left) and the fourth (IV ADM, right) of the first chemotherapy cycle.

Limit of Detection, Limit of Quantification, Selectivity and Matrix Effect. The LOD, defined as the concentration at which the S/N was at least 3, was 0.13 ng/mL for PTX and 0.19 ng/mL for 6α-OH-PTX. As shown in Panel C of Figure 29, reporting the S/N values obtained (22.5 and 15.5 for PTX and 6α-OH-PTX, respectively), the LLOQ was fixed at 1 ng/mL for both PTX and its metabolite 6α-OH-PTX and was validated through analysis of six replicates. The accuracy and precision at the LLOQ were determined by analyzing six replicates of the sample at the LLOQ concentration. The accuracy and CV% were, respectively, 109.8% and 5.0% for PTX and 106.5% and 8.1% for 6α-OH-PTX.

The method was not affected by endogenous components in the matrix or other components in the sample; on spiking six different sources of human plasma with PTX and 6α-OH-PTX at a concentration corresponding to the LLOQ the precision was 12.5 and 6.5 % for PTX and 6α-OH-PTX, respectively and the accuracy was 107.5 and 104.0%, respectively. There were no significant variations (<15%) in the peak area of each analyte in the six lots of matrix, therefore it was possible to exclude the presence of any matrix effect of ion suppression or enhancement. The absence of the matrix effects has been determined also by the post column infusion test and by comparing the peak area of the analyte extracted from plasma QC samples with the peak area of the extracted matrix prepared in five replicates and added with the same amount of the analyte (data not shown).

Stability. The stability of PTX and its metabolite 6α-OH-PTX, under different conditions, was assessed by analyzing QC samples, prepared in triplicate. All these analytes in human plasma were stable for 4 h at room temperature and for 72 h in the autosampler at 4°C after extraction (Table 15). PTX and 6α-OH-PTX were stable in human plasma over two freeze/thaw cycles: precision as CV% and accuracy for freeze/thaw samples were ≤3.1% and within 102.4-107.1% for PTX and ≤12.8% and within 94.0-112.2% for 6α-OH-PTX (Table 16). After 7 months of storage in human plasma, at approximately -80°C, precision (CV%) and accuracy obtained were ≤4.5% and within 94.6-103.2% for PTX, and ≤4.9% and within 89.6-102.8% for 6α-OH-PTX (Table 16).The standard working solutions of PTX and 6α-OH-PTX used for calibration curve and QC samples, prepared in methanol and stored at –80°C, were stable after 27

months: CV% and accuracy were ≤3.6% and within 106.6-113.3% for PTX and ≤8.8% and within 105.6-113.6% for 6α-OH-PTX (Table 17).

Table 15 Short term stability of PTX and its metabolite 6α-OH-PTX in human plasma samples.

Analytes	Nominal conc. (ng/mL)	T = 4h (RT)			T = 72h in autosampler (4°C)		
		Mean ± SD	Prec. %	Acc. %	Mean ± SD	Prec. %	Acc. %
PTX	3	2.71 ± 0.21	7.7	90.2	3.03 ± 0.03	1.1	101.1
	625	561.64 ± 26.83	4.8	89.9	617.20 ± 15.39	2.5	98.8
	7500	6658.95 ± 378.35	5.7	88.8	6703.78 ± 435.30	6.5	89.4
6α-OH-PTX	3	2.58 ± 0.02	0.7	86.0	2.74 ± 0.19	7.1	91.4
	75	66.60 ± 1.64	2.5	88.8	76.88 ± 1.55	2.0	102.5
	750	666.35 ± 36.97	5.5	88.8	725.84 ±25.13	3.5	96.8

Table 16 Stability of PTX and 6α-OH-PTX, in human plasma samples, after 2 freeze-thaw cycles and after 7 months of storage at -80°C.

Analytes	Nominal conc. (ng/mL)	After 2 freeze-thaw cycles			Stored at -80°C over 7 months		
		Mean ± SD	Prec. %	Acc. %	Mean ± SD	Prec. %	Acc. %
PTX	3	3.21 ± 0.03	0.9	107.1	2.97 ± 0.11	3.8	99.0
	625	706.72 ± 15.66	2.2	113.1	591.47 ± 8.31	1.4	94.6
	7500	7683.00 ± 236.01	3.1	102.4	7739.55 ± 354.80	4.5	103.2
6α-OH-PTX	3	2.82 ± 0.36	12.8	94.0	2.69 ±0.1	3.8	89.6
	75	84.19 ± 2.57	3.1	112.2	76.19 ± 2.35	3.1	101.6
	750	814.86 ± 2.24	0.3	108.6	771.01 ± 37.96	4.9	102.8

Table 17 Stability of the working solutions of PTX and 6α-OH-PTX stored at -80°C over 27 months.

Analytes	Nominal conc. (ng/mL)	Stored at -80°C over 27 months		
		Mean ± SD	Prec. %	Acc. %
PTX	3	3.20 ± 0.12	3.6	106.6
	625	704.35 ± 4.68	0.7	112.7
	7500	8499.14 ± 153.41	1.8	113.3
6α-OH-PTX	3	3.17 ± 0.28	8.8	105.6
	75	83.78 ± 0.28	0.3	111.7
	750	851.94 ± 4.27	0.5	113.6

4.1.3 High-performance liquid chromatography–tandem mass spectrometry method for the simultaneous determination of sunitinib and its main metabolite N-desethyl sunitinib in human plasma

4.1.3.1 Study on the Z/E isomerization

Most of the published analytical methods developed for the quantification of sunitinib and its main metabolite describe the sample handling under strict light protection, which is time-consuming and requires a dark room. Thus, in order to obtain a fast, specific, and easy to use method, we set up a processing procedure able to avoid the light protection relying on the peculiar characteristics of sunitinib isomerization. Sistla et al.(Sistla and Shenoy, 2005), indeed, showed that the E isomer of the sunitinib precursor semaxanib reverted to the Z-isomer following storage in the dark with an increase in the reconversion rate at higher temperatures (lnK vs. 1/T: r^2=0.96). This observation indicates that the E- to Z-isomer reversion is a thermal reversion. Based on these data we have studied the reversion kinetics of sunitinib in the dark at different temperatures (Figure 32).

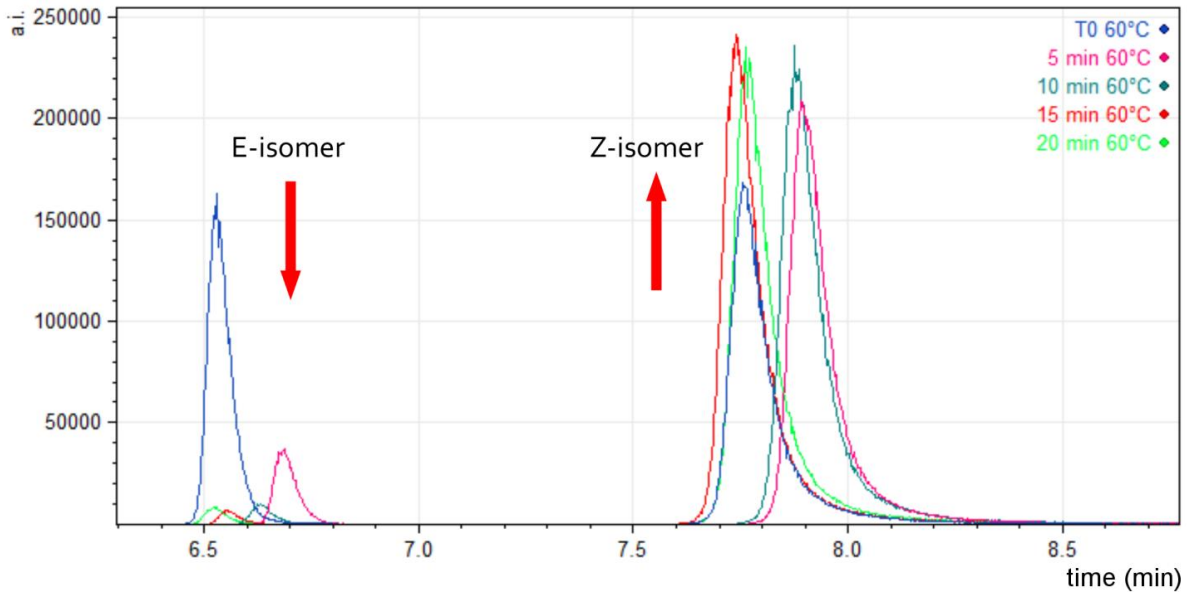

Figure 32 E/Z-isomer conversion of sunitinib (0.9 µg/mL) under different temperature conditions. The samples were analyzed at T0, without any heating process (blue line), and respectively after 5 (pink line), 10 (dark green line), 15 (red line), and 20 min (light green line) at 60°C.

During these initial experiments on the sunitinib reversion kinetics, a provisional and non optimized LC-MS/MS method has been used. More in detail, at first, an extracted sample of sunitinib (1 µg/mL), after light exposure, (for the extraction method, see "Material and Methods" Section) was split in five different glass vials: four aliquots were put in a heated bath, at 60°C for 5 (T1), 10 (T2), 15 (T3) and 20 (T4) min, while one aliquot was directly analyzed without heating process (T0).The peak area of the two isomers obtained after the heated bath step (T1,2,3,and 4 samples) were compared to those obtained from the same extracted light-exposed sample without heating process (T0 sample). Figure 32 shows the differences in terms of peak area of the samples treated at the different conditions. Already after 5 min at 60°C the peak area of E-isomer was more than 5-fold lower than T0 sample while the peak area of the Z-isomer resulted proportionally increased. Table 18 shows the area of E- and Z-isomers at different time points and the sum of the two isomers areas.

Table 18 Areas of E-isomer, Z-isomer, and the sum of the two isomers areas, together with the percentages respect to the total area, measured at T0 (without any heating process), T1, T2, T3, and T4 at 60°C.

Time	**E-isomer Area·10^5 (%)**		**Z-isomer Area·10^5 (%)**		**Total Area·10^5 (%)**	
T0	6.94	(44.12)	8.79	(55.87)	15.73	(100)
T1 (5 min)	1.34	(8.69)	14.14	(91.30)	15.48	(100)
T2 (10 min)	0.36	(2.27)	15.72	(97.72)	16.08	(100)
T3 (15 min)	0.23	(1.44)	16.00	(98.55)	16.23	(100)
T4 (20 min)	0.30	(1.95)	15.53	(98.04)	15.83	(100)

The peak area percentage of the two isomers respect to the total peak area is also reported. The reproducibility of the total area guaranteed that the decrease of the E-isomer area was due to its conversion in the active isomer and excluded the possibility of analyte degradation. After 10 min at 60°C, the equilibrium between E- and Z-isomers was reached and no variations in their areas were observed prolonging the time of incubation in the heated bath.

In order to further decrease the E-isomer signal and to reduce the time required for the treatment, additional experiments have been planned and the heated bath temperature has been progressively scaled up to 90°C. The best performance in terms

of E-isomer reconversion and time required for the treatment, has been obtained with highest temperature evaluated (90°C), which allowed a reduction of the sample treatment time to 5 min. Thus, further experiments have been performed in order to study the reconversion kinetics that takes place into the autosampler (i.e. in the dark and at 40°C), in order to understand if prolonging the time in the autosampler could further increase the Z- to E-isomers ratio. Therefore, extracted samples were heated at 90°C for 5 min and then placed in the autosampler to be analyzed by means of LC-MS/MS. Repeated analyses have been conducted to investigate the kinetics of the isomer reconversion for about 3 hours. Moreover, with the aim to test whether the kinetics depends on the sunitinib concentration, the following experiments were performed at 50 and 500 ng/mL.

In Figure 33, the peaks of Z-and E-isomers of samples prepared at the concentration of 50 ng/mL are reported.

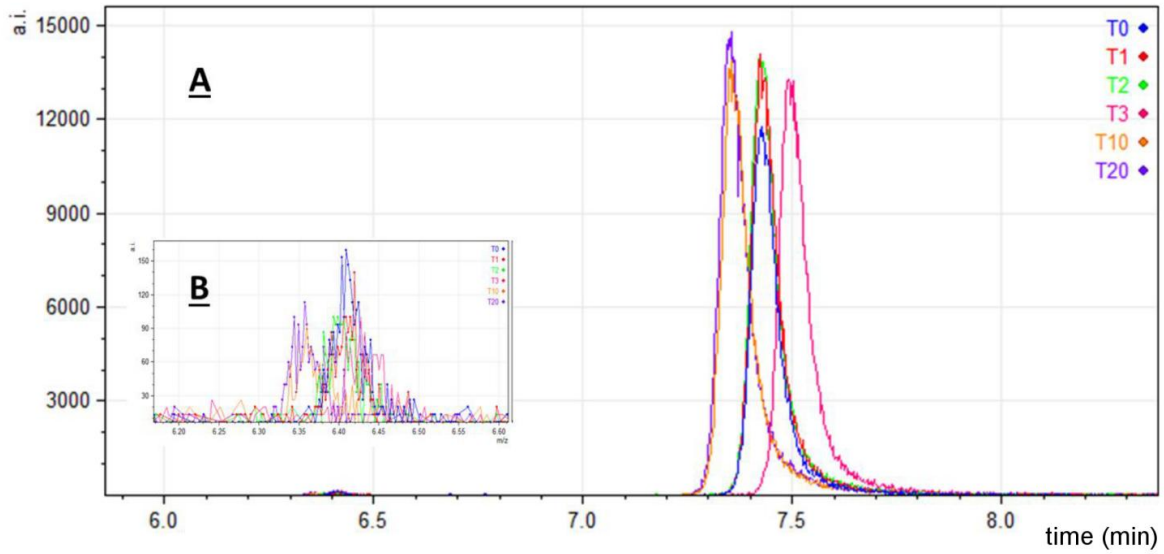

Figure 33 Panel A: Z- and E-isomer peaks of sunitinib at a concentration of 50 ng/mL after different intervals in dark condition and 40°C. The sample was analyzed at T0, immediately after the step at 90°C for 5 min (blue line), and then re-analyzed after 10 (T1), 20 (T2), 30 (T3), 100 min (T10), and 200 (T20) min in the autosampler. **Panel B**: enlargement of the E-isomer peaks.

As clear by the previous figure, at 50 ng/mL, the signal of the E-isomer was barely noticeable from the noise signal, anyway, an attempt of quantification was done and the results are reported in the following table (Table 19).

Table 19 Areas of E-isomer, Z-isomer, and the sum of the two isomers areas of sunitinib at a concentration of 50 ng/mL. The percentages of E- and Z-isomers respect to the total areas are reported. The samples were analyzed immediately after the step at 90°C for 5 min (T0), and after 10 (T1), 20 (T2), 30 (T3), 100 (T10), and 200 (T20) min in the autosampler (dark and at 40°C).

Sunitinib 50 ng/mL						
Time	**E-isomer Area·10^5 (%)**		**Z-isomer Area·10^5 (%)**		**Total Area·10^5 (%)**	
T0	0.004	(0,67)	0,582	(99,33)	0,586	(100)
T1 (10 min)	0.003	(0,41)	0,681	(99,59)	0,684	(100)
T2 (20 min)	0.003	(0,41)	0,697	(99,59)	0,700	(100)
T3 (30 min)	0.003	(0,38)	0,692	(99,62)	0,695	(100)
T10 (100 min)	0.002	(0,32)	0,706	(99,68)	0,708	(100)
T20 (200 min)	0.003	(0,35)	0,766	(99,65)	0,769	(100)

The results obtained using the concentration of 500 ng/mL are reported in Figure 34 and Table 20.

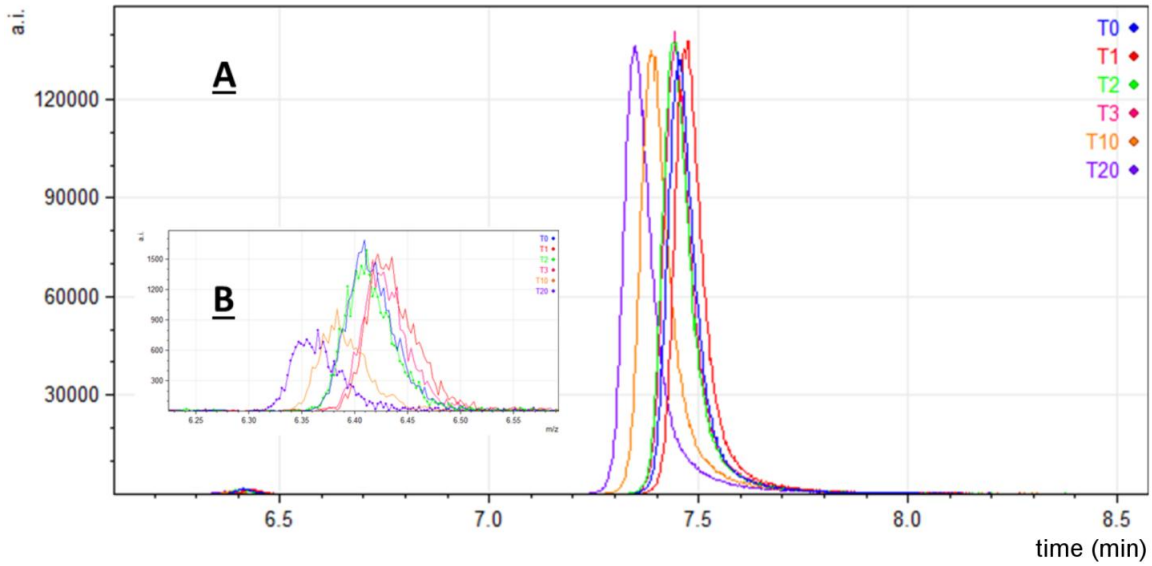

Figure 34 Panel A: Z- and E-isomer peaks of sunitinib at a concentration of 500 ng/mL after different intervals in dark condition and at 40°C. The sample was analyzed at T0, immediately after the step at 90°C for 5 min (blue line), and then re-analyzed after 10 (T1), 20 (T2), 30 (T3), 100 (T10), and 200 (T20) min in the autosampler. **Panel B**: enlargement of the E isomer peaks.

Table 20 Areas of E-isomer, Z-isomer, and the sum of the two isomers areas of sunitinib at a concentration of 500 ng/mL. The percentages of E- and Z-isomers respect to the total areas are reported. The samples were analyzed immediately after the step at 90°C for 5 min (T0), and after 10 (T1), 20 (T2), 30 (T3), 100 (T10), and 200 (T20) min in the autosampler (dark and at 40°C).

Suntinib 500 ng/mL						
Time	**E-isomer Area·10^5 (%)**		**Z-isomer Area·10^5 (%)**		**Total Area·10^5 (%)**	
T0	0.049	(0.73)	6.669	(99.26)	6.718	(100)
T1 (10 min)	0.048	(0.67)	7.084	(99.33)	7.132	(100)
T2 (20 min)	0.046	(0.64)	7.106	(99.35)	7.152	(100)
T3 (30 min)	0.042	(0.59)	7.083	(99.41)	7.125	(100)
T10 (100 min)	0.027	(0.37)	7.240	(99.63)	7.267	(100)
T20 (200 min)	0.023	(0.32)	7.247	(99.68)	7.270	(100)

The increasing of the temperature from 60 to 90°C augmented the E- to Z-isomer reconversion, thus increasing the Z-isomer signal and decreasing the E-isomer signal at both the investigated concentrations (50 and 500 ng/mL). In fact, the percentage of the E-isomer even after 20 min at 60°C was equal to 1.95% (T4, Figure 32), while after only 5 min at 90°C it resulted reduced to 0.67 and 0.73% at 50 (T0, Figure 33) and 500 ng/mL (T0, Figure 34), respectively. Moreover, the maintenance of the samples into the autosampler, thus in dark condition and at 40°C, resulted to be not worth of consideration for the set up of the method due to the very slightly difference between different re-injected samples. In fact, the E-isomer percentage decreased from 0.67% to 0.35% and from 0.73 to 0.32% in about 3 hours at 50 and 500 ng/mL, respectively. However, in each analytical run a series of samples, collectively called system suitability test, are requested to be analyzed before samples injection to verify instrument conditions. The system suitability test requires about 1 hour and, from these results, it is reliable to assume that this period is enough for stabilize the Z- to E-isomer ratio.

The same set of tests have been performed in samples at low (50 ng/mL) and high (500 ng/mL) concentration of the metabolite N-desethyl sunitinib heated at 90°C for 5 min. The results obtained are comparable with those observed with sunitinib samples: the E-isomer signal was indeed barely observable from the noise signal after the heated bath,

and it resulted even lower than the sunitinib one (Figure 35 and Figure 36, Table 21 and Table 22).

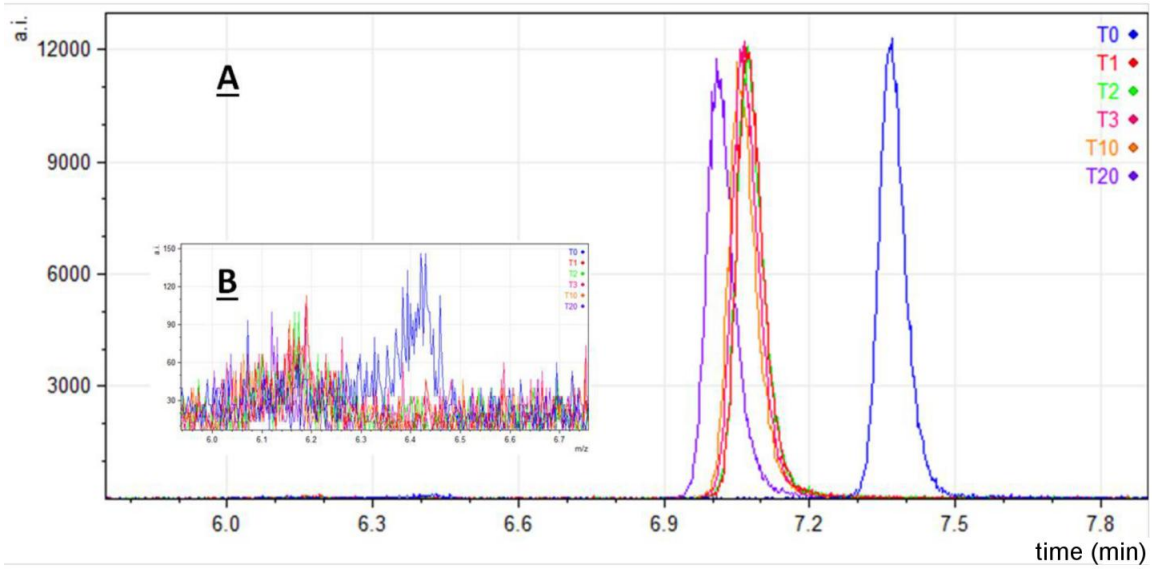

Figure 35 Panel A: Z- and E-isomer peaks of N-desethyl sunitinib at a concentration of 50 ng/mL after different intervals in dark condition and at 40°C. The sample was analyzed at T0, immediately after the step at 90°C for 5 min (blue line), and then re-analyzed after 10 (T1), 20 (T2), 30 (T3), 100 min (T10), and 200 (T20) min in the autosampler. **Panel B**: enlargement of the E-isomer peaks.

Table 21 Areas of E-isomer, Z-isomer, and the sum of the two isomers areas of N-desethyl sunitinib at a concentration of 50 ng/mL. The percentages of E- and Z-isomers respect to the total areas are reported. The samples were analyzed immediately after the step at 90°C for 5 min (T0), and after 10 (T1), 20 (T2), 30 (T3), 100 (T10), and 200 (T20) min in the autosampler (dark and at 40°C).

N-desethyl sunitinib 50 ng/mL						
Time	**E-isomer Area·10^5 (%)**		**Z-isomer Area·10^5 (%)**		**Total Area·10^5 (%)**	
T0	0.004	(0.89)	0.480	(98.61)	0.484	(100)
T1 (10 min)	0.004	(0.75)	0.478	(99.24)	0.482	(100)
T2 (20 min)	0.002	(0.53)	0.476	(99.47)	0.478	(100)
T3 (30 min)	0.002	(0.36)	0.481	(99.64)	0.483	(100)
T10 (100 min)	0.001	(0.30)	0.468	(99.70)	0.469	(100)
T20 (200 min)	0.001	(0.23)	0.472	(99.77)	0.473	(100)

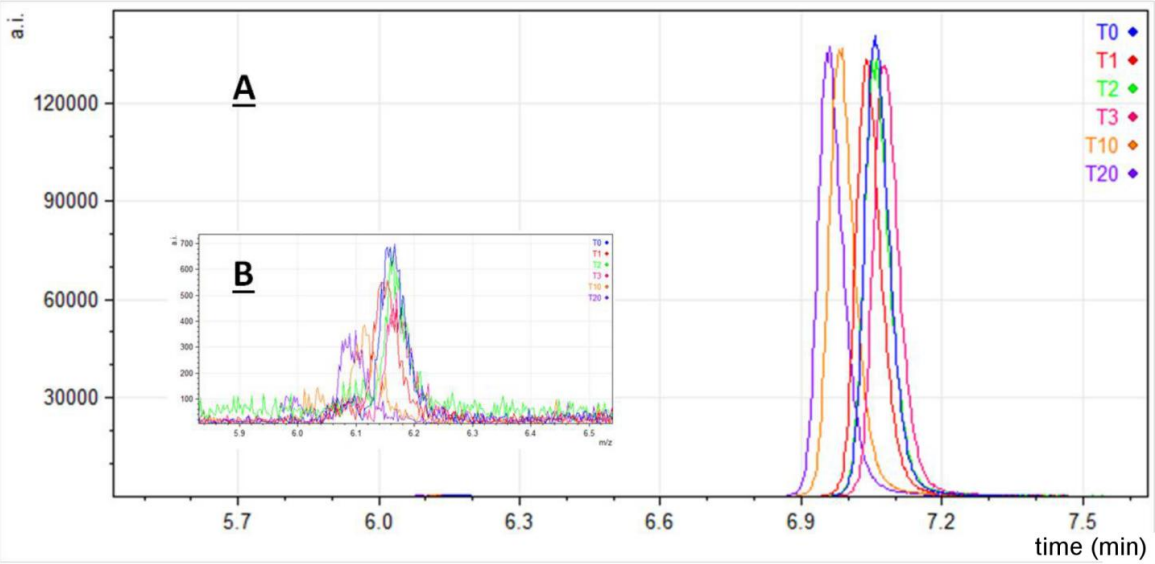

Figure 36 Panel A: Z- and E-isomer peaks of N-desethyl sunitinib at a concentration of 500 ng/mL after different intervals in dark condition and at 40°C. The sample was analyzed at T0, immediately after the step at 90°C for 5 min (blue line), and then re-analyzed after 10 (T1), 20 (T2), 30 (T3), 100 min (T10), and 200 (T20) min in the autosampler. **Panel B**: enlargement of the E isomer peaks.

Table 22 Areas of E-isomer, Z-isomer, and the sum of the two isomers areas of N-desethyl sunitinib at a concentration of 500 ng/mL. The percentages of E- and Z-isomers respect to the total areas are reported. The samples were analyzed immediately after the step at 90°C for 5 min (T0), and after 10 (T1), 20 (T2), 30 (T3), 100 (T10), and 200 (T20) min in the autosampler (dark and at 40°C).

N-desethyl sunitinib 500 ng/mL						
Time	**E-isomer Area·10^5 (%)**		**Z-isomer Area·10^5 (%)**		**Total Area·10^5 (%)**	
T0	0.022	**(0.40)**	5.473	**(99.60)**	5.495	**(100)**
T1 (10 min)	0.019	**(0.37)**	5.257	**(99.63)**	5.276	**(100)**
T2 (20 min)	0.015	**(0.29)**	5.324	**(99.71)**	5.339	**(100)**
T3 (30 min)	0.014	**(0.26)**	5.398	**(99.74)**	5.412	**(100)**
T10 (100 min)	0.010	**(0.19)**	5.472	**(99.81)**	5.482	**(100)**
T20 (200 min)	0.010	**(0.19)**	5.456	**(99.81)**	5.466	**(100)**

Also in the case of N-desethyl sunitinib, the maintenance of the samples into the autosampler resulted to be not worth of consideration in the E-isomer reconversion process and can be neglected.

To conclude, the conditions chosen for E-isomer reconversion to Z-isomer consisted of a heating process at 90°C for 5 min. At these conditions, it is possible to assume the E-isomer peak to be negligible, respect to the Z-isomer.

4.1.3.2 HPLC-MS/MS

To optimize the mass spectrometer conditions, an infusion of each standard solution and IS at 50 ng/mL in mobile phases (50:50) was used. The response of sunitinib and its main metabolite was assessed in positive and negative ion mode but the better one was obtained in positive mode. Using an ESI source in positive ion mode, sunitinib and its main metabolite formed mainly a protonated molecule $[M+H]^+$. The precursor ion of sunitinib, N-desethyl sunitinib, and sunitinib D-10 as IS (*m/z* 399.2, *m/z* 371.2, and *m/z* 409.3 respectively) passed through the first quadrupole into the collision cell and the collision energy (CE) and the Collision Cell Exit Potential (CXP) were optimized to obtain their product ions with a high signal (Table 23).

Table 23 Source- and compound-dependent parameters and ion transitions of each analyte and IS used for the mass spectrometer method. The dwell time of each transition was set up at 50 msec. DP: declustering potential; EP: entrance potential; CE: collision energy; CXP: collision cell exit potential.

Compound	Q1 (m/z)	DP (V)	EP (V)	Q3 (m/z)	CE (V)	CXP (V)
sunitinib	399	72	11	**326.2**	**28**	**21**
				283.1	36	18
				238.1	60	14
N-desethyl-sunitinib	371	57	10	**283.2**	**27**	**14**
				326.2	22	18
				238.2	54	21
sunitinib-D10 (IS)	409	67	11	**326.2**	**30**	**21**
				283.2	39	18
				238.2	63	14

The fragmentation pattern of sunitinib is represented in Figure 37, the same fragmentation pattern has been observed for its metabolite and IS.

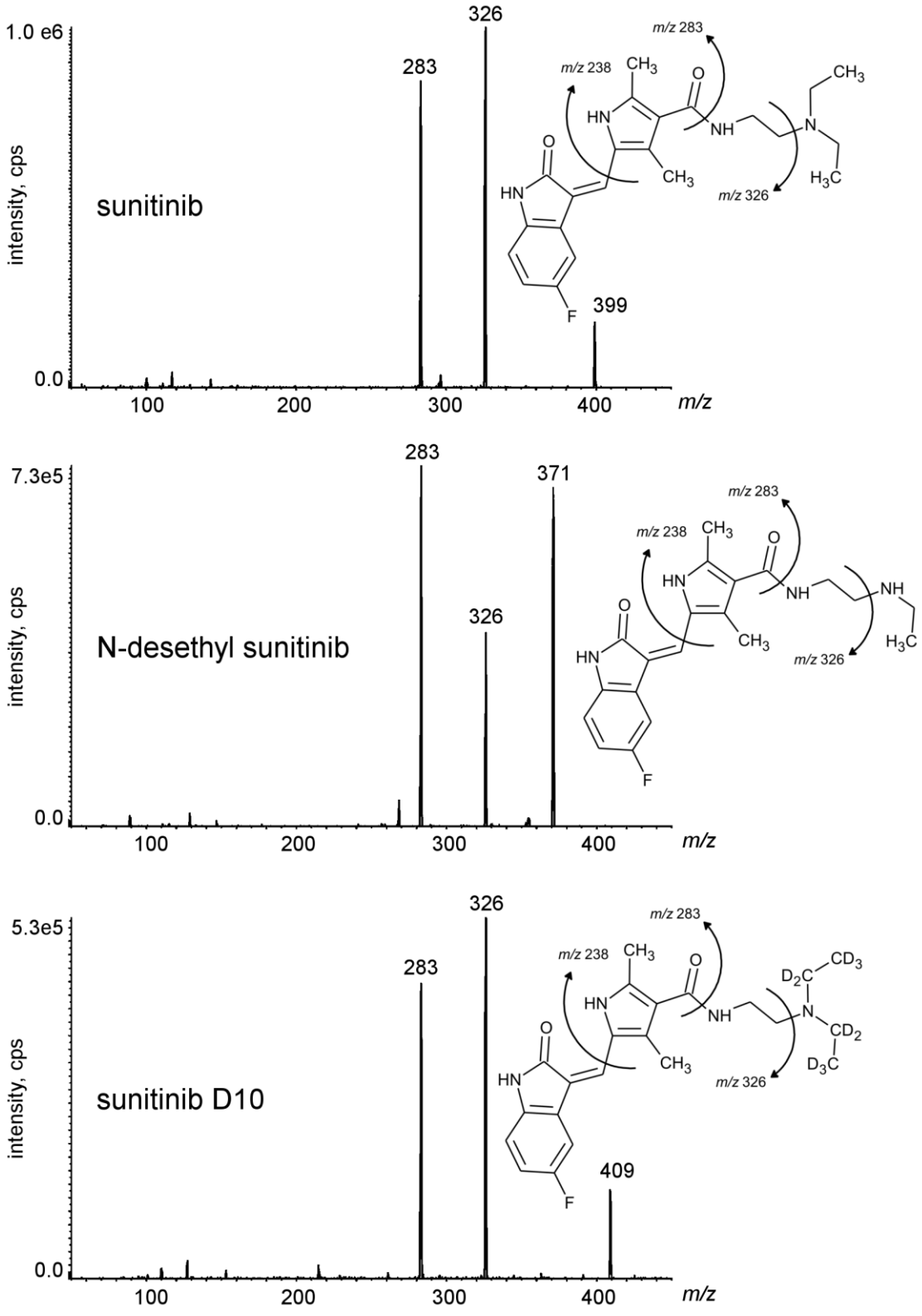

Figure 37 MS/MS mass spectra of sunitinib, N-desethyl sunitinib and sunitinib D10 (IS) with chemical structures and identification of the main fragment ions. The fragment ion at 238 m/z of the three compounds is not shown in the MS/MS mass spectra because it requires, for its formation, a higher CE than the other fragments.

For each compound, the daughter ion with the highest signal was used as quantifier, as follows: 399.2>326.2 for sunitinib, 371.2>283.2 for N-desethyl sunitinib, 409.3>326.2 for IS, all expressed in *m/z*. Two additional daughter ions, for each analyte and IS, were chosen as qualifiers and the details of the transitions and the correspondent CE and CXP were reported in Table 23.

Figure 38 presents typical SRM chromatograms, using the quantifier transitions noted above.

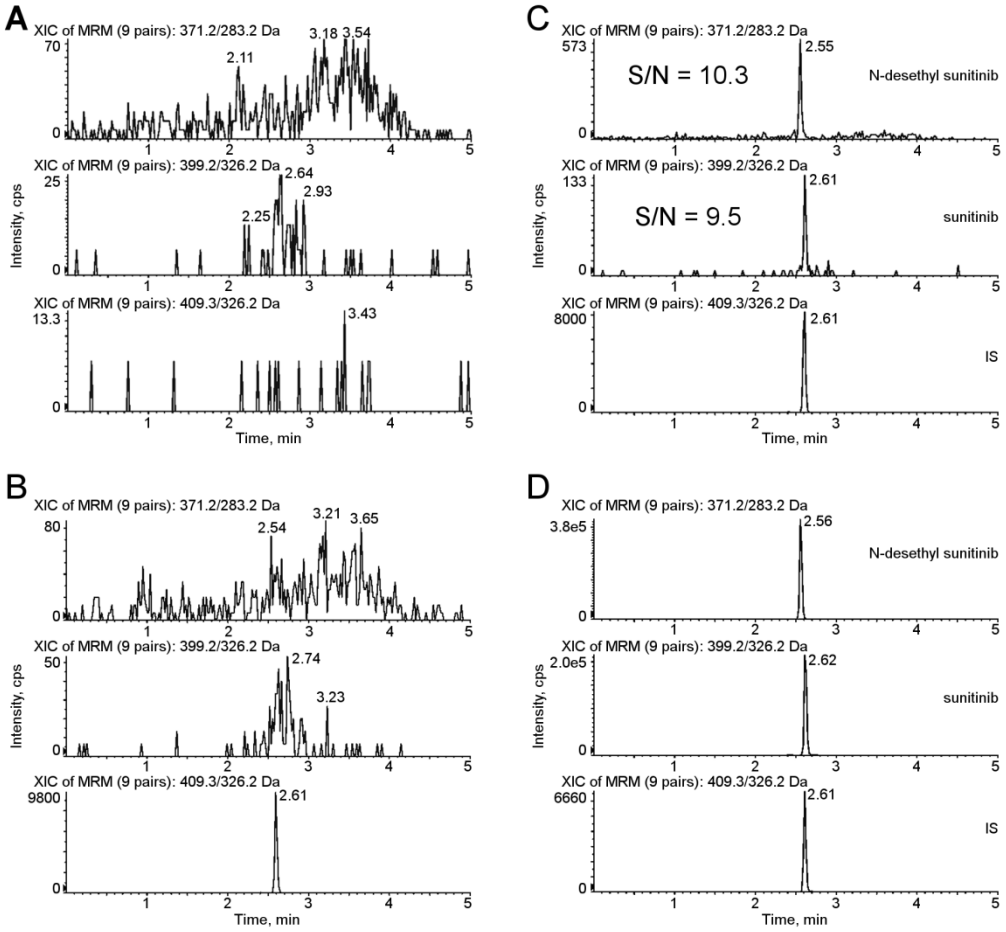

Figure 38 Representative SRM chromatograms. **Panel A**: SRM chromatograms of a human blank plasma sample; **Panel B**: SRM chromatograms of a human blank plasma sample with IS added; **Panel C**: S/N of sunitinib and N-desethyl sunitinib at the LLOQ (0.1 ng/mL for both the analytes); **Panel D**: SRM chromatograms of an extracted plasma sample of a calibration curve point (B: 250 ng/mL for sunitinib and 100 ng/mL for N-desethyl sunitinib).

Panel A shows an extracted blank plasma sample; Panel B displays an extracted blank plasma sample with IS added; Panel C shows an extracted plasma sample at the LLOQ

with IS added, and Panel D displays a point of the calibration curve at a concentration equal to 250 ng/mL for sunitinib and 100 ng/mL for N-desethyl sunitinib. The elution of the analytes was rapid and selective with adequate separation of all the peaks within 2.5 min: sunitinib, N-desethyl sunitinib and IS were eluted at approximately 2.61, 2.55, and 2.61 min, respectively. No interfering peaks were observed at these retention times, and the peaks were completely resolved from plasma matrix, with a good shape.

4.1.3.3 Validation of the method

The validation process has not yet been concluded. In fact, for a completely validation it is necessary to test the method in real patients samples and to conduct the ISR to verify the reliability of the reported subject sample analyte concentrations, as reported in Section 3.3 (Materials and Methods Section). At present, a request for plasma samples from patients treated with sunitinib has been presented at the internal ethical committee of the CRO institute. As soon as patients plasma samples will be available, these final assessment will be performed and the validation will be concluded.

Recovery. The extraction method is based on simple deproteinization with five volumes of CH_3OH relative to plasma sample. The recovery, evaluated in five replicates at three QC concentrations, was in the range 93.9-111.1% (CV ≤ 9.2%) for sunitinib and 95.7-108.1% (CV≤ 12.3%) for N-desethyl sunitinib, as shown in Table 24. The recovery of IS was evaluated in five replicates at a concentration of 100 ng/mL and it was 104.9 % (CV 5.2 %).

Table 24 Recovery of the analytes and the IS from human plasma.

Analyte	Nominal conc. (ng/mL)	Recovery (%) ± SD	CV %
sunitinib	0.25	100.5±9.3	9.2
	25	93.9±5.4	5.8
	400	111.1±1.0	0.9
N-desethyl sunitinib	0.25	104.6±12.9	12.3
	25	95.7±5.9	6.1
	200	108.1±2.9	2.7
sunitinib-D10 (IS)	100	104.9±5.4	5.2

Calibration Curves. Table 25 reports the results for the calibration curves of sunitinib and its main metabolite freshly prepared every day during the validation study, and the accuracy and precision for each standard.

Table 25 Linearity, accuracy, and precision data for calibration curves of sunitinib and N-desethyl sunitinib.

Analytes	**Nominal conc. (ng/mL)**	**Mean ± SD**	**Precision %**	**Accuracy %**
sunitinib	0.1	0.10±0.00	1.6	101.0
	0.5	0.48±0.04	7.7	95.8
	2.5	2.41±0.14	5.6	96.5
	10	10.25±0.47	4.6	102.5
	50	49.38±2.04	4.1	98.8
	250	256.67±12.29	4.8	102.7
	500	514.50±16.16	3.1	102.9
N-desethyl sunitinib	0.1	0.10±0.00	0.8	101.2
	0.5	0.47±0.02	3.9	94.2
	2.5	2.31±0.11	4.8	92.3
	10	9.72±1.05	10.8	97.2
	50	51.48±2.96	5.7	103.0
	100	104.93±9.07	8.6	104.9
	250	265.41±19.16	7.2	106.2

The calibration curves prepared on five different days showed good linearity and acceptable results of the back-calculated concentrations over the validated range of 0.1–500 ng/mL for sunitinib and 0.1-250 ng/mL for N-desethyl sunitinib (Figure 39). Pearson's coefficient of determination R^2 was ≥0.9931 for each run, the mean accuracy was always close to 100% (range from 95.8% to 102.9% for sunitinib and from 92.3 to 106.2% for N-desethyl sunitinib) and the precision, expressed as CV%, ranged from 1.6 to 7.7 % for sunitinib and from 0.8 to 10.8% for N-desethyl sunitinib. The carry-over effect was minimized injecting three samples of mobile phase between successive test

samples and after the injection of the ULOQ. This action guaranteed peak response no higher than 10% of LLOQ.

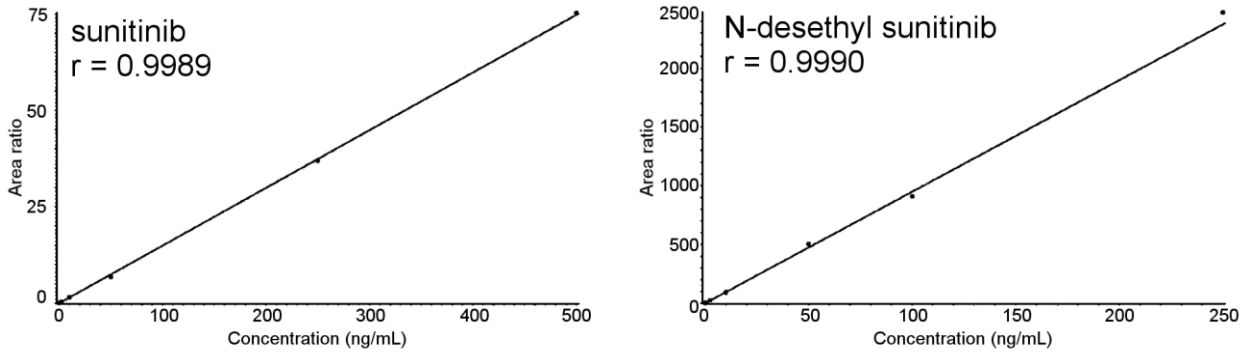

Figure 39 Calibration curves of sunitinib and N-desethyl sunitinib in human plasma.

Intra-day and inter-day Precision and Accuracy. The precision and accuracy of the method were evaluated by analyzing three replicates of QC samples (QCL, QCM and QCH) within a single-run analysis for intra-day assessment and over five consecutive runs for inter-day assessment. The accuracy and precision (CV%) obtained are shown in Table 26.

Table 26 Intra and inter-day precision and accuracy of the method for the analysis of sunitinib and its main metabolite in human plasma samples.

	Analytes	**Nominal conc. (ng/mL)**	**Mean ± SD**	**Prec. %**	**Acc. %**
Intra-day (N=5)	sunitinib	0.25	0.25±0.03	11.0	98.5
		25	25.93±0.69	2.7	103.7
		400	447.86±5.10	1.1	112.0
	N-desethyl sunitinib	0.25	0.26±0.03	11.7	103.7
		25	26.71±2.57	9.6	106.9
		200	223.30±6.28	2.8	111.7
Inter-day (N=15)	sunitinib	0.25	0.26±0.02	6.1	102.5
		25	25.40±1.27	5.0	101.6
		400	423.48±29.23	6.9	105.9
	N-desethyl sunitinib	0.25	0.25±0.02	9.1	99.1
		25	24.18±1.76	7.3	96.7
		200	214.45±14.17	6.6	107.2

The method was very precise, with intra- and inter-day CV ≤ 11.0 % and ≤ 6.9% for sunitinib, ≤11.7% and ≤9.1% for N-desethyl sunitinib. Moreover, the method showed intra- and inter-day accuracy within the range from 98.5 ad 112.0% and from 101.6 and 105.9% for sunitinib, from 103.7 to 111.7% and from 96.7 and 107.2% for N-desethyl sunitinib.

Limit of Detection, Limit of Quantification, Selectivity and Matrix Effect. The LOD was defined as the concentration at which the S/N was at least 3. On the basis of the S/N ratio obtained and reported in Figure 38, the LOD was 32 pg/mL for sunitinib and 29 pg/mL for N-desethyl sunitinib. The LLOQ was fixed at 0.1 ng/mL for both sunitinib and N-desethyl sunitinib and the accuracy and precision were determined by analyzing six replicates of the sample at the LLOQ concentration. The accuracy and CV% were, respectively, 87.4% and 14.7% for sunitinib, 107.8% and 8.0% for N-desethyl sunitinib. The method was not affected by endogenous components in the matrix or other components in the sample. In fact, spiking six different sources of human plasma with sunitinib and its main metabolite at a concentration corresponding to the LLOQ, the precision was 8.4% for sunitinib and 5.9% for N-desethyl sunitinib, respectively, and the accuracy was 89.5% for sunitinib and 114.9% for N-desethyl sunitinib, respectively. There were no significant variations (<15%) in the peak area of each analyte in the six lots of matrix, therefore it was possible to exclude the presence of any matrix effect of ion suppression or enhancement. The absence of the matrix effect has been determined, for sunitinib and N-desethyl sunitinb, also by the post column infusion test and by comparing the peak area of the analyte extracted from plasma QC samples with the peak area of the extracted matrix prepared in five replicates and added with the same amount of the analyte (data not shown).

Stability. The stability of sunitinib and its main metabolite, under different conditions, was assessed by analyzing QC samples, prepared in triplicate. Both the analytes in human plasma were stable for 4 h at room temperature (Table 27). For the peculiarity of this method, it was particularly important to assess the stability in the autosampler after the extraction. In fact, the autosampler temperature was set at 40°C in order to enhance and stabilize the conversion to the active Z-isomer, while usually the

autosampler temperature is fixed at 4°C. Therefore, we demonstrated the stability of the extracted samples up to 48 h in the autosampler at 40°C (Table 27).

Table 27 Short term stability of sunitinib and its main metabolite in human plasma samples at room temperature (RT) and in autosampler (40°C).

Analytes	Nominal conc. (ng/mL)	T = 4h (RT)			T = 48h in autosampler (40°C)		
		Mean ± SD	Prec. %	Acc. %	Mean ± SD	Prec. %	Acc. %
sunitinib	0.25	0.23±0.01	5.9	90.6	0.23±0.02	8.4	90.6
	25	23.37±0.86	3.7	93.5	23.94±1.95	8.1	95.8
	400	440.84±22.23	5.0	110.2	418.56±24.90	5.9	104.6
N-desethyl sunitinib	0.25	0.25±0.03	12.6	101.0	0.25±0.02	7.2	101.3
	25	22.81±1.12	4.9	91.2	25.20±0.45	1.8	100.8
	200	227.44±4.10	1.8	113.7	209.57±7.56	3.6	104.8

Sunitinib and N-desethyl sunitinib were stable in human plasma over two freeze/thaw cycles: precision as CV% and accuracy for freeze/thaw samples were ≤8.6% and within 99.9–108.2% for sunitinib and ≤12.4% and within 101.9–106.1% for N-desethyl sunitinib, (Table 28).

Table 28 Stability of sunitinib and its main metabolite, in human plasma samples, after 2 freeze-thaw cycles.

Analytes	After 2 freeze-thaw cycles			
	Nominal conc. (ng/mL)	Mean ± SD	Prec. %	Acc. %
sunitinib	0.25	0.26±0.02	6.5	105.9
	25	24.97±0.74	3.0	99.9
	400	432.80±37.20	8.6	108.2
N-desethyl sunitinib	0.25	0.26±0.02	9.2	104.8
	25	26.52±0.26	1.0	106.1
	200	203.82±25.24	12.4	101.9

Several aliquots of QC plasma samples have been stored at -80°C in order to complete the assessment of the long-term stability. This part of the validation will be conducted

in the next months in order to define the stability of the analytes in plasma at 6 months (after 5 months at -70°C have been already verified by Rodamer et al. (Rodamer et al., 2011). Moreover, the long term stability of standard working solutions of sunitinib and N-desethyl sunitinib used for the calibration curves and QC samples prepared in methanol and stored at –80°C will be assessed in the next months.

4.2 Phase Ib clinical trials

4.2.1 Collection and storage of the samples

The collection and storage of the samples from the three clinical trials followed the same procedures. Patients were hospitalized for 3 days during the two treatments (I and II administration for the phase I of FOLFIRI in combination with bevacizumab and cetuximab; I and IV administration for the phase I of weekly PTX) of the first therapy cycle and the drug administration and sampling were strictly monitored by the dedicated staff (MD clinical staff and research nurses dedicated to clinical studies).

The blood samples were collected into tubes containing K_2-EDTA and plasma was obtained immediately by centrifugation of the blood samples at 3000 g for 10 min at 4°C. Then the plasma was separated, split into 2 polypropylene tubes and stored as two independent aliquots at -80°C pending analysis. All blood samples were collected under the full ethical approval of the ethics committee of the participating centers and only after the signature of informed consent from all the enrolled patients.

The samplings were recorded, in details, in forms suitable to indicate the correct timing and any possible variation from it. Some basic information of the patient, such as the performance status (PS), the BSA, the scheduled treatment, the CPT-11/PTX dose, and the date and time of the therapy start were also reported (Appendix 1).

4.2.2 Genotype-guided phase I study of irinotecan administered in combination with 5-fluorouracil/leucovorin (FOLFIRI) and bevacizumab in advanced colorectal cancer patients

4.2.2.1 Patients characteristics and dose escalation

This dose finding study was concluded in December 2014. A total of 48 patients were enrolled in the trial, 25 with *UGT1A1 *1/*1* genotype and 23 with **1/*28* genotype. The main characteristics of the patients enrolled are shown in Table 29.

Table 29 Patients characteristics (n=48 patients who received at least one dose of protocol therapy). *One patient was not evaluable for safety because his treatment was delayed for personal reasons in the absence of DLT.

Number of evaluable patients	
For safety*	47
For pharmacokinetics	47 (43 for interaction with bevacizumab)
For efficacy	33
Accrual site	
Aviano, Italy	28 (58%)
Chicago, USA	17 (35%)
Rome, Italy	3 (6%)
Age, years	
Median, range	56, 32-76
Sex	
Male	28 (58%)
Female	20 (42%)
Race	
White	41 (85%)
Black	6 (13%)
Asian	1 (2%)
Body-surface area (BSA), m^2	
Median, range	1.80, 1.42-2.52
ECOG performance status	
0	45 (94%)
1	3 (6%)
Primary site	
Colon	37 (77%)
Rectum	11 (23%)
Number of metastatic sites	
1	29 (60%)
≥2	19 (40%)

The dose of CPT-11 was escalated from 260 mg/m^2 to 310 mg/m^2 and eventually to 370 mg/m^2 in both **1/*1* and **1/*28* patients, as reported in Table 30 where the overall results of the dose escalation are schematized.

Table 30 Dose escalation of CPT-11 and observed DLTs in patients treated with FOLFIRI plus bevacizumab.

CPT-11 dose (mg/m²)	***1/*1* patients (DLTs)**	***1/*28* patients (DLTs)**
260	**10 (1)** Grade 3 diarrhoea	**10 (2)** Grade 3 arrhythmia Grade 4 neutropenia
310	**10 (2)** Grade 3 diarrhoea x 2	**10 (4)** Grade 3 diarrhoea Grade 3 mucositis Grade 4 neutropenia x 2
370	**4 (2)** Grade 3 nausea/vomiting Grade 5 neutropenic sepsis	**3 (2)** Grade 3 diarrhoea Grade 4 neutropenia x 2

In the **1/*28* patients, 370 mg/m² was not tolerated (2 DLTs out of 3 patients), and the 310 mg/m² cohort was expanded to 10 patients, where 4 DLTs were observed. Hence, the 260 mg/m² cohort was expanded to 10 patients, and because 2 DLTs were observed among those 10 patients, 260 mg/m² was declared the MTD in **1/*28* patients. In the **1/*1* patients, 2 DLTs occurred among the first 3 patients treated at 310 mg/m². The 260 mg/m² was expanded to 10 patients and only 1 DLT was observed. Therefore, the 310 mg/m² cohort was expanded and no additional patients had a DLT (total 2 DLTs out of 10 patients). Thus, the dose was escalated to 370 mg/m², but 2 DLTs occurred among the first 4 patients treated, including a death from neutropenic sepsis. Hence, the 310 mg/m² dose was declared the MTD in **1/*1* patients.

The most common DLTs were neutropenia (6 of 13; 46%) and diarrhoea (5 of 13; 38%). Three of 6 neutropenia DLTs were febrile neutropenia. The other two DLTs were grade 3 mucositis and grade 3 arrhythmia (Table 30). Common (> 10% of patients) and/or severe toxicities during the first cycle of therapy are reported in Table 31. The median number of treatment cycles was 6 (range 0.5-10.5) in all treated patients. In the 20 **1/*1* and **1/*28* patients treated at the MTD, the median number of treatment cycles was 6 (range 1.5-10), and 65% of the patients treated at the MTD did not require a dose reduction of CPT-11. The doses of 5-FU and bevacizumab were not modified.

Table 31 Toxicities during the first cycle of FOLFIRI plus bevacizumab. Number of patients (%) is indicated. Toxicities were included if they occurred in at least 10% of patients or if they were grade 3 or greater, and if they were at least possibly related to treatment.

	Grade 1	**Grade 2**	**Grade 3**	**Grade 4**	**Grade 5**
Anaemia	13 (27)	9 (19)	1 (2)	0	0
Leukopenia	7 (15)	8 (17)	2 (4)	0	0
Neutropenia	4 (8)	12 (25)	10 (21)	5 (10)	1 (2)
Febrile neutropenia	0	0	1 (2)	1 (2)	1 (2)
Thrombocytopenia	3 (6)	0	0	0	0
Abdominal pain	12 (25)	2 (4)	0	0	0
Alopecia	3 (6)	3 (6)	1 (2)	0	0
Anorexia	6 (13)	0	0	0	0
Arrhythmia	0	0	1 (2)	0	0
Asthenia	16 (33)	1 (2)	0	0	0
Constipation	19 (40)	2 (4)	0	0	0
Diarrhoea	15 (31)	6 (13)	5 (10)	0	0
Elevated ALT	14 (29)	2 (4)	0	0	0
Elevated AST	24 (50)	4 (8)	0	0	0
Epistaxis	5 (10)	0	0	0	0
Fatigue	11 (23)	2 (4)	0	0	0
Fever	4 (8)	0	0	0	0
Mucositis	7 (15)	2 (4)	1 (2)	0	0
Nausea/Vomiting	26 (54)	7 (15)	5 (10)	0	0
Pain (from mucositis)	1 (2)	0	1 (2)	0	0

4.2.2.2 Pharmacokinetics of irinotecan and its main metabolites and interaction with bevacizumab

Pharmacokinetic data were obtained from 47 patients applying the LC-MS/MS method for the quantification of CPT-11 and its main metabolites in plasma samples (for the development and validation of the method see Section 4.1.1).

As examples of the pharmacokinetic profiles obtained, Figure 40 (Panel A and B) shows the plasma concentration-versus-time curves of CPT-11, SN-38, SN-38G and APC

determined, during the first cycle of therapy in two patients receiving respectively 310 (Panel A) and 370 (Panel B) mg/m^2 of CPT-11.

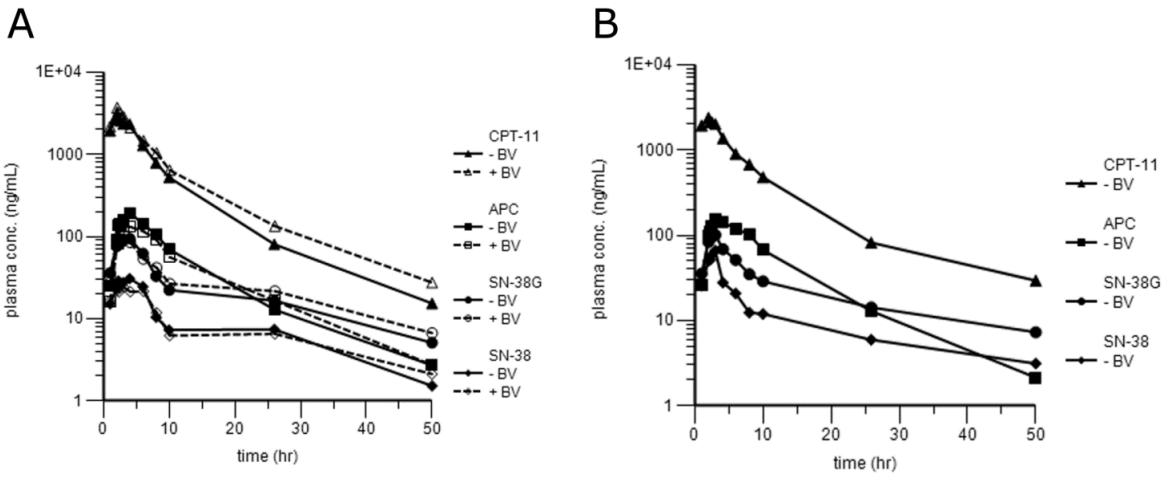

Figure 40 Plasma concentration-*versus*-time profiles of CPT-11 and its main metabolites: SN-38, SN-38G and APC. **Panel A**: Plasma concentration-*versus*-time profiles of CPT-11, SN-38, SN-38G and APC in one patient receiving 310 mg/m^2 of CPT-11 during the I and the II administration of the first therapy cycle; **Panel B**: Plasma concentration-*versus*-time profiles of CPT-11, SN-38, SN-38G and APC in one patient receiving 370 mg/m^2 of CPT-11 during the I administration of the first therapy cycle. BV: bevacizumab.

Panel A shows two pharmacokinetic profiles for each analyte because the patient received both the administrations of the first cycle whereas Panel B shows just one profile (referring to the first treatment) for analyte because the patient experienced DLTs. Therefore, he received additional treatment with a 25% reduction in the dose of CPT-11 and, consequently, blood samples were not drawn during the second administration.

For both the patients, CPT-11 plasma concentrations appeared to decline in a bi-exponential manner, with a rapid initial phase and an extended terminal phase. Moreover, it is possible to observe that APC presents a curve very similar to CPT-11 while the two regarding SN-38 and SN-38G show the same multi-exponential manner to decline with a very prolonged terminal phase. The principal pharmacokinetic parameters determined by the profiles reported in Figure 40 and related to the two patients treated with 310 or 370 mg/m^2 of CPT-11 are reported in Table 32 and Table 33, respectively.

Table 32 Pharmacokinetic parameters obtained from one patient treated at 310 mg/m^2 of CPT-11 during the first (Day 1-3) and the second (Day 15-17) treatment of the first chemotherapy cycle.

Days 1-3							
Compound	**C_{max} (ng/mL)**	**t_{max} (h)**	**AUC_{last} (h·ng/mL)**	**AUC_{inf} (h·ng/mL)**	**$t_{1/2}$ (h)**	**V_d (L/m^2)**	**Cl (L/h/m^2)**
CPT-11	3003.21	2.00	21298.29	21475.55	8.00	16.66	14.43
SN-38	30.70	4.00	415.40	452.34	16.81	-	-
SN-38G	94.36	4.00	1128.51	1263.11	18.31	-	-
APC	194.08	4.00	1994.79	2028.70	8.67	-	-
Days 15-17							
Compound	**C_{max} (ng/mL)**	**t_{max} (h)**	**AUC_{last} (h·ng/mL)**	**AUC_{inf} (h·ng/mL)**	**$t_{1/2}$ (h)**	**V_d (L/m^2)**	**Cl (L/h/m^2)**
CPT-11	3682.62	2.08	25613.15	25967.08	8.92	15.37	11.94
SN-38	24.12	3.08	375.22	449.63	24.31	-	-
SN-38G	104.41	3.08	1304.04	1491.75	19.44	-	-
APC	131.36	3.08	1714.92	1751.17	9.19	-	-

Table 33 Pharmacokinetic parameters obtained from one patient treated at 370 mg/m^2 of CPT-11 during the first (Day 1-3) treatment of the first chemotherapy cycle.

Days 1-3							
Compound	**C_{max} (ng/mL)**	**t_{max} (h)**	**AUC_{last} (h·ng/mL)**	**AUC_{inf} (h·ng/mL)**	**$t_{1/2}$ (h)**	**V_d (L/m^2)**	**Cl (L/hrm^2)**
CPT-11	2370.47	2.00	17759.90	18194.43	10.27	30.12	20.34
SN-38	65.95	3.00	515.52	601.46	21.04	-	-
SN-38G	100.72	3.00	1130.06	1330.56	19.07	-	-
APC	155.16	3.00	1817.06	1842.21	8.14	-	-

As reported in Table 33, in comparison with the patient treated at 310 mg/m^2, the patient treated at 370 mg/m^2 reached a SN-38 C_{max} that was more than double (65.95 vs. 30.70 ng/mL) and the SN-38 AUC_{last} was almost 25% higher (515.42 h vs. 415.40 ng/mL). This could explain the development of DLTs as CPT-11 is just a pro-drug rapidly converted to the active metabolite (SN-38).

Moving from a specific to a more general view of the pharmacokinetic results, in Figure 41, the mean plasma concentrations versus time profiles of CPT-11, SN-38, SN-38G and APC per dose level are reported.

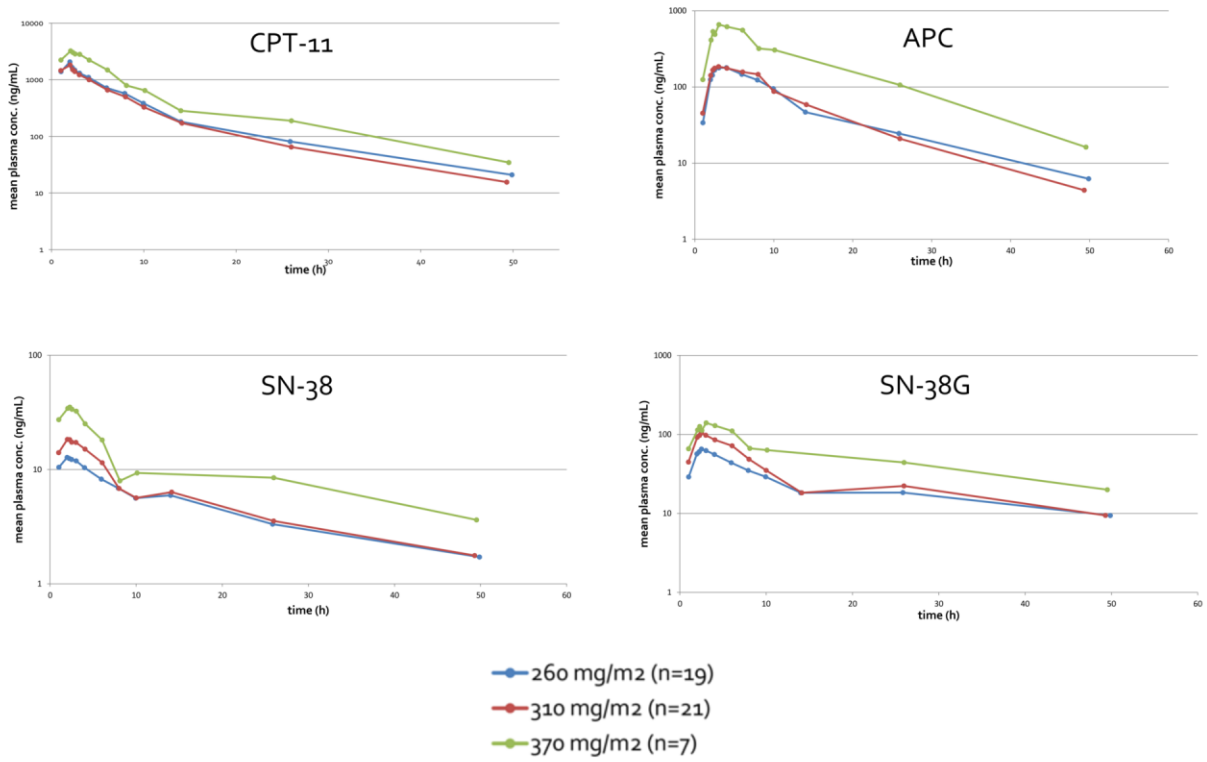

Figure 41 Mean plasma concentrations versus time profiles of CPT-11, SN-38, SN-38G and APC per dose level in patients enrolled in the phase I study.

Only the concentrations found during the first administration, with no effect derived by bevacizumab, have been used for the calculation of the mean values, and they include both the two genotype cohorts (Table 34). For all the quantifications of each patient, the highest concentrations found were within the dynamic range of the assay without the need for further dilution steps even if the independence of analysis from the dilution was previously assessed at the dilution factors of 1:10 and 1:100 (data not shown). If the blood sample at T=14 h should be done during the night, our policy was not to collect it for patient's respect. For this reason, for some patients the T=14 h sample was missed. In particular, this was the case of the seven patients treated at 370 mg/m^2.

Table 34 Data used for the generation of the mean plasma concentrations versus time profiles of CPT-11, SN-38, SN-38G and APC.

CPT-11				**APC**		
Time (h)	**260 (mg/m²)**	**310 (mg/m²)**	**370 (mg/m²)**	**260 (mg/m²)**	**310 (mg/m²)**	**370 (mg/m²)**
1	1395.28 ± 657.24	1454.00 ± 473.00	2232.70 ± 831.02	33.93 ± 23.62	45.31 ± 62.95	125.09 ± 117.60
2	2069.36 ± 876.71	1821.89 ± 562.43	3233.45 ± 1203.40	124.92 ± 71.46	142.18 ± 152.84	413.65 ± 332.28
2.25	1643.80 ± 696.46	1512.78 ± 477.03	3040.31 ± 1090.12	142.70 ± 82.58	166.92 ± 187.63	534.96 ± 473.18
2.5	1486.28 ± 601.02	1399.62 ± 437.10	2857.57 ± 1122.81	167.01 ± 100.36	176.80 ± 187.31	490.45 ± 402.79
3	1305.00 ± 558.31	1224.16 ± 394.26	2814.81 ± 1107.33	178.51 ± 112.01	185.17 ± 191.76	660.27 ± 596.25
4	1103.07 ± 502.06	1001.99 ± 419.86	2227.54 ± 930.41	179.30 ± 127.07	176.58 ± 159.47	619.02 ± 503.22
6	719.76 ± 341.02	658.09 ± 235.26	1488.96 ± 657.65	146.63 ± 86.74	157.52 ± 139.76	557.56 ± 434.17
8	573.98 ± 245.75	499.16 ± 166.92	792.76 ± 312.69	123.59 ± 65.35	146.55 ± 151.60	319.98 ± 367.70
10	383.99 ± 167.82	328.24 ± 88.63	646.42 ± 329.15	95.03 ± 64.20	87.54 ± 79.08	305.92 ± 391.86
14	181.51 ± 64.80	171.52 ± 21.93	-	46.83 ± 41.21	58.73 ± 7.95	-
26	81.19 ± 61.51	64.89 ± 27.18	188.72 ± 147.36	24.55 ± 19.61	20.98 ± 22.18	106.23 ± 116.89
50	20.94 ± 18.31	15.55 ± 10.63	34.52 ± 26.23	6.23 ± 8.01	4.41 ± 5.94	16.24 ± 20.39
SN-38				**SN-38G**		
1	10.47 ± 4.85	14.06 ± 6.00	27.32 ± 23.11	28.96 ± 17.95	44.69 ± 34.58	65.76 ± 61.53
2	12.77 ± 6.13	18.35 ± 8.16	34.32 ± 29.55	56.68 ± 28.77	91.86 ± 61.52	113.59 ± 83.89
2.25	12.50 ± 6.44	18.28 ± 8.00	35.16 ± 29.57	60.21 ± 30.79	97.04 ± 64.39	125.84 ± 96.19
2.5	12.25 ± 6.87	17.37 ± 8.02	33.67 ± 28.14	65.24 ± 34.09	104.42 ± 72.69	112.52 ± 79.66
3	11.91 ± 7.26	17.28 ± 9.13	32.42 ± 21.93	62.38 ± 33.35	97.65 ± 58.10	139.95 ± 105.97
4	10.38 ± 5.01	15.09 ± 8.56	25.13 ± 12.46	55.74 ± 30.30	85.35 ± 45.37	129.10 ± 90.03
6	8.25 ± 4.77	11.47 ± 7.41	18.13 ± 6.97	43.84 ± 23.07	71.71 ± 47.55	110.48 ± 77.32

8	6.87 ± 3.22	6.83 ± 4.76	7.96 ± 4.36	34.98 ± 15.50	48.51 ± 39.85	66.54 ± 76.62
10	5.62 ± 3.16	5.65 ± 3.39	9.33 ± 4.28	29.06 ± 14.64	35.03 ± 30.28	63.30 ± 77.49
14	5.94 ± 4.46	6.35 ± 5.78	-	18.25 ± 7.78	18.22 ± 13.40	-
26	3.33 ± 1.59	3.54 ± 1.59	8.48 ± 7.34	18.36 ± 11.54	22.27 ± 15.58	44.12 ± 37.04
50	1.72 ± 1.12	1.77 ± 0.84	3.62 ± 2.42	9.39 ± 7.75	9.43 ± 7.47	19.93 ± 14.50

The same considerations about the shape of the pharmacokinetic profiles of CPT-11, SN-38, SN-38G, and APC reported above can be done for the mean plasma concentrations versus time curves. CPT-11 and APC present a curve very similar each other, with concentrations declining in a bi-exponential manner, with a rapid initial phase and an extended terminal phase. At the same time, SN-38 and SN-38G show the same multi-exponential manner to decline with a very prolonged terminal phase.

In Figure 41 the standard deviation was not reported for major clarity. In fact, in Table 34 it is possible to see the huge variability, in term of standard deviation, obtained from the pharmacokinetic profiles of patients enrolled. In the following tables (Table 35, Table 36) the mean values of the principal pharmacokinetic parameters obtained from all the patients enrolled in the phase I study are reported, divided by administrations (I administration, i.e. without bevacizumab; II administration, i.e. with bevacizumab) and genotype group. In these tables dose adjustments were made for both C_{max} and AUC_{last}. Even in this case, looking at the standard deviation values, a great interindividual variability in the pharmacokinetic parameters has been observed.

The glucuronidation ratio (GR), defined as the ratio of SN38G AUC_{last} and SN38 AUC_{last}, has been calculated between the two genotype groups. Once more, in order to overcome the different concentrations among patients, the dose adjustment has been done for AUC_{last} values. No difference between the two cohorts has been obtained in GR values: indeed, GR equal to 6.10 ± 3.42 and 5.89 ± 4.02 has been obtained for **1/*1* patients and **1/*28* patients, respectively. These data suggest no pharmacokinetic differences between the two genotype groups.

Table 35 Summary of the main pharmacokinetic parameters of CPT-11, SN-38, SN-38G and APC without bevacizumab (I adm) obtained in the two genotype groups (**1/*1* and **1/*28* patients) during the I administration of the first chemotherapy cycle. Dose adjustments were made for C_{max} and AUC_{last}.

I adm (days 1-3)						
Genotype group	**compound**	**C_{max} (ng/mL)/ dose (mg/m²)**	**t_{max} (h)**	**AUC_{last} (h·ng/mL)/ dose (mg/m²)**	**$t_{1/2}$ (h)**	**Cl (L/h/m²)**
***1/*1**	CPT-11	8.12 ± 3.43	2.14 ± 0.55	59.64 ± 30.18	8.70 ± 1.41	20.77 ± 10.54
	SN-38	0.09 ± 0.05	2.89 ± 1.14	1.09 ± 0.46	18.43 ± 6.63	
	SN-38G	0.41 ± 0.23	3.19 ± 0.84	5.92 ± 3.22	20.05 ± 11.05	
	APC	1.09 ± 1.11	3.37 ± 0.98	13.46 ± 13.85	9.20 ± 3.00	
***1/*28**	CPT-11	6.59 ± 2.26	2.03 ± 0.20	49.09 ± 18.02	9.10 ± 1.92	22.65 ± 8.07
	SN-38	0.06 ± 0.04	2.18 ± 1.18	0.83 ± 0.37	32.54 ± 31.77	
	SN-38G	0.26 ± 0.17	2.95 ± 0.87	4.66 ± 2.95	23.85 ± 10.00	
	APC	0.75 ± 0.66	3.59 ± 1.25	9.81 ± 7.64	9.03 ± 1.57	

Table 36 Summary of the main pharmacokinetic parameters of CPT-11, SN-38, SN-38G and APC with bevacizumab (II adm) obtained in the two genotype groups (**1/*1* and **1/*28* patients) during the II administration of the first chemotherapy cycle. Dose adjustments were made for C_{max} and AUC_{last}.

II adm (days 15-17)						
Genotype group	**compound**	**C_{max} (ng/mL)/ Dose (mg/m²)**	**t_{max} (h)**	**AUC_{last} (h·ng/mL)/ dose (mg/m²)**	**$t_{1/2}$ (h)**	**Cl (L/h/m²)**
***1/*1**	CPT-11	8.74 ± 4.89	1.97 ± 0.43	63.80 ± 41.96	9.11 ± 1.29	20.21 ± 10.34
	SN-38	0.08 ± 0.04	2.39 ± 1.17	1.02 ± 0.52	24.72 ± 10.25	
	SN-38G	0.37 ± 0.18	2.89 ± 0.86	6.16 ± 3.95	20.99 ± 8.20	
	APC	0.62 ± 0.58	3.64 ± 1.12	8.87 ± 7.31	9.65 ± 2.52	
***1/*28**	CPT-11	6.81 ± 2.26	1.90 ± 0.52	49.78 ± 20.80	9.20 ± 1.60	25.83 ± 22.33
	SN-38	0.05 ± 0.03	1.83 ± 1.12	0.70 ± 0.32	32.99 ± 34.45	
	SN-38G	0.26 ± 0.18	2.71 ± 0.61	4.01 ± 3.02	22.96 ± 10.91	
	APC	0.42 ± 0.29	3.02 ± 0.59	6.56 ± 4.05	9.45 ± 2.13	

To conclude, as it is shown in Figure 42, CPT-11 Cl seems to be constant across the different dose levels (Spearman correlation coefficient = -0.02432, p = 0.8210), thus indicating a linear PK.

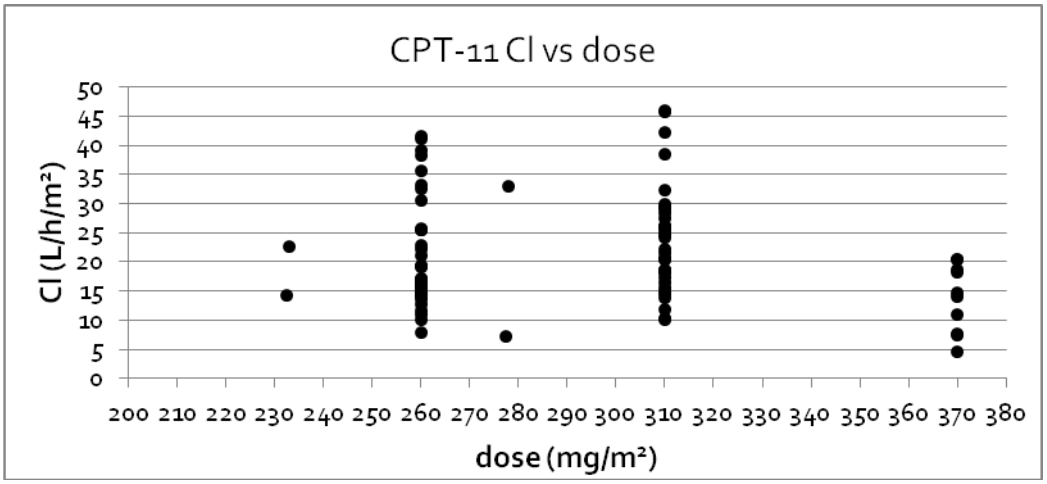

Figure 42 CPT-11 clearance (Cl) versus the doses (mg/m^2) in each patients.

Interaction with bevacizumab

In order to analyse the interaction between CPT-11 and bevacizumab, it has been considered only the PK of CPT-11 and SN-38, because of their clinical interest. Moreover, 4 out of the 47 patients enrolled were excluded because they did not receive a second dose of CPT-11 due to DLTs. In Table 37, the summary of CPT-11 and SN-38 pharmacokinetic parameters with and without bevacizumab is reported.

Table 37 CPT-11 and SN-38 pharmacokinetic parameters with and without bevacizumab (BV)

		Mean, range (% CV) without BV	**Mean, range (% CV) With BV**	**p**
CPT-11	C_{max} (ng/mL)/Dose (mg/m^2)	7.2, 3.3-14.1 (39)	7.8, 1.2-27.4 (50)	0.08
	T_{max} (h)	2.1, 1.0-4.0 (21)	1.9, 1.0-3.0 (24)	0.23
	AUC_{last} (h·ng/mL)/Dose (mg/m^2)	53.2, 21.6-129 (45)	57.0, 8.2-213 (59)	0.05
	$t_{1/2}$ (h)	8.8, 5.3-14.3 (18)	9.2, 5.4-12.0 (16)	0.48
	CL (L/h/m^2)	22.4, 7.7-46.3 (42)	23.5, 4.7-122 (76)	0.06
SN-38	C_{max} (ng/mL)/Dose (mg/m^2)	0.07, 0.02-0.22 (57)	0.06, 0.02-0.17 (58)	0.10
	T_{max} (h)	2.5, 1.0-6.0 (49)	2.1, 1.0-6.0 (55)	0.05
	AUC_{last} (h·ng/mL)/Dose (mg/m^2)	0.93, 0.33-2.3 (46)	0.86, 0.31-2.6 (53)	0.03
	$t_{1/2}$ (h)	25.4, 7.8-148 (96)	28.8, 8.4-178 (88)	0.02

No major differences were observed in all the pharmacokinetic parameters of CPT-11 and SN-38 in the presence or absence of bevacizumab. CPT-11 Cl was slightly higher when administered with bevacizumab compared to without bevacizumab (p = 0.06). The presence of bevacizumab was also associated with very small changes in the dose-adjusted AUC_{last} of CPT-11 (increased, p = 0.05) and SN-38 (reduced, p = 0.03). This is even graphically shown in the following figure (Figure 43).

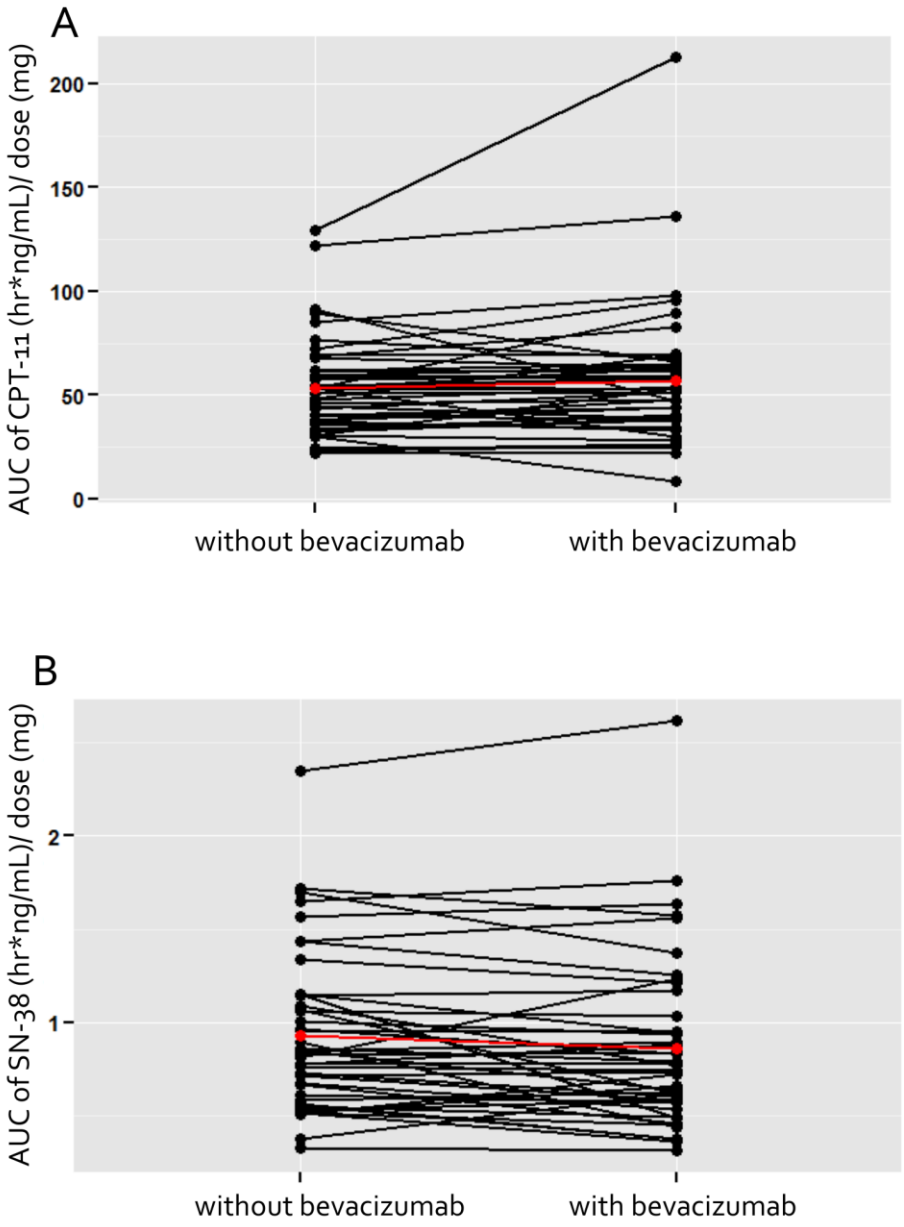

Figure 43 AUC_{last} of CPT-11 (A) and SN-38 (B) normalized for the CPT-11 dose, with and without concomitant treatment with bevacizumab. Each black line represents an individual subject, while the red lines connect the means for the two groups.

The overall median PFS was 9.0 months (95% CI = 6.6 - 13.1 months). PFS curves do not clearly separate by *UGT1A1* genotype, and a trend of PFS with CPT-11 dose is not evident (Table 38 and Figure 44).

Anyway, one patient with extensive liver and lymph node metastases and **1/*1* genotype treated at 310 mg/m^2 (dose reduced to 233 mg/m^2 after a DLT of grade 3 diarrhoea) had a complete response that has been durable for 5 years since the start of therapy (as of CT scan dated September 21, 2015).

Table 38 Response rate, overall and by CPT-11 dose and *UGT1A1*28* genotype. CR: complete response; PD: progressive disease; PR: partial response; SD: stable disease. Response rates between groups were compared using Fisher's exact test for count data. *One patient with **1/*1* genotype treated at 310 mg/m^2 (the MTD) had a CR that has been durable for 5 years since the start of chemotherapy.

	Patients	**CR+PR (responders)**	**SD+PD (non-responders)**	**p value and odds ratio (95% CI)**
Overall	33	13 (39%) 2 CR* + 11 PR	20 (61%) 15 SD + 5 PD	
260 mg/m^2	13	6 (46%) 1 CR + 5 PR	7 (54%) 6 SD + 1 PD	p = 0.61
310 mg/m^2	16	5 (31%) 1 CR* + 4 PR	11 (69%) 9 SD + 2 PD	
370 mg/m^2	4	2 (50%) 2 PR	2 (50%) 2 PD	
****1/*1***	16	6 (38%) 2 CR* + 4 PR	10 (63%) 7 SD + 3 PD	p = 1 OR = 0.86 (0.17 - 4.3)
****1/*28***	17	7 (41%) 7 PR	10 (59%) 8 SD + 2 PD	
Below MTD	6	2 (33%) 1 CR + 1 PR	4 (67%) 3 SD + 1 PD	p = 1 OR = 0.73 (0.06 - 6.2)
At or above MTD	27	11 (41%) 1 CR* + 10 PR	16 (59%) 12 SD + 4 PD	

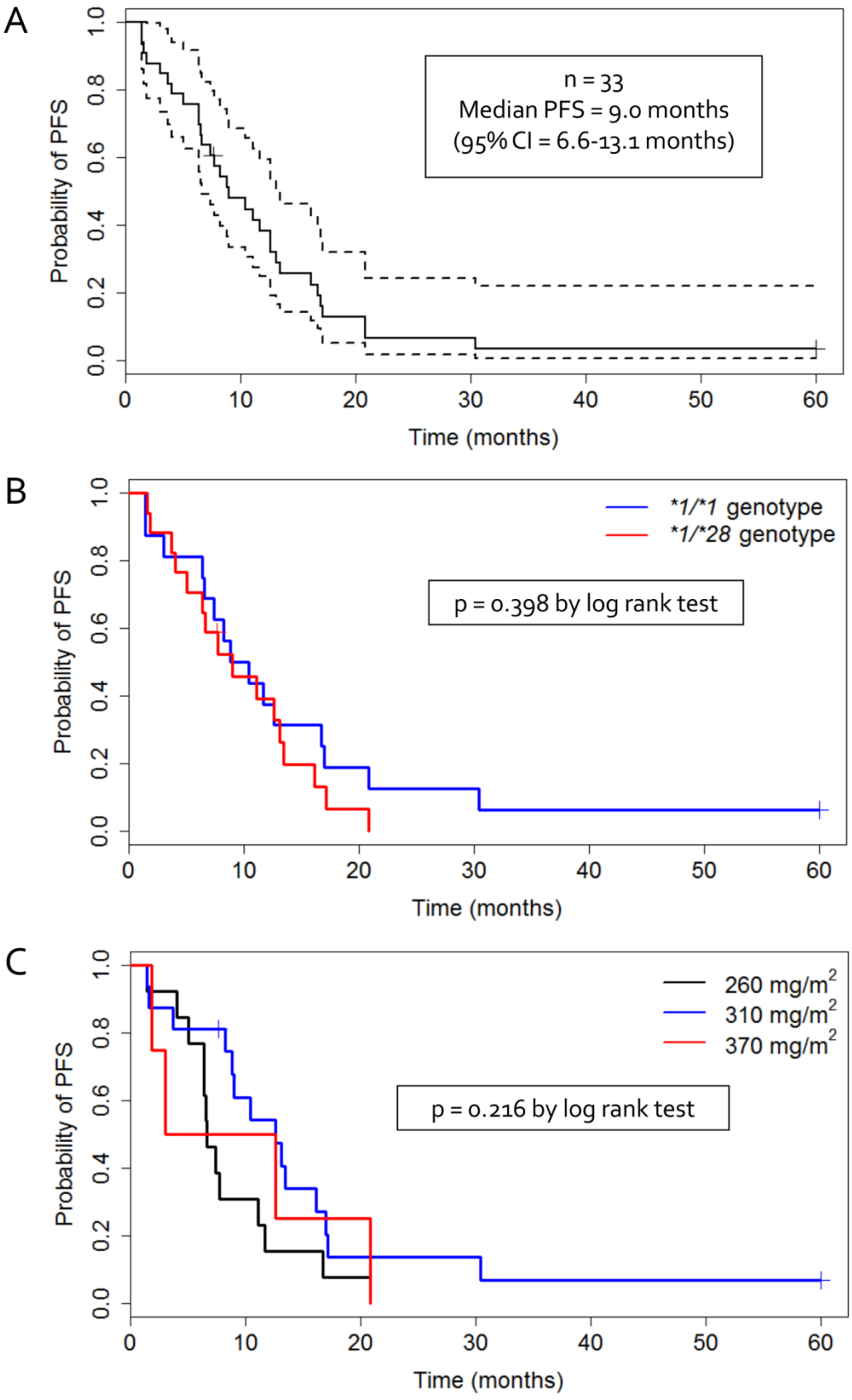

Figure 44 Progression-free survival (PFS) overall (A), by *UGT1A1* genotype (B), and by CPT-11 dose (C).

4.2.3 Genotype-guided phase I study of irinotecan administered in combination with 5-fluorouracil/leucovorin (FOLFIRI) and cetuximab as first-line therapy in metastatic colorectal cancer patients

4.2.3.1 Patients characteristics and dose escalation

To be eligible for this study, patients have to be *UGT1A1* wild type or heterozygous and RAS wild type. More in detail, the mutational analysis for *K-RAS/N-RAS/B-RAF* is necessary to assess that the patient is wild-type for all the mutations present in the exons 2, 3 and 4 of *K-RAS* and *N-RAS* in correspondence of the amino acid residues 12, 13, 59, 61, 117, and 146 (AIOM and SIAPEC-IAP, 2015).

Moreover, the wild-type status needs to be assessed for the *B-RAF* mutation within the exon 15 at the residue 600.

In the two centers involved in this ongoing study, seven patients were screened for the panel of mutations within the *RAS* and *RAF* genes family but, due to the relative high frequencies of these mutations in CRC patients and to the additional step of the *UGT1A1*28* screening, the enrollment is quite low and, at the moment, only two patients resulted eligible for this study.

The details of the enrollment status of this trial are summarized in Table 39.

Table 39 Genotype information about the seven screened patients.

Patient	Eligible	UGT1A1	EXON 2		EXON 3		EXON 4		EXON 15
		UGT1A1*28	K-RAS	N-RAS	K-RAS	N-RAS	K-RAS	N-RAS	B-RAF
1	Yes	*1/*1	wt	wt	wt	wt	wt	wt	wt
2	No	*28/*28	wt	wt	wt	wt	wt	wt	wt
3	No	*1/*1	wt	wt	wt	Q61H	wt	wt	wt
4	No	*28/*28	wt	wt	wt	wt	wt	wt	wt
5	Yes	*1/*28	wt	wt	wt	wt	wt	wt	wt
6	No	*1/*1	G12S	wt	wt	wt	wt	wt	wt
7	No	*1/*1	wt	G12S	wt	wt	wt	wt	wt

4.2.3.2 Pharmacokinetic analysis

Till now, just two patients completed both the treatments of the first therapy cycle and the PK followed during the days 1-3 and the days 15-17, accordingly to the protocol design. Even if, during the validation process, the stability of CPT-11 and its main metabolites was assessed at 4 months in plasma, patients' samples are analyzed as soon as possible after the collection. For this reason, the data regarding the first patient enrolled in this study are already available. In Figure 45 the plasma concentration-versus-time curves of CPT-11, SN-38, SN-38G, and APC are shown. They were determined, using the validated LC-MS/MS method (Marangon et al., 2015), described in the Section 4.1.1 in the first patient enrolled and receiving 260 mg/m^2 (first dose level) of CPT-11 as a 2-h continuous intravenous infusion.

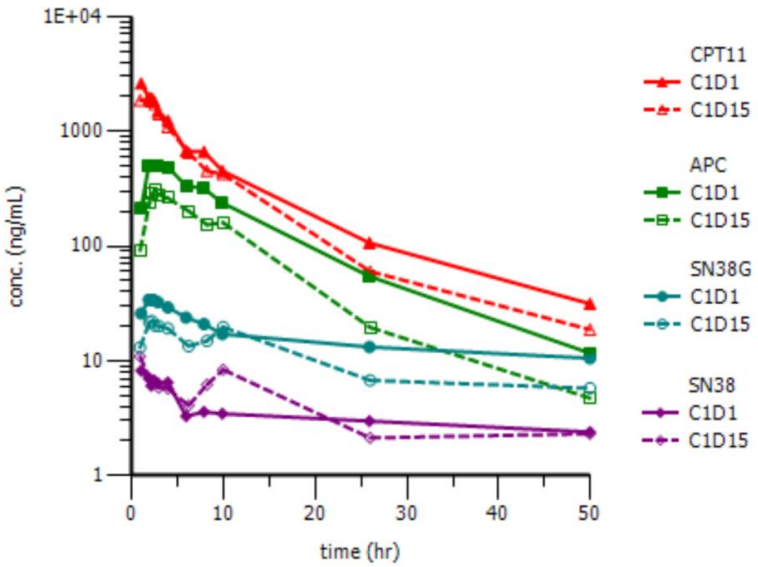

Figure 45 Plasma concentration-versus-time profiles of CPT-11 and its main metabolites (SN-38, SN-38G, and APC) in one patient receiving 260 mg/m^2 of CPT-11 during the I (C1D1) and the II (C1D15) administration of the first therapy cycle.

As regards the pharmacokinetic profiles of CPT-11 and its main metabolites, a good agreement between these curves and those obtained during the previous study has been observed, both in terms of shape and intensity. In fact, CPT-11 plasma concentrations appeared to decline in a bi-exponential manner, with a rapid initial phase and an extended terminal phase. The same trend has been shown with APC, which presents a curve very similar to CPT-11. As already observed, the two profiles

regarding SN-38 and SN-38G have shown the same multi-exponential manner to decline with a very prolonged terminal phase.

In order to define the pharmacokinetic interaction between CPT-11 and cetuximab, CPT-11 PK was evaluated in absence and presence of the monoclonal antibody in the same patient. The pharmacokinetic profile of CPT-11 alone was assessed at the first chemotherapy treatment in which cetuximab was administered on day 3 (50 h after the start of CPT-11 infusion). Whereas, CPT-11 PK in combination with cetuximab was performed during the second treatment of the first cycle, when the antibody was administered before CPT-11 dosage.

In the following tables (Table 40, Table 41) the main pharmacokinetic parameters of CPT-11 and its metabolites, obtained during the first and the second treatment respectively, are reported. They were determined applying a non-compartmental analysis.

Table 40 PK parameters obtained in one patient receiving 260 mg/m^2 of CPT-11 as a 2-h continuous intravenous infusion during the first administration (Day 1-3) of the first chemotherapy cycle.

Days 1-3							
Compound	**C_{max} (ng/mL)**	**t_{max} (h)**	**AUC_{last} (h·ng/mL)**	**AUC_{inf} (h·ng/mL)**	**$t_{1/2}$ (h)**	**V_d (L/m^2)**	**Cl (L/h/m^2)**
CPT-11	2599.96	1.08	16968.01	17448.08	10.60	227,85	14,90
SN-38	8.20	1.08	164.16	426.44	75.66	-	-
SN-38G	33.97	1.92	767.06	1652.60	58.24	-	-
APC	507.14	2.47	6576.38	6732.95	9.31	-	-

Table 41 PK parameters obtained in one patient receiving 260 mg/m^2 of CPT-11 as a 2-h continuous intravenous infusion during the second administration (Day 15-17) of the first chemotherapy cycle.

Days 15-17							
Compound	**C_{max} (ng/mL)**	**t_{max} (h)**	**AUC_{last} (h·ng/mL)**	**AUC_{inf} (h·ng/mL)**	**$t_{1/2}$ (h)**	**V_d (L/m^2)**	**Cl (L/h/m^2)**
CPT-11	1933.13	2.25	14420.32	14667.84	9.15	234,10	17,73
SN-38	10.93	0.97	198.31	277.22	23.57	-	-
SN-38G	22.18	2.25	521.74	722.15	24.05	-	-
APC	304.92	2.58	3644.86	3700.01	8.07	-	-

4.2.4 Genotype-guided phase I study for weekly paclitaxel in ovarian cancer patients

4.2.4.1 Patients characteristics and dose escalation

This third dose finding study is still on-going. Until now, a total of 37 patients were enrolled in the trial but only 35 patients were evaluable: 10 in the group 1 (*ABCB1-2677GG* genotype) and 25 in the group 2 (*ABCB1-2677GT; GA*, *AA*, *TT*, *AT* genotypes). The overall results of the dose escalation are schematized in Table 42.

Table 42 Dose escalation and observed DLTs in patients treated with weekly PTX. Group 1: *ABCB1-2677GG* genotype; group 2: *ABCB1-2677GT; GA*, *AA*, *TT*, *AT* genotypes.

PTX (mg/m^2)	group 1 patients (DLT)	group 2 patients (DLT)
80	**3 (0)**	**3 (0)**
90	/	**3 (0)**
100	**3 (0)**	**3 (0)**
110	**4 (1)** Prolonged G3 neutropenia	**3 (0)**
120		**10 (0)**
130		**3 (2)** Prolonged G3 neutropenia; Dermatological toxicity

The patients' enrollment in the group 2 was concluded: the dose of PTX was escalated from 80 to 130 mg/m^2, with steps of 10 mg/m^2. The dose of 130 mg/m^2 was not tolerated (2 patients out of 3 experienced DLTs), thus the 120 mg/m^2 dose level has been expanded to 10 patients, and due to no DLTs were observed among them, 120 mg/m^2 was declared the MTD for the group 2. In the group 1 patients, 1 DLT occurred among the first 3 patients treated at 110 mg/m^2. Hence, the 110 mg/m^2 cohort needs to be expanded to 6 patients before escalating the dose to the next dose level (120 mg/m^2) if no additional DLT will be observed. As reported in Table 42, the dose escalation conducted in this cohort was modified and the dose level of 90 mg/m^2 was omitted, thanks to a protocol emendation. Since 3 patients belonging to the group 2

characterized, according to the protocol rationale, by high risk of toxicity, were treated at the dose level of 100 mg/m^2 and no one exhibited DLT, it has been proposed to pass over the dose level of 90 mg/m^2 in patients belonging to group 1 (low risk of toxicity). Therefore, for this group of patients, the dose escalation passed directly from 80 mg/m^2 to 100 mg/m^2. Up to now, two of the three DLTs occurred were prolonged G3 neutropenia (67%), while the other DLT was a dermatological toxicity (Table 42).

4.2.4.2 Pharmacokinetics of paclitaxel and its 6α-hydroxy metabolite

Pharmacokinetic data were obtained from 34 out of the 35 patients (for one patient the PK was not performed) enrolled and evaluable till now in the phase I study. For this purpose, the validated LC-MS/MS method specifically developed for the quantification of PTX and its 6α-hydroxy metabolite in plasma samples (for the development and validation of the method see Section 4.1.2) has been applied. Figure 46 (Panel A and B) shows, as an example, the plasma concentration-versus-time curves of PTX and 6α-OH-PTX determined, during the first cycle of therapy, in two patients receiving respectively the lowest (80 mg/m^2, Panel A) and the highest (130 mg/m^2, Panel B) dose level of PTX as 1-h continuous intravenous infusion. In each panel, the two pharmacokinetic profiles of each analyte related to the first and fourth administration of PTX were shown.

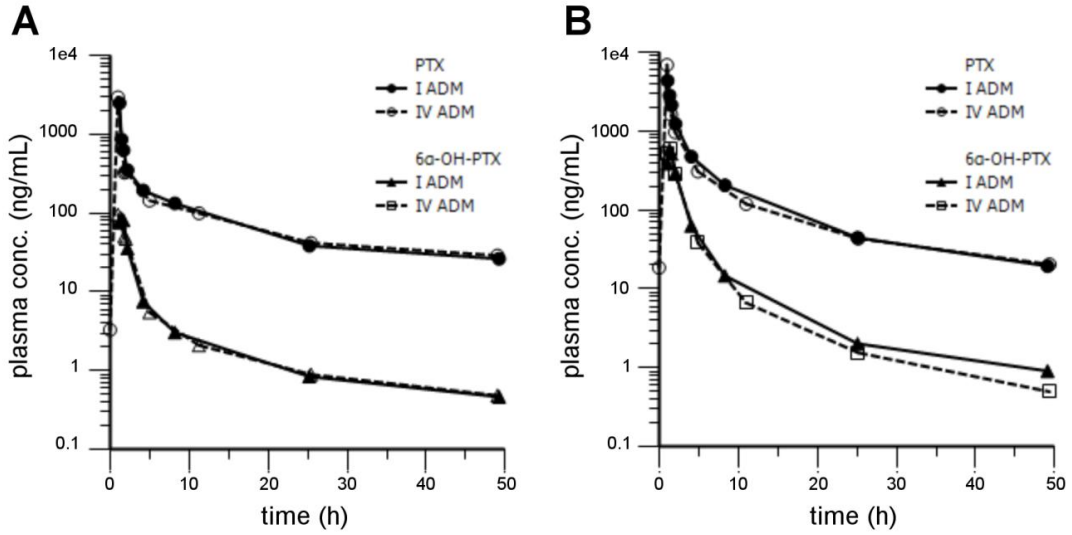

Figure 46 Plasma concentration-*versus*-time profiles of PTX and 6α-OH-PTX. **Panel A**: Plasma concentration-*versus*-time profiles of PTX and 6α-OH-PTX in one patient receiving 80 mg/m^2 of PTX during the I and the IV administration; **Panel B**: Plasma concentration-*versus*-time profiles of PTX and 6α-OH-PTX in one patient receiving 130 mg/m^2 of PTX during the I and the IV administration.

The principal pharmacokinetic parameters related to these two patients are reported in the following tables (Table 43 and Table 44).

Table 43 PK parameters obtained in one patient receiving 80 mg/m^2 of PTX during the first (I adm) and the fourth (IV adm) administration.

I adm						
compounds	**C_{max} (ng/mL)**	**t_{max} (h)**	**AUC_{last} (h·ng/mL)**	**$t_{1/2}$ (h)**	**V_z (L/m^2)**	**Cl (L/h/m^2)**
PTX	2467.60	1.20	5740.15	18.31	328.41	12.43
6α-OH-PTX	85.40	1.45	228.87	15.64		
IV adm						
PTX	2920.76	1.00	6169.61	22.40	364.02	11.26
6α-OH-PTX	95.20	1.00	256.76	18.49		

Table 44 PK parameters obtained in one patient receiving 130 mg/m^2 of PTX during the first (I adm) and the fourth (IV adm) administration.

I adm						
compounds	**C_{max} (ng/mL)**	**t_{max} (h)**	**AUC_{last} (h·ng/mL)**	**$t_{1/2}$ (h)**	**V_z (L/m^2)**	**Cl (L/h/m^2)**
PTX	4302.20	1.08	10644.14	12.34	210.62	11.83
6α-OH-PTX	576.86	1.33	1359.89	10.56		
IV adm						
PTX	6817.95	1.00	11325.75	15.65	248.99	11.03
6α-OH-PTX	580.35	1.53	1439.60	10.60		

In order to have a more general view of the pharmacokinetic profiles determined for PTX and 6α-OH-PTX in all the patients enrolled in this phase I study, the mean plasma concentrations versus time profiles of the two compounds per dose level have been calculated and they are reported in Table 45.

For all the quantifications of each patient, the highest concentration found in plasma samples was within the dynamic range of the assay without the need for further dilution steps even if the independence of analysis from the dilution was previously assessed at the dilution factors of 1:10 and 1:100 (data not shown).

Table 45 Data used for the generation of the mean plasma concentrations versus time profiles of PTX and 6α-OH-PTX.

PTX (ng/mL)								
Dose (mg/m²)	**Time (h)**							
	1	**1.25**	**1.5**	**2**	**4**	**8**	**25**	**49**
80 n=6	2377.67 ± 562.23	948.74 ± 239.36	551.20 ± 98.34	309.22 ± 59.68	138.16 ± 30.46	74.25 ± 30.99	23.61 ± 7.83	11.07 ± 7.87
90 n=3	1836.46 ± 905.99	834.41 ± 452.56	514.71 ± 339.84	442.73 ± 158.96	208.37 ± 53.33	91.89 ± 28.11	29.45 ± 7.45	13.15 ± 1.72
100 n=6	3576.32 ± 549.40	1713.80 ± 80.89	984.62 ± 109.63	499.79 ± 36.63	213.13 ± 25.96	102.36 ± 26.10	29.77 ± 6.36	12.13 ± 5.87
110 n=7	3941.74 ± 891.07	1900.47 ± 311.48	1166.74 ± 198.76	625.43 ± 126.73	236.87 ± 64.95	119.20 ± 35.98	25.47 ± 10.34	11.62 ± 3.24
120 n=9	5634.44± 764.94	2689.76 ± 814.16	1690.66 ± 475.60	984.84 ± 317.74	373.53 ± 128.54	146.24 ± 49.82	34.82 ± 11.44	15.24 ± 4.10
130 n=3	5254.80 ± 2341.28	3013.22 ± 1613.81	2323.08 ± 1339.06	1367.46 ± 896.90	440.83 ± 240.02	198.32 ± 87.69	56.13 ± 28.93	19.28 ± 5.16
6α-OH-PTX (ng/mL)								
Dose (mg/m²)	**Time (h)**							
	1	**1.25**	**1.5**	**2**	**4**	**8**	**25**	**49**
80 n=6	75.32 ± 12.24	73.72 ± 18.72	48.99 ± 19.24	22.87 ± 12.87	4.22 ± 1.92	1.76 ± 0.97	0.70 ± 0.22	0.25 ± 0.27
90 n=3	92.20 ± 58.21	92.20 ± 58.21	66.71 ± 57.49	52.43 ± 38.38	7.55 ± 3.25	2.53 ± 0.34	0.79 ± 0.26	0.33 ± 0.29
100 n=6	205.48 ± 81.28	228.62 ± 120.05	163.42 ± 113.18	65.34 ± 49.15	10.18 ± 8.78	3.07 ± 2.79	0.82 ± 0.64	0.27 ± 0.47
110 n=7	300.25 ± 212.77	348.85 ± 268.06	245.86 ± 188.00	83.67 ± 42.80	13.13 ± 8.88	4.39 ± 2.53	0.78 ± 0.34	0.17 ± 0.29
120 n=9	279.19 ± 144.78	327.14 ± 161.05	236.40 ± 98.07	110.36 ± 44.13	16.03 ± 6.36	4.36 ± 1.70	0.71 ± 0.30	0.23 ± 0.27
130 n=3	365.12 ± 116.25	468.40 ± 196.19	453.05 ± 234.17	269.73 ± 193.42	36.01 ± 27.24	9.30 ± 5.68	1.70 ± 0.72	0.66 ± 0.22

Noteworthy, in 24 out of 34 patients (70.6%), during the IV administration, the To sample (collected immediately before the PTX infusion) presented a residual presence of PTX at the mean concentration of 7.93 ± 12.82 ng/mL, thus indicating that with the weekly schedule, PTX may not be completely cleared from the bloodstream.

The mean plasma concentrations versus time profiles seem to augment with the dose increasing. Even in the case of PTX, a notable interindividual variability in plasma concentration levels has been observed. Thus, the standard deviations, reported in Table 45, have been omitted in Figure 47 for major clarity.

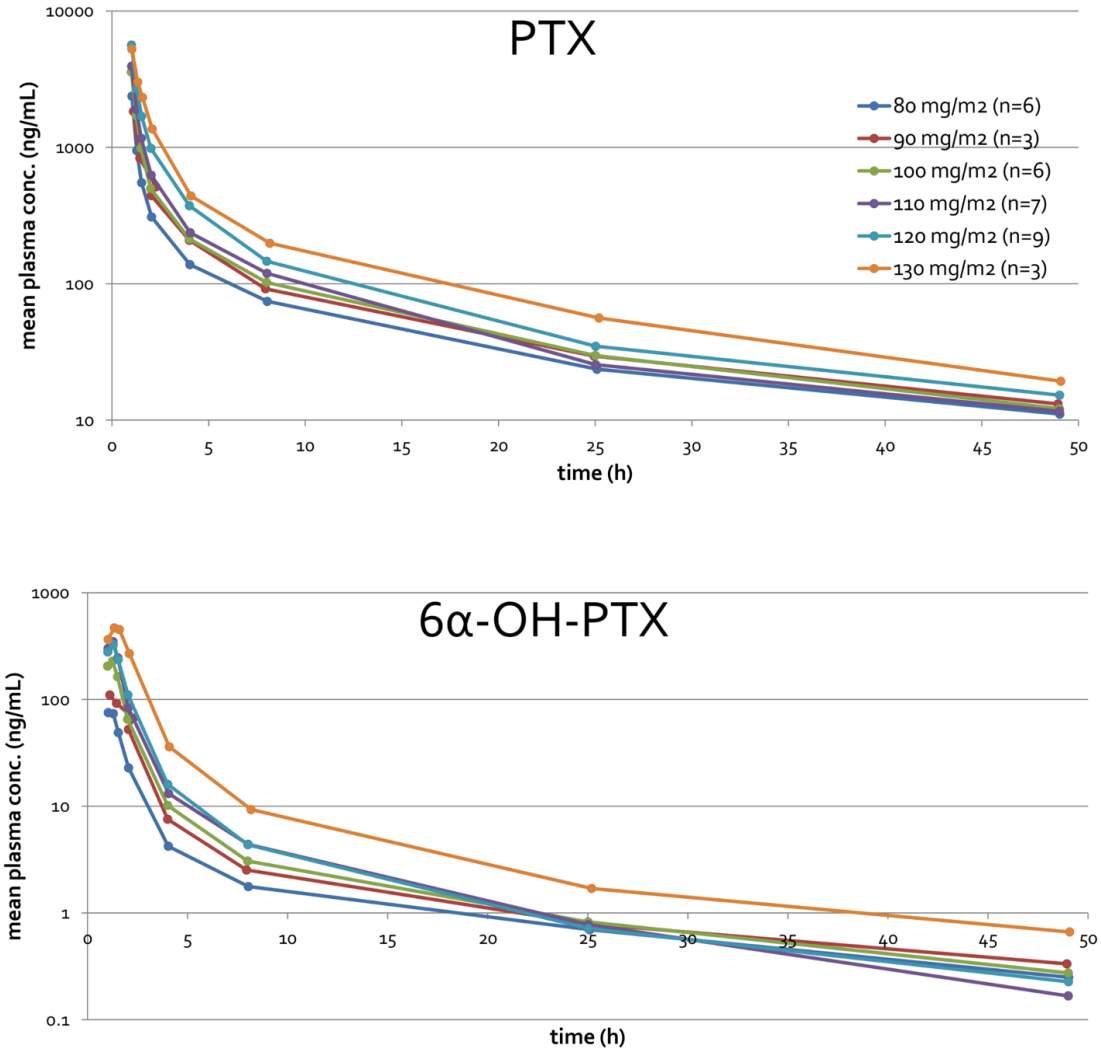

Figure 47 Mean plasma concentrations versus time profiles of PTX and 6α-OH-PTX per dose level determined in patients enrolled in the phase I study.

As reported for CPT-11 study, also in this case only the concentrations found during the first administration have been used for the calculation of the mean values, and they include both the two genotype cohorts.

In Table 46 and Table 47 the mean values of the principal pharmacokinetic parameters of PTX and 6α-OH-PTX per dose level are reported, respectively. No distinction between the two genotype groups has been done for these calculations.

Table 46 Summary of the mean pharmacokinetic parameters of PTX per dose level obtained during the first (I adm) and fourth (IV adm) administration.

PTX, I adm						
Dose (mg/m^2)	**C_{max} (ng/mL)**	**t_{max} (h)**	**AUC_{last} (h·ng/mL)**	**$t_{1/2}$ (h)**	**V_d (L/m^2)**	**Cl ($L/h/m^2$)**
80	2452.67 ± 550.26	1.03 ± 0.08	4221.73 ± 927.97	14.87 ± 2.18	394.55 ± 71.06	18.72 ± 4.23
90	2343.92 ± 310.70	1.00 ± 0.00	5064.95 ± 994.85	15.12 ± 4.17	379.27 ± 162.02	17.01 ± 2.73
100	3514.83 ± 527.26	1.00 ± 0.01	6045.01 ± 542.59	13.42 ± 2.63	308.01 ± 50.12	16.05 ± 1.59
110	3941.74 ± 891.07	1.02 ± 0.05	6830.04 ± 1409.31	12.76 ± 1.52	302.09 ± 93.86	16.32 ± 4.10
120	5175.00 ± 1552.96	1.06 ± 0.14	9339.32 ± 2337.45	13.09 ± 1.24	249.31 ± 67.91	13.21 ± 3.47
130	5254.80 ± 2341.28	1.03 ± 0.05	11843.56 ± 6246.63	12.72 ± 1.28	243.16 ± 147.05	12.82 ± 6.53
PTX, IV adm						
Dose (mg/m^2)	**C_{max} (ng/mL)**	**t_{max} (h)**	**AUC_{last} (h·ng/mL)**	**$t_{1/2}$ (h)**	**V_d (L/m^2)**	**Cl ($L/h/m^2$)**
80	2202.36 ± 448.63	1.01 ± 0.03	4109.80 ± 1112.49	20.39 ± 4.90	528.47 ±90.58	18.71 ± 4.75
90	2441.84 ± 915.05	1.00 ± 0.00	4513.99 ± 820.20	20.85 ± 0.71	555.34 ± 100.38	18.41 ± 2.76
100	3478.81 ± 1046.64	1.03 ± 0.04	5696.28 ± 1092.13	18.87 ± 2.46	458.63 ± 83.24	17.05 ± 3.86
110	3936.11 ± 859.69	1.01 ± 0.02	6508.20 ± 1283.91	16.12 ± 2.68	387.32 ± 81.12	16.89 ± 4.10
120	5367.92 ± 1739.55	1.01 ± 0.04	9138.38 ± 3256.79	17.02 ± 2.75	352.38 ± 167.33	14.15 ± 5.54
130	7342.52 ± 3231.71	1.00 ± 0.00	12297.64 ± 6345.87	16.80 ± 1.80	306.10 ± 191.85	12.21 ± 6.37

Table 47 Summary of the mean pharmacokinetic parameters of 6α-OH-PTX per dose level obtained during the first (I adm) and fourth (IV adm) administration.

6α-OH-PTX, I adm				
Dose (mg/m²)	**C_{max} (ng/mL)**	**t_{max} (h)**	**AUC_{last} (h·ng/mL)**	**$t_{1/2}$ (h)**
80	79.60 ± 16.08	1.14 ± 0.18	154.15 ± 51.62	14.58 ± 7.56
90	119.51 ± 29.73	1.19 ± 0.17	249.36 ± 82.52	14.49 ± 7.27
100	251.83 ± 122.42	1.14 ± 0.14	466.22 ± 281.68	10.15 ± 5.34
110	352.70 ± 264.97	1.23 ± 0.10	573.30 ± 364.34	7.91 ± 3.64
120	332.19 ± 158.48	1.23 ± 0.14	589.40 ± 237.63	9.32 ± 6.22
130	490.40 ± 218.48	1.42 ± 0.22	1138.57 ± 607.86	12.03 ± 2.93
6α-OH-PTX, IV adm				
Dose (mg/m²)	**C_{max} (ng/mL)**	**t_{max} (h)**	**AUC_{last} (h·ng/mL)**	**$t_{1/2}$ (h)**
80	74.17 ± 19.90	1.01 ± 0.03	149.08 ± 53.37	16.23 ± 13.71
90	99.30 ± 23.00	1.17 ± 0.29	236.84 ± 95.70	11.05 ± 4.04
100	176.55 ± 76.31	1.03 ± 0.04	350.30 ± 198.93	11.45 ± 8.88
110	233.44 ± 27.39	1.09 ± 0.19	436.66 ± 84.72	9.68 ± 6.92
120	263.60 ± 115.09	1.07 ± 0.18	532.47 ± 249.39	10.80 ± 5.45
130	495.92 ± 172.14	1.35 ± 0.31	1112.68 ± 490.56	8.86 ± 3.09

Differences between the first and the fourth administration

Although these data are not final due to the enrollment is still on-going, a preliminary comparison between the pharmacokinetic parameters obtained during the I and the IV administration has been performed among the patients enrolled till now, in order to investigate the possible autoinduction effect of PTX metabolism when administered in the weekly schedule (Gustafson et al., 2005). Thirty-two patients were evaluable in this analysis since in two patients the second PK was not performed due to DLT experience and venflon malfunction. Applying the Wilcoxon signed-rank test, no statistical differences were obtained in PTX C_{max}, t_{max}, AUC_{last}, and Cl ($p>0.05$) between the two administrations. These results, along with a significant increased of the PTX $t_{1/2}$ (from 13.61 ± 2.07 to 18.25 ± 3.38 h for the I and the IV administration, respectively) and a decreased V_d (from 316.51 ± 108.51 to 430.50 ± 139.19 L/m² for the I and the IV administration, respectively) during the IV administration ($p<0.0000$ in both the parameters), seem to exclude the autoinduction of PTX metabolism. As an example, in Figure 48 the mean PTX AUC_{last} obtained during the I and the IV administration are reported, divided per dose level for major clarity.

Furthermore, a significant decreasing in 6α-OH-PTX C_{max} (p=0.0028) and AUC_{last} (p=0.0455) has been observed during the IV administration. These results are in line with what reported for PTX.

Anyway, it should be considered that, in order to improve the patients' compliance, less sample time points were performed during the IV administration and, thus, the pharmacokinetic profile resulted less defined (Figure 22, Materials and methods Section). The sample time points omitted were specifically chosen in order to not invalidate the PTX PK. However, it is possible that during the IV administration the C_{max} of the metabolite has been missed in some patients, confirmed also by the variation of its t_{max} observed between the two administrations (decreased during the IV adm, p=0.0029). No difference in the $t_{1/2}$ value of the metabolite has been observed (p>0.05).

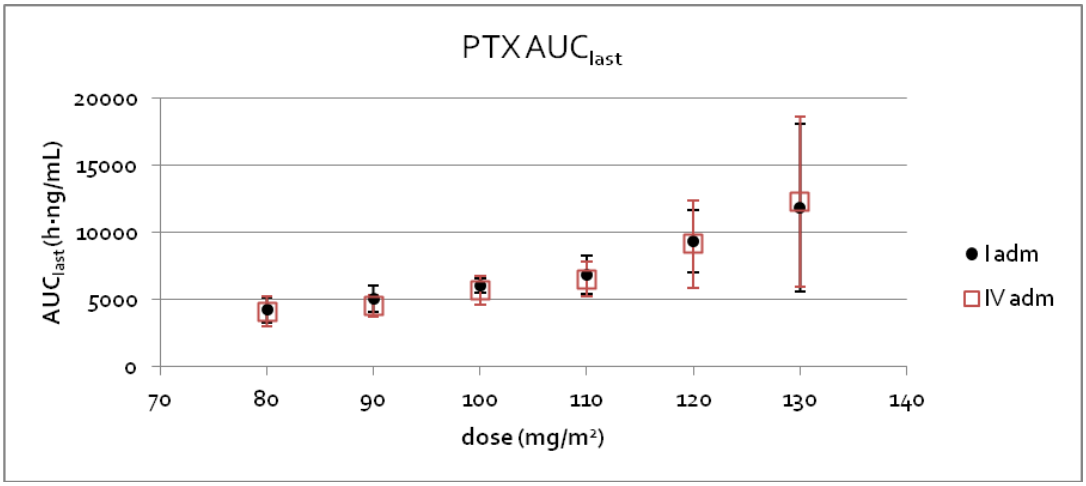

Figure 48 Comparison between the mean PTX AUC_{last} obtained during the I and the IV administration per dose level.

Differences between the two genotype groups

The effect of the patient's genotype on the PK of PTX and its main metabolite was also been investigated. As shown in the dose escalation scheme reported in Table 42, only the dose levels of 80, 100, and 110 mg/m^2 could be included for this analysis.

No significant (p>0.05) genotype-dependent differences in the main pharmacokinetic parameters of both PTX and 6α-OH-PTX have been obtained from this preliminary test.

PTX pharmacokinetics: linearity vs non linearity

In the literature, a disproportional increase in C_{max} and AUC at the increasing of the dose has been reported due to the saturation of both elimination and distribution processes

at higher concentrations of PTX (Henningsson et al., 2001) (Mross et al., 2000) (Gianni et al., 1995). The critical threshold for non-linear kinetics has not univocally determined. The evaluation of the PTX PK at different dose levels during this phase I study allowed us to investigate the drug's pharmacokinetic behaviour in a weekly schedule. Moreover, the closeness of the dose steps (10 mg/m^2) used for this dose escalation design could permit a precise definition of the critical threshold for non-linear PTX kinetics.

In Figure 49 the mean PTX AUC_{last} values, obtained during the first administration, versus the dose are reported.

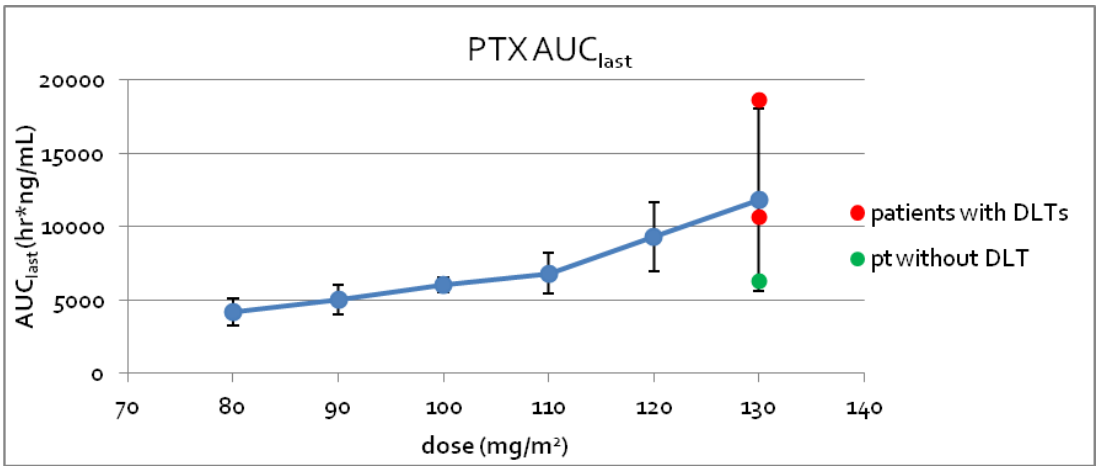

Figure 49 Mean PTX AUC_{last} obtained during the first administration versus the drug dose. The single AUC_{last} value of each patient treated at 130 mg/m^2 of PTX are reported (in red those related to patients experienced DLT; in green concerning the patient who did not experience DLT).

Looking at the blue line, it seems that the increasing of PTX AUC_{last} with the augment of the dose followed two distinct trends, one from 80 to 110 mg/m^2 and the other from 110 to 130 mg/m^2. In order to quantify this increase, the percentages of the dose and the relative AUC_{last} increment are reported in Table 48.

Table 48 PTX mean AUC_{last} values per dose level obtained during the first administration. For each dose level, the percentages of dose and relative AUC_{last} increasing, respect to the previous level, are reported.

Dose (mg/m^2)	AUC_{last} (h·ng/mL)	Dose increment %	AUC_{last} increment %
80	4221.73 ± 927.97	0	0
90	5064.95 ± 994.85	12.5	19.9
100	6045.01 ± 542.59	11.1	19.3
110	6830.04 ± 1409.31	10.0	13.0
120	9339.32 ± 2337.45	9.1	36.7
130	11843.56 ± 6246.63	8.3	26.8

Although the low number of patients per dose level represents a limitation, it seems that PTX AUC_{last} increased proportionally with the increment of the dose up to 110 mg/m^2. On the contrary, for doses higher than 110 mg/m^2, the increment is disproportionate respect to the dose increasing.

Looking at the single AUC_{last} value of each patient treated at 130 mg/m^2 (a total of 3 patients: 2/3 experienced DLT), as reported in Figure 49, it is clear that the huge AUC_{last} standard deviation observed at this dose level was due to the only patient who did not experience DLT. This patient exhibited indeed a particularly low AUC_{last} respect to the other two patients who experienced severe toxicity after the treatment. Excluding this patient from the calculation of the mean AUC_{last} at 130 mg/m^2, the increment respect to 120 mg/m^2 should be even greater than that reported in Table 48, thus emphasizing the non-linear behaviour of the PTX PK when doses higher than 110 mg/m^2 are administered. This result is in line with the literature that reports a variation of PTX kinetics from linear to non-linear with the increasing of the dose administered. Moreover, in our case, the critical threshold for non-linear kinetics seems to be the dose of 110 mg/m^2.

This consideration has been confirmed also by the Cl variations across the different dose levels, reported in Figure 50.

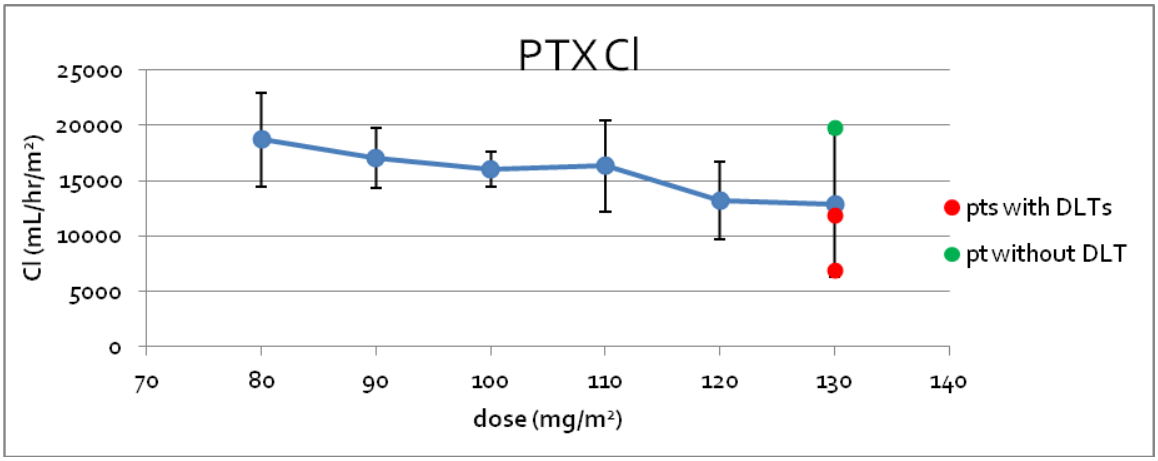

Figure 50 Mean PTX Cl obtained during the first administration versus the dose level. The single Cl value of each patient treated at 130 mg/m^2 of PTX is reported (in red those related to patients experienced DLT; in green concerning the patient who did not experience DLT).

Even in this case the Cl seems to follow two different trends, and the turning point seems to be the 110 mg/m^2 dose level: for doses lower than that the Cl can be

considered constant (linear PK), while for higher doses a decreased was observed (non-linear PK). This effect would be even stronger whether, as for AUC_{last}, the single Cl value of each patient treated at 130 mg/m^2 are considered. Even in this case, the large standard deviation was due to the only patient who did not experience DLT after the treatment.

More in general, the Spearman's rank correlation test was applied to analyse the overall correlation between PTX Cl and the dose. An inverse correlation has been found (Spearman correlation coefficient equal to -0.5191 and -0.4050 during the I and the IV administration, respectively), meaning that the Cl decreases with the increasing of the dose, and this trend is statistically significant (p = 0.0012 and 0.0175 during the I and the IV administration, respectively).

5 DISCUSSION

5.1 LC-MS/MS methods: development and validation

5.1.1 High-performance liquid chromatography–tandem mass spectrometry method for the simultaneous determination of irinotecan and its main metabolites in human plasma

The purpose of this work was to set up and validate a method to quantify irinotecan and its main metabolites (SN-38, SN-38G, and APC), in plasma of patients treated with both the standard doses, defined by different treatment protocols, and higher doses as expected in a dose escalation study.

Several methods are currently employed for the determination of CPT-11 and its metabolites in human plasma, most of them based on the use of fluorescence detectors, as reviewed by Chen et al. (Chen et al., 2012) and, more recently, by Crotti et al. (Crotti et al., 2015).

Anyway, to our knowledge, no method was available to simply measure irinotecan and, in particular, SN-38G with a high degree of sensitivity and in a wide concentration range. Among these methods, indeed, just few could quantify SN-38G but two (Sparreboom et al., 1998) (Owens et al., 2003) exploit a chromatographic runtime longer than 35 minutes and a too limited range (Owens et al.: 2-25 ng/mL for SN-38, SN-38G and APC and 5-300 ng/mL for CPT-11; Sparreboom et al.: 2-200 ng/mL for all the analytes). Since it has been mentioned the importance of quantifying SN-38G concentration, the method developed by Sai et al. (Sai et al., 2002) seemed not suitable because of a SN-38G lower limit of quantification (LLOQ) of 10 ng/mL that appears not fitting to accurately determine the elimination phase of the pharmacokinetic profile of this metabolite. Among the LC-MS/MS methods, just one, developed by our group, is suitable for simultaneously analyzing CPT-11, SN-38, SN-38G and APC (Corona et al., 2010) but the upper limit of quantification (ULOQ) (2 µg/mL for CPT-11) seemed not suitable for the quantification of samples collected by patients treated with high-dose irinotecan regimens (> 180 mg/m^2).

For this reason, a sensitive, specific and rapid method to quantify irinotecan and its main metabolites in human plasma has been developed and validated. The developed

method requires a small volume of plasma sample (100 µL), only simple treatment with methanol added with acetic acid (0.1% v/v) and a reasonable time of analysis (18 min). High selectivity and sensitivity was guaranteed by working in SRM mode (Kaye et al., 1992). In addition, as irinotecan and its main metabolites concentration needed to be determined on plasma collected by pluri-treated patients, more than one transition for each analyte (one used as quantifier and two as qualifiers) have been followed, in order to avoid interferences. Lastly, this method was developed using the reference standard of SN-38G avoiding any interferences related to the enzymatic conversion of SN-38. SN-38G reference compound, indeed, is not easy to find commercially available and many alternatives have been proposed: standard custom-synthesized by the analytical laboratory (Chen et al., 2012), biosynthesis of SN-38G from SN-38 precursor and the uridine-diphosphate (UDP) glucuronic acid substrate through the action of the UDP-glucuronosyl transferase 1A1 isoform enzyme (Corona et al., 2010), and hydrolysis of SN-38G in plasma by β-glucuronidase (Zhang et al., 2009). In this last case, the quantification of SN-38G was obtained through the increase of SN-38 after the hydrolysis.

We investigated a range of concentrations (10-10000 ng/mL for CPT-11, 1-500 ng/mL for SN-38 and SN-38G and 1-5000 ng/mL for APC) that we expected to cover those found in the patients' plasma even though, on the basis of our signal to noise ratio, we could have validated a lower LLOQ. Chromatographic separation was done on a Gemini C18 column (3 µM, 100 mm x 2.0 mm) using 0.1% acetic acid/bidistilled water and 0.1% acetic acid/acetonitrile as mobile phases. The mass spectrometer worked with electrospray ionization in positive ion mode. The method has been successfully validated according to the FDA-EMA guidance on bioanalytical method validation. The standard curves were linear (R^2 ≥0.9962) over the concentration ranges and had good back-calculated accuracy and precision. The intra- and inter-day precision and accuracy, determined on three quality control levels for all the analytes, were always <12.3% and between 89.4% and 113.0%, respectively. Moreover, we evaluated this bioanalytical method by re-analysis of incurred samples as an additional measure of assay reproducibility. The concentrations of irinotecan and its main metabolites determined on the two analytical runs were very similar in all samples, being the percentage difference of the results within 20% for more than 71% of the total amount of samples

re-analyzed. Finally, the present method was applied to a pharmacokinetic study in patients with metastatic CRC enrolled in a genotype-guided phase I study (dose-escalation study) of irinotecan administered in combination with 5-FU/leucovorin (FOLFIRI) and bevacizumab. The successful application of our method to a dose-escalation study, such as a phase I study, guarantees to have the possibility to employ this method to all irinotecan dosages currently used in clinical practice.

5.1.2 High-performance liquid chromatography–tandem mass spectrometry method for the simultaneous determination of paclitaxel and its main metabolite 6α-hydroxy-paclitaxel in human plasma

With the always stronger need of quantifying taxanes in samples derived from clinical studies or from treated patients due to the great inter-patient variability, and thanks to the identification of liquid chromatography coupled with mass spectrometry as the Gold Standard of drug testing, many LC-MS/MS assays have been developed and validated. In Table 49 a list of the published methods for the quantification of paclitaxel in human plasma is reported.

Noteworthy, the extraction procedure more frequently described in literature to quantify paclitaxel is surely LLE. The alternative sample treatment proposed in these published methods is the SPE, in some cases as on-line (Yamaguchi et al., 2013) or automatic (Sottani et al., 1998) SPE. Furthermore, in two assays the SPE has been associated to PP (Gardner et al., 2008) (Sottani et al., 1998). Instead, none of the published methods designed a sample treatment based on only PP, which is the fastest extraction method. The best LLOQs (0.1 ng/mL (Alexander et al., 2003)) in paclitaxel quantification were obtained applying LLE but this procedure is certainly more time-consuming than PP and on-line SPE. Thus, the first challenge in developing this method was to obtain a reasonable, from a clinical point of view, LLOQ concentration employing as sample treatment only PP in order to develop an analytical assay more suitable for a routine clinical application.

Table 49 List of publications related to the quantification of paclitaxel in human samples. (o)=on-line; (a)=automatic; (sa)=semi-automatic; DTX: docetaxel.

Ref.	Compound(s)	Sample (µL)	Sample prep	LLOQ (ng/mL)	ULOQ (ng/mL)	Runtime (min)
(Fernández-Peralbo et al., 2014)	PTX, 6α-OH-PTX, p-3′-OH-PTX	200	LLE	0.125, 0.5, 0.125	100	17.5
(Yamaguchi et al., 2013)	PTX, 6α-OH-PTX, p-3′-OH-PTX	90	(o)SPE	5, 0.87, 0.87	5000, 870, 435	30
(Zhang et al., 2011)	PTX, 6α-OH-PTX, p-3′-OH-PTX	100	LLE	0.5	500	7
(Zhang and Chen, 2008)	PTX	200	LLE	102.1	20420	2
(Gardner et al., 2008)	PTX	100	PP/SPE	10	2500	4
(Gao et al., 2006)	PTX	200	LLE	1	1000	4
(Gardner et al., 2006)	PTX	100	LLE	2	2500	8
(Gréen et al., 2006)	PTX, 6α-OH-PTX, p-3′-OH-PTX	500	SPE	0.5	7500,750,400	9
(Vainchtein et al., 2006)	PTX, 6α-OH-PTX, p-3′-OH-PTX	200	LLE	0.25	1000, 100, 100	9
(Mortier et al., 2004)	PTX	500	LLE	10	1000	2 & 0.8
(Stokvis et al., 2004)	PTX	200	LLE	0.25	1000	9
(Basileo et al., 2003)	PTX	100	(sa)LLE	1	1000	6
(Alexander et al., 2003)	PTX, 6α-OH-PTX, p-3′-OH-PTX	400	LLE	0.1, 0.1, 0.1	100, 100, 100	5
(Sottani et al., 1998)	PTX	500	PP/ (a)SPE	5	500	8
(Mortier et al., 2005)	DTX, PTX, 6α-OH-PTX, p-3′-OH-PTX	250	LLE	2	1000	11

Among the methods reported in Table 49, seven assays have been developed for the simultaneous quantification of the drug and its main metabolites, 6α-OH-PTX and p-3'-OH-PTX, while the other eight consider only the quantification of paclitaxel. Looking only at former seven, some of them employ a sample volume that ranges from 0.2 to 0.5 mL (Fernández-Peralbo et al., 2014) (Gréen et al., 2006) (Vainchtein et al., 2006) (Alexander et al., 2003) (Mortier et al., 2005). We could not employ these methods because we aimed at using a reduced volume of plasma (100 µL).

Another crucial feature was represented by the linearity range. Since we needed a method to be applied to a phase I study, the ULOQ had to be suitable for the quantification of samples collected by patients treated with higher than standard PTX doses, as expected in a dose escalation study. Most of the methods for the quantification of PTX and its main metabolites showed an ULOQ not appropriate for our purpose, being PTX upper limit of quantification equal or less than 2500 ng/mL (Fernández-Peralbo et al., 2014) (Zhang et al., 2011) (Alexander et al., 2003) (Mortier et al., 2005). The two methods with the highest ULOQs (5000 ng/mL (Yamaguchi et al., 2013) and 7500 ng/mL (Gréen et al., 2006)) have, instead, several other limitations, such as an unsatisfactory LLOQ (5 ng/mL) for paclitaxel (Yamaguchi et al., 2013) or a large plasma volume requirement (Gréen et al., 2006) together with a time-consuming sample treatment process (SPE).

Thus, due to the previously discussion on the methods already published, an LC-MS/MS assay has been developed and validated for the quantification of paclitaxel and its principal metabolite, 6α-OH-PTX. Our method requires a small volume of plasma sample (100 µL), only simple treatment with methanol added with formic acid (0.1% v/v) and a reasonable time of analysis (21 min). Chromatographic separation was done on a SunFireTM C18 column (3.5 µM, 92 Å, 2,1 x 150 mm) using 0.1% formic acid/bidistilled water and 0.1% formic acid/acetonitrile as mobile phases. The mass spectrometer worked with electrospray ionization in positive ion mode and selected reaction monitoring. The method has been fully validated according to the FDA-EMA guidance on bioanalytical method validation. The standard curves were linear (R^2 ≥0.9948) over the concentration ranges of 1-10000 and 1-1000 ng/mL for PTX and 6α-OH-PTX, respectively, and had good back-calculated accuracy and precision. The intra- and inter-day precision and accuracy, determined on three quality control levels for all

the analytes, were always <9.9% and between 91.1% and 104.8%, respectively. Moreover, we evaluated this bioanalytical method by re-analysis of incurred samples as an additional measure of assay reproducibility. The concentrations of PTX and its main metabolite determined on the two analytical runs were very similar in all samples, being the percentage difference of the results within 20% for more than 91.7% of the total amount of samples re-analyzed. Finally, the present method was successfully applied to a pharmacokinetic study in advanced ovarian cancer patients in a genotype-guided phase I study (dose-escalation study) of weekly paclitaxel.

5.1.3 High-performance liquid chromatography–tandem mass spectrometry method for the simultaneous determination of sunitinib and its main metabolite N-desethyl sunitinib in human plasma

Sunitinib is an oral multi-targeted tyrosine kinase inhibitor with antiangiogenic and antitumor activities attributable to the inhibition of several related tyrosine kinase receptors, including VEGF receptors types 1 and 2 (FLT1 and FLK1/KDR), platelet-derived growth factor receptors (PDGFR- α and PDGFR-β), stem cell factor receptor (c-KIT), and FMS-related tyrosine kinase 3 (FLT-3), which are implicated in tumour proliferation, angiogenesis, and metastasis (Giamas et al., 2010; Sawyers, 2004). Target total plasma concentrations of sunitinib plus active metabolite (N-desethyl sunitinib) are in the range of 50-100 ng/mL, as deduced from PK/PD relationship data (Faivre, 2006). Total trough concentrations <50 ng/mL have been associated with decreased therapeutic efficacy, whereas concentrations >100 ng/mL have been associated with an increased risk for toxicity. Taking into account the low therapeutic index, the large interindividual variability in the systemic exposure among patients treated with sunitinib, and the positive exposure-efficacy relationship of sunitinib, there is a strong rationale for TDM of this drug.

In the literature, previously published LC-MS/MS methods were developed for the detection of sunitinib alone or with its active metabolite. The main characteristics of these methods are reported in Table 50.

Table 50 List of publications related to the quantification of sunitinib and its active metabolite N-desethyl sunitinib.

Reference	Sunitinib and metabolites analized	Other analytes analized	Sample Volume (mL)	Extraction Method	LLOQ (ng/mL)	ULOQ (ng/mL)	Runtime (min)
(Minkin et al., 2008)	Sunitinib		0.2	LLE	0.2	500	3
(Haouala et al., 2009)	Sunitinib	Imatinib, nilotinib, dasatinib, sorafenib, lapatinib	0.1	PP	1	500	20
(de Bruijn et al., 2010)	Sunitinib, N-desethyl sunitinib		0.1	LLE	0.2	50	4
(Zhou and Gallo, 2010)	Sunitinib		0.01	PP	1.37	1000	3.2
(Honeywell et al., 2010)	Sunitinib	Erlotinib, sorafenib, gefitinib	0.02	PP	5	4000	<4
(Rodamer et al., 2011)	Sunitinib, N-desethyl sunitinib		0.1	PP	0.06	100	4
(Lankheet et al., 2013)	Sunitinib	Dasatinib, erlotinib gefitinib, imatinib, lapatinib, nilotinib, sorafenib	0.05	PP	5	2500	10
(Rais et al., 2012)	Sunitinib, N-desethyl sunitinib		0.05	LLE	0.1 sunitinib, 0.2 N-desethyl sunitinib	100 sunitinib, 200 N-desethyl sunitinib	5
(Qiu et al., 2013)	Sunitinib, N-desethyl sunitinib, N,N didesethyl		0.05	PP	0.1	100	4
(Götze et al., 2012)	Sunitinib	Erlotinib, imatinib, lapatinib, nilotinib, sorafenib	0.1	PP	10	1000	12
(Andriamanana et al., 2013)	Sunitinib	Bortezomib, dasatinib, erlotinib, imatinib, lapatinib, nilotinib, sorafenib, vandetanib	0.05	PP	2	250	10
(Lankheet et al., 2013a)	Sunitinib, N-desethyl sunitinib		0.5	PP	2.5	500	10
(Musijowski et al., 2014)	Sunitinib , N-desethyl sunitinib		0.5	LLE	0.1	150	6

Only six published methods considered the quantification of both sunitinib and N-desethyl sunitinib. One of the pivotal characteristics of a good method to be applicable to the clinical routine is the use of limited quantity of biological samples. The published methods employed a quantity of plasma that ranges from 50 µL (Lankheet et al., 2013a) (Qiu et al., 2013) to 500 µL (Musijowski et al., 2014). Instead, our method requires only 30 µL of plasma.

Another crucial point to consider in the development of a TDM method is surely the ease and the rapidity of the processing procedure. Three published methods use protein precipitation, whereas the other three require a more complex liquid-liquid extraction. Our processing method consists of an easy protein precipitation (PP) with 150 µL of methanol. Moreover, the major part of the methods aims to avoid the light exposure in any step, from the collection to the analysis of the sample, in order to prevent the conversion of the Z- to the unwanted E-isomer. This is a clear limit in the perspective of the applicability of the method to the clinical practice. For this reason, the method presented in this thesis does not require the protection from the light during the sample preparation but only a heating step with a heated water bath at 90°C for 5 min. The incubation of the sample, just before their introduction into the autosampler for the analysis, allows the rapid reconversion of the E-isomer, formed during the sample preparation, to the Z-form. Despite the additional heating step of 5 min little extends the processing time, it strongly facilitates the handling of the samples avoiding the necessity of sodium or UV-light (de Bruijn et al., 2010) and the setting of suitable dark rooms. Some authors (Lankheet et al., 2013a) found a way to bypass the light protection: as the two isomers showed equal mass spectrometry response, to process the data, the sum of single reaction monitoring responses of both separated isomers of each analyte was used. Consequently, protection from light during shipment, handling and processing of samples was not necessary employing the method developed by Lankheet et al. However, in order to apply this method, a quantifiable peak of both the isomers is necessary in any analytical run and this consideration could explain the LLOQ at 2.5 ng/mL. In our method, the LLOQ is 25 fold lower for both the analytes and the calibration range was 0.1-500 ng/mL for sunitinib and 0.1-250 ng/mL for N-desethyl sunitinib. Considering that the trough plasma concentration during the sunitinib therapy is typically in a range from 10 to 200 ng/mL for sunitinib and from 5 to 100

ng/mL for N-desethyl sunitinib, our method generously covered the clinical range and could be suitable also for pharmacokinetic studies in which really low concentrations should be detected in order to very accurately determine parameters as half-life.

Chromatographic separation was done on a Synergy Fusion RP C18 (4 µM, 80 Å, 2 x 50 mm) using 0.1% formic acid/bidistilled water and 0.1% formic acid/acetonitrile as mobile phases. The method resulted rapid, with retention times of the analytes at 2.61 and 2.55 min for sunitinib and N-desethyl sunitinib, respectively and a total analytical run, including the recondition time, of only 7 min. The mass spectrometer worked with electrospray ionization in positive ion mode and selected reaction monitoring. The method has been successfully validated according to the FDA-EMA guidance on bioanalytical method validation, although the long term stability and the incurred samples reanalysis still need to be performed in order to conclude this process. The standard curves were linear (R^2 ≥0.9931) over the concentration ranges and had good back-calculated accuracy and precision. The intra- and inter-day precision and accuracy, determined on three quality control levels for both the analytes, were always <11.7% and between 96.7% and 111.7%, respectively.

In conclusion, our method described an innovative approach to overtake the troublesome step of the light protection and a rapid and easy preparation process consistent with our aim of introducing the TDM of sunitinib in the clinical laboratory routine.

5.2 Phase Ib clinical trials

5.2.1 Genotype-guided phase I study of irinotecan administered in combination with 5-fluorouracil/leucovorin (FOLFIRI) and bevacizumab in advanced colorectal cancer patients

FOLFIRI is CPT-11 plus infusional 5-fluorouracil/leucovorin (5-FU/LV), and when combined with bevacizumab, is one of the standard first-line treatment options for patients with metastatic colorectal cancer (mCRC) (Benson et al., 2014). The recommended dose of CPT-11 in FOLFIRI is 180 mg/m^2 every two weeks based on a dose-finding study (Ducreux et al., 1999) that did not take into account the toxicity risk conferred by the *UGT1A1*28* allele. In fact, the *UGT1A1*28* allele confers reduced UGT1A1-mediated inactivation of SN-38, the active metabolite of CPT-11, and has been associated with severe neutropenia (Innocenti et al., 2004) (Toffoli et al., 2006) (Hoskins et al., 2007). The current U.S. prescribing information warns that the *UGT1A1 *28/*28* genotype is a risk factor for neutropenia and states that a dose reduction should be considered in these patients.

Moreover, it has been demonstrated, also in a previous phase I study conducted by our group (Toffoli et al., 2010) that patients with the **1/*1* and **1/*28* genotypes are able to tolerate more than the standard dose of CPT-11 (Marcuello et al., 2011) (Innocenti et al., 2014). Anyway, the effect of adding a biologic agent to genotype-guided dosing of FOLFIRI was unknown and the safe doses of CPT-11 in **1/*1* and **1/*28* patients treated with FOLFIRI plus bevacizumab needed to be identified.

This phase I trial has been designed in order to clarify these issues. Thus, the safe doses of CPT-11 that can be administered in mCRC patients treated with FOLFIRI in combination with bevacizumab according to their *UGT1A1*28* genotype (excluding those with the *28/*28 genotype) has been identified. The results support that CPT-11 can be safely administered at doses up to 310 mg/m^2, compared to the standard dose of 180 mg/m^2. In fact, the genotype-directed MTD of CPT-11 was 260 mg/m^2 for **1/*28* patients, and 310 mg/m^2 for **1/*1* patients. As previously reported (Innocenti et al.,

2004) (Toffoli et al., 2006) (Hoskins et al., 2007), the two genotypes confer different risk of toxicity and the **1/*28* patients do not tolerate the same dose of **1/*1* patients.

It is noteworthy that the MTDs for FOLFIRI plus bevacizumab are lower than those for FOLFIRI alone. In fact, in a previous phase I study with a similar design in front-line mCRC patients (Toffoli et al., 2010), the MTDs were 370 and 310 mg/m^2 for **1/*1* and **1/*28* patients, respectively. It is difficult to say whether this downward shift is caused by a pharmacodynamic effect of bevacizumab or other factors, as the two studies cannot be compared head to head.

Moreover, the analysis of the CPT-11 PK of in our study seems to rule out that the lower MTDs in FOLFIRI plus bevacizumab compared to those of FOLFIRI alone are due to an interaction between bevacizumab and CPT-11 increasing systemic exposure to either CPT-11 or SN-38. Pharmacokinetic parameters of exposure (C_{max} and AUC_{last}) are essentially unchanged (Table 37). A limited sampling pharmacokinetic substudy of the phase III FOLFIRI study in mCRC (Hurwitz et al., 2004) suggested a 33% increase in the $AUC_{0\text{-}5h}$ of SN-38 associated with the bevacizumab treatment. This difference has not been confirmed in three formal drug-drug interaction studies, including ours (Suenaga et al., 2014) (Denlinger et al., 2009).

This study concludes that, even with the addition of bevacizumab, a genotype-directed strategy leads to safe administration of higher doses of CPT-11. For patients treated at the MTD, the dose intensity of the regimen was preserved, as CPT-11 was dose-reduced only in 35% of patients and both 5-FU and bevacizumab dosing was unchanged. The limited number of patients evaluable for efficacy (n = 33) prevents drawing definitive conclusions on whether higher doses of CPT-11 lead to increased efficacy of FOLFIRI plus bevacizumab. Overall response was more frequently observed at the higher CPT-11 doses in previous FOLFIRI studies (Toffoli et al., 2010) (Marcuello et al., 2011), but in the present study no apparent association was found. The PFS analysis does not show a clear trend of improved PFS at the higher doses either (Figure 44).

Since the efficacy was not the primary endpoint of this study, the hypothesis that higher CPT-11 dosing might confer increased efficacy of FOLFIRI plus bevacizumab should be tested in a large population prospective study. Thus, based on the MTDs from the current study, a phase II clinical trial in front-line mCRC where CPT-11 is dosed at 310 and 260 mg/m^2 in patients with the **1/*1* and **1/*28* genotypes (respectively) is

currently ongoing and led by the University of North Carolina Lineberger Comprehensive Cancer Centre (NCT02138617 on clinicaltrials.gov). After the initial proof-of-concept studies with either FOLFIRI or single-agent irinotecan (Toffoli et al., 2010) (Marcuello et al., 2011) (Innocenti et al., 2014), this study provides definitive evidence for the role of genetic stratification to deliver safe doses of irinotecan in mCRC patients treated with a standard of care regimen. Even more importantly, this study suggests that the majority of mCRC patients currently treated with FOLFIRI plus bevacizumab may be underdosed with respect to irinotecan. The consequences of such underdosing on patient survival are unknown. With the advent of genomic screening in cancer patients and pre-emptive genotyping for pharmacogenomics prediction (Gillis et al., 2014), available genetic data on the *UGT1A1*28* status of patients in medical records can be utilized to reach the goal of improving precision in irinotecan-based therapies.

5.2.2 Genotype-guided phase I study of irinotecan administered in combination with 5-fluorouracil/leucovorin (FOLFIRI) and cetuximab as first-line therapy in metastatic colorectal cancer patients

FOLFIRI is a frequently used chemotherapy regimen for the first-line treatment of mCRC. Results of the phase III CRYSTAL trial showed that the addition in this setting of the EGFR antibody cetuximab improves the clinical outcome in patients whose tumours did not have mutations at *K-RAS* codons 12 and 13 (Van Cutsem et al., 2009). Some other striking results were observed by Heinemann and colleagues (Heinemann et al., 2014), in an open-label, randomized phase III clinical trial with the first aim of comparing the efficacy of cetuximab or bevacizumab in FOLFIRI first-line treatment of mCRC. Although the interpretation of the results is quite controversial (Pietrantonio et al., 2014), it seemed that a statistically significant overall survival advantage was reported in favour of cetuximab (median duration 28.7 months [95% CI 24.0–36.6] vs 25.0 months [22.7–27.6]; HR 0.77 [95% CI 0.62–0.96]; p=0.017) and this was further increased

in the subgroup of patients with tumours that were wild-type at all *RAS loci* (exon 2–4 *K-RAS* and *N-RAS*; 33.1 months vs 25.6 months; HR 0.70 [95% CI 0.53–0.92]; p=0.011).

Currently, the dose of CPT-11 in FOLFIRI schedule is 180 mg/m^2. However, our group demonstrated that a higher dose of CPT-11 is tolerated in *UGT1A1 *1/*1* and *UGT1A1 *1/*28* patients than *UGT1A1 *28/*28* also if the regimen is combined with bevacizumab (Eudract 2009-012227-28; Protocol code CRO-2009-25, NCT01183494).

However, at our knowledge, no data have been generated to demonstrate if these higher doses are tolerated when cetuximab is added.

Having regards to the intriguing results obtained from the previous genotype-guided phase Ib studies and the information in the literature that assessed the regimen FOLFIRI plus cetuximab as a promising treatment, there was a strong rationale to begin the phase Ib study entitled: "*A genotype-guided phase I study of irinotecan administered in combination with 5-fluorouracil/leucovorin (FOLFIRI) and cetuximab as first-line therapy in metastatic colorectal cancer patients*".

At the moment, due to the relative high frequencies of RAS mutations in CRC patients and to the additional step of the *UGT1A1*28* screening, just two patients resulted eligible and was enrolled in this new clinical study.

A proper statistical analysis of the PK data obtained during this clinical study will be done when the patient's enrollment will be concluded and the total plasma concentrations of CPT-11 and its three main metabolites will be obtained. In fact, only at the end of the clinical study, the evaluation of the effect of cetuximab on the CPT-11 PK could have a statistical significance.

Anyway, it can be interesting to compare the main PK parameters, such as C_{max} and AUC_{last}, obtained for the first patient enrolled with the mean values of those determined from the patients treated at the same CPT-11 dosage (260 mg/m^2) during the previous phase I clinical trial of CPT-11 in combination with bevacizumab. In order that the comparison is homogeneous, only patients with the same *UGT1A1*28* genotype (*UGT1A1*1/*1)* were considered in the calculation of the mean values. Moreover, as this clinical study is a phase Ib, that is a dose escalation study, only the data from the patients treated at the same CPT-11 dosage (260 mg/m^2) were taken into account for this preliminary analysis. CPT-11 C_{max} (2599.96 and 1933.13 ng/mL for the I and the II administration, respectively) and AUC_{last} (16968.01 and 14420.32 hr*ng/mL

for the I and the II administration, respectively) obtained were in good agreement with the mean C_{max} and AUC_{last} obtained in the previous study during both the I and the II administrations (C_{max}: 2354.46±958.98 and 1967.14±479.73 ng/mL for the I and the II administration, respectively; AUC_{last}: 15587.97±6996.21 and 13706.79±3824.02 hr*ng/mL for the I and the II administration, respectively). On the contrary, SN-38 C_{max} (8.20 and 10.93 ng/mL for the I and the II administration, respectively) and AUC_{last} (164.16 and 198.31 hr*ng/mL for the I and the II administration, respectively) were overall lower than the mean values previously obtained during both the I and II administrations (C_{max}: 22.51±14.15 and 15.90±4.92 ng/mL for the I and the II administration, respectively; AUC_{last}: 252.01±63.67 and 221.06±60.40 hr*ng/mL for the I and the II administration, respectively). The same observation could be done for SN-38G. In fact, SN-38G C_{max} (33.97 and 22.18 ng/mL for the I and the II administration, respectively) and AUC_{last} (767.06 and 521.74 hr*ng/mL for the I and the II administration, respectively) resulted lower than the mean values previously obtained during both the I and the II administrations (C_{max}: 94.56±40.78 and 82.95±35.72 ng/mL for the I and the II administration, respectively; AUC_{last}: 1326.29±499.24 and 1182.49±423.10 hr*ng/mL for the I and the II administration, respectively). Finally, also APC showed different results respect to the previous data. In fact, APC C_{max} (507.14 and 304.92 ng/mL for the I and the II administration, respectively) and AUC_{last} (6576.38 and 3644.86 hr*ng/mL for the I and the II administration, respectively) resulted higher than the mean values observed during the phase I of CPT-11 in combination with bevacizumab (C_{max}: 244.44±191.57 and 143.34±49.78 ng/mL for the I and the II administration, respectively; AUC_{last}: 2981.55±1859.81 and 1993.59±954.82 hr*ng/mL for the I and the II administration, respectively).

The formation of the two metabolites (SN-38 and APC), follows two different pathways (Figure 14). Therefore, the decrease of SN-38 and SN-38G concentrations and the parallel increase of APC plasma level, in comparison with the data concerning the previous clinical study, could probably be explained by a different activity of the enzymes involved in the metabolism.

5.2.3 Genotype-guided phase I study for weekly paclitaxel in ovarian cancer patients

PTX is a chemotherapeutic agent with broad antitumor activity. Its dosing and scheduling have been optimized during the last two decades, resulting in today's widely applied weekly regimens of 1-h infusions (Takano et al., 2002) (Mielke et al., 2005a).

The great interindividual differences observed in the PTX PK and the related pharmacodynamic profile (toxicity and tumour response) still remain the major concern related to this cytotoxic agent. The recent advances in the PGx field, pointed out as this high variability among patients could be related to the genetic characteristic of the patient. In fact, the recommended dose of weekly paclitaxel as 1-h i.v. infusion is 80 mg/m^2 based on a dose-finding study (Klaassen et al., 1996) that did not take into account the advances in the PGx research, which deserves the inclusion of patient genetic profiling in the optimization of anticancer drug dosage.

Several SNPs in genes encoding the well-known metabolizing enzymes (*CYP2C8*, *CYP3A4*) and transporters (such as *ABCB1*) of paclitaxel have been investigated in a large number of studies as genetic factors which may be of influence on paclitaxel induced adverse events, as recently revised by Frederiks et al. (Frederiks et al., 2015). Among them, the *2677G>T/A* SNP (responsible for the substitution from alanine to serine or threonine) has been shown to correlate with the P-gp expression and phenotype. In particular, the *2677G>T/A* allele has demonstrated to impact the PTX PK and PD in ovarian cancer patients (Hamidovic et al., 2010). Moreover, an association of the SNP with higher risk of severe haematological and non-haematological toxicity was demonstrated in 118 ovarian cancer patients of Asian ethnicity treated with PTX and carboplatin (Kim et al., 2009). Furthermore, a pilot study on 20 carboplatin/PTX treated ovarian cancer patients conducted by our group confirmed a lowered PTX Cl for patients carrying the variant *2677T/A* allele (unpublished data).

Thus, in order to render the treatment individualization feasible, our group designed a genotype-guided phase I clinical trial of weekly PTX in order to define the MTD and DLTs according to the *ABCB1-2677G>T/A* SNP in epithelial ovarian cancer patients. More specifically, patients enrolled in this trial have been divided in two different

cohorts based on the patients' genotype: group 1 (*ABCB1-2677GG* genotype), which is, according to the protocol rationale, the one characterized by low risk of toxicity and group 2 (*ABCB1-2677GT; GA, AA, TT, AT* genotypes), the one supposed to be at high risk of toxicities.

Although this dose finding study is still on-going, the safe dose of paclitaxel that can be administered in advanced ovarian cancer patients with *ABCB1-2677GT; GA, AA, TT, AT* genotypes (group 2) has been identified. In this cohort of patients, paclitaxel can be safely administered at doses up to 120 mg/m^2, compared to the standard dose of 80 mg/m^2. Concerning the patients with *ABCB1-2677GG* genotype (group 1), the dose escalation has not yet been concluded. Anyway, also in this group, doses higher than the standard one can be safely administered since the enrollment of patients' cohort is now at the dose level of 100 mg/m^2. Two of the three DLTs occurred till now were prolonged G3 neutropenia (67%), while the other DLT was a dermatological toxicity.

A deepened discussion of the clinical results of this phase I study, as reported for the previous trial related to FOLFIRI in combination with bevacizumab, should be premature, and will be completed when the study will be concluded. For instance, with the completion of the clinical data (PFS, ORR, the cumulative haematological and non haematological toxicities, number of dose reductions or delays between consecutive treatments) collection related to all the patients enrolled in this phase I study, the hypothesis of the threshold model, which seems to correlate the toxicity with the length of time that PTX concentration exceeds a threshold concentration (Gianni et al., 1995) (Henningsson et al., 2001) (Mielke et al., 2005b) (Mielke et al., 2005a) (Huizing et al., 1997), will be investigated.

At the moment, preliminary analyses have been done about the pharmacokinetic parameters obtained for both PTX and its major metabolite, 6α-OH-PTX. The first notable consideration refers to the comparison between the PK obtained during the first and the fourth administration, aimed at verifying the hypothesis of the autoinduction of PTX metabolism (Gustafson et al., 2005). Our results seemed to exclude this effect, since no statistical differences in PTX C_{max}, t_{max}, AUC_{last}, and Cl ($p>0.05$) between the two administrations has been obtained. Moreover, these results seems to be reinforced by the significant increased of the PTX $t_{1/2}$ along with a

decreased V_d during the IV administration that have been observed (p>0.0000 in both the parameters).

Noteworthy, up to now, no significant (p>0.05) differences in the main pharmacokinetic parameters of both PTX and 6α-OH-PTX between the two genotype groups have been obtained from this preliminary test. In particular, no difference in Cl between the two patients cohorts have been observed, although it has been reported in literature a lowered Cl in patients carrying the *2677T/A* genotype (Green, 2008) (Wong et al., 2005). Since this comparison has been conducted only at the dose level of 80, 100, and 110 mg/m^2, a further and more complete discussion related to this analysis will be done at the study conclusion.

Given the dose escalation nature of this study, an interesting investigation has been conducted on the dose dependent behaviour of PTX PK. In fact, several studies have reported a switching from linear to non linear PK when high doses of paclitaxel were administered (Henningsson et al., 2001) (Mross et al., 2000) (Gianni et al., 1995). The critical threshold for non-linear kinetics has not univocally determined, as it depends also from the administration schedule. Our results seemed to be in line with this behaviour, indicating the dose level of 110 mg/m^{2}as the turning point: with doses less than or equal to 110 mg/m^2, paclitaxel showed linear kinetics, which became non-linear for doses higher than 110 mg/m^2.

The overall trend of Cl, analysed by the Spearman's rank correlation test, has shown an inverse correlation with the paclitaxel dose (Spearman correlation coefficient = -0.5191 and 0.4050 during the I and the IV administration, respectively), meaning that the Cl decreases with the increasing of the dose (non-linear PK). Moreover, this trend has been found statistically significant (p = 0.0012 and 0.0175 during I and the IV administration, respectively). More in details, Cl seemed to show the same dual behaviour observed for AUC_{last}: for doses less than or equal to 100 mg/m^2 Cl appeared to be constant, while a clear decrease has been observed for doses higher than 100 mg/m^2. This consideration seemed to confirm the PTX PK switching from a linear to a non-linear behaviour for doses higher than 110 mg/m^2.

6 CONCLUSIONS

Innovative genotype-guided phase Ib clinical trials are intended to redefine the dose or the treatment modalities with conventional cytotoxic drugs taking into account the newer pharmacogenetic knowledge. In fact, among all the parameters responsible for the high variability, in term of both efficacy and toxicity, observed in patients with the same diagnosis and treated with the same drugs, great interest has been reserved to the effect of genetic differences among individuals on the response of cancer patients to chemotherapy. Thus, the aim of these particular phase I studies is to produce not a unique optimal dose for an unselected population ("one dose fits all" model), but different dose levels for patients with a different genetic background, as required by the *personalized medicine* approach.

In this PhD thesis, three genotype-guided phase Ib clinical trials have been described. Their principal aim was to define the MTDs and the DLTs of:

- CPT-11 administered in the FOLFIRI regimen plus bevacizumab or cetuximab in mCRC patients according to *UGT1A1*28* genotype;
- weekly PTX according to the *ABCB1-2677G>T/A* polymorphism in epithelial ovarian cancer patients.

At present, only the phase I related to FOLFIRI in combination with bevacizumab have been concluded. The MTD of genotype-directed irinotecan was 260 mg/m^2 for **1/*28* patients, and 310 mg/m^2 for **1/*1* patients. The obtained results support that the two genotypes confer a different risk of toxicity and **1/*28* patients do not tolerate the same dose of **1/*1* patients, although no significant difference in the pharmacokinetic parameters between the two genotype cohorts has been observed. Moreover, the MTDs for FOLFIRI plus bevacizumab resulted lower than those for FOLFIRI alone (370 and 310 mg/m^2 for **1/*1* and for **1/*28* patients, respectively), as found in a previous phase I with a similar design in front-line mCRC patients. In our study, the effect of the addition of bevacizumab to the genotype-guided dosing of FOLFIRI has been investigated by a pharmacokinetic point of view. The analysis of the PK of CPT-11 and its active metabolite seemed to rule out an effect of bevacizumab on CPT-11 and SN-38 PK.

Even if the efficacy was not the primary endpoint of this study since the limited number of patients evaluable for efficacy (n = 33) prevented drawing definitive conclusions on

whether higher doses of irinotecan lead to increased efficacy of FOLFIRI plus bevacizumab, no apparent association was found between the overall response and the higher CPT-11 doses. Anyway, this hypothesis should be tested in a large population prospective study.

The second phase I study of irinotecan, in FOLFIRI regimen in combination with cetuximab, has been recently started. Up to now, just two patients resulted eligible and were enrolled in this new clinical study, due to the relative high frequencies of RAS mutations in CRC patients. In fact, RAS mutations preclude the use of cetuximab and therefore the enrollment in this clinical study. Anyway, the pharmacokinetic profile of the first patient treated according to this protocol has already been determined.

Although it is still on-going, the third phase I study reported in this thesis has already demonstrated that a higher than standard dose of PTX could be safely administered in patients with *ABCB1-2677GT; GA, AA, TT, AT* genotypes, the group characterized, according to the protocol design, by a high risk of toxicity. In this cohort of patients, PTX can be tolerated at doses up to 120 mg/m^2, compared to the standard dose of 80 mg/m^2. Concerning the group of patients with *ABCB1-2677GG* genotype and defined as at low risk of toxicity, current data indicated that doses up to 100 mg/m^2 can be safely administered even if the MTD has not yet been determined.

Preliminary analyses have been done on the pharmacokinetic parameters determined for both PTX and its major metabolite, 6α-OH-PTX. The first notable result refers to the comparison between the PK obtained during the first and the fourth administration, which seemed to exclude the autoinduction of PTX metabolism (reported in literature), since no statistical differences in PTX systemic exposure between the two administrations has been observed.

Moreover, an initial comparison between the two genotype groups has been conducted at the dose levels of 80, 100, and 110 mg/m^2, and, up to now, no significant differences in the main pharmacokinetic parameters of both PTX and 6α-OH-PTX have been obtained. In particular, no difference in Cl between the two patients' cohorts has been observed, although it has been reported in literature a lowered Cl in patients carrying the *2677T/A* genotype. Noteworthy, the investigation on the dose dependent behaviour of PTX PK, conducted on the data collected till now, indicated a switching from linear to non-linear PK with doses higher than 110 mg/m^2 of PTX.

In order to support the phase I studies reported above, during this PhD project two LC-MS/MS methods have been set up for the quantification of the following drugs and their relative metabolites in human plasma:

- CPT-11 and its main metabolites, SN-38, SN-38G, and APC;
- PTX and its 6α-hydroxy metabolite (6α-OH-PTX).

Moreover, beyond the phase I projects, a third method has been developed, for the quantification of sunitinib and its active metabolite, N-desethyl sunitinib.

These methods have been conceived in order to be applied to both clinical studies and TDM and, for this reason, they were validated. Moreover, the development processes have taken in consideration the different and specific requirements that render an analytical assay suitable for clinical application.

First of all, all the three methods developed require a small plasma volume, ranging from 30 (sunitinib method) to 100 µL (in the case of CPT-11 and PTX methods). Furthermore, in the designed LC-MS/MS methods, the sample processing has been based on a simple protein precipitation. Sample preparation, indeed, is one of the most time-consuming steps in the bioanalysis aiming to extract the analytes of interest from biological matrices.

These methods have been developed in order to determine the pharmacokinetic profiles of the drugs under study. For this reason, the method sensitivity was crucial to accurately define the $t_{1/2}$ of the drugs and a properly low LLOQ was required (the designed methods have LLOQ concentrations ranging from 0.1 to 10 ng/mL). At the same time, also the ULOQ was important, in particular for those methods developed for dose escalation studies, where higher plasma concentrations than those reached with the standard dose are expected. The concentration ranges chosen for our new methods, in all the cases, generously covered the clinical expected drug concentrations, and resulted suitable for both for pharmacokinetic studies and for dose escalation trials (high doses).

A quite interesting result has been achieved in the case of the analytical method for the quantification of sunitinib, molecule that undergoes light induced Z-E isomerism. In order to prevent the E-isomer formation, most of the already published methods proposed to avoid the sample exposure to light in any steps, from the collection to the analysis, thus requiring the use of sodium or UV-light and the setting of suitable dark

rooms. Instead, our innovative approach has overtaken the troublesome step of the light protection by mean of an additional, but fast, step in sample preparation (a heated water bath at 90°C for 5 min) just before the sample analysis. The incubation in the water bath allowed the quantitatively reconversion of E to Z-isomer, formed during the sample handling. Thus, the method resulted surely more suitable to be used for TDM of sunitinib in the clinical laboratory routine.

Lastly, in order to apply the bioanalytical methods to clinical studies, it was essential to demonstrate that the analytical assay was reliable and reproducible for the intended use, by means of validating them according to the specific guidelines. In fact, the methods described in this thesis were fully validated in accordance to the FDA-EMA guidelines on bioanalytical method validation. Noteworthy, taking into account the recently revised version of the FDA guidance, we have introduced the incurred samples reanalysis assessment during the methods validation, as a further test to verify the reliability and reproducibility of the determined sample analyte concentrations.

References

Abigerges, D., Chabot, G.G., Armand, J.P., Hérait, P., Gouyette, A., Gandia, D., 1995. Phase I and pharmacologic studies of the camptothecin analog irinotecan administered every 3 weeks in cancer patients. J. Clin. Oncol. Off. J. Am. Soc. Clin. Oncol. 13, 210–221.

AIOM, SIAPEC-IAP, 2015. AIOM and SIAPEC-IAP recommendation for the evaluation of RAS mutations in colon rectum cancer.

Alexander, M.S., Kiser, M.M., Culley, T., Kern, J.R., Dolan, J.W., McChesney, J.D., Zygmunt, J., Bannister, S.J., 2003. Measurement of paclitaxel in biological matrices: high-throughput liquid chromatographic-tandem mass spectrometric quantification of paclitaxel and metabolites in human and dog plasma. J. Chromatogr. B Analyt. Technol. Biomed. Life. Sci. 785, 253–261.

Alnaim, L., 2007. Therapeutic drug monitoring of cancer chemotherapy. J. Oncol. Pharm. Pract. 13, 207–221. doi:10.1177/1078155207081133

Amado, R.G., Wolf, M., Peeters, M., Van Cutsem, E., Siena, S., Freeman, D.J., Juan, T., Sikorski, R., Suggs, S., Radinsky, R., Patterson, S.D., Chang, D.D., 2008. Wild-type KRAS is required for panitumumab efficacy in patients with metastatic colorectal cancer. J. Clin. Oncol. Off. J. Am. Soc. Clin. Oncol. 26, 1626–1634. doi:10.1200/JCO.2007.14.7116

Ando, Y., Ueoka, H., Sugiyama, T., Ichiki, M., Shimokata, K., Hasegawa, Y., 2002. Polymorphisms of UDP-glucuronosyltransferase and pharmacokinetics of irinotecan. Ther. Drug Monit. 24, 111–116.

Andriamanana, I., Gana, I., Duretz, B., Hulin, A., 2013. Simultaneous analysis of anticancer agents bortezomib, imatinib, nilotinib, dasatinib, erlotinib, lapatinib, sorafenib, sunitinib and vandetanib in human plasma using LC/MS/MS. J. Chromatogr. B Analyt. Technol. Biomed. Life. Sci. 926, 83–91. doi:10.1016/j.jchromb.2013.01.037

Arrondeau, J., Gan, H.K., Razak, A.R., Paoletti, X., Le Tourneau, C., 2010. Development of anti-cancer drugs. Discov. Med. 10, 355–362.

Bardin, C., Veal, G., Paci, A., Chatelut, E., Astier, A., Levêque, D., Widmer, N., Beijnen, J., 2014. Therapeutic drug monitoring in cancer--are we missing a trick? Eur. J. Cancer Oxf. Engl. 1990 50, 2005–2009. doi:10.1016/j.ejca.2014.04.013

Basileo, G., Breda, M., Fonte, G., Pisano, R., James, C.A., 2003. Quantitative determination of paclitaxel in human plasma using semi-automated liquid-liquid extraction in conjunction with liquid chromatography/tandem mass spectrometry. J. Pharm. Biomed. Anal. 32, 591–600.

Belani, C.P., Lee, J.S., Socinski, M.A., Robert, F., Waterhouse, D., Rowland, K., Ansari, R., Lilenbaum, R., Natale, R.B., 2005. Randomized phase III trial comparing cisplatin-etoposide to

carboplatin-paclitaxel in advanced or metastatic non-small cell lung cancer. Ann. Oncol. Off. J. Eur. Soc. Med. Oncol. ESMO 16, 1069–1075. doi:10.1093/annonc/mdi216

Benson, A.B., Venook, A.P., Bekaii-Saab, T., Chan, E., Chen, Y.-J., Cooper, H.S., Engstrom, P.F., Enzinger, P.C., Fenton, M.J., Fuchs, C.S., Grem, J.L., Hunt, S., Kamel, A., Leong, L.A., Lin, E., Messersmith, W., Mulcahy, M.F., Murphy, J.D., Nurkin, S., Rohren, E., Ryan, D.P., Saltz, L., Sharma, S., Shibata, D., Skibber, J.M., Sofocleous, C.T., Stoffel, E.M., Stotsky-Himelfarb, E., Willett, C.G., Gregory, K.M., Freedman-Cass, D.A., National Comprehensive Cancer Network, 2014. Colon cancer, version 3.2014. J. Natl. Compr. Cancer Netw. JNCCN 12, 1028–1059.

Berlin, N.I., Rall, D., Mead, J.A., Freireich, E.J., Vanscott, E., Hertz, R., Lipsett, M.B., 1963. FOLIC ACID ANTAGONIST. EFFECTS ON THE CELL AND THE PATIENT. COMBINED CLINICAL STAFF CONFERENCE AT THE NATIONAL INSTITUTES OF HEALTH. Ann. Intern. Med. 59, 931–956.

Bonfiglio, null, King, null, Olah, null, Merkle, null, 1999. The effects of sample preparation methods on the variability of the electrospray ionization response for model drug compounds. Rapid Commun. Mass Spectrom. RCM 13, 1175–1185. doi:10.1002/(SICI)1097-0231(19990630)13:12<1175::AID-RCM639>3.0.CO;2-0

Booth, B., Arnold, M.E., DeSilva, B., Amaravadi, L., Dudal, S., Fluhler, E., Gorovits, B., Haidar, S.H., Kadavil, J., Lowes, S., Nicholson, R., Rock, M., Skelly, M., Stevenson, L., Subramaniam, S., Weiner, R., Woolf, E., 2015. Workshop Report: Crystal City V—Quantitative Bioanalytical Method Validation and Implementation: The 2013 Revised FDA Guidance. AAPS J. 17, 277–288. doi:10.1208/s12248-014-9696-2

Bosma, P.J., Chowdhury, J.R., Bakker, C., Gantla, S., de Boer, A., Oostra, B.A., Lindhout, D., Tytgat, G.N., Jansen, P.L., Oude Elferink, R.P., 1995. The genetic basis of the reduced expression of bilirubin UDP-glucuronosyltransferase 1 in Gilbert's syndrome. N. Engl. J. Med. 333, 1171–1175. doi:10.1056/NEJM199511023331802

Bosó, V., Herrero, M.J., Santaballa, A., Palomar, L., Megias, J.E., de la Cueva, H., Rojas, L., Marqués, M.R., Poveda, J.L., Montalar, J., Aliño, S.F., 2014. SNPs and taxane toxicity in breast cancer patients. Pharmacogenomics 15, 1845–1858. doi:10.2217/pgs.14.127

Bowers, V.D., Locker, S., Ames, S., Jennings, W., Corry, R.J., 1991. The hemodynamic effects of Cremophor-EL. Transplantation 51, 847–850.

Brown, T., Havlin, K., Weiss, G., Cagnola, J., Koeller, J., Kuhn, J., Rizzo, J., Craig, J., Phillips, J., Von Hoff, D., 1991. A phase I trial of taxol given by a 6-hour intravenous infusion. J. Clin. Oncol. Off. J. Am. Soc. Clin. Oncol. 9, 1261–1267.

Brunton, L., Chabner, B., Knollman, B., 2011. Goodman and Gilman's The Pharmacological Basis of Therapeutics, Twelfth Edition. McGraw Hill Professional.

Canadian Minister of Health, 1991. GUIDANCE FOR INDUSTRY Conduct and Analysis of Bioavailability and Bioequivalence Studies - Part A: Oral Dosage Formulations Used for Systemic Effects. J. Comput. Assist. Tomogr. 15, 621–628.

Canal, P., Gay, C., Dezeuze, A., Douillard, J.Y., Bugat, R., Brunet, R., Adenis, A., Herait, P., Lokiec, F., Mathieu-Boue, A., 1996. Pharmacokinetics and pharmacodynamics of irinotecan during a phase II clinical trial in colorectal cancer. Pharmacology and Molecular Mechanisms Group of the European Organization for Research and Treatment of Cancer. J. Clin. Oncol. Off. J. Am. Soc. Clin. Oncol. 14, 2688–2695.

Cancer Facts and Figures, 2016. Cancer Facts and Figures. Am. Cancer Soc.

Carden, C.P., Sarker, D., Postel-Vinay, S., Yap, T.A., Attard, G., Banerji, U., Garrett, M.D., Thomas, G.V., Workman, P., Kaye, S.B., 2010. Can molecular biomarker-based patient selection in Phase I trials accelerate anticancer drug development? Drug Discov. Today 15, 88–97. doi:10.1016/j.drudis.2009.11.006

Catimel, G., Chabot, G.G., Guastalla, J.P., Dumortier, A., Cote, C., Engel, C., Gouyette, A., Mathieu-Boué, A., Mahjoubi, M., Clavel, M., 1995. Phase I and pharmacokinetic study of irinotecan (CPT-11) administered daily for three consecutive days every three weeks in patients with advanced solid tumors. Ann. Oncol. Off. J. Eur. Soc. Med. Oncol. ESMO 6, 133–140.

Chabot, G.G., Abigerges, D., Catimel, G., Culine, S., de Forni, M., Extra, J.M., Mahjoubi, M., Hérait, P., Armand, J.P., Bugat, R., 1995. Population pharmacokinetics and pharmacodynamics of irinotecan (CPT-11) and active metabolite SN-38 during phase I trials. Ann. Oncol. Off. J. Eur. Soc. Med. Oncol. ESMO 6, 141–151.

Chakravarti, A., 2001. Single nucleotide polymorphisms: . . .to a future of genetic medicine. Nature 409, 822–823. doi:10.1038/35057281

Chatelut, E., Pivot, X., Otto, J., Chevreau, C., Thyss, A., Renée, N., Milano, G., Canal, P., 2000. A limited sampling strategy for determining carboplatin AUC and monitoring drug dosage. Eur. J. Cancer Oxf. Engl. 1990 36, 264–269.

Chen, X., Peer, C.J., Alfaro, R., Tian, T., Spencer, S.D., Figg, W.D., 2012. Quantification of irinotecan, SN38, and SN38G in human and porcine plasma by ultra high-performance liquid chromatography-tandem mass spectrometry and its application to hepatic chemoembolization. J. Pharm. Biomed. Anal. 62, 140–148. doi:10.1016/j.jpba.2012.01.008

Ciardiello, F., Tortora, G., 2008. EGFR antagonists in cancer treatment. N. Engl. J. Med. 358, 1160–1174. doi:10.1056/NEJMra0707704

Combes, O., Barré, J., Duché, J.C., Vernillet, L., Archimbaud, Y., Marietta, M.P., Tillement, J.P., Urien, S., 2000. In vitro binding and partitioning of irinotecan (CPT-11) and its metabolite, SN-38, in human blood. Invest. New Drugs 18, 1–5.

Conti, J.A., Kemeny, N.E., Saltz, L.B., Huang, Y., Tong, W.P., Chou, T.C., Sun, M., Pulliam, S., Gonzalez, C., 1996. Irinotecan is an active agent in untreated patients with metastatic colorectal cancer. J. Clin. Oncol. Off. J. Am. Soc. Clin. Oncol. 14, 709–715.

Cordon-Cardo, C., O'Brien, J.P., Boccia, J., Casals, D., Bertino, J.R., Melamed, M.R., 1990. Expression of the multidrug resistance gene product (P-glycoprotein) in human normal and tumor tissues. J. Histochem. Cytochem. Off. J. Histochem. Soc. 38, 1277–1287.

Corona, G., Elia, C., Casetta, B., Toffoli, G., 2010. Fast liquid chromatography-tandem mass spectrometry method for routine assessment of irinotecan metabolic phenotype. Ther. Drug Monit. 32, 638–646. doi:10.1097/FTD.0b013e3181ec3bf5

Cresteil, T., Monsarrat, B., Alvinerie, P., Tréluyer, J.M., Vieira, I., Wright, M., 1994. Taxol metabolism by human liver microsomes: identification of cytochrome P450 isozymes involved in its biotransformation. Cancer Res. 54, 386–392.

Crotti, S., Posocco, B., Marangon, E., Nitti, D., Toffoli, G., Agostini, M., 2015. Mass spectrometry in the pharmacokinetic studies of anticancer natural products. Mass Spectrom. Rev. doi:10.1002/mas.21478

Crotti, S., Seraglia, R., Traldi, P., 2011. Some thoughts on electrospray ionization mechanisms. Eur. J. Mass Spectrom. Chichester Engl. 17, 85–99. doi:10.1255/ejms.1129

Dawood, S., Leyland-Jones, B., 2009. Pharmacology and pharmacogenetics of chemotherapeutic agents. Cancer Invest. 27, 482–488. doi:10.1080/07357900802574660

de Bruijn, P., Sleijfer, S., Lam, M.-H., Mathijssen, R.H.J., Wiemer, E.A.C., Loos, W.J., 2010. Bioanalytical method for the quantification of sunitinib and its n-desethyl metabolite SU12662 in human plasma by ultra performance liquid chromatography/tandem triple-quadrupole mass spectrometry. J. Pharm. Biomed. Anal. 51, 934–941. doi:10.1016/j.jpba.2009.10.020

de Graan, A.-J.M., Elens, L., Sprowl, J.A., Sparreboom, A., Friberg, L.E., van der Holt, B., de Raaf, P.J., de Bruijn, P., Engels, F.K., Eskens, F.A.L.M., Wiemer, E.A.C., Verweij, J., Mathijssen, R.H.J., van Schaik, R.H.N., 2013. CYP3A4*22 genotype and systemic exposure affect paclitaxel-induced neurotoxicity. Clin. Cancer Res. Off. J. Am. Assoc. Cancer Res. 19, 3316–3324. doi:10.1158/1078-0432.CCR-12-3786

de Hoffmann, E., 1996. Tandem mass spectrometry: A primer. J. Mass Spectrom. 31, 129–137. doi:10.1002/(SICI)1096-9888(199602)31:2<129::AID-JMS305>3.0.CO;2-T

Denlinger, C.S., Blanchard, R., Xu, L., Bernaards, C., Litwin, S., Spittle, C., Berg, D.J., McLaughlin, S., Redlinger, M., Dorr, A., Hambleton, J., Holden, S., Kearns, A., Kenkare-Mitra, S., Lum, B., Meropol, N.J., O'Dwyer, P.J., 2009. Pharmacokinetic analysis of irinotecan plus bevacizumab in patients with advanced solid tumors. Cancer Chemother. Pharmacol. 65, 97–105. doi:10.1007/s00280-009-1008-7

De Roock, W., Piessevaux, H., De Schutter, J., Janssens, M., De Hertogh, G., Personeni, N., Biesmans, B., Van Laethem, J.-L., Peeters, M., Humblet, Y., Van Cutsem, E., Tejpar, S., 2008. KRAS wild-type state predicts survival and is associated to early radiological response in metastatic colorectal cancer treated with cetuximab. Ann. Oncol. Off. J. Eur. Soc. Med. Oncol. ESMO 19, 508–515. doi:10.1093/annonc/mdm496

DeVita, V.T., Chu, E., 2008. A history of cancer chemotherapy. Cancer Res. 68, 8643–8653. doi:10.1158/0008-5472.CAN-07-6611

Dhani, N., Tu, D., Sargent, D.J., Seymour, L., Moore, M.J., 2009. Alternate endpoints for screening phase II studies. Clin. Cancer Res. Off. J. Am. Assoc. Cancer Res. 15, 1873–1882. doi:10.1158/1078-0432.CCR-08-2034

DiMasi, J.A., Grabowski, H.G., 2007. Economics of new oncology drug development. J. Clin. Oncol. Off. J. Am. Soc. Clin. Oncol. 25, 209–216. doi:10.1200/JCO.2006.09.0803

Douillard, J.Y., Cunningham, D., Roth, A.D., Navarro, M., James, R.D., Karasek, P., Jandik, P., Iveson, T., Carmichael, J., Alakl, M., Gruia, G., Awad, L., Rougier, P., 2000. Irinotecan combined with fluorouracil compared with fluorouracil alone as first-line treatment for metastatic colorectal cancer: a multicentre randomised trial. Lancet Lond. Engl. 355, 1041–1047.

du Bois, A., Lück, H.-J., Meier, W., Adams, H.-P., Möbus, V., Costa, S., Bauknecht, T., Richter, B., Warm, M., Schröder, W., Olbricht, S., Nitz, U., Jackisch, C., Emons, G., Wagner, U., Kuhn, W., Pfisterer, J., Arbeitsgemeinschaft Gynäkologische Onkologie Ovarian Cancer Study Group, 2003. A randomized clinical trial of cisplatin/paclitaxel versus carboplatin/paclitaxel as first-line treatment of ovarian cancer. J. Natl. Cancer Inst. 95, 1320–1329.

DuBois, D., DuBois, E., 1916. A formula to estimate the approximate surface area if height and weight be known. Arch. Intern. Med. 17, 863–871.

Ducreux, M., Ychou, M., Seitz, J.F., Bonnay, M., Bexon, A., Armand, J.P., Mahjoubi, M., Méry-Mignard, D., Rougier, P., 1999. Irinotecan combined with bolus fluorouracil, continuous infusion fluorouracil, and high-dose leucovorin every two weeks (LV5FU2 regimen): a clinical dose-finding and pharmacokinetic study in patients with pretreated metastatic colorectal cancer. J. Clin. Oncol. Off. J. Am. Soc. Clin. Oncol. 17, 2901–2908.

Duffy, M.J., O'Donovan, N., Crown, J., 2011. Use of molecular markers for predicting therapy response in cancer patients. Cancer Treat. Rev. 37, 151–159. doi:10.1016/j.ctrv.2010.07.004

Dvorak, H.F., 2002. Vascular permeability factor/vascular endothelial growth factor: a critical cytokine in tumor angiogenesis and a potential target for diagnosis and therapy. J. Clin. Oncol. Off. J. Am. Soc. Clin. Oncol. 20, 4368–4380.

Eisenhauer, E.A., O'Dwyer, P.J., Christian, M., Humphrey, J.S., 2000. Phase I clinical trial design in cancer drug development. J. Clin. Oncol. 18, 684–684.

El-Kenawi, A.E., El-Remessy, A.B., 2013. Angiogenesis inhibitors in cancer therapy: mechanistic perspective on classification and treatment rationales. Br. J. Pharmacol. 170, 712–729. doi:10.1111/bph.12344

EMA, 2011. Guideline on bioanalytical method validation EMA.

Etienne-Grimaldi, M.-C., Boyer, J.-C., Thomas, F., Quaranta, S., Picard, N., Loriot, M.-A., Narjoz, C., Poncet, D., Gagnieu, M.-C., Ged, C., Broly, F., Le Morvan, V., Bouquié, R., Gaub, M.-

P., Philibert, L., Ghiringhelli, F., Le Guellec, C., Collective work by Groupe de Pharmacologie Clinique Oncologique (GPCO-Unicancer), French Réseau National de Pharmacogénétique Hospitalière (RNPGx), 2015. UGT1A1 genotype and irinotecan therapy: general review and implementation in routine practice. Fundam. Clin. Pharmacol. 29, 219–237. doi:10.1111/fcp.12117

Fabian, M.A., Biggs, W.H., Treiber, D.K., Atteridge, C.E., Azimioara, M.D., Benedetti, M.G., Carter, T.A., Ciceri, P., Edeen, P.T., Floyd, M., Ford, J.M., Galvin, M., Gerlach, J.L., Grotzfeld, R.M., Herrgard, S., Insko, D.E., Insko, M.A., Lai, A.G., Lélias, J.-M., Mehta, S.A., Milanov, Z.V., Velasco, A.M., Wodicka, L.M., Patel, H.K., Zarrinkar, P.P., Lockhart, D.J., 2005. A small molecule-kinase interaction map for clinical kinase inhibitors. Nat. Biotechnol. 23, 329–336. doi:10.1038/nbt1068

Faivre, S., 2006. Safety, Pharmacokinetic, and Antitumor Activity of SU11248, a Novel Oral Multitarget Tyrosine Kinase Inhibitor, in Patients With Cancer. J. Clin. Oncol. 24, 25–35. doi:10.1200/JCO.2005.02.2194

Farber, S., Diamond, L.K., 1948. Temporary remissions in acute leukemia in children produced by folic acid antagonist, 4-aminopteroyl-glutamic acid. N. Engl. J. Med. 238, 787–793. doi:10.1056/NEJM194806032382301

Fast, D.M., Kelley, M., Viswanathan, C.T., O'Shaughnessy, J., King, S.P., Chaudhary, A., Weiner, R., DeStefano, A.J., Tang, D., 2009a. Workshop report and follow-up--AAPS Workshop on current topics in GLP bioanalysis: Assay reproducibility for incurred samples--implications of Crystal City recommendations. AAPS J. 11, 238–241. doi:10.1208/s12248-009-9100-9

Fast, D.M., Kelley, M., Viswanathan, C.T., O'Shaughnessy, J., King, S.P., Chaudhary, A., Weiner, R., DeStefano, A.J., Tang, D., 2009b. Workshop report and follow-up--AAPS Workshop on current topics in GLP bioanalysis: Assay reproducibility for incurred samples--implications of Crystal City recommendations. AAPS J. 11, 238–241. doi:10.1208/s12248-009-9100-9

FDA, 2013a. Guidance for Industry Bioanalytical Method Validation DRAFT GUIDANCE.

FDA, 2013b. Paving the Way for Personalized Medicine.

FDA, 2001. Bioanalytical method validation for studies on pharmacokinetics, bioavailability and bioequivalence: Highlights of the FDA's Guidance 4, 5–13.

Fennelly, D., Aghajanian, C., Shapiro, F., O'Flaherty, C., McKenzie, M., O'Connor, C., Tong, W., Norton, L., Spriggs, D., 1997. Phase I and pharmacologic study of paclitaxel administered weekly in patients with relapsed ovarian cancer. J. Clin. Oncol. Off. J. Am. Soc. Clin. Oncol. 15, 187–192.

Fernández-Peralbo, M.A., Priego-Capote, F., Luque de Castro, M.D., Casado-Adam, A., Arjona-Sánchez, A., Muñoz-Casares, F.C., 2014. LC-MS/MS quantitative analysis of paclitaxel and its major metabolites in serum, plasma and tissue from women with ovarian cancer after

intraperitoneal chemotherapy. J. Pharm. Biomed. Anal. 91, 131–137. doi:10.1016/j.jpba.2013.12.028

Frederiks, C.N., Lam, S.W., Guchelaar, H.J., Boven, E., 2015. Genetic polymorphisms and paclitaxel- or docetaxel-induced toxicities: A systematic review. Cancer Treat. Rev. 41, 935–950. doi:10.1016/j.ctrv.2015.10.010

Freireich, E.J., Gehan, E.A., Rall, D.P., Schmidt, L.H., Skipper, H.E., 1966. Quantitative comparison of toxicity of anticancer agents in mouse, rat, hamster, dog, monkey, and man. Cancer Chemother. Rep. 50, 219–244.

Gabrielsson, J., Weiner, D., 2012. Non-compartmental Analysis, in: Reisfeld, B., Mayeno, A.N. (Eds.), Computational Toxicology. Humana Press, Totowa, NJ, pp. 377–389.

Gao, B., Yeap, S., Clements, A., Balakrishnar, B., Wong, M., Gurney, H., 2012. Evidence for therapeutic drug monitoring of targeted anticancer therapies. J. Clin. Oncol. Off. J. Am. Soc. Clin. Oncol. 30, 4017–4025. doi:10.1200/JCO.2012.43.5362

Gao, S., Zhang, Z.-P., Edinboro, L.E., Ngoka, L.C., Karnes, H.T., 2006. The effect of alkylamine additives on the sensitivity of detection for paclitaxel and docetaxel and analysis in plasma of paclitaxel by liquid chromatography-tandem mass spectrometry. Biomed. Chromatogr. BMC 20, 683–695. doi:10.1002/bmc.582

Gardner, E.R., Dahut, W., Figg, W.D., 2008. Quantitative determination of total and unbound paclitaxel in human plasma following Abraxane treatment. J. Chromatogr. B Analyt. Technol. Biomed. Life. Sci. 862, 213–218. doi:10.1016/j.jchromb.2007.12.013

Gardner, E.R., Liau, C.-T., Chu, Z.E., Figg, W.D., Sparreboom, A., 2006. Determination of paclitaxel in human plasma following the administration of Genaxol or Genetaxyl by liquid chromatography/tandem mass spectrometry. Rapid Commun. Mass Spectrom. RCM 20, 2170–2174. doi:10.1002/rcm.2577

Gelderblom, H., Verweij, J., Nooter, K., Sparreboom, A., 2001. Cremophor EL: the drawbacks and advantages of vehicle selection for drug formulation. Eur. J. Cancer Oxf. Engl. 1990 37, 1590–1598.

Gharwan, H., Groninger, H., 2015. Kinase inhibitors and monoclonal antibodies in oncology: clinical implications. Nat. Rev. Clin. Oncol. doi:10.1038/nrclinonc.2015.213

Giamas, G., Man, Y.L., Hirner, H., Bischof, J., Kramer, K., Khan, K., Ahmed, S.S.L., Stebbing, J., Knippschild, U., 2010. Kinases as targets in the treatment of solid tumors. Cell. Signal. 22, 984–1002. doi:10.1016/j.cellsig.2010.01.011

Gianni, L., Kearns, C.M., Giani, A., Capri, G., Viganó, L., Lacatelli, A., Bonadonna, G., Egorin, M.J., 1995. Nonlinear pharmacokinetics and metabolism of paclitaxel and its pharmacokinetic/pharmacodynamic relationships in humans. J. Clin. Oncol. Off. J. Am. Soc. Clin. Oncol. 13, 180–190.

Gillis, N.K., Patel, J.N., Innocenti, F., 2014. Clinical implementation of germ line cancer pharmacogenetic variants during the next-generation sequencing era. Clin. Pharmacol. Ther. 95, 269–280. doi:10.1038/clpt.2013.214

Gilman, A., Philips, F.S., 1946. The Biological Actions and Therapeutic Applications of the B-Chloroethyl Amines and Sulfides. Science 103, 409–436. doi:10.1126/science.103.2675.409

Glantz, M.J., Choy, H., Kearns, C.M., Mills, P.C., Wahlberg, L.U., Zuhowski, E.G., Calabresi, P., Egorin, M.J., 1995. Paclitaxel disposition in plasma and central nervous systems of humans and rats with brain tumors. J. Natl. Cancer Inst. 87, 1077–1081.

Goldman, J.M., Melo, J.V., 2003. Chronic myeloid leukemia--advances in biology and new approaches to treatment. N. Engl. J. Med. 349, 1451–1464. doi:10.1056/NEJMra020777

González, O., Blanco, M.E., Iriarte, G., Bartolomé, L., Maguregui, M.I., Alonso, R.M., 2014. Bioanalytical chromatographic method validation according to current regulations, with a special focus on the non-well defined parameters limit of quantification, robustness and matrix effect. J. Chromatogr. A 1353, 10–27. doi:10.1016/j.chroma.2014.03.077

Goodman, V.L., Rock, E.P., Dagher, R., Ramchandani, R.P., Abraham, S., Gobburu, J.V.S., Booth, B.P., Verbois, S.L., Morse, D.E., Liang, C.Y., Chidambaram, N., Jiang, J.X., Tang, S., Mahjoob, K., Justice, R., Pazdur, R., 2007. Approval Summary: Sunitinib for the Treatment of Imatinib Refractory or Intolerant Gastrointestinal Stromal Tumors and Advanced Renal Cell Carcinoma. Clin. Cancer Res. 13, 1367–1373. doi:10.1158/1078-0432.CCR-06-2328

Götze, L., Hegele, A., Metzelder, S.K., Renz, H., Nockher, W.A., 2012. Development and clinical application of a LC-MS/MS method for simultaneous determination of various tyrosine kinase inhibitors in human plasma. Clin. Chim. Acta Int. J. Clin. Chem. 413, 143–149. doi:10.1016/j.cca.2011.09.012

Gravitz, L., 2014. Therapy: This time it's personal. Nature 509, S52–54. doi:10.1038/509S52a

Green, H., 2008. Pharmacogenomics of importance for paclitaxel chemotherapy. Pharmacogenomics 9, 671–674. doi:10.2217/14622416.9.6.671

Gréen, H., Söderkvist, P., Rosenberg, P., Mirghani, R.A., Rymark, P., Lundqvist, E.A., Peterson, C., 2009. Pharmacogenetic studies of Paclitaxel in the treatment of ovarian cancer. Basic Clin. Pharmacol. Toxicol. 104, 130–137. doi:10.1111/j.1742-7843.2008.00351.x

Gréen, H., Vretenbrant, K., Norlander, B., Peterson, C., 2006. Measurement of paclitaxel and its metabolites in human plasma using liquid chromatography/ion trap mass spectrometry with a sonic spray ionization interface. Rapid Commun. Mass Spectrom. RCM 20, 2183–2189. doi:10.1002/rcm.2567

Grem, J.L., Tutsch, K.D., Simon, K.J., Alberti, D.B., Willson, J.K., Tormey, D.C., Swaminathan, S., Trump, D.L., 1987. Phase I study of taxol administered as a short i.v. infusion daily for 5 days. Cancer Treat. Rep. 71, 1179–1184.

Gupta, E., Mick, R., Ramirez, J., Wang, X., Lestingi, T.M., Vokes, E.E., Ratain, M.J., 1997. Pharmacokinetic and pharmacodynamic evaluation of the topoisomerase inhibitor irinotecan in cancer patients. J. Clin. Oncol. Off. J. Am. Soc. Clin. Oncol. 15, 1502–1510.

Gustafson, D.L., Long, M.E., Bradshaw, E.L., Merz, A.L., Kerzic, P.J., 2005. P450 induction alters paclitaxel pharmacokinetics and tissue distribution with multiple dosing. Cancer Chemother. Pharmacol. 56, 248–254. doi:10.1007/s00280-004-0988-6

Haaz, M.C., Rivory, L., Riché, C., Vernillet, L., Robert, J., 1998. Metabolism of irinotecan (CPT-11) by human hepatic microsomes: participation of cytochrome P-450 3A and drug interactions. Cancer Res. 58, 468–472.

Hamidovic, A., Hahn, K., Kolesar, J., 2010. Clinical significance of ABCB1 genotyping in oncology. J. Oncol. Pharm. Pract. Off. Publ. Int. Soc. Oncol. Pharm. Pract. 16, 39–44. doi:10.1177/1078155209104380

Haouala, A., Zanolari, B., Rochat, B., Montemurro, M., Zaman, K., Duchosal, M.A., Ris, H.B., Leyvraz, S., Widmer, N., Decosterd, L.A., 2009. Therapeutic Drug Monitoring of the new targeted anticancer agents imatinib, nilotinib, dasatinib, sunitinib, sorafenib and lapatinib by LC tandem mass spectrometry. J. Chromatogr. B Analyt. Technol. Biomed. Life. Sci. 877, 1982–1996. doi:10.1016/j.jchromb.2009.04.045

Harris, J.W., Katki, A., Anderson, L.W., Chmurny, G.N., Paukstelis, J.V., Collins, J.M., 1994. Isolation, structural determination, and biological activity of 6 alpha-hydroxytaxol, the principal human metabolite of taxol. J. Med. Chem. 37, 706–709.

Hegde, S.R., Sun, W., Lynch, J.P., 2008. Systemic and targeted therapy for advanced colon cancer. Expert Rev. Gastroenterol. Hepatol. 2, 135–149. doi:10.1586/17474124.2.1.135

Heinemann, V., von Weikersthal, L.F., Decker, T., Kiani, A., Vehling-Kaiser, U., Al-Batran, S.-E., Heintges, T., Lerchenmüller, C., Kahl, C., Seipelt, G., Kullmann, F., Stauch, M., Scheithauer, W., Hielscher, J., Scholz, M., Müller, S., Link, H., Niederle, N., Rost, A., Höffkes, H.-G., Moehler, M., Lindig, R.U., Modest, D.P., Rossius, L., Kirchner, T., Jung, A., Stintzing, S., 2014. FOLFIRI plus cetuximab versus FOLFIRI plus bevacizumab as first-line treatment for patients with metastatic colorectal cancer (FIRE-3): a randomised, open-label, phase 3 trial. Lancet Oncol. 15, 1065–1075. doi:10.1016/S1470-2045(14)70330-4

Heinrich, M.C., Maki, R.G., Corless, C.L., Antonescu, C.R., Harlow, A., Griffith, D., Town, A., McKinley, A., Ou, W.-B., Fletcher, J.A., Fletcher, C.D.M., Huang, X., Cohen, D.P., Baum, C.M., Demetri, G.D., 2008. Primary and secondary kinase genotypes correlate with the biological and clinical activity of sunitinib in imatinib-resistant gastrointestinal stromal tumor. J. Clin. Oncol. Off. J. Am. Soc. Clin. Oncol. 26, 5352–5359. doi:10.1200/JCO.2007.15.7461

Helgason, H.H., Kruijtzer, C.M.F., Huitema, A.D.R., Marcus, S.G., ten Bokkel Huinink, W.W., Schot, M.E., Schornagel, J.H., Beijnen, J.H., Schellens, J.H.M., 2006. Phase II and pharmacological study of oral paclitaxel (Paxoral) plus ciclosporin in anthracycline-pretreated metastatic breast cancer. Br. J. Cancer 95, 794–800. doi:10.1038/sj.bjc.6603332

Henningsson, A., 2005. Association of CYP2C8, CYP3A4, CYP3A5, and ABCB1 Polymorphisms with the Pharmacokinetics of Paclitaxel. Clin. Cancer Res. 11, 8097–8104. doi:10.1158/1078-0432.CCR-05-1152

Henningsson, A., Karlsson, M.O., Viganò, L., Gianni, L., Verweij, J., Sparreboom, A., 2001. Mechanism-based pharmacokinetic model for paclitaxel. J. Clin. Oncol. 19, 4065–4073.

He, P., Court, M.H., Greenblatt, D.J., von Moltke, L.L., 2006. Human pregnane X receptor: genetic polymorphisms, alternative mRNA splice variants, and cytochrome P450 3A metabolic activity. J. Clin. Pharmacol. 46, 1356–1369. doi:10.1177/0091270006292125

Hertz, D.L., Motsinger-Reif, A.A., Drobish, A., Winham, S.J., McLeod, H.L., Carey, L.A., Dees, E.C., 2012. CYP2C8*3 predicts benefit/risk profile in breast cancer patients receiving neoadjuvant paclitaxel. Breast Cancer Res. Treat. 134, 401–410. doi:10.1007/s10549-012-2054-0

Hollingsworth, S.J., Biankin, A.V., 2015. The Challenges of Precision Oncology Drug Development and Implementation. Public Health Genomics 18, 338–348. doi:10.1159/000441557

Honeywell, R., Yarzadah, K., Giovannetti, E., Losekoot, N., Smit, E.F., Walraven, M., Lind, J.S.W., Tibaldi, C., Verheul, H.M., Peters, G.J., 2010. Simple and selective method for the determination of various tyrosine kinase inhibitors used in the clinical setting by liquid chromatography tandem mass spectrometry. J. Chromatogr. B Analyt. Technol. Biomed. Life. Sci. 878, 1059–1068. doi:10.1016/j.jchromb.2010.03.010

Hopfgartner, G., Bourgogne, E., 2003. Quantitative high-throughput analysis of drugs in biological matrices by mass spectrometry. Mass Spectrom. Rev. 22, 195–214. doi:10.1002/mas.10050

Hoskins, J.M., Goldberg, R.M., Qu, P., Ibrahim, J.G., McLeod, H.L., 2007. UGT1A1*28 genotype and irinotecan-induced neutropenia: dose matters. J. Natl. Cancer Inst. 99, 1290–1295. doi:10.1093/jnci/djm115

Houk, B.E., Bello, C.L., Kang, D., Amantea, M., 2009. A Population Pharmacokinetic Meta-analysis of Sunitinib Malate (SU11248) and Its Primary Metabolite (SU12662) in Healthy Volunteers and Oncology Patients. Clin. Cancer Res. 15, 2497–2506. doi:10.1158/1078-0432.CCR-08-1893

Houk, B.E., Bello, C.L., Poland, B., Rosen, L.S., Demetri, G.D., Motzer, R.J., 2010. Relationship between exposure to sunitinib and efficacy and tolerability endpoints in patients with cancer: results of a pharmacokinetic/pharmacodynamic meta-analysis. Cancer Chemother. Pharmacol. 66, 357–371. doi:10.1007/s00280-009-1170-y

Huang, R.S., Ratain, M.J., 2009. Pharmacogenetics and pharmacogenomics of anticancer agents. CA. Cancer J. Clin. 59, 42–55. doi:10.3322/caac.20002

Huizing, M.T., Giaccone, G., van Warmerdam, L.J., Rosing, H., Bakker, P.J., Vermorken, J.B., Postmus, P.E., van Zandwijk, N., Koolen, M.G., ten Bokkel Huinink, W.W., van der Vijgh, W.J.,

Bierhorst, F.J., Lai, A., Dalesio, O., Pinedo, H.M., Veenhof, C.H., Beijnen, J.H., 1997. Pharmacokinetics of paclitaxel and carboplatin in a dose-escalating and dose-sequencing study in patients with non-small-cell lung cancer. The European Cancer Centre. J. Clin. Oncol. Off. J. Am. Soc. Clin. Oncol. 15, 317–329.

Huizing, M.T., Keung, A.C., Rosing, H., van der Kuij, V., ten Bokkel Huinink, W.W., Mandjes, I.M., Dubbelman, A.C., Pinedo, H.M., Beijnen, J.H., 1993. Pharmacokinetics of paclitaxel and metabolites in a randomized comparative study in platinum-pretreated ovarian cancer patients. J. Clin. Oncol. Off. J. Am. Soc. Clin. Oncol. 11, 2127–2135.

Hurwitz, H., Fehrenbacher, L., Novotny, W., Cartwright, T., Hainsworth, J., Heim, W., Berlin, J., Baron, A., Griffing, S., Holmgren, E., Ferrara, N., Fyfe, G., Rogers, B., Ross, R., Kabbinavar, F., 2004. Bevacizumab plus irinotecan, fluorouracil, and leucovorin for metastatic colorectal cancer. N. Engl. J. Med. 350, 2335–2342. doi:10.1056/NEJMoa032691

Innocenti, F., Schilsky, R.L., Ramírez, J., Janisch, L., Undevia, S., House, L.K., Das, S., Wu, K., Turcich, M., Marsh, R., Karrison, T., Maitland, M.L., Salgia, R., Ratain, M.J., 2014. Dose-finding and pharmacokinetic study to optimize the dosing of irinotecan according to the UGT1A1 genotype of patients with cancer. J. Clin. Oncol. Off. J. Am. Soc. Clin. Oncol. 32, 2328–2334. doi:10.1200/JCO.2014.55.2307

Innocenti, F., Undevia, S.D., Iyer, L., Chen, P.X., Das, S., Kocherginsky, M., Karrison, T., Janisch, L., Ramírez, J., Rudin, C.M., Vokes, E.E., Ratain, M.J., 2004. Genetic variants in the UDP-glucuronosyltransferase 1A1 gene predict the risk of severe neutropenia of irinotecan. J. Clin. Oncol. Off. J. Am. Soc. Clin. Oncol. 22, 1382–1388. doi:10.1200/JCO.2004.07.173

Ivy, S.P., Siu, L.L., Garrett-Mayer, E., Rubinstein, L., 2010. Approaches to Phase 1 Clinical Trial Design Focused on Safety, Efficiency, and Selected Patient Populations: A Report from the Clinical Trial Design Task Force of the National Cancer Institute Investigational Drug Steering Committee. Clin. Cancer Res. 16, 1726–1736. doi:10.1158/1078-0432.CCR-09-1961

Iyer, L., Das, S., Janisch, L., Wen, M., Ramírez, J., Karrison, T., Fleming, G.F., Vokes, E.E., Schilsky, R.L., Ratain, M.J., 2002. UGT1A1*28 polymorphism as a determinant of irinotecan disposition and toxicity. Pharmacogenomics J. 2, 43–47.

Jain, R.K., 2009. A new target for tumor therapy. N. Engl. J. Med. 360, 2669–2671. doi:10.1056/NEJMcibr0902054

Johnatty, S.E., Beesley, J., Paul, J., Fereday, S., Spurdle, A.B., Webb, P.M., Byth, K., Marsh, S., McLeod, H., AOCS Study Group, Harnett, P.R., Brown, R., DeFazio, A., Chenevix-Trench, G., 2008. ABCB1 (MDR 1) polymorphisms and progression-free survival among women with ovarian cancer following paclitaxel/carboplatin chemotherapy. Clin. Cancer Res. Off. J. Am. Assoc. Cancer Res. 14, 5594–5601. doi:10.1158/1078-0432.CCR-08-0606

Jones, P.R.M., Wilkinson, S., Davies, P.S.W., 1985. A revision of body surface area estimations. Eur. J. Appl. Physiol. 53, 376–379. doi:10.1007/BF00422858

Kaestner, S.A., Sewell, G.J., 2007. Chemotherapy Dosing Part I: Scientific Basis for Current Practice and Use of Body Surface Area. Clin. Oncol. 19, 23–37. doi:10.1016/j.clon.2006.10.010

Kang, M.H., Figg, W.D., Ando, Y., Blagosklonny, M.V., Liewehr, D., Fojo, T., Bates, S.E., 2001. The P-glycoprotein antagonist PSC 833 increases the plasma concentrations of 6alpha-hydroxypaclitaxel, a major metabolite of paclitaxel. Clin. Cancer Res. Off. J. Am. Assoc. Cancer Res. 7, 1610–1617.

Karapetis, C.S., Khambata-Ford, S., Jonker, D.J., O'Callaghan, C.J., Tu, D., Tebbutt, N.C., Simes, R.J., Chalchal, H., Shapiro, J.D., Robitaille, S., Price, T.J., Shepherd, L., Au, H.-J., Langer, C., Moore, M.J., Zalcberg, J.R., 2008. K-ras mutations and benefit from cetuximab in advanced colorectal cancer. N. Engl. J. Med. 359, 1757–1765. doi:10.1056/NEJMoa0804385

Karlsson, M.O., Molnar, V., Freijs, A., Nygren, P., Bergh, J., Larsson, R., 1999. Pharmacokinetic models for the saturable distribution of paclitaxel. Drug Metab. Dispos. Biol. Fate Chem. 27, 1220–1223.

Kaye, B., Clark, M.W., Cussans, N.J., Macrae, P.V., Stopher, D.A., 1992. The sensitive determination of abanoquil in blood by high-performance liquid chromatography/atmospheric pressure ionization mass spectrometry. Biol. Mass Spectrom. 21, 585–589. doi:10.1002/bms.1200211110

Kebarle, P., Verkerk, U.H., 2009. Electrospray: from ions in solution to ions in the gas phase, what we know now. Mass Spectrom. Rev. 28, 898–917. doi:10.1002/mas.20247

Kehrer, D.F., Yamamoto, W., Verweij, J., de Jonge, M.J., de Bruijn, P., Sparreboom, A., 2000. Factors involved in prolongation of the terminal disposition phase of SN-38: clinical and experimental studies. Clin. Cancer Res. Off. J. Am. Assoc. Cancer Res. 6, 3451–3458.

Khosravan, R., 2012. A retrospective analysis of data from two trials of sunitinib in patients with advanced renal cell carcinoma (RCC): Pitfalls of efficacy subgroup analyses based on dose-reduction status. [WWW Document]. URL http://meetinglibrary.asco.org/print/569354 (accessed 1.25.16).

Kim, H.S., Kim, M.-K., Chung, H.H., Kim, J.W., Park, N.H., Song, Y.S., Kang, S.B., 2009. Genetic polymorphisms affecting clinical outcomes in epithelial ovarian cancer patients treated with taxanes and platinum compounds: a Korean population-based study. Gynecol. Oncol. 113, 264–269. doi:10.1016/j.ygyno.2009.01.002

Kita, T., Kikuchi, Y., Takano, M., Suzuki, M., Oowada, M., Konno, R., Yamamoto, K., Inoue, H., Seto, H., Yamamoto, T., Shimizu, K., 2004. The effect of single weekly paclitaxel in heavily pretreated patients with recurrent or persistent advanced ovarian cancer. Gynecol. Oncol. 92, 813–818. doi:10.1016/j.ygyno.2003.12.002

Klaassen, U., Wilke, H., Strumberg, D., Eberhardt, W., Korn, M., Seeber, S., 1996. Phase I study with a weekly 1 h infusion of paclitaxel in heavily pretreated patients with metastatic breast and ovarian cancer. Eur. J. Cancer Oxf. Engl. 1990 32A, 547–549.

Kola, I., Landis, J., 2004. Can the pharmaceutical industry reduce attrition rates? Nat. Rev. Drug Discov. 3, 711–715. doi:10.1038/nrd1470

Krämer, I., Lipp, H.-P., 2007. Bevacizumab, a humanized anti-angiogenic monoclonal antibody for the treatment of colorectal cancer. J. Clin. Pharm. Ther. 32, 1–14. doi:10.1111/j.1365-2710.2007.00800.x

Kumar, G.N., Walle, U.K., Bhalla, K.N., Walle, T., 1993. Binding of taxol to human plasma, albumin and alpha 1-acid glycoprotein. Res. Commun. Chem. Pathol. Pharmacol. 80, 337–344.

Lankheet, N. a. G., Hillebrand, M.J.X., Rosing, H., Schellens, J.H.M., Beijnen, J.H., Huitema, A.D.R., 2013. Method development and validation for the quantification of dasatinib, erlotinib, gefitinib, imatinib, lapatinib, nilotinib, sorafenib and sunitinib in human plasma by liquid chromatography coupled with tandem mass spectrometry. Biomed. Chromatogr. BMC 27, 466–476. doi:10.1002/bmc.2814

Lankheet, N.A.G., Steeghs, N., Rosing, H., Schellens, J.H.M., Beijnen, J.H., Huitema, A.D.R., 2013. Quantification of sunitinib and N-desethyl sunitinib in human EDTA plasma by liquid chromatography coupled with electrospray ionization tandem mass spectrometry: validation and application in routine therapeutic drug monitoring. Ther. Drug Monit. 35, 168–176. doi:10.1097/FTD.0b013e31827efd9e

Lesar, T.S., 1998. Errors in the use of medication dosage equations. Arch. Pediatr. Adolesc. Med. 152, 340–344.

Leskelä, S., Jara, C., Leandro-García, L.J., Martínez, A., García-Donas, J., Hernando, S., Hurtado, A., Vicario, J.C.C., Montero-Conde, C., Landa, I., López-Jiménez, E., Cascón, A., Milne, R.L., Robledo, M., Rodríguez-Antona, C., 2011. Polymorphisms in cytochromes P450 2C8 and 3A5 are associated with paclitaxel neurotoxicity. Pharmacogenomics J. 11, 121–129. doi:10.1038/tpj.2010.13

Lesser, G.J., Grossman, S.A., Eller, S., Rowinsky, E.K., 1995. The distribution of systemically administered [3H]-paclitaxel in rats: a quantitative autoradiographic study. Cancer Chemother. Pharmacol. 37, 173–178.

Le Tourneau, C., Lee, J.J., Siu, L.L., 2009. Dose Escalation Methods in Phase I Cancer Clinical Trials. JNCI J. Natl. Cancer Inst. 101, 708–720. doi:10.1093/jnci/djp079

Le Tourneau, C., Raymond, E., Faivre, S., 2007. Sunitinib: a novel tyrosine kinase inhibitor. A brief review of its therapeutic potential in the treatment of renal carcinoma and gastrointestinal stromal tumors (GIST). Ther. Clin. Risk Manag. 3, 341–348.

Lièvre, A., Bachet, J.-B., Boige, V., Cayre, A., Le Corre, D., Buc, E., Ychou, M., Bouché, O., Landi, B., Louvet, C., André, T., Bibeau, F., Diebold, M.-D., Rougier, P., Ducreux, M., Tomasic, G., Emile, J.-F., Penault-Llorca, F., Laurent-Puig, P., 2008. KRAS mutations as an independent prognostic factor in patients with advanced colorectal cancer treated with cetuximab. J. Clin. Oncol. Off. J. Am. Soc. Clin. Oncol. 26, 374–379. doi:10.1200/JCO.2007.12.5906

Lokiec, F., du Sorbier, B.M., Sanderink, G.J., 1996. Irinotecan (CPT-11) metabolites in human bile and urine. Clin. Cancer Res. Off. J. Am. Assoc. Cancer Res. 2, 1943–1949.

Longnecker, S.M., Donehower, R.C., Cates, A.E., Chen, T.L., Brundrett, R.B., Grochow, L.B., Ettinger, D.S., Colvin, M., 1987. High-performance liquid chromatographic assay for taxol in human plasma and urine and pharmacokinetics in a phase I trial. Cancer Treat. Rep. 71, 53–59.

Loos, W.J., Verweij, J., Gelderblom, H.J., de Jonge, M.J., Brouwer, E., Dallaire, B.K., Sparreboom, A., 1999. Role of erythrocytes and serum proteins in the kinetic profile of total 9-amino-20(S)-camptothecin in humans. Anticancer. Drugs 10, 705–710.

Lorusso, D., Pietragalla, A., Mainenti, S., Masciullo, V., Di Vagno, G., Scambia, G., 2010. Review role of topotecan in gynaecological cancers: current indications and perspectives. Crit. Rev. Oncol. Hematol. 74, 163–174. doi:10.1016/j.critrevonc.2009.08.001

Lu, C.-Y., Huang, C.-W., Wu, I.-C., Tsai, H.-L., Ma, C.-J., Yeh, Y.-S., Chang, S.-F., Huang, M.-L., Wang, J.-Y., 2015. Clinical Implication of UGT1A1 Promoter Polymorphism for Irinotecan Dose Escalation in Metastatic Colorectal Cancer Patients Treated with Bevacizumab Combined with FOLFIRI in the First-line Setting. Transl. Oncol. 8, 474–479. doi:10.1016/j.tranon.2015.11.002

Manish, S., 2014. A UGT1A1 genotype-guided dosing study of irinotecan in metastatic colorectal cancer (mCRC) patients (pts) treated with FOLFIRI plus bevacizumab (BEV). [WWW Document]. URL http://meetinglibrary.asco.org/print/1417186 (accessed 1.25.16).

Marangon, E., Posocco, B., Mazzega, E., Toffoli, G., 2015a. Development and validation of a high-performance liquid chromatography-tandem mass spectrometry method for the simultaneous determination of irinotecan and its main metabolites in human plasma and its application in a clinical pharmacokinetic study. PloS One 10, e0118194. doi:10.1371/journal.pone.0118194

Marangon, E., Posocco, B., Mazzega, E., Toffoli, G., 2015b. Development and validation of a high-performance liquid chromatography-tandem mass spectrometry method for the simultaneous determination of irinotecan and its main metabolites in human plasma and its application in a clinical pharmacokinetic study. PloS One 10, e0118194. doi:10.1371/journal.pone.0118194

Marcuello, E., Páez, D., Paré, L., Salazar, J., Sebio, A., del Rio, E., Baiget, M., 2011. A genotype-directed phase I-IV dose-finding study of irinotecan in combination with fluorouracil/leucovorin as first-line treatment in advanced colorectal cancer. Br. J. Cancer 105, 53–57. doi:10.1038/bjc.2011.206

Markman, M., Hall, J., Spitz, D., Weiner, S., Carson, L., Van Le, L., Baker, M., 2002. Phase II trial of weekly single-agent paclitaxel in platinum/paclitaxel-refractory ovarian cancer. J. Clin. Oncol. Off. J. Am. Soc. Clin. Oncol. 20, 2365–2369.

Marsh, S., Paul, J., King, C.R., Gifford, G., McLeod, H.L., Brown, R., 2007. Pharmacogenetic assessment of toxicity and outcome after platinum plus taxane chemotherapy in ovarian

cancer: the Scottish Randomised Trial in Ovarian Cancer. J. Clin. Oncol. Off. J. Am. Soc. Clin. Oncol. 25, 4528–4535. doi:10.1200/JCO.2006.10.4752

Mathijssen, R.H.J., Sparreboom, A., Verweij, J., 2014. Determining the optimal dose in the development of anticancer agents. Nat. Rev. Clin. Oncol. 11, 272–281. doi:10.1038/nrclinonc.2014.40

Mathijssen, R.H., Van Alphen, R.J., Verweij, J., Loos, W.J., Nooter, K., Stoter, G., Sparreboom, A., 2001. Clinical pharmacokinetics and metabolism of irinotecan (CPT-11). Clin. Cancer Res. 7, 2182–2194.

McCormack, P.L., Keam, S.J., 2008. Bevacizumab: a review of its use in metastatic colorectal cancer. Drugs 68, 487–506.

Mei, H., Hsieh, Y., Nardo, C., Xu, X., Wang, S., Ng, K., Korfmacher, W.A., 2003. Investigation of matrix effects in bioanalytical high-performance liquid chromatography/tandem mass spectrometric assays: application to drug discovery. Rapid Commun. Mass Spectrom. RCM 17, 97–103. doi:10.1002/rcm.876

Mendel, D.B., Laird, A.D., Xin, X., Louie, S.G., Christensen, J.G., Li, G., Schreck, R.E., Abrams, T.J., Ngai, T.J., Lee, L.B., Murray, L.J., Carver, J., Chan, E., Moss, K.G., Haznedar, J.O., Sukbuntherng, J., Blake, R.A., Sun, L., Tang, C., Miller, T., Shirazian, S., McMahon, G., Cherrington, J.M., 2003. In vivo antitumor activity of SU11248, a novel tyrosine kinase inhibitor targeting vascular endothelial growth factor and platelet-derived growth factor receptors: determination of a pharmacokinetic/pharmacodynamic relationship. Clin. Cancer Res. Off. J. Am. Assoc. Cancer Res. 9, 327–337.

Mick, R., Gupta, E., Vokes, E.E., Ratain, M.J., 1996. Limited-sampling models for irinotecan pharmacokinetics-pharmacodynamics: prediction of biliary index and intestinal toxicity. J. Clin. Oncol. Off. J. Am. Soc. Clin. Oncol. 14, 2012–2019.

Mielke, S., Sparreboom, A., Behringer, D., Mross, K., 2005a. Paclitaxel pharmacokinetics and response to chemotherapy in patients with advanced cancer treated with a weekly regimen. Anticancer Res. 25, 4423–4427.

Mielke, S., Sparreboom, A., Steinberg, S.M., Gelderblom, H., Unger, C., Behringer, D., Mross, K., 2005b. Association of Paclitaxel pharmacokinetics with the development of peripheral neuropathy in patients with advanced cancer. Clin. Cancer Res. Off. J. Am. Assoc. Cancer Res. 11, 4843–4850. doi:10.1158/1078-0432.CCR-05-0298

Miller, F.G., Joffe, S., 2008. Benefit in phase 1 oncology trials: therapeutic misconception or reasonable treatment option? Clin. Trials 5, 617–623. doi:10.1177/1740774508097576

Minkin, P., Zhao, M., Chen, Z., Ouwerkerk, J., Gelderblom, H., Baker, S.D., 2008. Quantification of sunitinib in human plasma by high-performance liquid chromatography-tandem mass spectrometry. J. Chromatogr. B Analyt. Technol. Biomed. Life. Sci. 874, 84–88. doi:10.1016/j.jchromb.2008.09.007

Moertel, C.G., Schutt, A.J., Reitemeier, R.J., Hahn, R.G., 1972. Phase II study of camptothecin (NSC-100880) in the treatment of advanced gastrointestinal cancer. Cancer Chemother. Rep. 56, 95–101.

Monsarrat, B., Alvinerie, P., Wright, M., Dubois, J., Guéritte-Voegelein, F., Guénard, D., Donehower, R.C., Rowinsky, E.K., 1993. Hepatic metabolism and biliary excretion of Taxol in rats and humans. J. Natl. Cancer Inst. Monogr. 39–46.

Monsarrat, B., Royer, I., Wright, M., Cresteil, T., 1997. Biotransformation of taxoids by human cytochromes P450: structure-activity relationship. Bull. Cancer (Paris) 84, 125–133.

Mortier, K.A., Renard, V., Verstraete, A.G., Van Gussem, A., Van Belle, S., Lambert, W.E., 2005. Development and validation of a liquid chromatography-tandem mass spectrometry assay for the quantification of docetaxel and paclitaxel in human plasma and oral fluid. Anal. Chem. 77, 4677–4683. doi:10.1021/ac0500941

Mortier, K.A., Verstraete, A.G., Zhang, G.-F., Lambert, W.E., 2004. Enhanced method performance due to a shorter chromatographic run-time in a liquid chromatography-tandem mass spectrometry assay for paclitaxel. J. Chromatogr. A 1041, 235–238.

Motzer, R.J., Michaelson, M.D., Rosenberg, J., Bukowski, R.M., Curti, B.D., George, D.J., Hudes, G.R., Redman, B.G., Margolin, K.A., Wilding, G., 2007. Sunitinib efficacy against advanced renal cell carcinoma. J. Urol. 178, 1883–1887. doi:10.1016/j.juro.2007.07.030

Mross, K., Holländer, N., Hauns, B., Schumacher, M., Maier-Lenz, H., 2000. The pharmacokinetics of a 1-h paclitaxel infusion. Cancer Chemother. Pharmacol. 45, 463–470.

Muggia, F.M., Creaven, P.J., Hansen, H.H., Cohen, M.H., Selawry, O.S., 1972. Phase I clinical trial of weekly and daily treatment with camptothecin (NSC-100880): correlation with preclinical studies. Cancer Chemother. Rep. 56, 515–521.

Musijowski, J., Piórkowska, E., Rudzki, P.J., 2014. Determination of sunitinib in human plasma using liquid chromatography coupled with mass spectrometry: Liquid Chromatography. J. Sep. Sci. 37, 2652–2658. doi:10.1002/jssc.201400231

Newton, K.F., Newman, W., Hill, J., 2012. Review of biomarkers in colorectal cancer. Colorectal Dis. Off. J. Assoc. Coloproctology G. B. Irel. 14, 3–17. doi:10.1111/j.1463-1318.2010.02439.x

Nováková, L., 2013. Challenges in the development of bioanalytical liquid chromatography-mass spectrometry method with emphasis on fast analysis. J. Chromatogr. A 1292, 25–37. doi:10.1016/j.chroma.2012.08.087

Nussbaumer, S., Bonnabry, P., Veuthey, J.-L., Fleury-Souverain, S., 2011. Analysis of anticancer drugs: a review. Talanta 85, 2265–2289. doi:10.1016/j.talanta.2011.08.034

Ohtsu, T., Sasaki, Y., Tamura, T., Miyata, Y., Nakanomyo, H., Nishiwaki, Y., Saijo, N., 1995. Clinical pharmacokinetics and pharmacodynamics of paclitaxel: a 3-hour infusion versus a 24-hour infusion. Clin. Cancer Res. Off. J. Am. Assoc. Cancer Res. 1, 599–606.

Owens, T.S., Dodds, H., Fricke, K., Hanna, S.K., Crews, K.R., 2003. High-performance liquid chromatographic assay with fluorescence detection for the simultaneous measurement of carboxylate and lactone forms of irinotecan and three metabolites in human plasma. J. Chromatogr. B Analyt. Technol. Biomed. Life. Sci. 788, 65–74.

Paci, A., Veal, G., Bardin, C., Levêque, D., Widmer, N., Beijnen, J., Astier, A., Chatelut, E., 2014. Review of therapeutic drug monitoring of anticancer drugs part 1 – Cytotoxics. Eur. J. Cancer 50, 2010–2019. doi:10.1016/j.ejca.2014.04.014

Panday, V.R., Huizing, M.T., van Warmerdam, L.J., Dubbelman, R.C., Mandjes, I., Schellens, J.H., Huinink, W.W., Beijnen, J.H., 1998. Pharmacologic study of 3-hour 135 mg M-2 paclitaxel in platinum pretreated patients with advanced ovarian cancer. Pharmacol. Res. 38, 231–236. doi:10.1006/phrs.1998.0360

Parmar, M.K.B., Ledermann, J.A., Colombo, N., du Bois, A., Delaloye, J.-F., Kristensen, G.B., Wheeler, S., Swart, A.M., Qian, W., Torri, V., Floriani, I., Jayson, G., Lamont, A., Tropé, C., ICON and AGO Collaborators, 2003. Paclitaxel plus platinum-based chemotherapy versus conventional platinum-based chemotherapy in women with relapsed ovarian cancer: the ICON4/AGO-OVAR-2.2 trial. Lancet Lond. Engl. 361, 2099–2106.

Patel, J.N., 2014. Application of genotype-guided cancer therapy in solid tumors. Pharmacogenomics 15, 79–93. doi:10.2217/pgs.13.227

Pietrantonio, F., Iacovelli, R., Di Bartolomeo, M., de Braud, F., 2014. FOLFIRI with cetuximab or bevacizumab: FIRE-3. Lancet Oncol. 15, e581. doi:10.1016/S1470-2045(14)70397-3

Pignon, T., Lacarelle, B., Duffaud, F., Guillet, P., Catalin, J., Durand, A., Monjanel, S., Favre, R., 1994. Pharmacokinetics of high-dose methotrexate in adult osteogenic sarcoma. Cancer Chemother. Pharmacol. 33, 420–424.

Pinkel, D., 1998. Cancer chemotherapy and body surface area. J. Clin. Oncol. Off. J. Am. Soc. Clin. Oncol. 16, 3714–3715.

Pinkel, D., 1958. The use of body surface area as a criterion of drug dosage in cancer chemotherapy. Cancer Res. 18, 853–856.

Posocco, B., Dreussi, E., de Santa, J., Toffoli, G., Abrami, M., Musiani, F., Grassi, M., Farra, R., Tonon, F., Grassi, G., Dapas, B., 2015. Polysaccharides for the Delivery of Antitumor Drugs. Materials 8, 2569–2615. doi:10.3390/ma8052569

Presta, L.G., Chen, H., O'Connor, S.J., Chisholm, V., Meng, Y.G., Krummen, L., Winkler, M., Ferrara, N., 1997. Humanization of an anti-vascular endothelial growth factor monoclonal antibody for the therapy of solid tumors and other disorders. Cancer Res. 57, 4593–4599.

Qiu, F., Bian, W., Li, J., Ge, Z., 2013. Simultaneous determination of sunitinib and its two metabolites in plasma of Chinese patients with metastatic renal cell carcinoma by liquid

chromatography-tandem mass spectrometry. Biomed. Chromatogr. BMC 27, 615–621. doi:10.1002/bmc.2836

Rahman, A., Korzekwa, K.R., Grogan, J., Gonzalez, F.J., Harris, J.W., 1994. Selective biotransformation of taxol to 6 alpha-hydroxytaxol by human cytochrome P450 2C8. Cancer Res. 54, 5543–5546.

Rais, R., Zhao, M., He, P., Xu, L., Deeken, J.F., Rudek, M.A., 2012. Quantitation of unbound sunitinib and its metabolite N-desethyl sunitinib (SU12662) in human plasma by equilibrium dialysis and liquid chromatography-tandem mass spectrometry: application to a pharmacokinetic study. Biomed. Chromatogr. BMC 26, 1315–1324. doi:10.1002/bmc.2697

Rayleigh, F.R.., 1882. XX. On the equilibrium of liquid conducting masses charged with electricity. Philos. Mag. Ser. 5 14, 184–186. doi:10.1080/14786448208628425

Reynolds, D.J., Aronson, J.K., 1993. ABC of monitoring drug therapy. Making the most of plasma drug concentration measurements. BMJ 306, 48–51.

Rivory, L.P., Chatelut, E., Canal, P., Mathieu-Boué, A., Robert, J., 1994. Kinetics of the in vivo interconversion of the carboxylate and lactone forms of irinotecan (CPT-11) and of its metabolite SN-38 in patients. Cancer Res. 54, 6330–6333.

Rivory, L.P., Haaz, M.C., Canal, P., Lokiec, F., Armand, J.P., Robert, J., 1997. Pharmacokinetic interrelationships of irinotecan (CPT-11) and its three major plasma metabolites in patients enrolled in phase I/II trials. Clin. Cancer Res. Off. J. Am. Assoc. Cancer Res. 3, 1261–1266.

Rodamer, M., Elsinghorst, P.W., Kinzig, M., Gütschow, M., Sörgel, F., 2011. Development and validation of a liquid chromatography/tandem mass spectrometry procedure for the quantification of sunitinib (SU11248) and its active metabolite, N-desethyl sunitinib (SU12662), in human plasma: Application to an explorative study. J. Chromatogr. B 879, 695–706. doi:10.1016/j.jchromb.2011.02.006

Rothenberg, M.L., Eckardt, J.R., Kuhn, J.G., Burris, H.A., Nelson, J., Hilsenbeck, S.G., Rodriguez, G.I., Thurman, A.M., Smith, L.S., Eckhardt, S.G., Weiss, G.R., Elfring, G.L., Rinaldi, D.A., Schaaf, L.J., Von Hoff, D.D., 1996. Phase II trial of irinotecan in patients with progressive or rapidly recurrent colorectal cancer. J. Clin. Oncol. Off. J. Am. Soc. Clin. Oncol. 14, 1128–1135.

Rothenberg, M.L., Kuhn, J.G., Burris, H.A., Nelson, J., Eckardt, J.R., Tristan-Morales, M., Hilsenbeck, S.G., Weiss, G.R., Smith, L.S., Rodriguez, G.I., 1993. Phase I and pharmacokinetic trial of weekly CPT-11. J. Clin. Oncol. Off. J. Am. Soc. Clin. Oncol. 11, 2194–2204.

Rowinsky, E.K., Grochow, L.B., Ettinger, D.S., Sartorius, S.E., Lubejko, B.G., Chen, T.L., Rock, M.K., Donehower, R.C., 1994. Phase I and pharmacological study of the novel topoisomerase I inhibitor 7-ethyl-10-[4-(1-piperidino)-1-piperidino]carbonyloxycamptothecin (CPT-11) administered as a ninety-minute infusion every 3 weeks. Cancer Res. 54, 427–436.

Sai, K., Kaniwa, N., Ozawa, S., Sawada, J., 2002. An analytical method for irinotecan (CPT-11) and its metabolites using a high-performance liquid chromatography: parallel detection with fluorescence and mass spectrometry. Biomed. Chromatogr. BMC 16, 209–218. doi:10.1002/bmc.137

Saint-Marcoux, F., Sauvage, F.-L., Marquet, P., 2007. Current role of LC-MS in therapeutic drug monitoring. Anal. Bioanal. Chem. 388, 1327–1349. doi:10.1007/s00216-007-1320-1

Sakamoto, K.M., 2004. Su-11248 Sugen. Curr. Opin. Investig. Drugs Lond. Engl. 2000 5, 1329–1339.

Saltz, L.B., Douillard, J.Y., Pirotta, N., Alakl, M., Gruia, G., Awad, L., Elfring, G.L., Locker, P.K., Miller, L.L., 2001. Irinotecan plus fluorouracil/leucovorin for metastatic colorectal cancer: a new survival standard. The Oncologist 6, 81–91.

Sanavio, B., Krol, S., 2015. On the Slow Diffusion of Point-of-Care Systems in Therapeutic Drug Monitoring. Front. Bioeng. Biotechnol. 3. doi:10.3389/fbioe.2015.00020

Santos, A., Zanetta, S., Cresteil, T., Deroussent, A., Pein, F., Raymond, E., Vernillet, L., Risse, M.L., Boige, V., Gouyette, A., Vassal, G., 2000. Metabolism of irinotecan (CPT-11) by CYP3A4 and CYP3A5 in humans. Clin. Cancer Res. Off. J. Am. Assoc. Cancer Res. 6, 2012–2020.

Sawyers, C., 2004a. Targeted cancer therapy. Nature 432, 294–297. doi:10.1038/nature03095

Sawyers, C., 2004b. Targeted cancer therapy. Nature 432, 294–297.

Sawyers, C.L., 2008. The cancer biomarker problem. Nature 452, 548–552. doi:10.1038/nature06913

Schaeppi, U., Fleischman, R.W., Cooney, D.A., 1974. Toxicity of camptothecin (NSC-100880). Cancer Chemother. Rep. [3] 5, 25–36.

Schiff, P.B., Horwitz, S.B., 1981. Taxol assembles tubulin in the absence of exogenous guanosine 5'-triphosphate or microtubule-associated proteins. Biochemistry (Mosc.) 20, 3247–3252.

Schiff, P.B., Horwitz, S.B., 1980. Taxol stabilizes microtubules in mouse fibroblast cells. Proc. Natl. Acad. Sci. U. S. A. 77, 1561–1565.

Schlessinger, J., 2000. Cell signaling by receptor tyrosine kinases. Cell 103, 211–225.

Schork, N.J., 2015. Personalized medicine: Time for one-person trials. Nature 520, 609–611. doi:10.1038/520609a

Schuurhuis, G.J., Broxterman, H.J., Pinedo, H.M., van Heijningen, T.H., van Kalken, C.K., Vermorken, J.B., Spoelstra, E.C., Lankelma, J., 1990. The polyoxyethylene castor oil Cremophor EL modifies multidrug resistance. Br. J. Cancer 62, 591–594.

Seymour, L., Ivy, S.P., Sargent, D., Spriggs, D., Baker, L., Rubinstein, L., Ratain, M.J., Le Blanc, M., Stewart, D., Crowley, J., Groshen, S., Humphrey, J.S., West, P., Berry, D., 2010. The design of phase II clinical trials testing cancer therapeutics: consensus recommendations from the clinical trial design task force of the national cancer institute investigational drug steering committee. Clin. Cancer Res. Off. J. Am. Assoc. Cancer Res. 16, 1764–1769. doi:10.1158/1078-0432.CCR-09-3287

Shah, V.P., Midha, K.K., Dighe, S., McGilveray, I.J., Skelly, J.P., Yacobi, A., Layloff, T., Viswanathan, C.T., Cook, C.E., McDowall, R.D., 1991. Analytical methods validation: bioavailability, bioequivalence and pharmacokinetic studies. Conference report. Eur. J. Drug Metab. Pharmacokinet. 16, 249–255.

Shanholtz, C., 2001. Acute life-threatening toxicity of cancer treatment. Crit. Care Clin. 17, 483–502.

Shankaran, V., Wisinski, K.B., Mulcahy, M.F., Benson, A.B., 2008. The role of molecular markers in predicting response to therapy in patients with colorectal cancer. Mol. Diagn. Ther. 12, 87–98.

Sistla, A., Shenoy, N., 2005. Reversible Z-E Isomerism and Pharmaceutical Implications for SU5416. Drug Dev. Ind. Pharm. 31, 1001–1007. doi:10.1080/03639040500306260

Slatter, J.G., Schaaf, L.J., Sams, J.P., Feenstra, K.L., Johnson, M.G., Bombardt, P.A., Cathcart, K.S., Verburg, M.T., Pearson, L.K., Compton, L.D., Miller, L.L., Baker, D.S., Pesheck, C.V., Lord, R.S., 2000. Pharmacokinetics, metabolism, and excretion of irinotecan (CPT-11) following I.V. infusion of [(14)C]CPT-11 in cancer patients. Drug Metab. Dispos. Biol. Fate Chem. 28, 423–433.

Sledge, G.W., Neuberg, D., Bernardo, P., Ingle, J.N., Martino, S., Rowinsky, E.K., Wood, W.C., 2003. Phase III trial of doxorubicin, paclitaxel, and the combination of doxorubicin and paclitaxel as front-line chemotherapy for metastatic breast cancer: an intergroup trial (E1193). J. Clin. Oncol. Off. J. Am. Soc. Clin. Oncol. 21, 588–592.

Sonnichsen, D.S., Hurwitz, C.A., Pratt, C.B., Shuster, J.J., Relling, M.V., 1994. Saturable pharmacokinetics and paclitaxel pharmacodynamics in children with solid tumors. J. Clin. Oncol. Off. J. Am. Soc. Clin. Oncol. 12, 532–538.

Sottani, C., Minoia, C., D'Incalci, M., Paganini, M., Zucchetti, M., 1998. High-performance liquid chromatography tandem mass spectrometry procedure with automated solid phase extraction sample preparation for the quantitative determination of paclitaxel (Taxol) in human plasma. Rapid Commun. Mass Spectrom. RCM 12, 251–255. doi:10.1002/(SICI)1097-0231(19980314)12:5<251::AID-RCM145>3.0.CO;2-Z

Sparano, J.A., Wang, M., Martino, S., Jones, V., Perez, E.A., Saphner, T., Wolff, A.C., Sledge, G.W., Wood, W.C., Davidson, N.E., 2008. Weekly paclitaxel in the adjuvant treatment of breast cancer. N. Engl. J. Med. 358, 1663–1671. doi:10.1056/NEJMoa0707056

Sparreboom, A., de Bruijn, P., de Jonge, M.J., Loos, W.J., Stoter, G., Verweij, J., Nooter, K., 1998a. Liquid chromatographic determination of irinotecan and three major metabolites in human plasma, urine and feces. J. Chromatogr. B. Biomed. Sci. App. 712, 225–235.

Sparreboom, A., de Jonge, M.J., de Bruijn, P., Brouwer, E., Nooter, K., Loos, W.J., van Alphen, R.J., Mathijssen, R.H., Stoter, G., Verweij, J., 1998b. Irinotecan (CPT-11) metabolism and disposition in cancer patients. Clin. Cancer Res. Off. J. Am. Assoc. Cancer Res. 4, 2747–2754.

Sparreboom, A., Huizing, M.T., Boesen, J.J., Nooijen, W.J., van Tellingen, O., Beijnen, J.H., 1995. Isolation, purification, and biological activity of mono- and dihydroxylated paclitaxel metabolites from human feces. Cancer Chemother. Pharmacol. 36, 299–304. doi:10.1007/BF00689047

Sparreboom, A., van Tellingen, O., Nooijen, W.J., Beijnen, J.H., 1996. Nonlinear pharmacokinetics of paclitaxel in mice results from the pharmaceutical vehicle Cremophor EL. Cancer Res. 56, 2112–2115.

Spear, B.B., Heath-Chiozzi, M., Huff, J., 2001. Clinical application of pharmacogenetics. Trends Mol. Med. 7, 201–204.

Stokvis, E., Ouwehand, M., Nan, L.G. a. H., Kemper, E.M., van Tellingen, O., Rosing, H., Beijnen, J.H., 2004. A simple and sensitive assay for the quantitative analysis of paclitaxel in human and mouse plasma and brain tumor tissue using coupled liquid chromatography and tandem mass spectrometry. J. Mass Spectrom. JMS 39, 1506–1512. doi:10.1002/jms.747

Strimbu, K., Tavel, J.A., 2010. What are biomarkers? Curr. Opin. HIV AIDS 5, 463–466. doi:10.1097/COH.0b013e32833ed177

Suenaga, M., Fuse, N., Yamaguchi, T., Yamanaka, Y., Motomura, S., Matsumoto, H., Hamamoto, Y., Mizunuma, N., Doi, T., Hatake, K., Iwasaki, J., Ohtsu, A., 2014. Pharmacokinetics, safety, and efficacy of FOLFIRI plus bevacizumab in Japanese colorectal cancer patients with UGT1A1 gene polymorphisms. J. Clin. Pharmacol. 54, 495–502. doi:10.1002/jcph.246

Takano, M., Kikuchi, Y., Kita, T., Suzuki, M., Ohwada, M., Yamamoto, T., Yamamoto, K., Inoue, H., Shimizu, K., 2002. Phase I and pharmacological study of single paclitaxel administered weekly for heavily pre-treated patients with epithelial ovarian cancer. Anticancer Res. 22, 1833–1838.

Tamura, T., Sasaki, Y., Eguchi, K., Shinkai, T., Ohe, Y., Nishio, M., Kunikane, H., Arioka, H., Karato, A., Omatsu, H., 1994. Phase I and pharmacokinetic study of paclitaxel by 24-hour intravenous infusion. Jpn. J. Cancer Res. Gann 85, 1057–1062.

Taylor, G., 1964. Disintegration of Water Drops in an Electric Field. Proc. R. Soc. Lond. Math. Phys. Eng. Sci. 280, 383–397. doi:10.1098/rspa.1964.0151

ten Tije, A.J., Verweij, J., Loos, W.J., Sparreboom, A., 2003. Pharmacological effects of formulation vehicles : implications for cancer chemotherapy. Clin. Pharmacokinet. 42, 665–685. doi:10.2165/00003088-200342070-00005

Thall, P.F., 2008. A review of phase 2-3 clinical trial designs. Lifetime Data Anal. 14, 37–53. doi:10.1007/s10985-007-9049-x

Therasse, P., Arbuck, S.G., Eisenhauer, E.A., Wanders, J., Kaplan, R.S., Rubinstein, L., Verweij, J., Van Glabbeke, M., van Oosterom, A.T., Christian, M.C., Gwyther, S.G., 2000. New guidelines to evaluate the response to treatment in solid tumors. European Organization for Research and Treatment of Cancer, National Cancer Institute of the United States, National Cancer Institute of Canada. J. Natl. Cancer Inst. 92, 205–216.

Thiebaut, F., Tsuruo, T., Hamada, H., Gottesman, M.M., Pastan, I., Willingham, M.C., 1987. Cellular localization of the multidrug-resistance gene product P-glycoprotein in normal human tissues. Proc. Natl. Acad. Sci. U. S. A. 84, 7735–7738.

Thurston, D.E., 2006. Chemistry and Pharmacology of Anticancer Drugs. CRC Press.

Toffoli, G., Cecchin, E., Corona, G., Russo, A., Buonadonna, A., D'Andrea, M., Pasetto, L.M., Pessa, S., Errante, D., De Pangher, V., Giusto, M., Medici, M., Gaion, F., Sandri, P., Galligioni, E., Bonura, S., Boccalon, M., Biason, P., Frustaci, S., 2006. The role of UGT1A1*28 polymorphism in the pharmacodynamics and pharmacokinetics of irinotecan in patients with metastatic colorectal cancer. J. Clin. Oncol. Off. J. Am. Soc. Clin. Oncol. 24, 3061–3068. doi:10.1200/JCO.2005.05.5400

Toffoli, G., Cecchin, E., Gasparini, G., D'Andrea, M., Azzarello, G., Basso, U., Mini, E., Pessa, S., De Mattia, E., Lo Re, G., Buonadonna, A., Nobili, S., De Paoli, P., Innocenti, F., 2010a. Genotype-driven phase I study of irinotecan administered in combination with fluorouracil/leucovorin in patients with metastatic colorectal cancer. J. Clin. Oncol. Off. J. Am. Soc. Clin. Oncol. 28, 866–871. doi:10.1200/JCO.2009.23.6125

Toffoli, G., Cecchin, E., Gasparini, G., D'Andrea, M., Azzarello, G., Basso, U., Mini, E., Pessa, S., De Mattia, E., Lo Re, G., Buonadonna, A., Nobili, S., De Paoli, P., Innocenti, F., 2010b. Genotype-driven phase I study of irinotecan administered in combination with fluorouracil/leucovorin in patients with metastatic colorectal cancer. J. Clin. Oncol. Off. J. Am. Soc. Clin. Oncol. 28, 866–871. doi:10.1200/JCO.2009.23.6125

Tsao, Y.P., Russo, A., Nyamuswa, G., Silber, R., Liu, L.F., 1993. Interaction between replication forks and topoisomerase I-DNA cleavable complexes: studies in a cell-free SV40 DNA replication system. Cancer Res. 53, 5908–5914.

Tukey, R.H., Strassburg, C.P., Mackenzie, P.I., 2002. Pharmacogenomics of human UDP-glucuronosyltransferases and irinotecan toxicity. Mol. Pharmacol. 62, 446–450.

Urso, R., Blardi, P., Giorgi, G., 2002. A short introduction to pharmacokinetics. Eur. Rev. Med. Pharmacol. Sci. 6, 33–44.

Vainchtein, L.D., Thijssen, B., Stokvis, E., Rosing, H., Schellens, J.H.M., Beijnen, J.H., 2006. A simple and sensitive assay for the quantitative analysis of paclitaxel and metabolites in human plasma using liquid chromatography/tandem mass spectrometry. Biomed. Chromatogr. BMC 20, 139–148. doi:10.1002/bmc.544

Van Cutsem, E., Köhne, C.-H., Hitre, E., Zaluski, J., Chang Chien, C.-R., Makhson, A., D'Haens, G., Pintér, T., Lim, R., Bodoky, G., Roh, J.K., Folprecht, G., Ruff, P., Stroh, C., Tejpar, S., Schlichting, M., Nippgen, J., Rougier, P., 2009a. Cetuximab and chemotherapy as initial treatment for metastatic colorectal cancer. N. Engl. J. Med. 360, 1408–1417. doi:10.1056/NEJMoa0805019

Van Cutsem, E., Köhne, C.-H., Hitre, E., Zaluski, J., Chang Chien, C.-R., Makhson, A., D'Haens, G., Pintér, T., Lim, R., Bodoky, G., Roh, J.K., Folprecht, G., Ruff, P., Stroh, C., Tejpar, S., Schlichting, M., Nippgen, J., Rougier, P., 2009b. Cetuximab and chemotherapy as initial treatment for metastatic colorectal cancer. N. Engl. J. Med. 360, 1408–1417. doi:10.1056/NEJMoa0805019

Van Tellingen, O., Huizing, M.T., Panday, V.N., Schellens, J.H.M., Nooijen, W.J., Beijnen, J.H., 1999. Cremophor EL causes (pseudo-) non-linear pharmacokinetics of paclitaxel in patients. Br. J. Cancer 81, 330.

van Zuylen, L., Karlsson, M.O., Verweij, J., Brouwer, E., de Bruijn, P., Nooter, K., Stoter, G., Sparreboom, A., 2001. Pharmacokinetic modeling of paclitaxel encapsulation in Cremophor EL micelles. Cancer Chemother. Pharmacol. 47, 309–318. doi:10.1007/s002800000215

Walczak, C.E., Cai, S., Khodjakov, A., 2010. Mechanisms of chromosome behaviour during mitosis. Nat. Rev. Mol. Cell Biol. 11, 91–102. doi:10.1038/nrm2832

Walker, I., Newell, H., 2009. Do molecularly targeted agents in oncology have reduced attrition rates? Nat. Rev. Drug Discov. 8, 15–16. doi:10.1038/nrd2758

Walle, T., Walle, U.K., Kumar, G.N., Bhalla, K.N., 1995. Taxol metabolism and disposition in cancer patients. Drug Metab. Dispos. Biol. Fate Chem. 23, 506–512.

Wall, M.E., Wani, M.C., 1995. Camptothecin and taxol: discovery to clinic--thirteenth Bruce F. Cain Memorial Award Lecture. Cancer Res. 55, 753–760.

Wall, M.E., Wani, M.C., Cook, C.E., Palmer, K.H., McPhail, A.T., Sim, G.A., 1966. Plant Antitumor Agents. I. The Isolation and Structure of Camptothecin, a Novel Alkaloidal Leukemia and Tumor Inhibitor from Camptotheca acuminata1,2. J. Am. Chem. Soc. 88, 3888–3890. doi:10.1021/ja00968a057

Wani, M.C., Taylor, H.L., Wall, M.E., Coggon, P., McPhail, A.T., 1971. Plant antitumor agents. VI. The isolation and structure of taxol, a novel antileukemic and antitumor agent from Taxus brevifolia. J. Am. Chem. Soc. 93, 2325–2327.

Weisberg, E., Manley, P.W., Breitenstein, W., Brüggen, J., Cowan-Jacob, S.W., Ray, A., Huntly, B., Fabbro, D., Fendrich, G., Hall-Meyers, E., Kung, A.L., Mestan, J., Daley, G.Q., Callahan, L., Catley, L., Cavazza, C., Azam, M., Mohammed, A., Neuberg, D., Wright, R.D., Gilliland, D.G., Griffin, J.D., 2005. Characterization of AMN107, a selective inhibitor of native and mutant Bcr-Abl. Cancer Cell 7, 129–141. doi:10.1016/j.ccr.2005.01.007

Whitesides, G.M., Goe, G.L., Cope, A.C., 1969. Irradiation of cis, cis- 1,5-cyclooctadiene in the presence of copper (I) chloride. J. Am. Chem. Soc. 91, 2608– 2616.

Widmer, N., Bardin, C., Chatelut, E., Paci, A., Beijnen, J., Levêque, D., Veal, G., Astier, A., 2014. Review of therapeutic drug monitoring of anticancer drugs part two – Targeted therapies. Eur. J. Cancer 50, 2020–2036. doi:10.1016/j.ejca.2014.04.015

Wiernik, P.H., Schwartz, E.L., Strauman, J.J., Dutcher, J.P., Lipton, R.B., Paietta, E., 1987. Phase I clinical and pharmacokinetic study of taxol. Cancer Res. 47, 2486–2493.

Wong, M., Evans, S., Rivory, L.P., Hoskins, J.M., Mann, G.J., Farlow, D., Clarke, C.L., Balleine, R.L., Gurney, H., 2005. Hepatic technetium Tc 99m-labeled sestamibi elimination rate and ABCB1 (MDR1) genotype as indicators of ABCB1 (P-glycoprotein) activity in patients with cancer. Clin. Pharmacol. Ther. 77, 33–42. doi:10.1016/j.clpt.2004.09.002

Yamaguchi, H., Fujikawa, A., Ito, H., Tanaka, N., Furugen, A., Miyamori, K., Takahashi, N., Ogura, J., Kobayashi, M., Yamada, T., Mano, N., Iseki, K., 2013. Quantitative determination of paclitaxel and its metabolites, 6α-hydroxypaclitaxel and p-3′-hydroxypaclitaxel, in human plasma using column-switching liquid chromatography/tandem mass spectrometry. Biomed. Chromatogr. BMC 27, 539–544. doi:10.1002/bmc.2826

Ye, M., Zhu, Z., Fu, Q., Shen, K., Li, D.K., 2000. Nonlinear pharmacokinetics of paclitaxel in ovarian cancer patients. Acta Pharmacol. Sin. 21, 596–599.

Zhang, L., Borysenko, C.W., Albright, T.A., Bittner, E.R., Lee, T.R., 2001. The cis-trans isomerization of 1,2,5,6-tetrasilacycloocta-3,7-dienes: analysis by mechanistic probes and density functional theory. J. Org. Chem. 66, 5275–5283.

Zhang, S.-Q., Chen, G.-H., 2008. Determination of Paclitaxel in Human Plasma by UPLC-MS-MS. J. Chromatogr. Sci. 46, 220–224.

Zhang, W., Dutschman, G.E., Li, X., Cheng, Y.-C., 2011. Quantitation of paclitaxel and its two major metabolites using a liquid chromatography-electrospray ionization tandem mass spectrometry. J. Chromatogr. B Analyt. Technol. Biomed. Life. Sci. 879, 2018–2022. doi:10.1016/j.jchromb.2011.05.024

Zhang, W., Dutschman, G.E., Li, X., Ye, M., Cheng, Y.-C., 2009. Quantitation of Irinotecan and its two major metabolites using a liquid chromatography-electrospray ionization tandem mass spectrometric. J. Chromatogr. B Analyt. Technol. Biomed. Life. Sci. 877, 3038–3044. doi:10.1016/j.jchromb.2009.07.025

Zhou, Q., Gallo, J.M., 2010. Quantification of sunitinib in mouse plasma, brain tumor and normal brain using liquid chromatography-electrospray ionization-tandem mass spectrometry and pharmacokinetic application. J. Pharm. Biomed. Anal. 51, 958–964. doi:10.1016/j.jpba.2009.10.006

Appendix 1

EudraCT n. 2009-012227-28
CRO-2009-25

A genotype-guided phase I study of irinotecan administered in combination with 5-fluorouracil/leucovorin (FOLFIRI) and bevacizumab in advanced colorectal cancer patients

SAMPLING FOR THE PK OF CPT-11

Date of start of the therapy: _____

Protocol n°_CRO-2009-25_____ Medical record n° _____ Paz.n° _____

First name and last name _____ Sigla _____

Date of birth_____ PS(Karnowsky) _____ BSA (m^2) _____

Weight (kg) _____ Height (cm) _____

Center _____

Sheduled Therapy

CPT-11	LV	5-FU	BV
|_____| mg/m^2 2h i.v. (day 1 and day 15)	200 mg/m^2 2h i.v. (day 1 and day 15)	400 mg /m^2 bolus (day 1 and day 15) 2.4 gr/m^2 46h i.v. (day 1 and day 15)	5 mg/kg 90 min i.v.

Therapy cycle n° _____ Date and time of the therapy_____

CPT-11 dose (mg/m^2) _____ Total CPT-11 dose (mg) _____

N°	Aliquote	Time	Teoric time	Real time	Administration	Note
1		0'			Before CPT-11 infusion (IV)	
2		1.0 h			1 h after start of IV	
3		2.0 h			End of the IV	
4		2.25 h			15 min after the end of IV	
5		2.50 h			30 min after the end of IV	
6		3.0 h			1 h after the end of IV	
7		4.0 h			2 h after the end of IV	
8		6.0 h			4 h after the end of IV	
9		8.0 h			6 h after the end of IV	
10		10.0 h			8 h after the end of IV	
12		26.0 h			24 h after the end of IV	
13		50.0 h			48 h after the end of IV	

EudraCT n. 2013-005618-37
CRO-2014-01

A genotype-guided phase I study of irinotecan administered in combination with 5-fluorouracil/leucovorin (FOLFIRI) and cetuximab as first-line therapy in metastatic colorectal cancer patients

SAMPLING FOR THE PK OF CPT-11

Date of start of the therapy: _____

Protocol n°_CRO-2014-01_____ Medical record n° _____ Paz.n° _____

First name and last name _____ Sigla _____

Date of birth_____ PS(Karnowsky) _____ BSA (m^2) _____

Weight (kg) _____ Height (cm) _____

Center _____

Sheduled Therapy

CPT-11	LV	5-FU	CTX
|_____| mg/m^2 2h i.v. (day 1 and day 15)	200 mg/m^2 2h i.v. (day 1 and day 15)	400 mg /m^2 bolus (day 1 and day 15) 2.4 gr/m^2 46h i.v. (day 1 and day 15)	500 mg /m^2

Therapy cycle n° _____ Date and time of the therapy_____

CPT-11 dose (mg/m^2) _____ Total CPT-11 dose (mg) _____

N°	Aliquote	Time	Teoric time	Real time	Administration	Note
1		0'			Before CPT-11 infusion (IV)	
2		1.0 h			1 h after start of IV	
3		2.0 h			End of the IV	
4		2.25 h			15 min after the end of IV	
5		2.50 h			30 min after the end of IV	
6		3.0 h			1 h after the end of IV	
7		4.0 h			2 h after the end of IV	
8		6.0 h			4 h after the end of IV	
9		8.0 h			6 h after the end of IV	
10		10.0 h			8 h after the end of IV	
12		26.0 h			24 h after the end of IV	
13		50.0 h			48 h after the end of IV	

EudraCT n. 2010-021619-18
CRO-2010-42

A genotype-guided phase I study for weekly paclitaxel in ovarian cancer patients

SAMPLING FOR THE PK OF PTX

Date of start of the therapy: _____

Protocol n°_CRO-2010-42_____ Medical record n° _____ Paz.n° _____

First name and last name _____ Sigla _____

Date of birth_____ PS(Karnowsky) _____ BSA (m^2) _____

Weight (kg) _____ Height (cm) _____

Center _____

Sheduled Therapy

PTX
|_____| mg/m^2 1h i.v.

Therapy cycle n° _____ Date and time of the therapy_____

PTX dose (mg/m^2) _____ Total PTX dose (mg) _____

N°	Aliquote	Time	Teoric time	Real time	Administration	Note
1		0'			Before PTX infusion (IV)	
2		1.0 h			End of the IV	
3		1.25 h			15 min after the end of IV **(I adm only)**	
4		1.50 h			30 min after the end of IV	
5		2.0 h			1 h after the end of IV	
6		4.0 h			3 h after the end of IV	
7		8.0 h			7 h after the end of IV	
8		25.0 h			24 h after the end of IV	
9		49.0 h			48 h after the end of IV	